12738-6016-R0-00

STUDY OF ELECTRIC PROPULSION SPACECRAFT PLASMAS AND FIELD INTERACTIONS

by

Robert K. Cole, H. S. Ogawa, and J. M. Sellen, Jr.

prepared for

NATIONAL AERONAUTICS AND SPACE ADMINISTRATION

CONTRACT NAS7-100

TRW SYSTEMS GROUP

ONE SPACE PARK • REDONDO BEACH CALIFORNIA 90278

12738-6016-R0-00

FINAL REPORT
STUDY OF ELECTRIC PROPULSION SPACECRAFT PLASMAS AND FIELD INTERACTIONS

by

Robert K. Cole, H. S. Ogawa and J. M. Sellen, Jr.

Prepared for

NATIONAL AERONAUTICS AND SPACE ADMINISTRATION

July 1, 1970

Contract 952414

Technical Management
Jet Propulsion Laboratory
Pasadena, California

Propulsion Research and Advanced Concepts Section

Daniel J. Kerrisk

TRW Systems Group
One Space Park
Redondo Beach, California 90278

TABLE OF CONTENTS

I. INTRODUCTION

A previous program[1] has examined possible problem areas in the acquisition and interpretation of data by a science payload which might result from the operation of the thrusting units of an electrically propelled spacecraft. The analyses and experiments described in this report are a continuation of that program. In the earlier work, principal emphasis was upon the isolation of problem areas, the general categorization of the liklihood of occurrence of a problem, a definition of the region in space in which particular problem areas might arise, and an enumeration of those scientific experiments whose results might be influenced by the operation of the thrusting units. In the present work, emphasis has been restricted. Conjectural interactions, whose definition cannot improve within the limitations of laboratory testing or of analyses, have not been treated. Possible and probable problem areas have been taken up, but in a framework aligned, as much as is possible, to the configuration which an electrically propelled spacecraft might possess. An attempt has been made to quantify the extent of an interaction as it might affect the operation of the science payload and to determine conditions under which interference effects may be minimized or eliminated.

The program findings may be discussed in terms of four categories of contamination to the spacecraft and its environment. These categories are magnetic, electrostatic, space plasma, and electromagnetic contamination. Possible sources of magnetic contamination are in current flows in the ion engine (both beam generation and neutralization), in the electrical equilibration of the thrust beam with the space plasma, and in the (assumed) solar array. Current flows in the solar array include both the conventional circulating current in the power generation and dissipation loops, and that particle current which may result from the drainage between the space plasma and the solar array (which returns to the space plasma via the ion engine neutralizer and thrust beam). Electrostatic contamination of the spacecraft may result from the equilibration potentials established in the electrical equilibration between the thrust beam and the space plasma. A contributing factor here, but generally of diminished importance in the overall interaction is the electrical equilibration between the spacecraft and the space plasma. Space plasma contamination is the deposition in the regions near the spacecraft of particles whose properties are dissimilar to those of the unperturbed ambient environment. Such particles may

arise through the electrical interchange between the space plasma and the thrust beam. The final area of contamination, electromagnetic, may proceed from the electrical equilibration between the thrust beam and the space plasma or may be of a more conventional nature, arising from the operation of the systems which comprise the thrusting unit.

In the sections which follow, the several forms of possible contamination will be discussed in greater detail, together with the means for the control of contaminant levels. These discussions will establish that the operation of the thrusting units of an electrically propelled spacecraft is compatible with the operation of the science payload.

II. PROGRAM REVIEW

The findings of the overall program are contained in the technical reports and published papers that have resulted from the research effort. These documents are given in Section IV of this report. The discussion in this section will review principal aspects of the various portions of Section IV.

A. Magnetic Contamination

1. Solar Arrays

a. General Features

The Introduction has noted that, where possible, problem areas will be considered in the configuration which an electrically propelled spacecraft might possess. Accordingly, the analysis of contaminant magnetic fields did not consider all possible cell stack arrangements. Rather, the calculations used the cell stack of the General Electric 30' roll-up array. The number of arms, physical dimensions, current levels, and numbers of strings are those of the cited array. The analysis did not, however, utilize all of the features of that system. The number of backwires, backwire placement, injection and collection busbar arrangement, and polarities to the various strings will be different from the conditions in the original 30' array. Such changes have been introduced in order to reduce contaminant field levels to that point where they are no longer of concern to either the measurements of the ambient magnetic field or of the directionality of low energy charged particles.

b. Mirror Properties

In a system of current flows, and with the assumption that design considerations allow for an assignment of direction as well as magnitude in the current, it is possible to ascribe certain "mirroring" properties to the flow. For a given array, a system of planes may be specified, and, through selection of the direction of current flow for elements which are at mirror points for these planes, conditions may be generated in which contaminant field cancellation occurs for certain field components within a plane. The 30' roll-up array is particularly adaptable to such an approach in contamiant field cancellation. "Contaminant Magnetic Fields from Large Area Solar Arrays" (Reference 2 and Section IV.A. of this report) discusses such mirroring properties in detail. For the 30' array, through the use of a "mirror-mirror" symmetry property, cancellation of the "Z" component of contaminant field (the array is contained in the x-y plane) occurs along the central axis of the array, everywhere throughout a series of some eight planes, and along the "central" axes of each of the separate arms. Components of contaminant field in the x and y directions also vanish along the central axis of the array, and in the x-y plane containing the array.

The property of contaminant field cancellation along certain lines and planes of the system allows the selection of a "clean" location for magnetometers measuring the ambient magnetic field. In addition, the feature of cancellation within certain planes leads to a reversal of contaminant field direction in regions separated by the planes. A low energy charged particle moving through the overall space near the array will be subjected to $\vec{v} \times \vec{B}$ forces, but perturbations to directionality are minimized as a result of field reversal. Thus, measurements of low energy charged particle directionality may also proceed without the introduction of perturbations from array operation.

In this first analysis, an assumption has been made of equal current flows within each of the strings of the array. In practice, the magnitudes of current flows in the strings will vary to an extent depending upon many factors that cannot be taken up in detail in this present analysis. If, however, the configuration of current flow within each string is such as to minimize contaminant field generation, then variations in the magnitude of the string current (including the possible condition of complete loss of a string

current) will not result in any substantive contaminant field. The principal factors for reduction of individual string contaminant fields are in the granularity of the backwiring circuits and in the geometry of the injection and collection busbars. These features of the array will be discussed in II.A.1. d, e, and f.

c. Current Polarities For Strings Within an Arm

The selection of the mirror property of an array provides a zero failure mode condition (identical string currents) in which contaminant field cancellation occurs in certain planes or along certain axes. In regions away from those planes and axes, cancellation does not occur. However, some degree of cancellation may be obtained through the assignment of current polarities to the strings. (It should be noted that the accepted "mirror" condition does not result in an individual specification of string current polarities.) Reference 3 (also Section IV.B. of this report) has evaluated the contaminant fields at a series of selected points near an arm of the array for two different assignments of polarity to the string currents. For those calculations a single balanced backwire condition is assumed(II.A.1.d and e). By utilizing a reversal of current flow direction between adjacent strings (within the limits of a required mirror condition), substantial reductions of contaminant field levels may be realized. (Table I, Section IV.B.) The specification of the mirror property and the polarities of string currents does complete the major elements in configuring the current of the array. The remaining elements are in the detailed features of the string current patterns and the array arm collection and injection patterns.

d. Backwire Placement

In the discussion of this section it will be assumed that a single backwire is utilized for a string. Section II. A.1.e. will consider multiple backwiring arrangements. The backwire carries the total current of the string and is assumed to be "concentrated" (physical dimensions of the wire are small compared to the total width of the cells in the string). Since the currents in the cells are distributed over a larger area than in the backwire, field cancellation through equal-and-opposite currents on a point by point basis cannot occur. There are, however, arrangements which substantially reduce contaminant field levels, for only this single backwire case.

Reference 3 has considered two cases of backwire placement. The first of these is "balanced" (located at the mid line of the string) while the second is "offset" (located at the edge of the string). For this latter case it is possible to describe the current elements of the string and backwire as a series of linear dipoles. Field generation for these dipoles is large and diminishes only slowly in moving away from the string. For the balanced backwire, cancellation of the dipole terms occurs, and the remaining term of highest magnitude is of linear quadrupole form. Field magnitudes here are reduced significantly, even near the string, and fall off more rapidly in moving away from the string. Table II of Section IV.B. provides calculated values of the partial derivatives of the components of contaminant field for variations in the string current and for balanced and offset single backwires. A representation in terms of partial derivatives with respect to string current is to allow the analysis to treat the likely condition that operation will proceed with variations present in the string currents (mirror properties and string polarities have been selected assuming identical currents in all strings). The calculations, made at a point on the central axis of the array for which magnetometer placement might be considered likely, revealed intolerably large values of contaminant field variation with respect to string current for the single offset backwire, even if utilized for those strings which are outermost at the array arms. For the single balanced backwire, contaminant fields (even those resulting after the complete failure of a string) are of sufficiently small magnitude that interference with interplanetary field measurements would not result. This condition is obtained for both the inboard and outboard locations on the array arms. A conclusion from these calculations is that balanced backwiring must be utilized if measurements of interplanetary magnetic fields are to be performed.

e. Backwire Granularity

For the cell stack utilized in the 30' array, the physical width of a string is approximately .4 meters. If a single backwire is used, then elements of the current flow may be separated as much as .2 meters from the oppositely directed current in the backwire. This separation, a, enters into the magnitude of the linear quadrupole term for contaminant field generation, as a^2. By increasing the number of backwires (reducing backwire granularity) the line current quadrupolar term diminishes, and, for particular

conditions detailed in Reference 2, may be made to vanish. The condition of a quadrupole null may be achieved by using no more than two backwires and proper spacing. The remaining higher order multipolar contributions are greatly reduced in magnitude, and use of the quadrupole null condition can lead to contaminant field level for a single string as low as 1 milligamma (10^{-8} gauss) at separation distances of the order of 1 meter. There would appear to be reason, then, for the use of such backwiring spacing. However, a suitable failure mode analysis must also be undertaken relative to the possible failure of one of the multiple backwires. If this should occur as an open circuit failure and if the failed backwire is offset with respect to the central line of the string, then the contaminant field generation reverts to that of line current dipoles whose magnitude, as previously noted, is not tolerable if ambient space field measurements are to be made. An appropriate systems analysis here must weigh the advantages of contaminant field reduction through multiple backwiring against the possible failure of a non-central wire with large resulting contaminant fields. A final consideration here is that, with multiple backwiring, the open circuit failure mode of a backwire does not result in the loss of power generated by the string.

f. Injection and Collection Busbars

The contaminant magnetic fields generated by the solar array also derive from the current flows in those busbars which collect and inject into the cells of the string and the backwire. This injection and collection may be "central" (at a point on the central line of the string) or it may be "offset" (other than central). If the injection is central, contaminant fields depend directly upon the square of the length of the injection busbar and inversely as the cube of the distance from the busbar to the point at which the field is evaluated. For an offset injection, the relevant behavior is as the first power of busbar length and with an inverse square dependence on separation distance. Since the distance from a field point to a busbar is, in general, very much larger than the length of the busbar, an offset injection produces contaminant fields at least an order of magnitude larger than central injection. The contaminant field level on the central axis of the entire array for an offset injection at the outermost strings of the array is comparable to or in excess of the interplanetary field and cannot be considered tolerable.

The use of central injection and collection on the strings produces a condition of contaminant field level which is acceptable for those outermost strings of the array. For those strings near the spacecraft, however, some further means of field reduction would appear to be necessary. Such reductions are obtained when the number of backwires is increased. References 2 and 3 provide detailed calculations for strings with 2 and 3 backwiring elements. These latter cases result in acceptably small contaminant fields for those regions of the spacecraft where magnetometer placement is likely.

From the analysis, the use of offset injection and collection does not provide sufficiently reduced contaminant fields. Central injection and collection and the use of multiple backwires does provide sufficient magnetic cleanliness for interplanetary field measurements. The use of multiple backwiring, however, involves other considerations, as discussed in the previous section, and an appropriate failure mode analysis for the case of an open circuit backwire must be performed in order to fully treat the use of multiple backwiring.

g. Solar Array Blanket Injection and Collection Busbars

For the 30'-roll-up array the currents from the various strings are brought together into the array blanket collection busbars. Since these busbars are located on the inboard edge of the array and near the possible locations for a magnetometer, their geometry and current flow patterns are of major importance. For the original configuration of these conductors[4], contaminant fields well in excess of the interplanetary magnetic fields will result even for separation distances from the busbars of several meters. A revised configuration for these elements is given in Reference 3. In the revised configuration mirror properties are utilized so that, for equal current in all strings, exact cancellation of contaminant field occurs along specific planes and axes of the overall array. The revised arrangement also forms the current paths into higher order multipoles, with the near placement of opposing multipolar structures. In this manner the essentially dipolar current structures present in the original design are restated in terms of opposing octupoles (of slightly different magnitude). The combination of mirror properties and use of higher multipoles provide for a condition in which contaminant fields diminish rapidly in moving away from the busbars.

From this result, acceptable levels of magnetic cleanliness may be realized at points near the body of the craft and at points for which magnetometer placement can be achieved with acceptable boom lengths.

2. Ion Engine Operation

a. Electron Bombardment Discharge

An electron bombardment ion engine has been utilized in the analysis, because of the considered likelihood of the use of this thruster for electrically propelled missions. For this thruster, three possible sources of contaminant field must be considered. The currents flowing in the electron bombardment discharge may create contaminant fields. Also the current flow from the discharge region to and into the plasma thrust beams may generate fields. Finally to be considered are the magnetic fields required to establish and sustain the electron bombardment discharge.

This section will consider the current flows in the electron bombardment discharge. Reference 5 has illustrated two conditions in this current flow pattern. The first is highly asymmetric and does produce a net magnetic moment and resultant contaminant fields. In the second condition, the discharge currents are symmetric about the axis of the thruster, and magnetic field lines are wholly contained within the discharge region. The highly asymmetric discharge condition cannot be considered likely and should such a condition occur, the spacecraft operation would be presented with a variety of problems ranging from loss of thruster effectiveness to realignment of the thrust vector from the ion source. The condition of a discharge which is essentially symmetric is the most likely condition. Surface conditions and the particular properties of elements of the discharge may, however, introduce some variations away from the perfectly symmetric discharge. Evaluation of possible contaminant field generation from such asymmetries would require appropriate systems tests with the actual thrusting device.

b. Bombardment Discharge to Neutralizer Currents

In the bombardment discharge, electrons are removed from the neutral propellant material. The ion-electron pairs formed in the discharge proceed eventually into the thrust beam. Their progress is, however,

along different paths and contaminant field generation may result from the physical separation of the negative and positive currents. Reference 5 illustrates conditions of an axially symmetric discharge with, however, an asymmetric current path from the discharge region to the thrust beam neutralizer. This condition creates contaminant fields which are not confined to the discharge region. In a second case, an axially symmetric current flow from the discharge region to the neutralizer is utilized. For this arrangement, magnetic field lines created by the current flow are wholly contained in the discharge region. The principal point of emphasis here is that containment of contaminant fields is possible through appropriate systems design.

c. Currents in the Neutralization Injection Region

In a neutralized thrust beam, the space charge density of ions and electrons must be everywhere equal. There is no requirement, however, for a point-by-point condition of equal current densities of the two species. In Section II.A.3., conditions of electron "streaming", which lead to contaminant fields will be discussed. This present section will be concerned with current flows from the neutralizer into regions near the injection point. Since it is unlikely that electrons will enter the beam from an axially symmetric neutralizer, but, rather that injection occurs from a single neutralizer, current flows in this region will not be such as to produce cancellation in the magnetic fields generated. If it is assumed that at some axial point the current densities of the two species are equal, then only the current flows from the face of the thruster to this axial point may create contaminant fields. If the beam current is I, the beam diameter D, and the distance from the thruster face to that point at which current density neutralization occurs is d, the maximum possible magnetic moment of the current flows is less than $\sim\frac{1}{2}\mu_o IdD(MKS)$. Evaluation of this dipole term for typical ion engine parameters and the assumption d=D leads to contaminant field levels of the order of $1\gamma(10^{-5}\text{gauss})$ at distances of 1 meter and with an inverse cubic dependence in the distance from the current flows to the field point. At separation distances of the order of 2 meters, measurements of the interplanetary field would not be affected by a current flow system as given here. It is important to note, however, that the present case rests on assumed values of distance along the plasma column until ion and electron current densities are everywhere equal. In practice, this condition may occur only at points very distantly

removed from the spacecraft. In the overall electrical equilibration of the spacecraft, the only requirement upon currents is that the algebraic sum of all currents leaving the craft sum to zero. Section II.A.3 will discuss a condition in the electrical equilibration of the thrust beam with the space plasma in which gross inequalities in the current densities occur with resultant contaminant field generation.

d. Ion Thruster Magnetic Field

In the operation of the electron bombardment discharge thruster, a magnetic field is required. If this field were to be supplied by an air-core solenoid, then regions within 50 meters of the thruster would possess contaminant fields which exceed the interplanetary field. Various means for the reduction of this field are discussed in Reference 5. Emphasis should not be directed toward the air core solenoid engine, however. While this form received extensive earlier use, more recently developed ion engines have utilized external flux concentraters and magnetic materials in the thruster proper which tend to contain the thruster field more effectively. Appropriate systems testing of the specific thruster design to be utilized on a spacecraft should be made to determine and correct contaminant fields to acceptable levels.

3. Thrust Beam Equilibration With The Space Plasma

Section II.A.2.c. has discussed a condition in which, over a comparatively localized region, inequalities in the current densities of ions and electrons occur and generate contaminant magnetic fields. Because of the limited physical extent of the flow system through which these inequalities exist, the magnitudes of the magnetic fields so generated are reduced to tolerable levels for relatively modest separation distances. If, however, the distances over which inequalities exist between ion and electron current densities are large, then the fields so generated fall off slowly in moving from the flow system and large separation distances may be required to realize acceptable low contaminant field levels.

Figure 4 of Reference 5 has illustrated several possible current flow systems in which contaminant fields result. One of these cases is that of particle drainage to the spacecraft and returning to the space plasma via

the thrust beam. This condition will be discussed further in II.A.4. Present emphasis will be placed upon possible circulating current loops between the thrust beam and the space plasma and the case of electron "streaming".

For the thrust beam equilibration with the space plasma, a required condition is that the total electron interchange must balanced. If a net outward diffusion of electrons from the thrust beam to the space plasma exists at one point, net inward diffusion must exist at another. Balanced interchange may occur, then, under a condition of circulating current loops. Such loops do generate magnetic fields. If, however, the current flow system possesses symmetry about the axis of the thrust beam, then the magnetic field lines so generated are wholly contained within the current flow system. Axial symmetry, in turn, is the most likely condition provided that the thrust beam itself is axially symmetric and if the space plasma merging with the thrust beam is axially symmetric. It may be noted that wake effects of the spacecraft may create conditions in which the space plasma in the near neighborhood of the thrust beam is no longer axially symmetric. The particular details of the spacecraft wake in the space plasma involve many factors beyond the scope of this discussion, however, and this discussion will merely note the general features of possible equilibration situations.

The existence of an axially symmetric current flow system in the thrust beam-space plasma equilibration will also depend upon the patterns of motion of freshly injected neutralizing electrons. If the electrons are injected with large energies and if the conditions in the bi-plasma equilibration allow the back diffusion of a colony of essentially stagnant electrons, then electron streaming is a likely condition. Reference 6 has treated at length factors which may contribute to a streaming situation and the present discussion will be restricted to the general behavior for this case. The freshly injected electrons move directly into the space plasma thereby providing an extended current flow situation of excess electron current density and at overall current levels of the magnitude of the ion engine current. The ions leaving the engine move through a stagnant colony of electrons. Here ion current density is finite and ordered and may generate magnetic fields. The stagnant electron colony has no net drift and generates no compensating fields. The net result of these several current flows are

contaminant magnetic fields which are large near the thrust beam and which fall off only slowly in moving away from the beam. For ampere level beams and a streaming condition, separation distances of as much as 20 meters may be required to attain acceptably low contaminant levels.

Appropriate measures to avoid conditions of streaming appear to be the operation of the neutralization system at comparatively modest injection potentials and the possible use of material structures to separate the two plasmas over the initial portion of the thrust beam flight path. This approach to "delayed" coupling may not be necessary in the case of the interplanetary plasma where coupling is already reduced because of the extremely low level of this ambient plasma.

4. Drainage Current To Solar Array

For an electrically propelled craft, a steady state drainage of electrons to exposed points on a positive solar array may be returned to the space plasma via the thrust beam. Figure 4 of Reference 5 illustrates such a current flow, and Figure 33 of Reference 6 also displays such a flow. In the latter case, the current flow pattern is rather arbitrarily drawn with the principal consideration being that the contaminant field energy density be calculable and allow the specification of a self inductance to the flow. The actual drainage of particles to an array or to a spacecraft will depend upon many factors that are beyond inclusion in this present study. Specific evaluation of drainage levels will proceed from testing of the actual system under plasma wind tunnel conditions set up to duplicate the ambient space plasma density.

Some estimate of allowable drainage levels may be made. If a total drainage current of 1 milliampere is in circulation about the spacecraft, then contaminant fields of .1γ would be present at distances of ~ 2 meters from the central axis of the craft (here assumed to also coincide with the thrust beam axis and with axial symmetry assumed in the current flow). Since the level of electron current diffusing to a plane in the interplanetary medium is of the order of 10^{-9} amperes/cm^2, a total drainage of 1 milliampere would require the capture of those electrons diffusing to an area of $\sim 10^6 cm^2$. This is approximately equal to the total area of the four arms of the 30'

roll-up array. Thus, a drainage condition in which all electrons diffusing to the general region of a solar array proceed to drainage points on the array would yield ~1 milliampere and for the array in the interplanetary region. (Much higher drainage levels are, of course, possible in the ionosphere with its comparatively dense plasma). Reference 7 and Reference 8 detail experimental studies in which drainages were observed, with particular concern for comparatively large positive array potentials. These studies are not immediately interpretable in terms of a generalized array with some specified number of drainage points and with some specified physical size. However, for array potentials sufficiently positive with respect to the plasma and for drainage points of sufficient physical extent and number, the collection of the bulk of electrons diffusing into the vicinity of the array is possible. In further evaluations of possible drainages, the principal factors will be array voltage, initial drainage point density and configuration, drainage point creation through micrometeorite impact, and drainage point growth through long term deterioration of the insulation material separating the array from the plasma. If the drainage should reach to the possible level of 1 milliampere for the interplanetary example given, then contaminant fields will be $\sim .2\gamma d^{-1}$ where d is the separation distance (in meters) from the spacecraft to the field point. Thus, at 2 meters from the craft, the contaminant field level is $\sim .1\gamma$.

B. Electrostatic Contamination

1. Thrust Beam-Space Plasma Equilibration

In this present section, attention will be restricted to the electrical interaction between the thrust beam and the space plasma. These two plasmas may interchange particles, and the steady state electrical equilibration will be one of balanced interchange. The neutralizing currents of electrons must equal the thrust ion current, and electrons diffusing across the boundary between the two plasmas must balance (net inward flow equal to net outward flow). Balance on a point-by-point basis is not required, but balance over larger regions of the boundary between the two plasmas will occur. (At some distant point along the axis of the thrust beam, the thrust beam density diminishes to the level of the ambient plasma. Electron diffusion properties for this region of the merging contour are somewhat indeterminate).

The conditions of balanced interchange, current neutralization, and the required potential difference between the neutralizer and the thrust beam in order to extract and transport the neutralizing current will determine a state of electrical equilibration. In this state, the potential of the neutralizer will be at some value relative to the potential of the space plasma. If the spacecraft is also at the neutralizer potential, then this same value of potential difference will exist between the spacecraft and the space plasma. If the potential difference is non-zero, then a state of electrostatic contamination exists and results of some scientific measurements may be affected. If the spacecraft and the space plasma are at identical potentials, then a state of electrostatic "cleanliness" exists. This is a desirable condition, particularly for low-energy charged particle energy and directionality measurements.

For a conventional passive spacecraft the properties of the electrical equilibration are determined by the interaction between the craft and the plasma. For an electrically propelled spacecraft, the bi-plasma equilibration is, in general, the dominant reaction, and spacecraft-space plasma interactions act as a perturbation to the basic equilibration between the thrust beam and the space plasma. This condition of relative magnitudes to the interactions will be assumed to exist and the basic equilibration state will be determined by the bi-plasma interaction. Section II.B.2. will consider the alteration of spacecraft equilibration potential as a result of particle interchange between the vehicle and the space plasma.

For the bi-plasma equilibration, two possible "end-point" conditions appear, and the actual equilibration state for a given thrust beam and space plasma may range from one to the other of these conditions. The first of these end point conditions is a state in which the injection potential is "recovered" in the thrust beam, and the second is a state of full electron "streaming". In the first case, the potential in the thrust beam in moving along the axis of the beam diminishes from its value at the beam origin and eventually reaches a level approximately that of the neutralizer before merging with the space plasma. The space plasma potential and the neutralizer are, then, at approximately the same potential, and the rise of potential in moving from the neutralizer to the thrust beam has been then "recovered". For a spacecraft at the neutralizer potential, the level of

electrostatic contamination is reduced, and, with appropriate further bias voltages, may be eliminated.

In the second end-point condition, the potential in the thrust beam has only minor variations in moving from the beam origin to the eventual merging with the space plasma. The neutralizer must be at a negative potential with respect to the thrust beam in order for the extraction and transport of neutralizing electrons to occur. The freshly injected electrons, however, are not confronted, after their entry into the thrust beam, with a potential structure that would tend to retain them within the beam, and, are allowed to stream directly into the space plasma. This direct streaming results in a contamination of the space plasma and in the generation of contaminant magnetic fields. Further, the neutralizer is now at a potential difference with respect to the space plasma of, essentially, the injection potential. If the spacecraft is at the same potential of the neutralizer a condition of substantial electrostatic contamination may exist.

The two states that have been outlined differ considerably in the manner in which the plasmas interact and a major question in analyzing a possible equilibration state is the extent, toward one end point or another, to which the interaction will proceed. A crucial factor here appears to be the possibility of the space plasma acting to back diffuse an essentially stagnant colony of cold electrons into the thrust beam. These electrons act to charge neutralize the ions in the thrust beam while the electrons from the neutralizer serve merely to current neutralize the thrust ion current.

Reference 5 has treated some of the general considerations that exist in the electrostatic equilibration. Reference 6 presents a much more detailed series of factors relative to this interaction. Both analyses and experiments have been conducted in order to gain some insight into possible space behavior. It should be emphasized that, because of limitations in the physical extent of ground testing facilities and because of uncertainties in the occurrence or importance of certain plasma phenomena, both experiments and analyses must serve primarily to give indications of what might occur in space. The actual determination of equilibration must proceed in situ.

While primary concern is for those conditions in which streaming may occur, with attendant electrostatic contamination, the behavior of the

thrust beam may be examined initially without regard for changes in behavior which result from the presence of another plasma. Such a restricted initial emphasis is meaningful if the circumstances under which the ambient plasma is later introduced can be so as not to alter the thrust beam behavior in any substantive manner.

For thrust beams neutralized with withdrawn hot wires and for injection potentials which are "moderate" (of the order of a few volts) the following properties have been generally obtained:

1) The electrons in the thrust beam possess a distribution which appears, from Langmuir probes, to be Maxwellian.

2) The value of kT_e for those electrons is proportionally related to the injection potential, which is the potential difference between the neutralizer and the thrust beam.

3) The dependence in the plasma column of ρ, V, T_e (plasma density, potential, and electron temperature) is essentially "barometric" (see Reference 6).

The occurrence of a Maxwellianized distribution is of interest. An interaction of electrons with the plasma based on conservative single particle interactions would predict electrons randomized in direction but possessing a single velocity magnitude at any given point in the plasma. The Maxwellianization may be the result of two aspects of the interaction: 1) L'iouville trapping in the plasma potential structure (which allows a prolonged period for collective interactions) and 2) collective interactions (possibly of the two electron stream form). A relationship between T_e and the injection energy of the electrons can be approximately determined using a conservative conversion of injection energy into electron temperature and electron potential energy in the plasma potential structure (here using the barometric relationship in ρ, V, T_e). Values of T_e from analyses are in best agreement with experimental results if attention is restricted in the equilibration to a comparatively short axial region of the beam.

The existence of barometric conditions in the plasma result in a potential structure which moves negative in potential by the magnitude of kT_e

for each downward e-folding in density. Thus in moving from the most dense portion of the plasma to very dilute portions of the plasma, considerable potential differences may result unless some limiting processes are involved. Some limiting process may be seen as necessary if steady state current flows exist. For example, if electrons leaving the neutralizer must eventually diffuse to and through outlying regions of very dilute plasma, and if the potential in these regions is negative with respect to the neutralizer, then an energy flow from some source to the electrons must exist. The ions in the flow possess large energies and, in principle, at least, a coupling of ion energy to electrons would allow the steady state flow of electron currents into regions at potentials negative with respect to the neutralizer. Using the barometric relationship without restriction for the case of SERT I's equilibration with the ionospheric plasma, and for the possible electron temperatures in the thrust beam, lead to a prediction of a positive vehicle potential with respect ot the space plasma. Such a conclusion was consistent with the experimentally observed signals from the spacecraft's rotating vane surface electric field meter. Energy flow to permit the neutralizing electrons to move from the neutralizer into a space plasma which is negative with respect to their source would be required. In the laboratory tests that have since been conducted, no definitive proof of such an energy flow has been obtained. In one series of experiments, potentials in the plasma have been negative with respect to the neutralizer by small amounts, but not by the larger amounts which obtain from the unqualified use of the barometric equation. In other cases, potentials in the plasma through the measured points remained positive with respect to the neutralizer. As a result of these experiments it must be concluded that any energy flow that may exist is of a limited nature and that the most likely condition is that potentials in the downstream regions of the plasma are, at best, at or near the neutralizer potential. This necessarily infers that spacecraft equilibration potentials with respect to the space plasma may be near zero or may be negative. Positive equilibration potentials appear unlikely and a proper review of the SERT I equilibration would focus upon the evidence supplied by the surface electric field meters.

There appear to be, then, limitations to the use of the barometric equation. Also of interest are apparent declines in the value of electron temperature in moving to more dilute regions of the plasma. Since

the potential increment in the plasma under barometric conditions is kT_e per e-folding in density, a diminishing temperature would lead to diminishing potential increments. In this manner, the use of the barometric equation would continue to be valid on a local basis and for a local value of T_e without necessarily leading to the generation of potentials which move negative with respect to the neutralizer. Utilizing this last possible condition a general pattern of thrust beam behavior may be formed for conditions of moderate injection potential. An injection of electrons provides these particles with an energy which is conservatively converted to both thermal and potential energy. Behavior of ρ, V, and T_e is consistent with a barometric condition and the local value of T_e. Declines in electron temperature for the bulk of those electrons present at a point in space occur in moving into more dilute regions of the plasma. Integration of the various potential increments from the most dense portion of the plasma into a dilute region produces potentials which, at best, recover the injection potential. The eventual potential of the thrust beam as it merges with a space plasma would be at or slightly positive with respect to the neutralizer.

This first analysis of the thrust beam behavior has neglected the possible alteration to that plasma which might result from the presence of an ambient plasma. Under certain circumstances this may be a justifiable approximation. In experiments described in Reference 6 a bi-plasma equilibration was examined in which, for balanced interchange, a "hot" thrust beam was in contact with a "cold" space plasma with little or no apparent alteration of properties away from that of the "hot" beam as a single plasma. Several factors may be of importance here. Among these are the density of the "cold" plasma, the total amount of contact area between the two plasmas and the axial position in the thrust beam at which the ambient plasma is first allowed to engage in equilibration (see experimental configuration, Reference 6). If the thrust beam has completed a reasonable fraction of the "recovery" process prior to engaging in equilibration with the ambient plasma, then the introduction of that second plasma may not result in a substantive alteration of the thrust beam. The interchange of electrons occurs at a potential which is approximately the neutralizer potential and hence there is no apparent reason for a substantial energy loss to occur as the beam electron interchanges with the space electron. Since beam electrons may be lower in temperature at these downstream points, the differences in temperature between beam and space is now reduced. A principal feature of

the interaction, then, may be whether the interchange results in a substantial net loss of electron injection energy. If it does not, then the beam-in-plasma retains the general features of the single beam.

While the experimental observation that a "hot" thrust beam remained essentially unchanged following the addition of a "cold" ambient plasma is a basis for the argument above that electron interchange need not effect the thrust beam, there are, at least qualitative arguments for conclusions directly opposite to this view. Reference 6 presents such a discussion. An initial configuration is assumed in which the beam electrons are energetic, and potential gradients in the thrust beam are at values determined by barometric conditions,density gradients and this electron temperature. The potential gradients act to recover the bulk of the injection potential so that the plasma potential in downstream regions approaches the value of the neutralizer potential. An interchange is then assumed in which the outgoing beam electron is more energetic than the inwardly diffusing space plasma electron. This net loss of energy results in a diminution in beam electron temperature and diminished values of potential gradients (through both reduced temperatures, and, because of reduced electron pressure, reduced beam divergence and subsequently reduced density gradients). The extent of the potential increment from the origin of the thrust beam diminishes because of reduced potential gradients. However, the potential increment from the neutralizer to the thrust beam in order to extract and transport the neutralizing current remains fixed, so that the neutralizer potential moves in a negative direction with respect to the space plasma. This, in turn, creates a circumstance in which the immediate escape of the thrust beam electron into space becomes more likely (reduced L'iouville trapping) and, upon escape and interchange an even larger kinetic energy difference exists between the beam and space electrons. The process that has been described feeds back upon itself in phase, and, would appear, thus, to be unstable in an intermediate state of equilibration. The final stable state would be that of a completely stagnant colony of back diffused space plasma electrons which charge neutralize the ion flow, and, whose low energies leads to comparatively modest potential increments between the thrust beam origin and the space plasma. The neutralizer potential relative to the space plasma would be negative and at essentially the value of the injection potential. Freshly injected electrons, confronted with only weak electric

fields in the thrust beam proper would escape directly to the space plasma, acting only as a current neutralization to the thrust ions. Electrostatic, magnetic, and space plasma contamination would be a resulting condition of this equilibration state.

The postulated interaction above and the earlier observations of stable interchange without major change in the thrust beam properties are contradictory and indicate the importance of other, as yet unspecified, processes. Two features of the interaction of interest here appear to be the availability of back diffusing electrons (strength of the coupling between the two plasmas) and the time of retention of those colder electrons which have back-diffused into the plasma column. Reference 6 describes experiments in which fast electrons were allowed to stream through stagnant or semi-stagnant electrons. Coupling of energy from the fast to the stagnant electrons was not observable which would indicate that a less energetic electron, back diffusing into the plasma column, would not be heated by more energetic streaming electrons and, hence, returned to the space. This would allow significant retention of a colder colony and allow streaming to space of freshly injected energetic electrons to persist. Build-up of a cold colony would, however, depend upon the number of space plasma electrons readily available. The escape of a fast electron without interchange does result in a positive movement of the spacecraft and thrust beam potential relative to the space plasma. If the space plasma is very dilute, the electric fields (and accompanying potentials) required to pull in a distant electron may be of such magnitude that this inwardly drawn electron eventually reaches energies comparable to that of the electron which escaped. Steady state equilibration could be set up then with substantial potential increments remaining in the thrust beam, and the recovery of the bulk of the injection potential would result.

Of the several conditions described thus far the following possibilities now may be made. In the dilute interplanetary space plasma, the availability of ambient electrons is at comparatively low levels. The quantity of these electrons which may be injected into the thrust beam near the thrust beam origin is not a current of comparable magnitude to the beam neutralization current. The thrust beam, then, undergoes an injection and thermalization of neutralizing electrons in essentially the same manner as

would be the case for the beam alone with no ambient plasma. Under these conditions, the injection potential is largely recovered within a short axial distance in the thrust beam. The thrust beam potential then remains near the neutralizer potential and merges eventually with the space plasma with a net potential difference from neutralizer to space plasma which is small compared to the injection potential. Conditions of electrostatic cleanliness on the spacecraft may be achieved with modest bias potentials between the neutralizer and the spacecraft.

For a thrust beam in the comparatively dense plasma of the ionosphere, much larger quantities of back diffusing electrons are available. If the contact between the two plasma is immediate, the interchange may occur before any recovery of injection potential has been realized and establishment of electron streaming conditons is likely. "Delayed coupling" (see Reference 6) could offset the effects of the ambient plasma on the beam by allowing the thrust plasma an opportunity to thermalize its neutralizing electrons, and recover its injection potential prior to beginning an interchange with the space plasma.

From a systems standpoint several recommendations may be made. The first of these is a reaffirmation on the limitation of allowed injection potential. Earlier discussions have set forth a figure of approximately 10 volts as an upper limit to neutralizer injection potential. That value is reaffirmed from the present analysis. The second recommendation is that appropriate field sensing instruments and appropriate bias systems be active in the spacecraft to detect that fraction of the injection potential which remains unrecovered and to correct accordingly to derive electrostatic cleanliness. For spacecraft in the dilute interplanetary plasma these two measures may be considered sufficient. For spacecraft operating in the ionospheric plasma an additional system element to "delay" the coupling between the two plasmas (see Reference6) would permit electrostatic cleanliness to be achieved with less reliance upon biasing voltages from the spacecraft to the thrust beam neutralizer.

2. Solar Panel and Spacecraft Drainage Current

The discussion of the previous section was restricted to the electrical equilibration between the thrust beam and space plasma. Since the

principal coupling in the spacecraft-thrust beam-space plasma system will generally be in the bi-plasma equilibration, a reasonable approach is to consider this interaction first, and to add the spacecraft-space plasma interaction as a qualifying element. The principal concern of the spacecraft-space plasma interaction is the particle current. If this current sums algebraically to zero then there will be no perturbation to the equilibration state between the thrust beam and the space plasma. If, however, a non-zero current exists to the spacecraft, then its return to the space plasma will affect the bi-plasma equilibration state. Assuming the perturbation to be small, an estimate of the shift in the equilibration potential is the product of the spacecraft current times the dynamic resistance from the spacecraft to the neutralizer, from the neutralizer to the thrust beam and from the thrust beam to the space plasma (see Reference 6). For example, if the zeroth order equilibration potential of the spacecraft is calculated using only the bi-plasma equilibration and relative potentials from the neutralizer to the spacecraft, and if V_{so} is the spacecraft potential relative to the space plasma in this zeroth order state, and if i_D is the drainage current to the spacecraft at V_{so}, then the change of spacecraft potential due to the drainage current is $i_D(R_{sc-n} + R_{n-tb} + R_{tb-sp})$ where the resistances are dynamic resistances. The dynamic resistance from the spacecraft to the neutralizer will very likely be of a conventional nature. The remaining dynamic resistances are more complicated and may be negative in value (see discussion, Reference 6). The principal concern in stable equilibration is that the ΣR given above have a net positive value. In order to minimize shifts in the equilibration potential due to shifts in the spacecraft drainage current, the value of ΣR should not be large. For example, if $\Sigma R = 10^3\Omega$, a shift in spacecraft drainage current of 1 milliampere leads to a 1 volt shift in spacecraft equilibration potential.

The drainage to the spacecraft may be directly to the craft and may also be to exposed points on the (assumed) solar array powering the craft. Since the array potentials may range upward to comparatively large voltages, the effective isolation of the array elements from the space plasma is a requirement if perturbations due to drainage currents are to be avoided. Factors in this electrostatic equilibration are discussed in Reference 7 and 8.

The discussion here has assumed that currents between the spacecraft and the space plasma are small in comparison to the currents of thrust ions and their accompanying neutralizing electrons. For a large spacecraft in a comparatively dense plasma, and for low level of current in the thrusting device, this condition may not obtain. Here the equilibration state may be determined primarily by the vehicle-space plasma interaction with the thrust beam-space plasma interaction acting as a perturbation. A discussion of the general case here is not possible in view of the many factors which may be of importance in the electrical interaction between the craft and the ambient plasma.

C. Space Plasma Contamination

1. Particle Interchange

The ion thruster releases both neutral and charged particles which move into regions around the spacecraft which vary with the type of particle release. Neutral particles which leave the thruster at large angles of divergence with respect to the thrust beam may intercept spacecraft surfaces depending upon craft configuration. Subsequent evaporation of the neutral from the spacecraft surface may release the particle into those regions of the craft at which particle detectors are placed. Similar considerations also apply to low energy charge exchange ions emerging at large angles with respect to the beam. Reference 5 discusses these processes and lists various treatments of these particle depositions. These forms of particle release do not appear to provide operational problems to the science payload, provided that appropriate systems design has minimized the initial interception and with proper placement of the science payload.

The thrust ions released into the space plasma move in essentially straight lines and do not constitute an area of concern for the science payload. Electrons moving from the thrust beam into the space plasma, however, are not necessarily on straight line trajectories. In the regions near the Earth the magnetic field causes these particles to execute essentially helical paths. For electrons of the order of electron volts in energy and with gauss-level magnetic fields, radii of curvature are small and the helix, in general, does not have points of interception on spacecraft surfaces unless those

surfaces are in the near neighborhood of the thruster. In the interplanetary space, field levels are reduced to the order of γ's, and radii of curvature for electrons released into the space plasma are in the range from meters to tens of meters. Under these conditions electrons released on one side of a spacecraft may move and intercept the opposite side (see Reference 5). In principle, then, an electron moving from a thrust beam into the space plasma may intercept surfaces of the spacecraft which are well removed from the thruster.

Reference 5 has discussed the interchange of electrons between the two plasmas, and, considering that this interchange need not be balanced on a point-by-point basis, has noted the possible advantages of a "local sink-distant source" condition. For such a condition, an imbalance in the interchange exists such that space plasma particles intercepting the thrust beam near the beam origin are absorbed, while the thrust beam retains its own electrons. For the overall interchange to be balanced, there must be points at which electron release from the beam exceeds the quantity of electrons entering. This "distant source" condition is of minor concern, however, in that the electrons so released are at remote points from the craft and have extremely low probabilities of diffusing back into the immediate neighborhood of the science payload.

While the local sink-distant source condition is desirable, the practical achievement is not apparent. In the injection region the thrust beam electrons are at their largest values of temperature and escape from the potential structure of the plasma column is possible, at least for the most energetic of these electrons. (It is assumed here that electron streaming has not occurred, and that the bulk of the injection potential has been recovered.) For electrons escaping into the space plasma it is not likely that the spectrum of energy or of directions is identical to that of the space plasma. The principal avenue of relief would appear to be in the maximum possible separation of any electron detection instruments from the thrust beam. This placement is beneficial even for a passive spacecraft in that it can provide some removal from surfaces which possess comparatively high fluxes of photo electrons from the solar UV. A second step, once the instrument location is assigned is a trajectory analysis. At the instrument location an energy and direction is assigned to an electron <u>leaving</u> the instrument. The trajectory

in the space plasma for this particle is calculated using possible values and directions of the interplanetary magnetic field. If the trajectory so calculated eventually intercepts the thrust beam (and without the interception at any material surface), then it is possible for an electron of this energy and mvoing in the reverse direction along this trajectory to leave the thrust beam and to proceed to the detector. If the electron detector possesses a very broad range of "look angles", then some trajectories may be possible paths between beam and detector. For more restricted look angles these possibilities diminish. Actual analysis is complicated and cannot be stated generally. Rather the analysis should be performed for a considered base condition of instrument placement, look angles, energy ranges and separation from the thrust beam.

A further consideration here relates to spacecraft moving to very large heliocentric distances. The drop off in the interplanetary field makes electron trajectories in the space plasma move with larger and larger radii of curvature and connection of the payload to the near regions of the thrust beam become even less likely.

Finally, attention should be paid to the condition of electrostatic cleanliness which is possible for electrically propelled craft with appropriate nulling bias potentials between the spacecraft and the neutralizer. These conditions have not been realized on previous passive spacecraft whose electrical equilibration in the interplanetary space is dominated by photo emission from the spacecraft under solar UV. These photo electrons also constitute a source of contamination to the space plasma. For the electrically propelled craft, operation without interference from these particles is possible and opens the way to a more rigorous examination of the electron properties of the interplanetary space than has been previously achieved.

2. Electron Content Measurements

The presence of a thrust beam exhausting into the space plasma may have an impact upon the measurement of the interplanetary electron content [9,10]. These measurements are performed by directing radio waves at a higher and lower frequency from the earth to a distant spacecraft. The variation in wave time-of-flight provides a measure of the intergrated electron density

along the flight path from transmitter to the spacecraft. If the flight path of the waves should traverse the thrust beam before reaching the spacecraft then two effects must be considered. The first of these is that an additional quantity of electrons is now encountered along the flight path. This effect, it develops, is of minor concern for presently considered levels of thrust beam. The second effect is the refraction and absorption of the waves as they move through the thrust plasma. For the lower of the two wave frequencies commonly used, both refraction and absorption effects will be of concern. Even comparatively small bendings of the wave front may cause signal loss if the receiving antenna is very narrowly directionally sensitive.

References 9 and 10 have treated the interaction of propagating waves with plasma thrust beams considering both absorption and refraction. These effects relate both to electron content measurements and to the transmission and reception links covering other spacecraft operations. In both areas loss of signal or data may occur if the transmission path should proceed through the more dense, upstream, regions of the thrust beam. Appropriate avenues of relief to avoid these perturbing effects are through craft orientation, receiver placement relative to the thrust beam, and thrust beam orientation relative to the transmission path from earth to spacecraft.

D. Electromagnetic Contamination

1. Thrust Beam-Space Plasma Equilibration

The release of a thrust beam into an ambient plasma creates a condition in which various particle species possess gross motion relative to other species and relative to the magnetic field in space. Reference 1 has reviewed several possible situations in regard to the generation of electromagnetic signals. Such wave generation would constitute a source of electromagnetic contamination which could impact upon the operation of wave detectors in the science payload. The discussion of Reference 1 concluded that such wave generation was conjectural. A subsequent review of wave generation in the bi-plasma equilibration cannot assess any liklihood to the occurrence of such contamination. Laboratory testing is not appropriate in this area because of the near presence of bounding material walls which would complicate and qualify any observed interaction.

Reference 5 has treated briefly certain aspects of electromagnetic contamination and has concluded that the principal area of concern for an interplanetary spacecraft would be for frequencies in the VLF range. The relevant geometry for possible VLF generation is the unbounded geometry in space. Recommended procedure here would be for in situ tests. VLF detectors are a recommended portion of a technology payload to observe whether such radiations are generated in the bi-plasma equilibration.

2. Electromagnetic Interference

In the section above, attention was restricted to the plasma interaction alone. However, electromagnetic interference of purely conventional nature may also occur. Reference 5 has presented a discussion of observed behavior on the SNAP-10A flight. Here the cycling of the high voltage supply to the ion thruster is believed to have created observed difficulties in spacecraft operation. The EMI detected in later ground based simulations was both radiated and conducted, and it was concluded that low frequency (below 1 MHz) conducted EMI was the cause of observed flight operational problems.

Reference 5 has stated that:"This flight evidence should not be considered as a general and unavoidable feature of electric thruster operation. Arcing during ion engine startup was observed on SERT I, but there was no apparent loss of data channels or inadvertent changes in spacecraft circuitry. The evidence does indicate some of the problems of thruster system integration into specific spacecraft, and points out an area for additional emphasis in system integration and testing".

III. SUMMARY

The operation of a solar-electric spacecraft has been studied relative to a possible impact upon the operation of the science payload. Magnetic, electrostatic, space plasma, and electromagnetic contamination levels from the operation of the electric thruster and the associated solar array have been analyzed.

The analysis of magnetic contamination from solar array operation has utilized the basic cell stack of the 30' roll-up array. The following recommendations have resulted:

1) Construction of the array should result in current flows with mirror-mirror configurations about the x = o and y = 0 planes (see Reference 2,3). This requires identical construction of all array blankets and "balanced" construction on each blanket.

2) Solar cell current flow direction should reverse between the inboard and corresponding outboard string of a solar array blanket.

3) Solar cell current flow direction should reverse between exterior (blanket edge) strings and interior strings.

4) Backwiring for the solar cells of a string should be balanced. Offset backwiring should not be utilized. Injection and collection of currents on a string should be central.

5) Multiple backwiring should be used for the various strings. Three backwire systems with spacing such as to produce a "quadrupole null" should be utilized. An engineering failure mode analysis should be made for the failure mode of an open circuit backwire condition.

6) Busbars collecting the string currents for a solar array blanket should be balanced on the blanket. Arrangements to produce opposing octupoles are recommended.

Following these various recommended procedures, the calculated contaminant fields are substantially reduced so that interplanetary magnetic field measurements may be performed without interference from the solar array provided that modest separation distances are present between the array and the magnetometer. Contaminant fields are also sufficiently reduced to levels where they do not constitute a perturbation to low energy charged particle directionality measurements.

Operation of the ion thruster results in a series of current flows which have been analyzed. Those currents in the thruster and in the ion generation to ion neutralization regions are capable of configuration so that contaminant fields are contained to the immediate region of the thruster. The central remaining problem of current flows which may produce contaminant fields are those current flows in the electrical equilibration of the thrust beam and

the space plasma. This interaction will also be a crucial element in the areas of electrostatic contamination and space plasma contamination.

The principal concern in the electrostatic equilibration is whether the freshly injected beam neutralizing electrons are retained in the thrust column for sufficiently prolonged dwell times or stream directly into the space plasma. If the thrust beam potential structure results in significant L'iouville trapping of the injected electron, then recovery of the bulk of the injection potential is likely. Thrust beam electrons will interchange with space plasma electrons but this interchange may occur over an extensive bounding area between the two plasmas. Significant loss of electron injection energy will not occur in the interchange. Interchange currents, because of their broad distribution in area will possess symmetry properties that result in the local containment of the magnetic fields generated by those currents. The retention of the neutralizing electrons for more prolonged periods before interchange, results in diminished near-spacecraft alterations in the electron properties of the space plasma. Magnetic contamination and space plasma contamination levels are at tolerable magnitudes provided that modest separation distances exist between the science payload and the thrust beam. Electrostatic cleanliness of the spacecraft may be achieved by modest bias potentials between the spacecraft and the thrust beam neutralizer.

If conditions obtain, however, in which electrons from the space plasma provide a stagnant or semi-stagnant neutralizing colony for the thrust ions, then the potential structure in the plasma column is no longer determined by the properties of the injected neutralizing electrons. If these freshly injected electrons are energetic, and if the back diffusing space plasma electrons are comparatively cold, then the electric fields in the thrust beam will not be sufficient to prevent direct streaming of a neutralizing electron from the neutralizer to space. The neutralizer electron current serves merely to current neutralize the ion thrust beam. Neutralizer potential relative to the thrust beam is that necessary to extract and conduct the neutralizing current to the beam. Since the potential increment from the thrust beam to the space plasma may be at a reduced level (cold stagnant electrons in the beam), the equilibration potential of the neutralizer relative to space is essentially the injection potential. Electrostatic contamination, magnetic contamination, and space plasma contamination levels are at significant levels.

From an experimental and analytical examination of factors in the electrostatic equilibration the area of principal concern is for "large" injection potentials for thrust beams immersed in comparatively dense ambient plasmas such as the ionosphere. Previous discussions of allowable injection potential have indicated an upper limit design figure of 10 volts. The findings of this program confirm that earlier figure. Neutralizer design should yield injection potentials less than 10 volts in magnitude. Further, if the thrust beam is immersed in an ionospheric plasma, the use of material structures may be advisable in order to delay the coupling between the thrust beam and the space plasma. The thrust beam in this protected axial region may entrap its electrons, build potential structures which recover the bulk of the injection potential and allow for equilibration between thrust beam electrons at lower energy levels in comparison with space plasma electrons. Actual use of such material structures to provide an initial isolation of the thrust beam will depend, of course, upon many factors relating to the configuration of the spacecraft.

For spacecraft operating in the interplanetary space, the dilute levels of that plasma and the consequent reduced level of coupling already provide the thrust beam with sufficient initial isolation. However, the overall neutralization system should still include a capability of variable bias potentials from neutralizer to spacecraft (and appropriate surface field sensing devices) to null any remaining potential difference between the spacecraft and the space plasma. Here, as before, an upper limit of 10 volts on the injection potential from neutralizer to thrust beam remains in effect.

Under the recommended limitations on injection potential and with the recommended systems for the completion of the nulling of the spacecraft equilibration potential, operation of the science payload will not be affected by the thruster operation. Even further, the condition of electrostatic cleanliness possible on electrically active spacecraft will allow low energy charged particle energy and directionality measurements under circumstances not previously achieved with conventional passive craft.

Electrically propelled spacecraft, because of their excursion capabilities, both in space and in time, provide many opportunities for scientific exploration. From the experiments and analysis conducted here, the operation of the electric thrusting units will be compatable with the operation of the science payload.

REFERENCES

1. "Study of Electric Spacecraft Plasmas and Field Interactions", Robert K. Cole, H. S. Ogawa, and J.M. Sellen, Jr., Final Report, Contract NAS 7-564, TRW 07677-6013-R000, 1 May 1968.

2. "Contaminant Magnetic Fields from Large Area Solar Arrays", J. M. Sellen, Jr. TRW 12738-6006-R000, 16 June 1969.

3. "Backwire and Busbar Placement for Magnetic Cleanliness on Large Area Solar Arrays", J. M. Sellen, Jr., TRW 12738-6007-R000, 30 June 1969.

4. "Feasibility Study -- 30 Watts per Pound Roll-Up Solar Array", NAS 7-100, General Electric Report 68 SD 4301, June 1968.

5. "Interaction of Spacecraft Science and Engineering Subsystems with Electric Propulsion Systems", J. M. Sellen, Jr., Presented at the 6th AIAA Annual Meeting and Technical Display, Anaheim, California, 20-24 October 1969. AIAA preprint 69-1106.

6. "Factors in the Electrostatic Equilibration Between a Plasma Thrust Beam and the Ambient Space Plasma", H.S. Ogawa, Robert K. Cole, and J.M. Sellen, Jr., Presented at the AIAA 8th Electric Propulsion Conference, Stanford California, 31 August - 2 September 1970. AIAA Preprint 70-1142.

7. "Operation of Solar Cell Arrays in Dilute Streaming Plasmas", Robert K. Cole, H. S. Ogawa, and J. M. Sellen, Jr., NASA CR 72376, TRW 09357-6006-R000, 15 March 1968.

8. "Operation of Solar Cell Arrays in Dilute Streaming Plasmas", Robert K. Cole, H. S. Ogawa, and J. M. Sellen, Jr., Presented at the AIAA 7th Electric Propulsion Conference, Williamsburg, Virginia, 3-5 March 1969, AIAA preprint 69-262. (NOTE: References 7 and 8 are similarly titled and authored and contain some common portions. Additional topics individual to each reference are present, however.)

9. "Plane Wave Refraction at the Boundary of a Plasma Thrust Beam", J. M. Sellen, Jr., TRW 9884-64-1, August 1969.

10. "Plasma Thrust Beam Total Electron Content and Possible Perturbations to Radio Propagation Measurements", J. M. Sellen, Jr., TRW 9884-64-3, September 1969.

SECTION IV.

TECHNICAL REPORTS AND PUBLISHED PAPERS

SECTION IV. A.

CONTAMINANT MAGNETIC FIELDS FROM LARGE AREA SOLAR ARRAYS

12738-6006-R000

CONTAMINANT MAGNETIC FIELDS FROM LARGE AREA SOLAR ARRAYS

J. M. Sellen, Jr.

H. S. Ogawa

Physical Research Center

TRW Systems

Redondo Beach, California

16 June 1969

CONTAMINANT MAGNETIC FIELDS FROM LARGE AREA SOLAR ARRAYS

J. M. Sellen, Jr. and H. S. Ogawa

I. INTRODUCTION

The flow of currents in the solar cell array providing spacecraft power may generate contaminant magnetic fields. For spacecraft engaged in the collection and interpretation of scientific data, and, in particular, for spacecraft determining the magnetic fields of interplanetary space, these contaminant fields must be reduced to acceptably small levels. Since ambient field levels in interplanetary regions are of the order of 1γ (10^{-5} gauss), required levels of magnetic cleanliness for spacecraft operation are of the order of tenths of gammas. By suitable back-wiring techniques in the solar cell array construction and by appropriate care in the design and location of electronic circuits, such levels of cleanliness have been achieved at the location of the spacecraft magnetometers for the Pioneer spacecraft.[1] Acceptable levels of magnetic cleanliness have also been achieved for the IMP and Mariner spacecraft.[2,3]

The successful determination of interplanetary magnetic fields by scientific spacecraft, thus far operating in the general region of 1 AU, does not indicate, per se, successful operation in the exploration of more distant interplanetary regions. Several factors are of concern for these advanced and vital missions. A principal consideration is the diminution of the interplanetary fields for greater heliocentric distances. At 5 AU, interplanetary fields are reduced to the order of tenths of gammas[4], with consequent required reductions in spacecraft contaminant field levels. Additional factors are introduced by the propulsive systems and power systems which such deep-space missions may require. Of particular interest here are electrically propelled spacecraft.[5,6,7] A variety of studies have demonstrated the desirability of final stage long term electrical propulsion of the spacecraft. The operation of such thrusting units requires the onboard generation of levels of power hitherto not realized by "conventional" vehicles. Estimated levels of required power generation are of the order of ten kilowatts during the initial portions of thrust unit operation. The power systems which supply the thrusting units, scientific measuring instruments, and required data handling and telemetry

circuits may be, in time, nuclear-electric. The near term means for such power generation appear more likely to be solar-electric. Of particular interest are the developing large scale roll-out and fold-out solar arrays.

From these considerations, an increased concern for possible contaminant magnetic fields from solar-electric spacecraft is required for the exploration and determination of deep space magnetic fields. It is therefore, the interest of this manuscript to investigate the contaminant fields generated from large scale solar cell arrays comensurate with the required power levels of solar-electric vehicles. The study will not consider a generalized cell stack, but, rather, will utilize, with minor modifications, the cell stack of the General Electric 30' roll-out array.[8] While specifications of the cell stack are not vital in the discussion of desirable symmetry properties of the array, the determination of contaminant fields away from the principal axis of the array and the resultant contaminant fields for conditions of failure in a module of the solar array do derive from specific details of the cell stack. The study will examine contaminant magnetic fields throughout regions of space comparable in size to the array under conditions of complete array operation (zero failure mode), and on the principal axis of the system for the failure mode of a single module, and will examine how each of these field conditions is affected by the "granularity" in the backwiring elements for the cell stack.

II. MIRROR PROPERTIES

A. General Consideations

The total array to be considered here consists of four "arms", each arm being capable of 2.5 kilowatts at 1 AU. Each arm is further divided into two "blankets", whose dimensions are here approximated to be 1.2 meters in width and 10 meters in length. A blanket possesses six "strings". A string consists of 19 solar cells in a parallel sub-module, with 242 sub-modules in series to form the string. The width of a string is .4 meter and the length is 5 meters. Total current in a string is $\sim$ 2 amperes, while string output voltage is $\sim$100 volts. The combined array, illustrated schematically in Figure 1, contains four arms, eight blankets, 48 strings. All strings are parallel connected to provide an array output of $\sim$100 amperes at $\sim$100 volts.

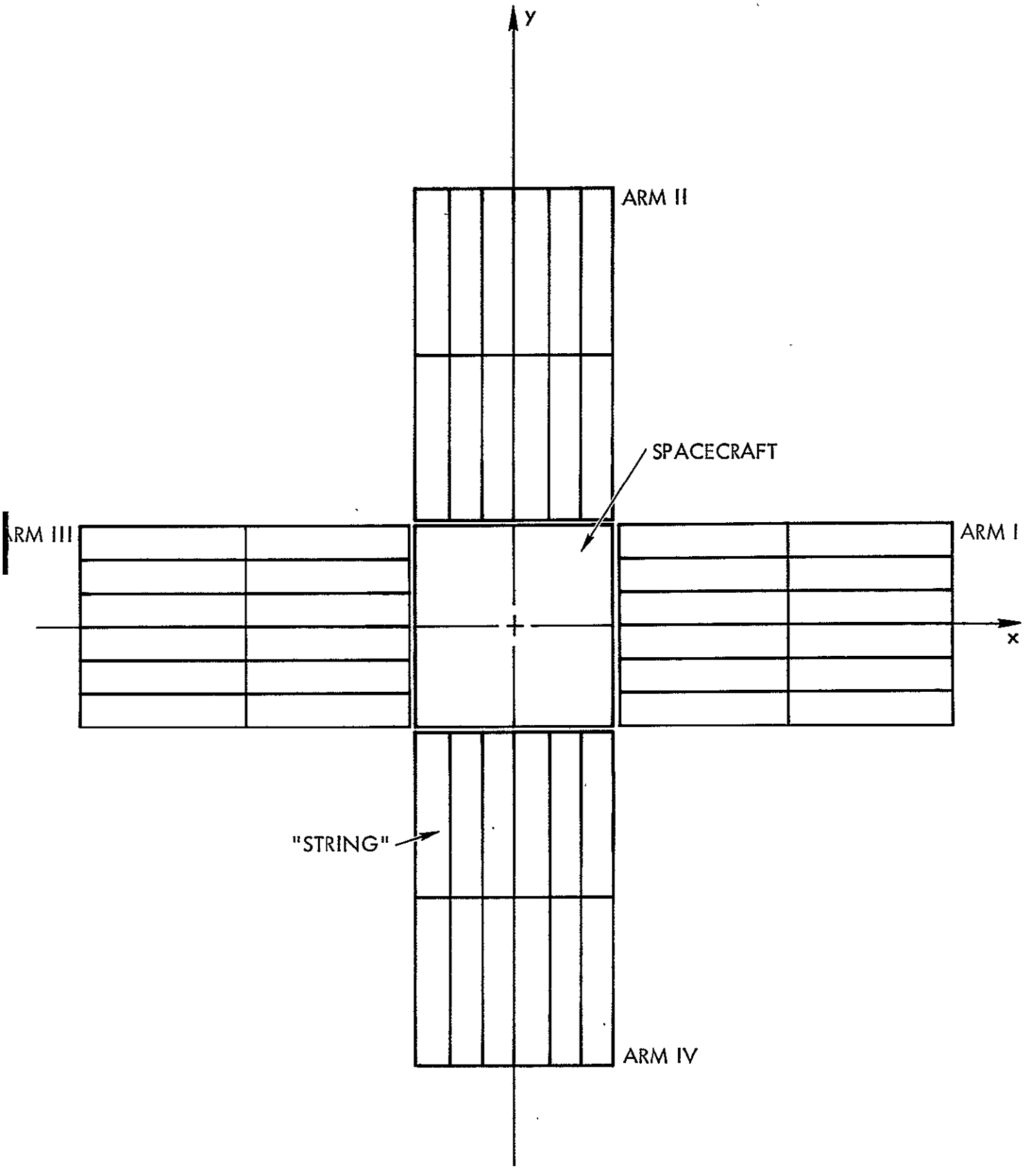

Figure 1. 10kw (1 AU) Spacecraft Solar Cell Panel Array

NOT TO SCALE

The principal concern in Section II will be the assignment of "polarity" to the strings comprising the array and the general properties of contaminant fields for certain configurations of polarity. It will be assumed that currents are identical in magnitude in all strings. It will also be assumed that the injection and collection of currents from a string is "central", rather than "offset" (See Section III C for further discussion of these features) and that backwiring elements are "balanced" (Section III B).

The assignment of polarity to the strings can establish certain "mirror" properties to the array, considered about various planes. The array currents are all contained in the plane $z = 0$, and mirror properties will be considered initially about the planes $y = 0$ and $x = 0$. Other planes, about which mirror properties may be established will be detailed.

B. Mirror Conditions: y = 0 plane

The discussion here will consider Arms II and IV of the total array. In the strings in these arms the currents in the solar cells and backwires are entirely in the y direction ("y-directed currents") while the currents in the injection and collection bus bars are "x-directed".

Consider first a condition in which y-directed currents are mirrored in the plane $y = 0$. This is illustrated in Fugure 2a. For this condition a current element $+\hat{j}\ I\ dl$ at (x, y) possesses an oppositely directed current element $-\hat{j}\ I\ dl$ at the mirror point $(x, -y)$. Here $\hat{i}$, $\hat{j}$, $\hat{k}$ are unit vectors in the indicated Cartesian system, and dl is the length of the current element. The magnetic field at a point (x_o, z_o) in the $y = 0$ plane is determined by a summation over all current elements, and, if mirror properties exist, then summation over pairs of elements, at mirror points, may be utilized.

$$\text{From } \vec{dB} = \frac{\mu_o}{4\pi} \frac{I\ \vec{dl} \times \vec{r}}{r^3} \qquad (1)\ (\text{MKS})$$

where $I\ \vec{dl}$ is the vector current element and $\vec{r}$ is vector from the current element to the field point, it may be seen that the reversal of the vector current at the mirror points leads to cancellation of magnetic fields in the x and z directions. Since y-directed currents cannot create magnetic fields in the y direction, all

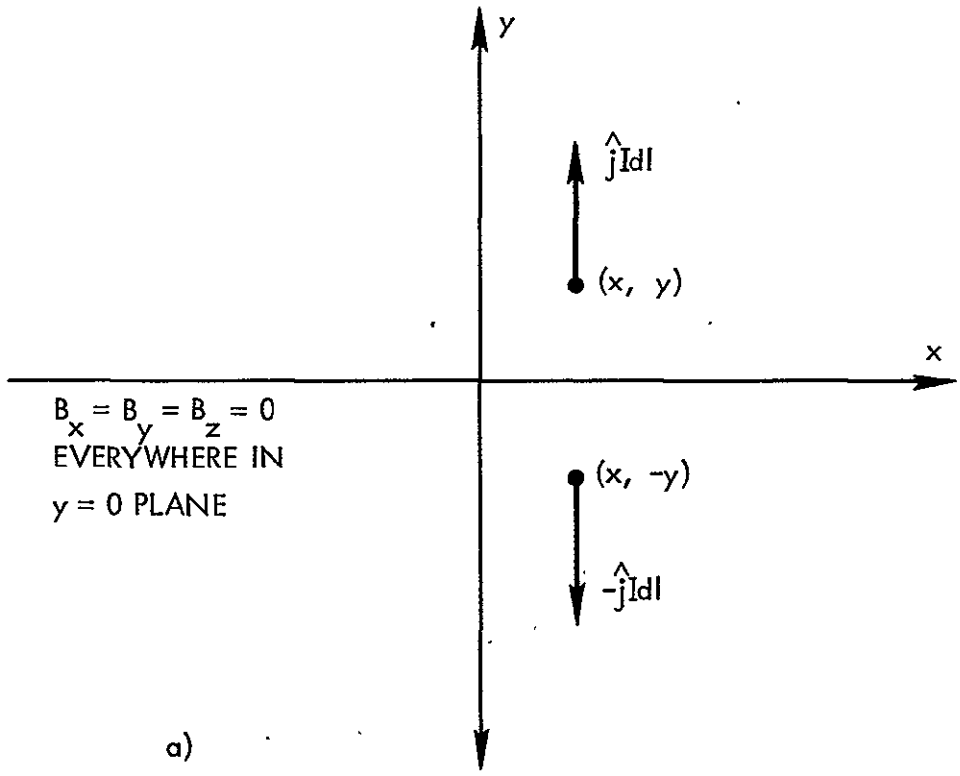

Figure 2a. Y-directed currents mirrored about the y = 0 plane. Contaminant B-fields vanish everywhere in the y = 0 plane.

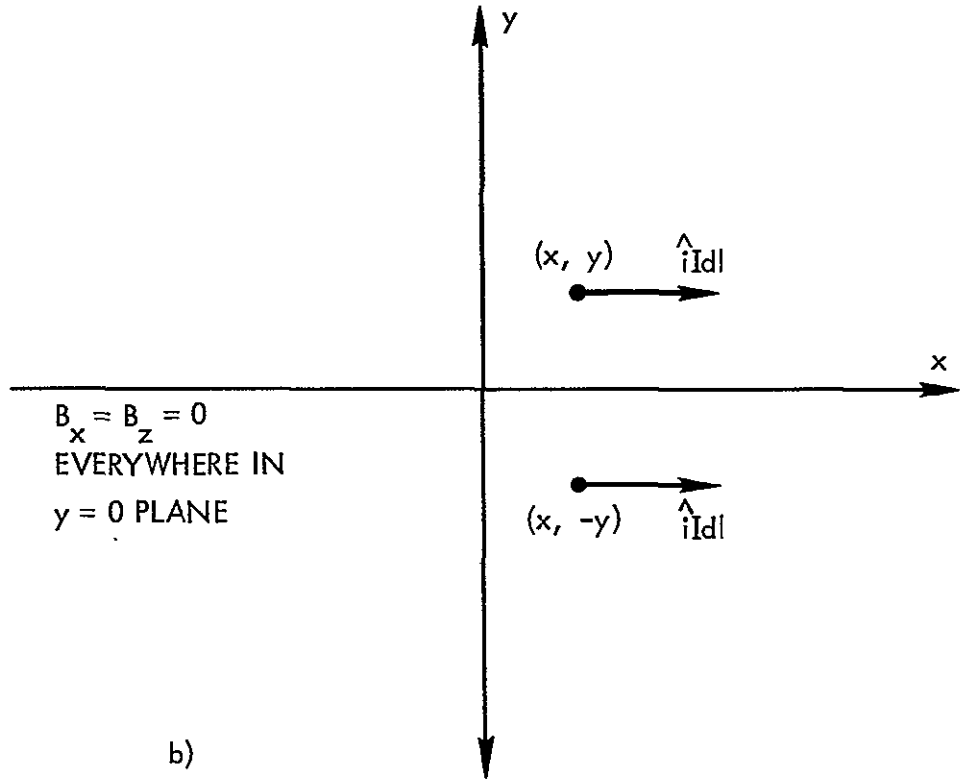

Figure 2b. X-directed currents mirrored about the y = 0 plane. $B_x = B_z = 0$ everywhere in the y = 0 plane. $B_y \neq 0$ in general.

ield components are, zero under this mirror condition. The extension of this mirror ondition to all y-directed currents in Arms I, III of the array leads to the esults:

> Mirror conditions of y-directed currents about the plane y = 0 yields $B_x = B_z = B_y = 0$ everywhere in the y = 0 plane.

t is important to note that the mirror condition does not require that all y-directed urrents be similarly directed, but merely that the y-current at (x, y) be oppositely irected to the y-current at (x,-y).

The mirror condition for x-directed currents about the plane y = 0 is illustrated in Figure 2b. If $\hat{i}$ I dl is a current element at (x, y), the mirror condition equires $\hat{i}$ I dl at (x, -y). From Equation 1 and summing over pairs of elements at irror points it follows:

> Mirror conditions of x-directed currents about the plane y = 0, lead to $B_x = B_z = 0$ everywhere in the y = 0 plane.

ıe field component B_y does not cancel in a summation by pairs of mirror elements. ancellation of B_y at certain locations in the y = 0 plane may occur if other mirror roperties exist about other planes. In general, however, $B_y \neq 0$ under this mirror ondition.

Since the present mirror condition for x-directed currents does not lead to ancellation of all components of B in the y = 0 plane, it is of interest to examine ı anti-mirror condition about this plane for x-directed currents. Examination here eveals that $B_x = B_y = 0$ in the y = 0 plane for this anti-mirror condition($\hat{i}$ I dl at x, y) and $-\hat{i}$ I dl at (x, -y). However, $B_z \neq 0$ in general in the y = 0 plane for ıe anti-mirror in x-directed currents. There would appear to be, no immediate dvantage to the anti-mirror condition relative to a mirror condition in x-directed urrents. However, it would appear that physical considerations in the construction of an actual array rule out the possibility of a mirror condition of y-irected currents and an anti-mirror condition of x-directed currents about the = 0 plane. It will be shown that similarly constructed blankets in Arms I and II lead to a mirror condition about the y = 0 plane for both x- and y-directed ırrents.

C. Mirror Conditions: x = 0 plane

The condition that y-directed currents mirror about the x = 0 plane is that $+\hat{j}\ I\ dl$ exists at (x, y) and $+\hat{j}\ I\ dl$ at (-x; y). This condition is illustrated in Figure 3a. By considerations similar to those of II.B it follows that:

> Mirror conditions of y-directed currents about the plane x = 0, lead to $B_y = B_z = 0$ everywhere in the x = 0 plane.

The summation over pairs of mirror elements here does not lead, in general, to cancellation of B_x.

The condition that x-directed currents mirror about the x = 0 plane is that $+\hat{i}\ I\ dl$ exists at (x, y) and $-\hat{i}\ I\ dl$ at (-x,y). This is illustrated in Figure 3b. It follows that:

> Mirror conditions of x-directed currents about the plane x = 0 lead to $B_x = B_y = B_z = 0$ everywhere in the x = 0 plane.

As before, if y-directed currents mirror in the x = 0 plane, then x-directed currents must also mirror in this plane from physical considerations in array construction. Note, however, that all currents may mirror in the y = 0 plane and anti-mirror in the x = 0 plane if this condition is desired. The choice of mirroring or anti-mirroring about y = 0 does not demand any specific mirror condition about the x = 0 plane.

D. Mirror Conditions: Both x = 0 and y = 0 planes

Figure 4a illustrates a mirror-mirror configuration in which x and y currents mirror about both y = 0 and x = 0. Figure 4b illustrates a mirror-anti-mirror configuration. As noted in II.C, either configuration is possible. An important factor, however, may be in the construction of the array. In Figure 4a all blankets are similarly constructed. Figure 4b would require the construction of two different blankets. Considerations of costs, both in construction of the primary array and in spare blanket units for the array would appear to favor the mirror-mirror configuration of Fig. 4a. Magnitudes of

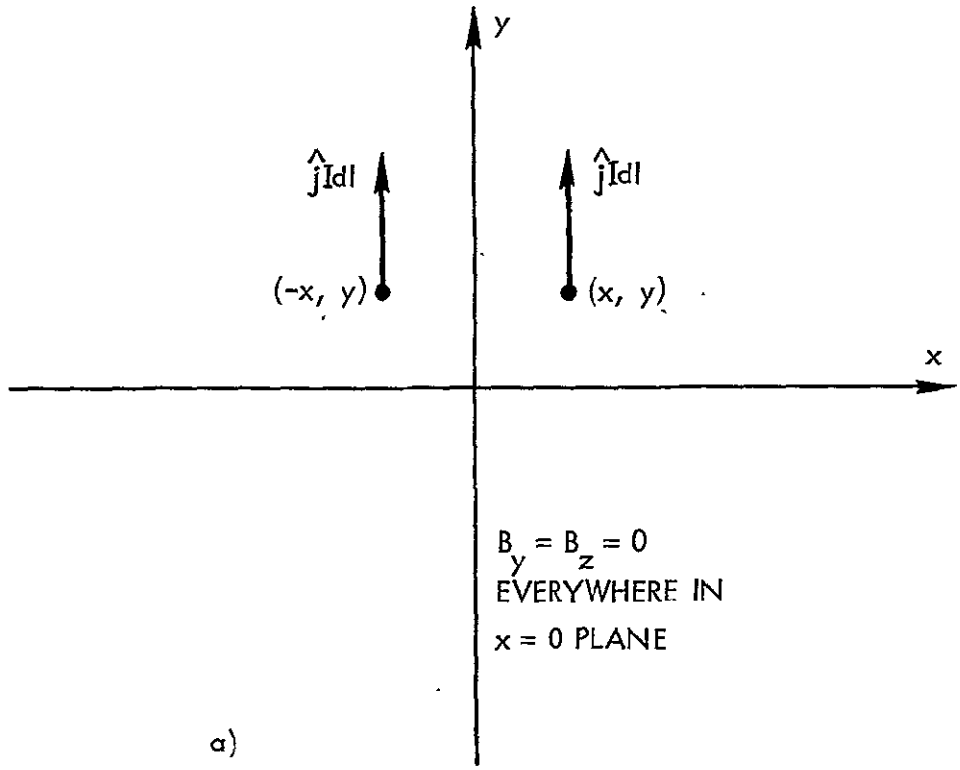

Figure 3a. Y-directed currents mirrored about the x = 0 plane. $B_y = B_z = 0$ everywhere in the x = 0 plane. $B_x \neq 0$ in general.

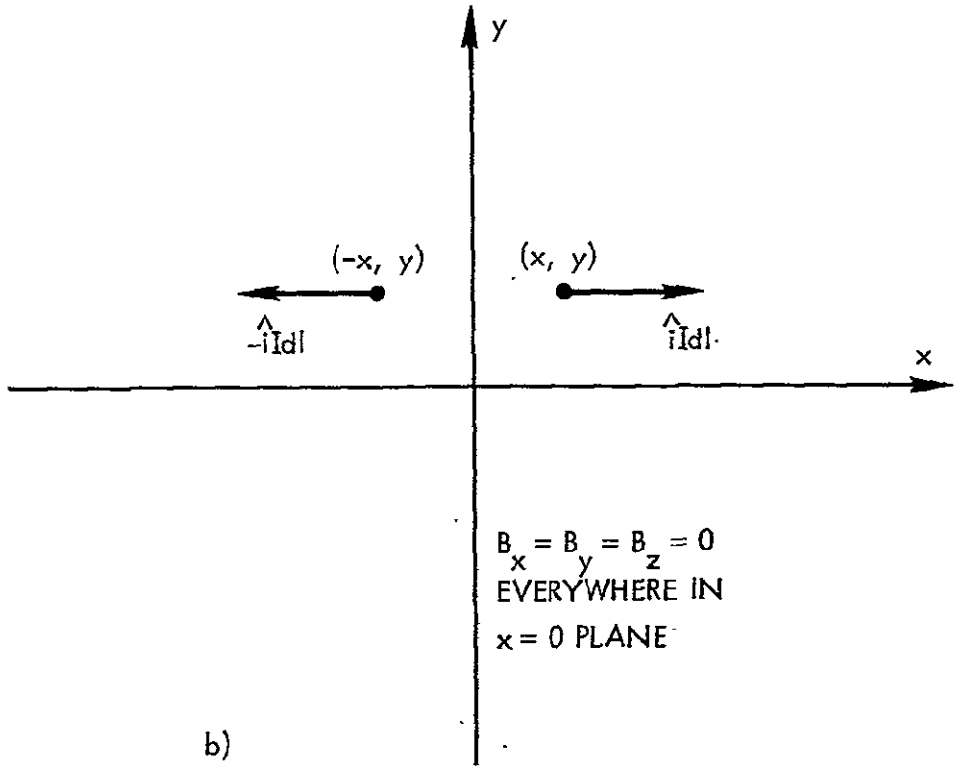

Figure 3b. X-directed currents mirrored about the x = 0 plane. $B_x = B_y = B_z = 0$ everywhere in the x = 0 plane.

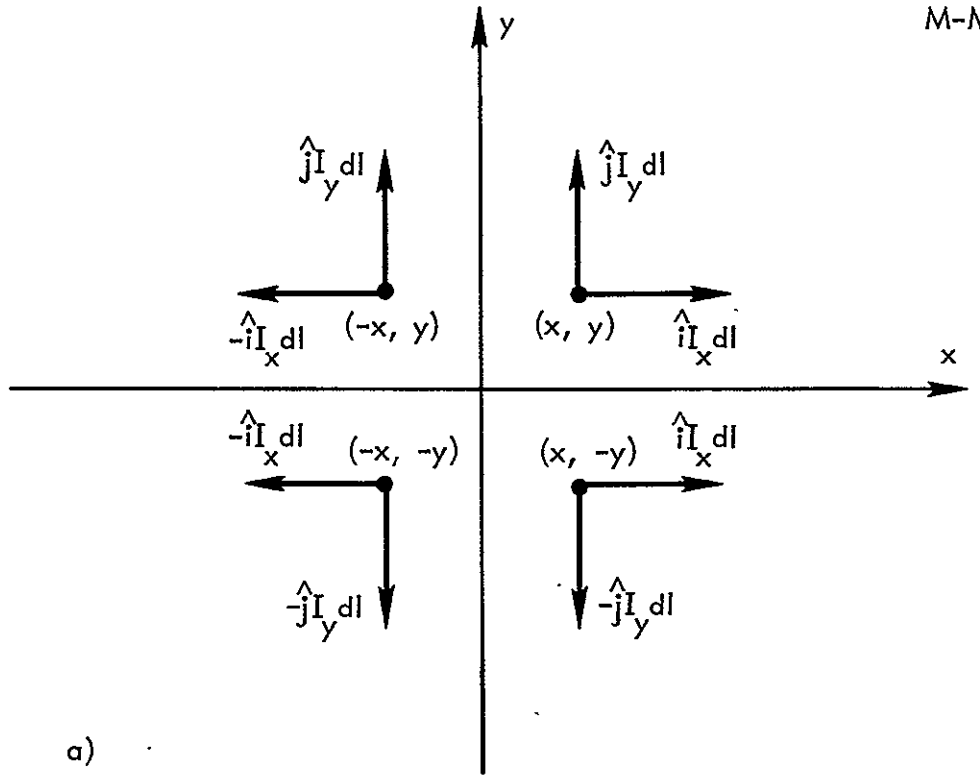

Figure 4a. Mirror-mirror configuration for which x and y-directed currents are both mirrored about x = 0 and y = 0.

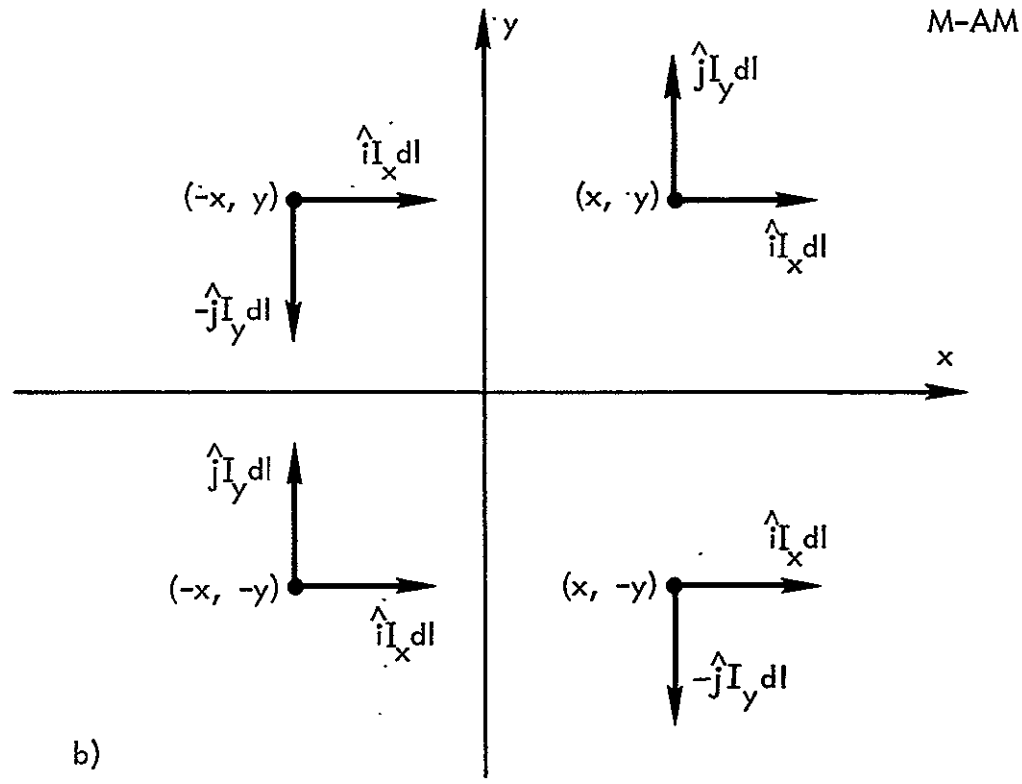

Figure 4b. Mirror-anti-mirror configuration for which x and y-directed currents are mirrored about y = 0 and anti-mirrored about x = 0.

perturbation magnetic fields away from the primary axis (x = y = 0) of the array are discussed in III.D for both mirror-mirror and mirror-anti-mirror configurations. Also treated are the magnitudes of contaminant fields for the failure mode of a single string for both mirror-mirror (MM) and mirror-anti-mirror (M-AM) conditions.

E. Additional Mirror Properties

The two arms of the solar array thus far considered contain some 12 "inboard" strings (adjacent to the spacecraft) and 12 "outboard" strings. The mirror properties of the array do not dictate any required polarity relationship between inboard and outboard strings. Figure 5a, b illustrate two arrangements of current, both of which are mirror-mirror configurations. (It should be noted that reversal of current in adjacent inboard strings has been utilized to the extent possible while still maintaining a mirror-mirror configuration. Such current reversal is not required by desired mirror properties, but simply by the obvious benefits in contaminant field reductions at points away from the central axis of the array.)

The first arrangement (5a) does possess additional mirror properties. The 12 strings in Arm II in Figure 5a possess a mirror-mirror property about the plane y = d + L, where d is the half-width of the spacecraft and L is the length of a string, and about the plane x = 0. Similarly, the strings in arm IV have a mirror-mirror configuration about the x = 0 and y = -d -L planes. Considering both arms, the mirror properties about y = ±(d + L) planes do not exist. However, the magnitude of the distance separating the center points of the two arms is such that perturbation fields from the one arm are insignificant at the center of the other arm. In effect, then, mirror-mirror conditions exist about the x = 0 plane and about the y = -(d + L), 0, and +(d + L) planes. This results in $B_x = B_z = 0$ everywhere in the three y-planes denoted, $B_y = B_z = 0$ everywhere in the x = 0 plane, $B_x = B_y = B_z = 0$ along the axis x = y = 0 and along the lines x = 0, y = ± (d + L).

The current configuration in Figure 5b is a mirror-mirror configuration about the x = 0 and y = 0 planes. However, all current effectively anti-mirror about the y = (d + L) plane and y = -(d + L) plane. This causes $B_x \neq 0$ and $B_z \neq 0$ in these planes. The general desirability of nulling B_z wherever possible (to provide more effective containment of the perturbation fields to zones near the solar array) would indicate that Figure 5b is not an optimum arrangement.

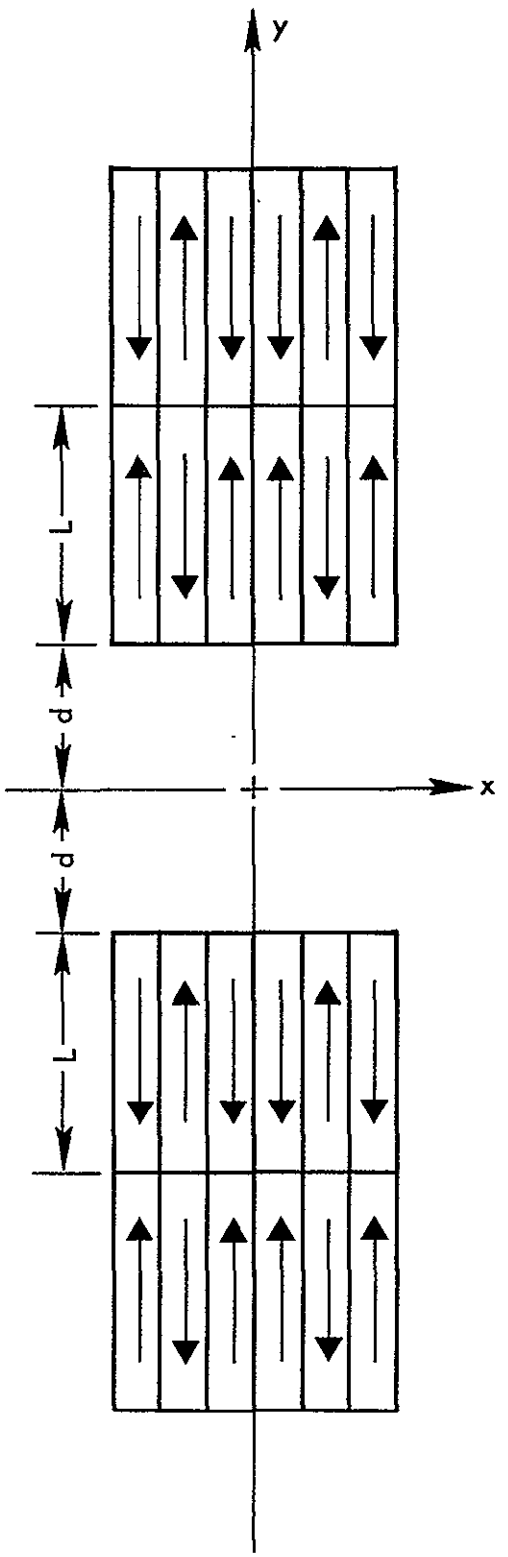

(a) M-M (x = 0 PLANE; y = 0 PLANE)
M-M (y = d + L PLANE; x = 0 PLANE)
M-M (y = - d - L PLANE; x = 0 PLANE)

Figure 5a. Mirror-mirror configuration for which the string currents reverse from adjacent strings and mirror about the x = 0, y = 0, ± (d + L) planes.

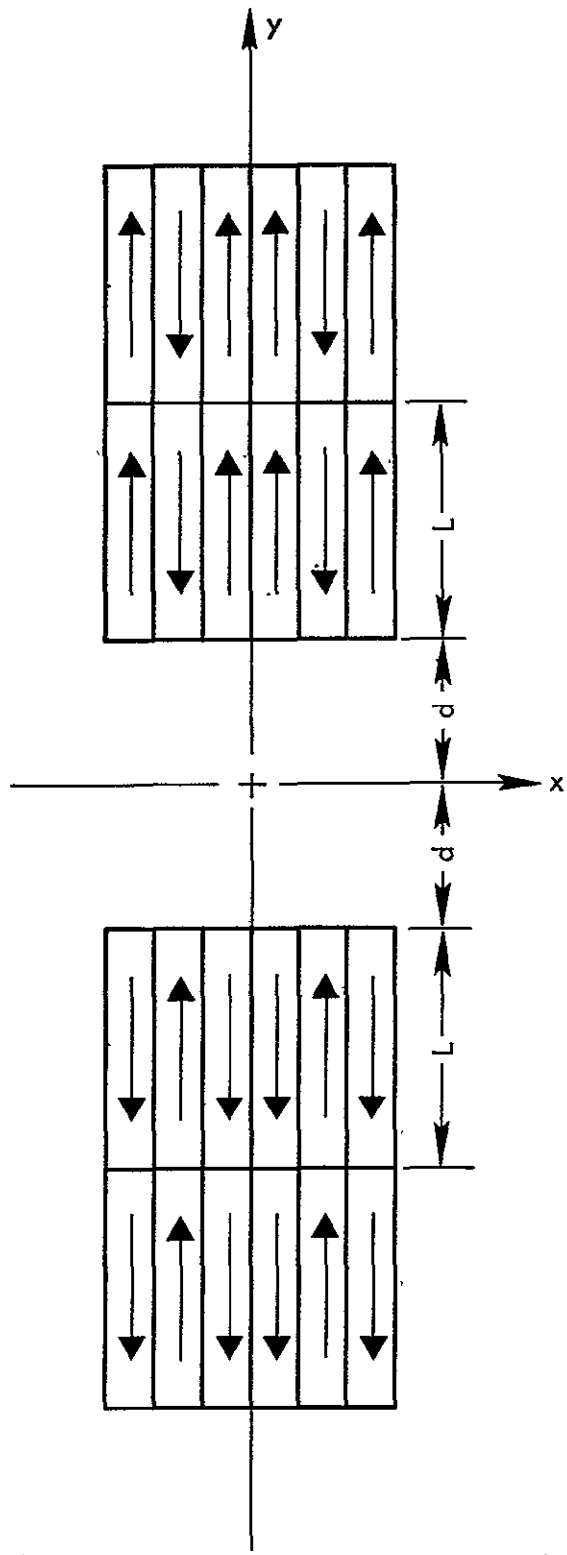

(b) M-M (x = 0 PLANE; y = 0 PLANE)
AM-M (y = d + L PLANE; x = 0 PLANE)
AM-M (y = - d - L PLANE; x = 0 PLANE)

Figure 5b. Mirror-mirror configuration for which the string currents mirror about the x = y = 0 planes and anti-mirror about the y = ± (d + L) planes.

F. Additional Arms to Solar Array

The total array consists of four arms. Arms II and IV have their principal dimensions along the y-axis, while Arms I and III have their principal dimensions along the x-axis. Factors of cost in construction of the array would indicate some desirability in having similar construction in all blankets. If this arrangement is utilized then, additional mirror properties are obtained. Figure 6 illustrates the complete array, four arms, eight blankets, 48 strings. The array has a mirror-mirror configuration about the planes $x = 0$, $y = 0$, $x = y$, and $x = -y$. Effective mirror-mirror configurations are obtained about the $y = \pm(d + L)$ and $x = \pm (d + L)$ planes. B_z vanishes rigorously in the first four planes and, for practical purposes, in the remaining four. Figure 6 illustrates the planes in which B_z vanishes and indicates the polarity of B_z in regions of non-zero field. Also indicated are the lines along which all field components vanish.

A final property of the system illustrated in Figure 6 is that contaminant fields in B_x, B_y at a plane in which B_z vanishes are such as to be perpendicular to that specific plane. Field directions are indicated in Figure 6. Note that $B_x = B_y = 0$ throughout the $z = 0$ plane so that indicated field directions are valid only for non-zero z.

G. Overall Field Magnitudes

The emphasis in this section has been directed toward specific benefits which derive from systems of varying mirror properties. If the system mirrors both x- and y-directed currents about the $x = 0$ and $y = 0$ planes, then one field component, B_z, vanishes throughout some eight planes, along the central axis of the system and along the separate "central" axes of each of the four arms. Also, B_x and B_y vanish along the central axis of total array. These features are desirable in that a specific location then does exist for the location of magnetometers and in this location contaminant fields are, in principle, zero. In practice, the currents flowing in the strings will not be precisely equal and net contaminant fields will result at points in space for which the zero-failure mode perfectly balanced currents indicate a rigorously zero field.

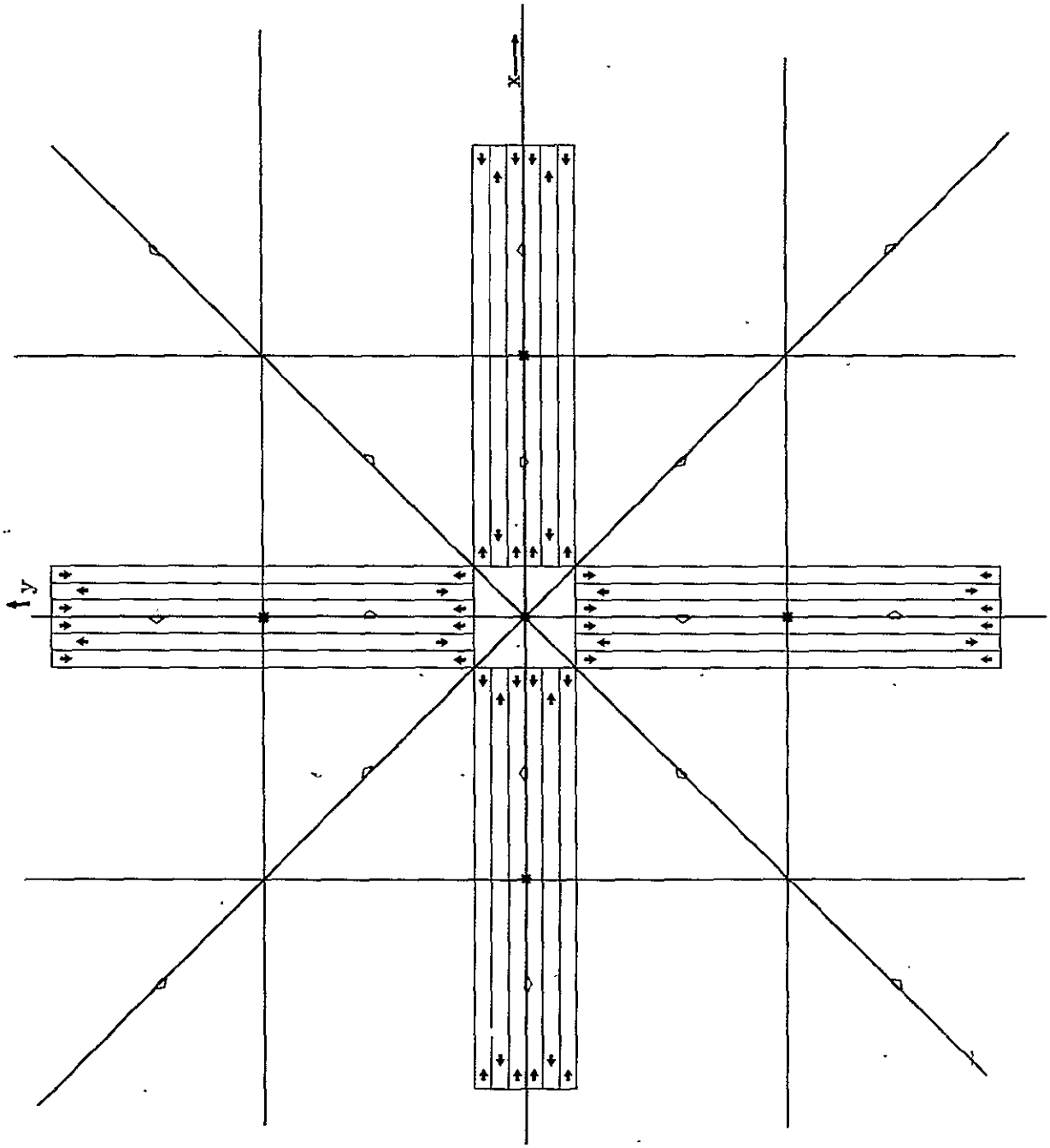

Figure 6. Solar array indicating string currents mirroring about x = 0, y = 0, x = y, and x = -y planes. $B_z = 0$ in these planes, and, y = ±(L+d) and x = ±(L+d) planes. All field components vanish on central axis of array and on central axes (*) of each arm. B_x and B_y vanish throughout z = 0 plane. Field directions at x = 0, y = 0, x = y, and x = -y planes indicated by open arrows (field does <u>not</u> connect from arrow to arrow but circulates through z = 0 plane).

The magnitude of contaminant fields for possible failure modes, or for imbalances in the current and the magnitude of contaminant fields away from the central axis for even the perfectly balanced array will depend not only on mirror properties, but also on use of, wherever possible, reverses in "polarity" between neighboring strings. Some reversals in polarity have already been utilized (Figure 5a) to provide obvious benefits in contaminant field cancellation. The following section will evaluate contaminant fields under conditions in which a single string has complete loss of current, all other strings operating at normal (and equal) currents. Since contaminant fields can result in the alteration of direction for charged particles traversing the region, a desirable condition is one that minimizes such fields over a region of as yet unspecified size centered, probably, on the central axis of the array. In this manner, particle detection apparatus located on the central axis would experience minimum perturbations to measured particle properties from contaminant fields.

III. CONTAMINANT FIELD MAGNITUDES

A. General Considerations

The discussion of the previous section has shown, by utilizing particular mirror properties in the overall solar array current flow, that magnetic fields vanish exactly along the central axis of the system and, for practical purposes, vanish along the separate central axes of the separate arms. In principle, a magnetometer located on the central axis of the array would have a zero level contaminant field regardless of the level of current flow in the array or of the granularity in the backwiring. The sole requirement for zero contaminant field is the maintenance of mirror properties. Several considerations impose further requirements on the current flow system if acceptably low contaminant fields are to be realized.

A first of these considerations is present even if a perfectly mirrored current flow system could be maintained. Strict cancellation of the fields occurs only along selected lines. For regions away from these axes, non-cancellation obtains and contaminant field levels are dependent on current flow magnitudes and upon backwiring granularity. The contaminant field level in these regions is of

concern to magnetometers, since magnetometer placement on a specific axis may not be consistent with other system demands and since physically realizable magnetometers are not lines but, rather, extend over finite spatial volumes. "Off axis" contaminant fields are of concern to charged particle detection devices since particles arriving at the magnetometer must traverse off axis regions and may acquire measurable changes in their direction during such traversals.

A second consideration obtains from the possibility of "failure modes" which are not of sufficient magnitude to terminate vehicle operation, but might impose perturbations upon active experiments. The partial loss of current in a string of the solar array may not be significant in terms of array output power, but may create serious contaminant fields, since the current loss does violate the mirror conditions considered for a perfectly operating array.

A final area of concern for contaminant field growth is under conditions of completely uniform current flow in the array strings, but with physical relocation of the array arms. Such physical perturbations also lead obviously to the loss of mirror properties.

The calculations of contaminant fields will be detailed in the following sections. Perturbations due to complete current loss in a single string will be evaluated and off axis fields for equal current flows in all strings will be computed. The magnitude of these fields will be examined as functions of the granularity in the backwiring. Perturbation fields due to physical relocation of array arms have been noted, but will not be further detailed.

B. Contaminant Fields from a Single String of the Solar Array Including Backwire Currents

The currents in a string are composed of those which flow through the solar cells, that which flows in the backwire, and those which are in the injection and collection bus bars. These injection and collection currents are considered in III.C. This present discussion will consider fields generated by the currents in the cells and in the backwire, here assumed to be "balanced" (centrally located). A sketch of these currents is given in Figure 7. The choice indicated there, is a string from Arm II (or IV) of the overall array. The x', y,'z' axes are a translation from the x, y axes utilized in Figures 1 - 6.

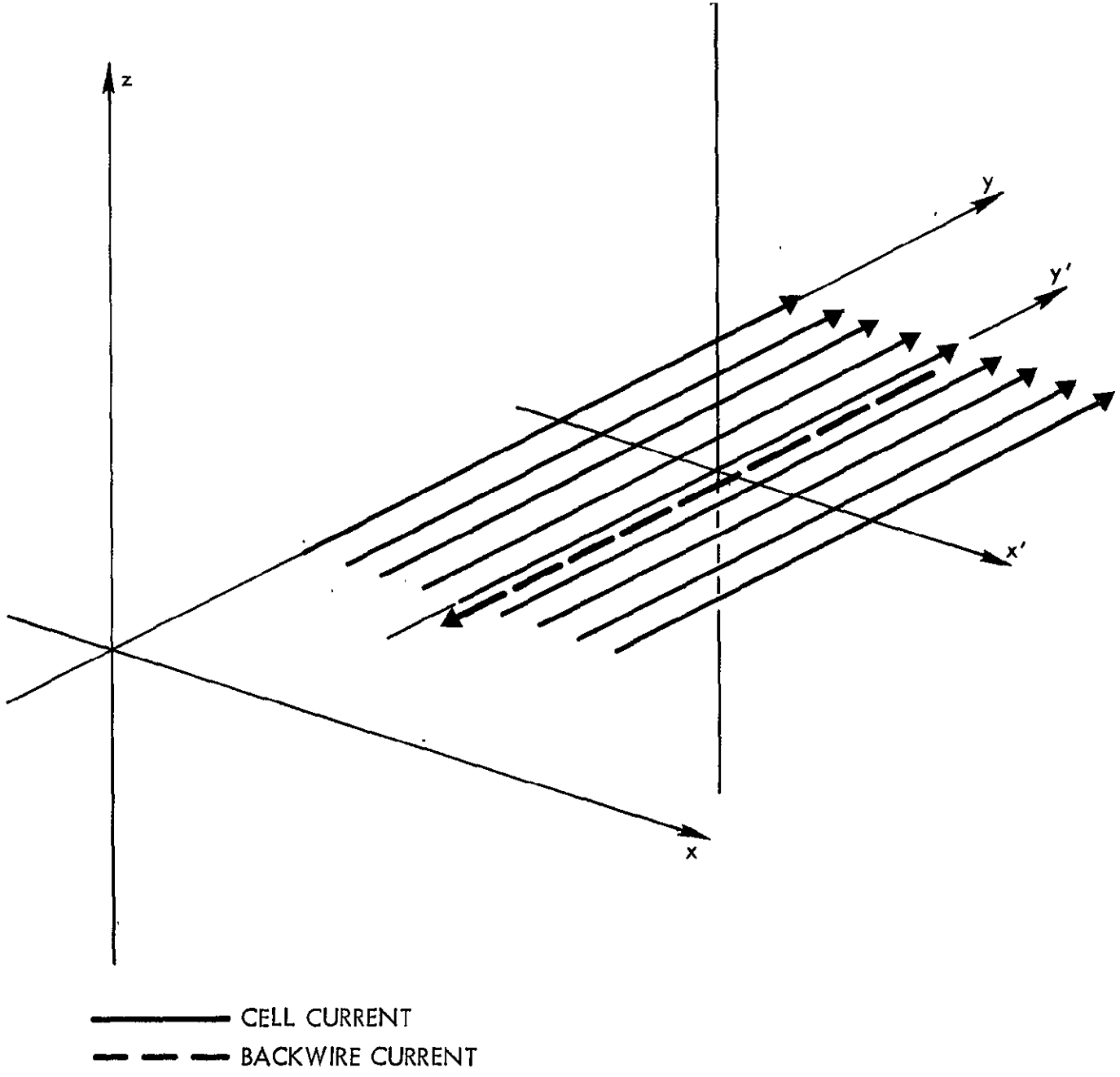

Figure 7. Solar cell currents for a single string and a single balanced backwire. Also shown are the x′, y′, z′ coordinates used in B-field calculations of the finite line current string.

Some general properties of the field from these currents may be stated. Figure 8a displaces a series of infinite line currents in a system of cylindrical coordinates. These currents may be viewed as a sum of line current quadrupoles. The field from one such quadrupole, Figure 8b, of spacing $\underline{a}$ and at points $r >> a$ is given by

$$B_r = \frac{\mu_o I a^2 \sin 2\alpha}{\pi r^3} \qquad (2)$$

QUADRUPOLE

and

$$B_\alpha = \frac{-\mu_o I a^2 \cos 2\alpha}{r^3} \qquad (3)$$

The angular dependence of B_r and B_α is essentially quadrupolar. However, the dependence on a and r is only as a^2/r^3 which is an essentially dipolar drop-off form. This results from the infinite extent of the line current. For finite lengths of the currents, the dependence a^2/r^3 will be preserved until $r \sim L/2$, the half-length of the current elements. Since the current elements in a string are separated by, at most, o.4 meters ($\underline{a}$ = 0.2 meters) and since L/2 = 2.5 meters, it follows that for a substantial region around a string that B_r, B_α are given with reasonable accuracy by (2) and (3) for a given linear current quadrupole. The field from the summation over all quadrupoles results in some "effective" value to the a^2 term in Equation (2) and Equation (3). The general form of the magnetic field in the plane perpendicular to the line currents is illustrated in Figure 8c.

Two properties of the fields from a single string (including backwiring) may be discussed in terms of systems of infinite line currents. The first property relates to backwire placement. If the backwire is "offset", as illustrated in Figure 9a, then the system of currents becomes a collection of line current dipoles. The field from one such dipole, Figure 9b, of spacing $\underline{a}$ and at points $r >> a$ is given by

Figure 8a. Series of infinite line currents with a single balanced return current.

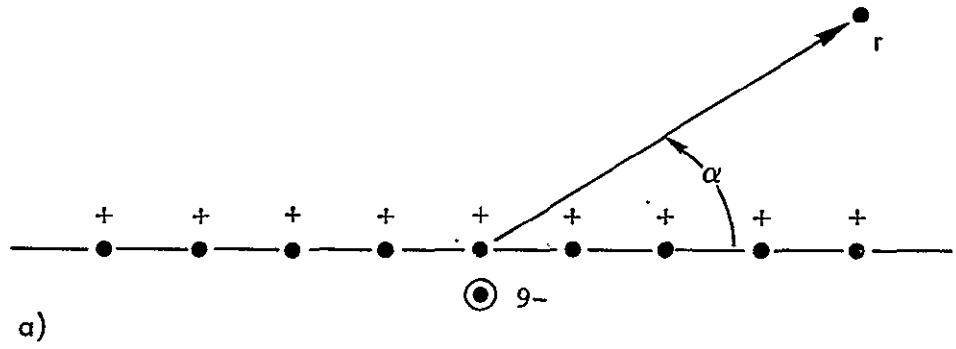

a)

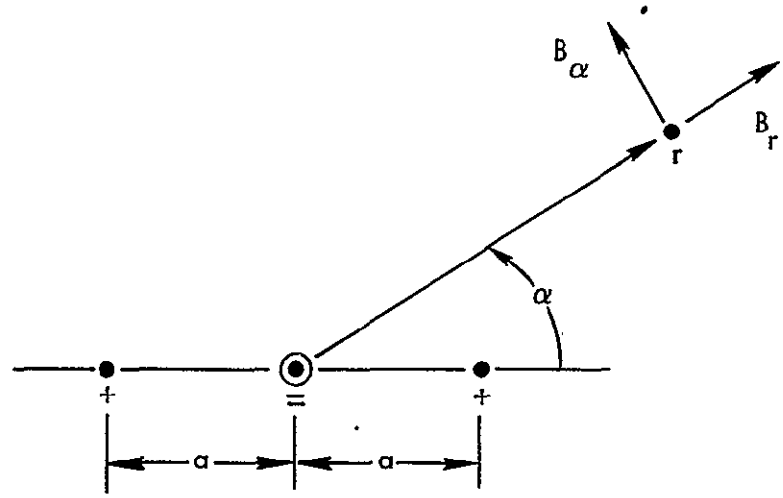

b)

Figure 8b. Line current quadrupole with spacing a.

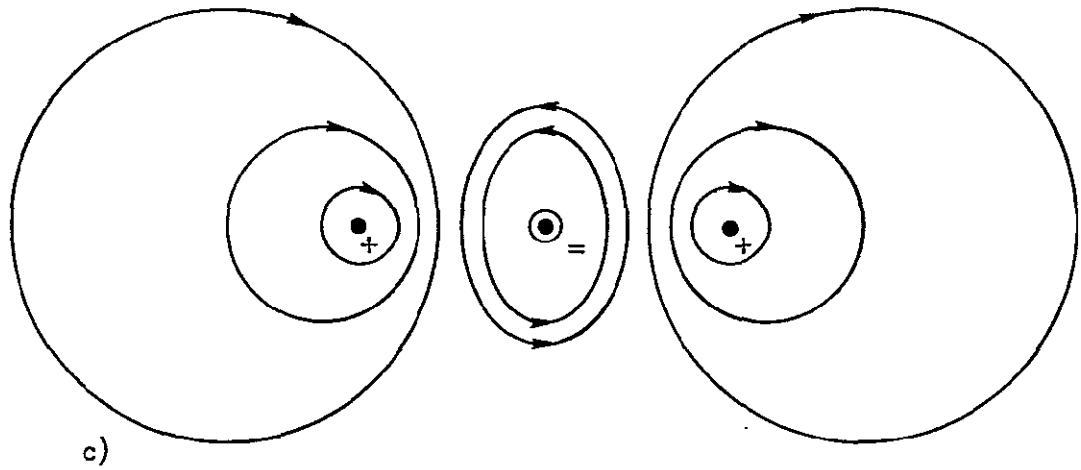

c)

Figure 8c. General form of the magnetic field produced by a line current

+ INTO PAPER
– OUT OF PAPER
• CELL CURRENT
⊙ BACKWIRE CURRENT

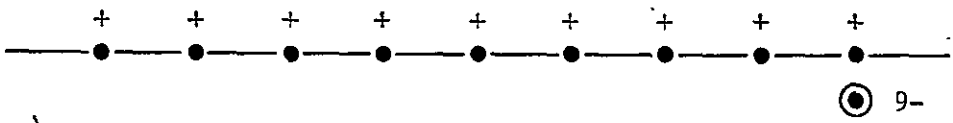

a)

Figure 9a. Series of infinite line currents with a single "off-set" return current.

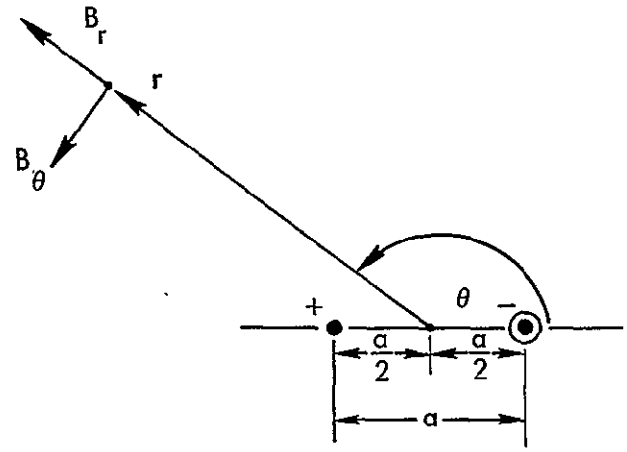

b)

Figure 9b . Line current dipole with spacing a.

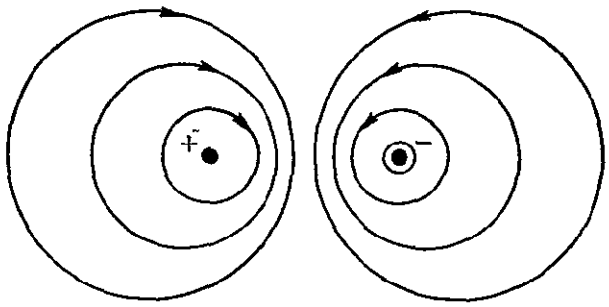

c)

Figure 9c. General form of magnetic field produced by line current dipole.

+ INTO PAPER
− OUT OF PAPER
● CELL CURRENT
⊙ BACKWIRE CURRENT

$$B_r = \frac{\mu_o I a \sin\theta}{2\pi r^2} \qquad (4)$$

and DIPOLE

$$B_\theta = \frac{-\mu_o I a \cos\theta}{2\pi r^2} \qquad (5)$$

The dipolar fields sketched in Figure 9c differ from the quadrupolar fields in Equation (2) and (3) both in the angular dependence and in the dependence on a and r. Since a << r, the additional power of a/r in the quadrupolar fields {(2), (3)} results in a great reduction in the magnitude of the magnetic fields when compared to the fields in Equation (4), (5). From this it follows that reduction of contaminant fields is markedly aided through the use of balanced backwiring circuits.

A second property of fields from the string and backwire (or backwires) is field magnitude as the granularity of the backwiring is varied. Figure 10a illustrates a system of nine line currents with a single backwire. These currents comprise four quadrupoles whose a values are δ, 2δ, 3δ, 4δ, and a summation over all quadrupoles yields $a^2_{eff} = \delta^2(1 + 4 + 9 + 16) = 30\ \delta^2$. In Fig. 10b the number of backwires is increased to three and the current system becomes three quadruples of spacing δ. Summation here yields $a^2_{eff} = 3\delta^2$, a reduction of one order of magnitude from the previous case. Diminution of field proceeds generally as N^{-2} where N is the number of backwiring elements. From this it follows that reduction of contaminant fields is markedly aided through the use of multiple backwires.

The field reduction through multiple backwiring has been described as generally proceeding as N^{-2}. Such a dependence is not exact. In point of fact, the variation in position of elements in the backwiring array can lead to a reversal of field polarity from the quadrupole contribution. In principle, then, backwire position may be chosen to set the quadrupole contribution of all current carrying members to zero. Figure 11a illustrates this quadruple null condition for a current array with two backwires. In Figure 11a, the 2n + 1 current elements with current I have

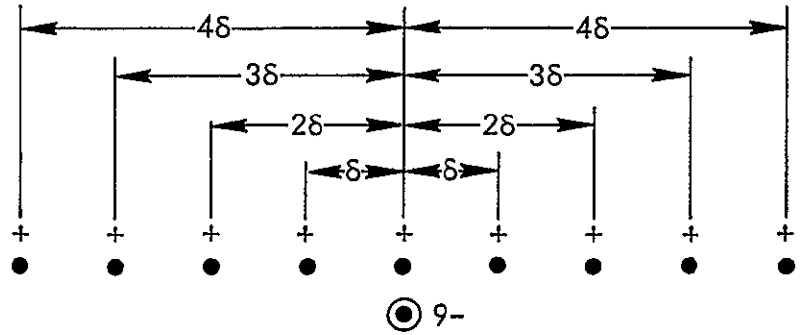

a)

Figure 10a. Nine line currents with a single balanced backwire. This system is comprised of four quadupoles with a values of δ, 2δ , 3δ , and 4δ .

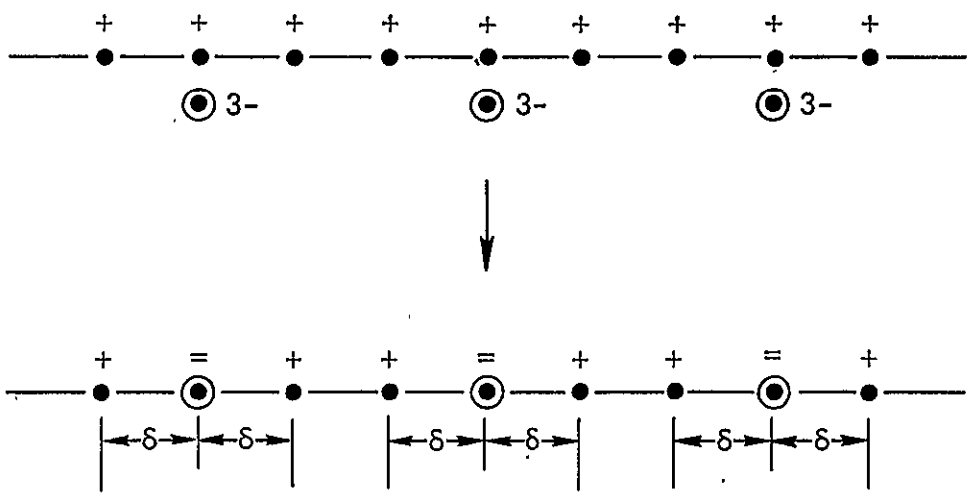

b)

Figure 10b. Nine line currents with three balanced backwires. This system is comprised of three quadrupoles with spacing a = δ.

Figure 11a. 2n + 1 current elements with a single return current of 2n + 1 units of current.

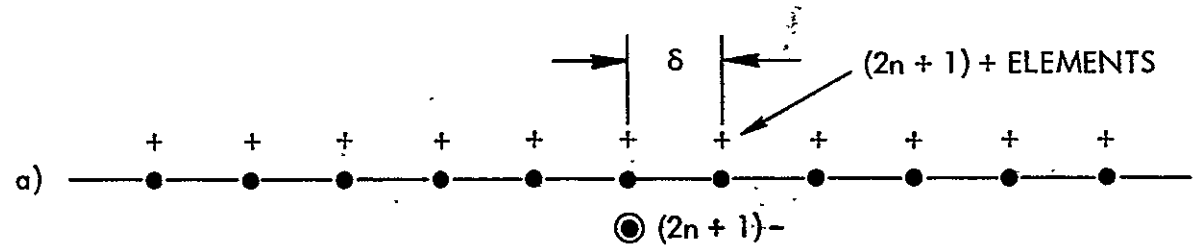

Figure 11b. Quadrupole of opposite polarity from condition 11a with spacing $\underline{a} = \lambda$.

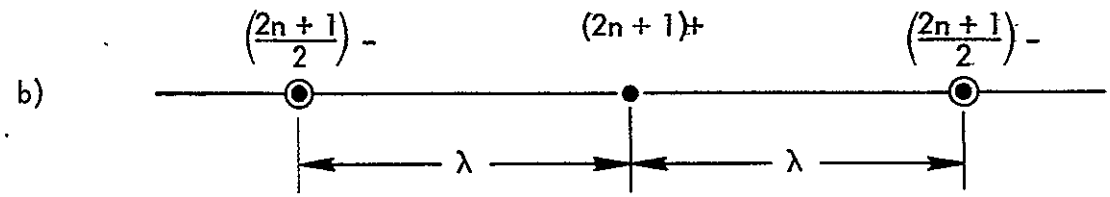

Figure 11c. Superposition of 11a and 11b to produce a magnetic field for which the quadrupole term vanishes, leaving only the octupole terms. Two backwire quadrupole null.

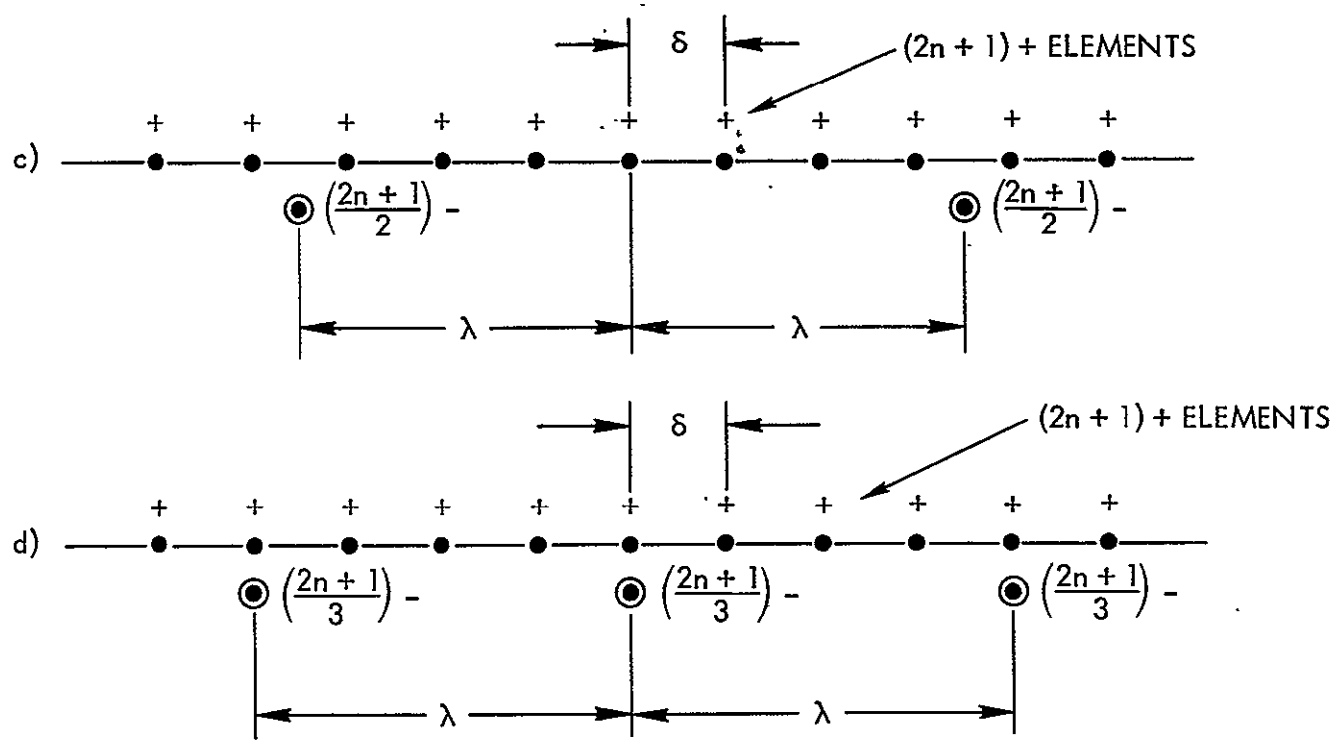

Figure 11d Three backwire quadrupole null.

a total Ia^2_{eff} of $I\delta^2 \sum_{1}^{n} (i)^2 = \frac{n}{6} (n + 1)(2n + 1)\ I\delta^2$. The quadrupole in Figure 11b has $Ia^2_{eff} = -\frac{2n + 1}{2} I\lambda^2$. The superposition of these two sets of currents leads to the configuration in Figure 11c. If

$$\frac{2n + 1}{2} I\lambda^2 = \frac{n}{6} (n + 1)\ (2N + 1)\ I\delta^2$$

or

$$\lambda = \delta\left(\frac{n\ (n + 1)}{3}\right)^{1/2} \qquad (6)$$

TWO BACKWIRE
QUADRUPOLE NULL

then the quadrupole contribution of all elements vanishes. Similar considerations for 3 balanced backwires, Figure 11d, show that

$$\lambda = \delta\left(\frac{n\ (n + 1)}{2}\right)^{1/2} \qquad (7)$$

THREE BACKWIRE
QUADRUPOLE NULL

yields zero net quadrupole contribution for the entire set of current elements.

The calculations leading to Equation (7) and Equation (8) have assumed infinite length to the line current elements. The current elements in a string are limited to 5 meters in length, and, variations in magnetic field away from the forms of Equation (2) and (3) will be experienced. The variations will prevent <u>exact</u> cancellation of contaminant fields for arrays utilizing a backwire spacing calculated from Equation (7) or (8). However, some benefits in contaminant field reduction may be obtained from the backwire placement. Calculated fields from single strings of the solar array from "quadrupole null" backwiring will be given later in this section.

The contaminant fields from a single string of 0.4 meter width and 5 meter length and various backwire configurations have been calculated at various positions in the x', y', z' space. The field $B_{z'}$ for $y' = 0$ and $z' = 0$ is given in Figure 12 as a function of x'. The total string current is 1.8 amperes, a value

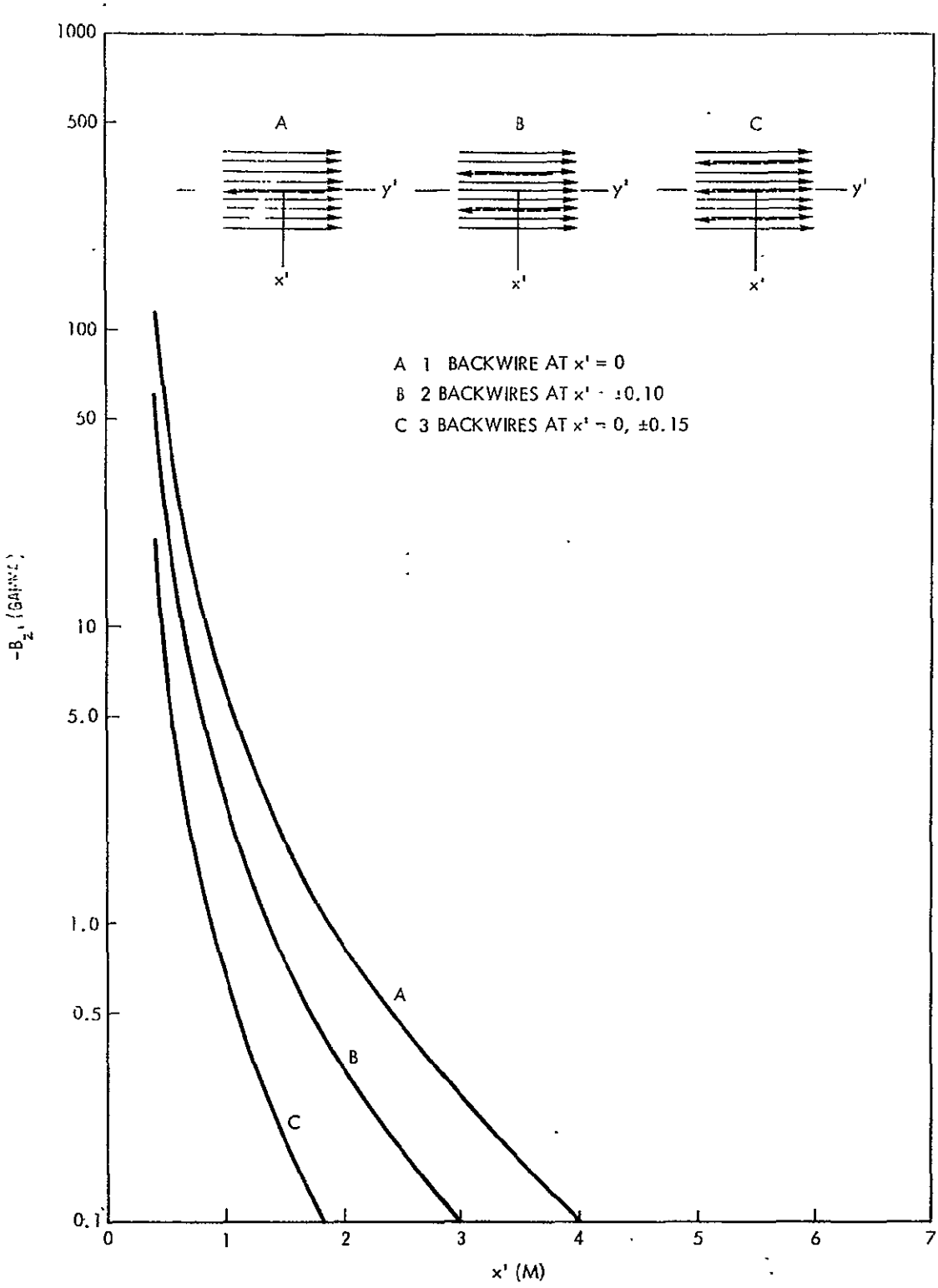

Figure 12. B_z-(x´, 0, 0) for single string of finite length for one, two, and three balanced backwires. Curve A single backwire at x´ = 0. Curve B two backwires at x´ = ±0.10 m. Curve C three backwires at x´ = 0, ±0.15 m.

slightly below the anticipated string currents of the 10 KW, 4 arm array. For the indicated string current, contaminant fields in excess of 100γ are obtained at ∿ .5 meters from the center of the string and, to obtain fields below the .1γ level, x′ distances of ∿ 4 meters are required.

The calculations illustrated in Figure 12 utilized nine current elements in the forward direction with a total width in the x′ direction of 40 cm rather than the 19 elements in the actual string. This simplification does lead to economies in computation time without the introduction of significant changes in the calculated fields. In Condition A a single balanced backwire was utilized. Condition B utilized two balanced backwires with spacing indicated on the Figure, while Condition C utilized three balanced backwires with the spacing illustrated in the Figure. For Condition C contaminant levels of 1γ are obtained at x′ ∿ 0.9 meters and the 0.1γ level occurs at x′ ∿ 1.8 meters. The significant improvement obtained by multiple backwires are to be noted.

The function $-B_{x'}(z')$ for $x'=0$ and $y'=0$ is given in Figure 13 for single, double, and triple backwires of the configuration shown in Figure 12. For a single balanced backwire, $-B_{x'}$ = 1γ at z′∿ 1.8 meters and = .1γ at z′∿ 3.6 meters. With three backwires at the indicated spacings, the 1γ level occurs at z′∿ 0.8 meters and .1γ level at z′∿ 1.8 meters. The triple backwire configuration utilized here succeeds in reducing contaminant fields to values well below the interplanetary level for distances removed from the string of ∿ 2 meters.

The field values thus far illustrated occur in the plane of the solar array and along the central axis of a single string. The magnetometer location is unlikely to be at either location. From Figure 6 and the discussion of Section II, magnetometer location along the central axis of the entire array would appear desirable. A location precisely on the axis may not be possible because of demands for the location of other subsystems. In addition, the failure mode of a single string results in magnetic fields along the central axis equal in magnitude to single string fields at that point. There is, thus, interest in single string fields for $y' \neq 0$. Figure 14 presents $-B_{x'}(z')$ at $y = -2.5$ meters. This axis

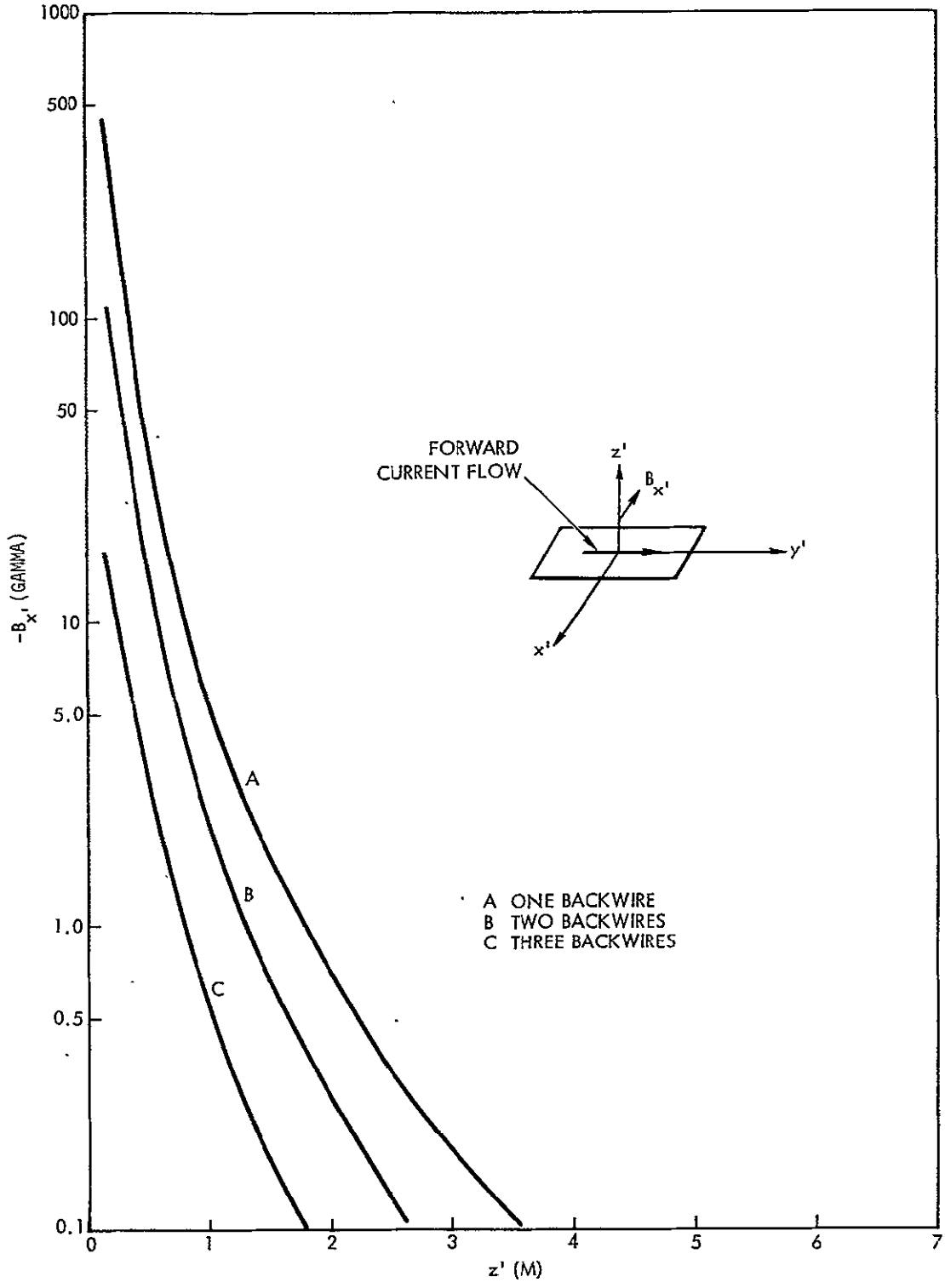

Figure 13. $B_{x'}(0, 0, z')$ for single string of finite length for one, two, and three balanced backwires. Curve A single backwire at $x' = 0$. Curve B two backwires at $x' = \pm 0.10$ m. Curve C three backwires at $x' = 0, \pm 0.15$ m.

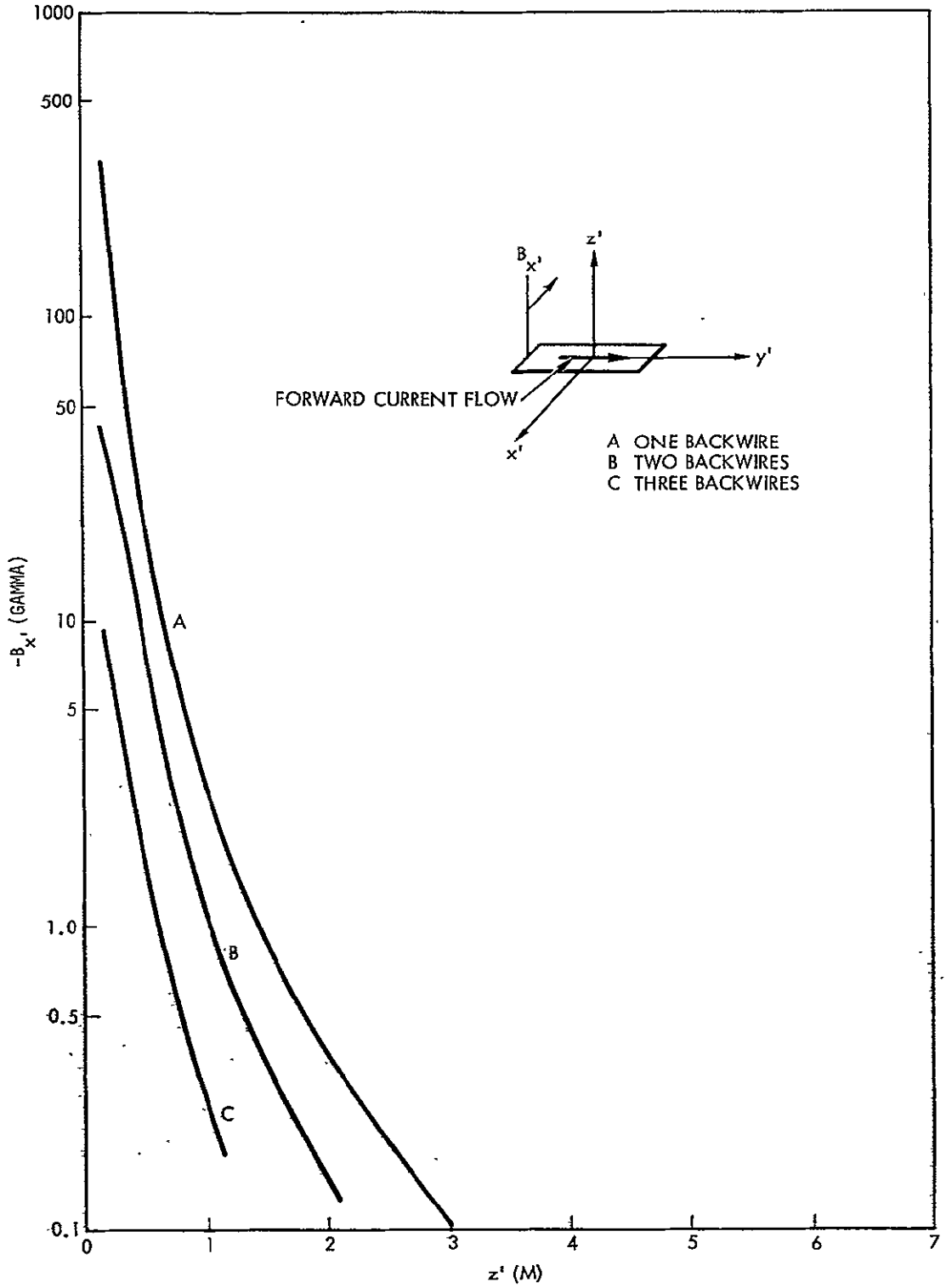

Figure 14. $B_{x'}(0, -2.5, z')$ for single string for one, two and three balanced backwires. Curve A single backwire at $x' = 0$. Curve B two backwires at $x' = \pm 0.10$ m. Curve C three backwires at $x' = 0, \pm 0.15$ m.

goes through the outer edge of the string. For the total array illustrated in Figure 6, $y' = -2.5$ meters is $\sim$1.2 meters from the axis $x = y = 0$. It may be seen that the movement in y' away from the central axis of the string (Figure 13) does not result in any major diminution of field strengths. Values of $z' \sim 3.1$ meters are still required to obtain the .1γ level for a single backwire. For three backwires the 0.1γ level is attained at $z \sim 1.3$ meters.

The accuracy of the quadrupole fields for infinite length current elements Equation (2), (3) may be examined further using the calculated fields in Figures 12 and 13. For a total current of 1.8 amperes distributed through nine wires with overall width of .4 meters and a single balanced backwire, the term $\frac{\mu_o\, i\, a^2_{eff}}{\pi}$ obtained by summing over all quadrupoles is equal to 6. Thus

$$B_r = \frac{6 \sin 2\alpha}{r^3} \qquad (2')$$

$$B_\alpha = \frac{-6 \cos 2\alpha}{r^3} \qquad (3')$$

where B is in γ and r is in meters. For $x' = y' = 0$, the term $r = z'$, $B_r = 0$, $B_\alpha = -B_{x'}$. Thus, from (3'), and at $z = 2$ meters (chosen to be large compared to total wire separation), $B_{x'} = -.75\gamma$. The calculated result, which rigorously includes finite wire length and wire positioning, yields, (Figure 13), $B_{x'} = -.694\gamma$, in good agreement with the "line current quadrupole" approximation. For $y' = z' = 0$, $r = x'$, $B_r = 0$, and $B_\alpha = B_z$. For $x = 2$ meters, B_z from the quadrupole approximation is, again, -0.75γ, while the calculated fields (Figure 12) are $B_{z'} = -.839\gamma$. Again, there is good agreement between the quadrupole form, Equation (2), (3), and the calculated results. Since $B_r^2 + B_\alpha^2$ is not dependent on α, the magnitude of the contaminant field has a simple r^{-3} dependence in this range of r. In estimating correct location for instruments relative to solar panel elements, this r^{-3} dependence in contaminant field magntidude is of value.

The effect of offsetting the backwire is as noted earlier, to generate a system of line current dipoles. The magnitude of these dipolar fields, from Equation (4) and (5), is proportional to a_{eff}/r^2 where a_{eff} is derived from a

summation over the various dipolar elements. Because of the comparatively weak drop-off rate (r^{-2}), these dipolar fields proceed to considerable distances. Figure 15 illustrates $B_{z'}$ for large values of y' (5 to 9 meters) and various z' values. It may be noted that $B_{z'}$ is still several tenths of a γ at y' values of 9 meters. Thus, contaminant fields from an offset backwire configuration are appreciable even if the string is an "outboard" string on the arm. The contaminant fields from injection and collection currents for an offset backwire are of comparable (or larger) magnitude and underscore the undesirability of the offset backwire configuration.

A final point of interest for the contaminant fields from single string cell and backwire currents is the field from a string whose backwires are oriented to produce a quadrupole null condition. Figure 16 illustrates the magnetic fields as a function of z' and $x'$for points over the center of the string for a two-wire quadrupole null and Figure 17 illustrates points over the end of the string for a three-wire quadrupole null. The reduction in field magnitude is $\sim$ 2 orders of magnitude through the use of quadrupole nulling; and contaminant field levels of a few milligamma are obtained at distances of 1 - 2 meters from the string. These calculations would indicate that multiple backwires, with quadrupole nulling, should be utilized.

C. Contaminant Fields from Injection and Collection Busbar Currents

The previous section has treated the contaminant fields from solar cell and backwire currents. For the string examined, in Arm II, these are y-directed currents, resulting in contaminant fields in the x and z directions. The injection and collection currents for this string are x-directed and produce magnetic fields in the y and z directions. Similar field component assignments exist for strings located in Arm IV. For Arms I and III the principal currents (solar cell and backwires) are x-directed (y and z fields) while injection and collection currents are y-directed (x and z fields). The present discussion will not take up additions or cancellations of field components from the variously directed currents but will be concerned with the magnitude of contaminant fields from the injection and collection currents.

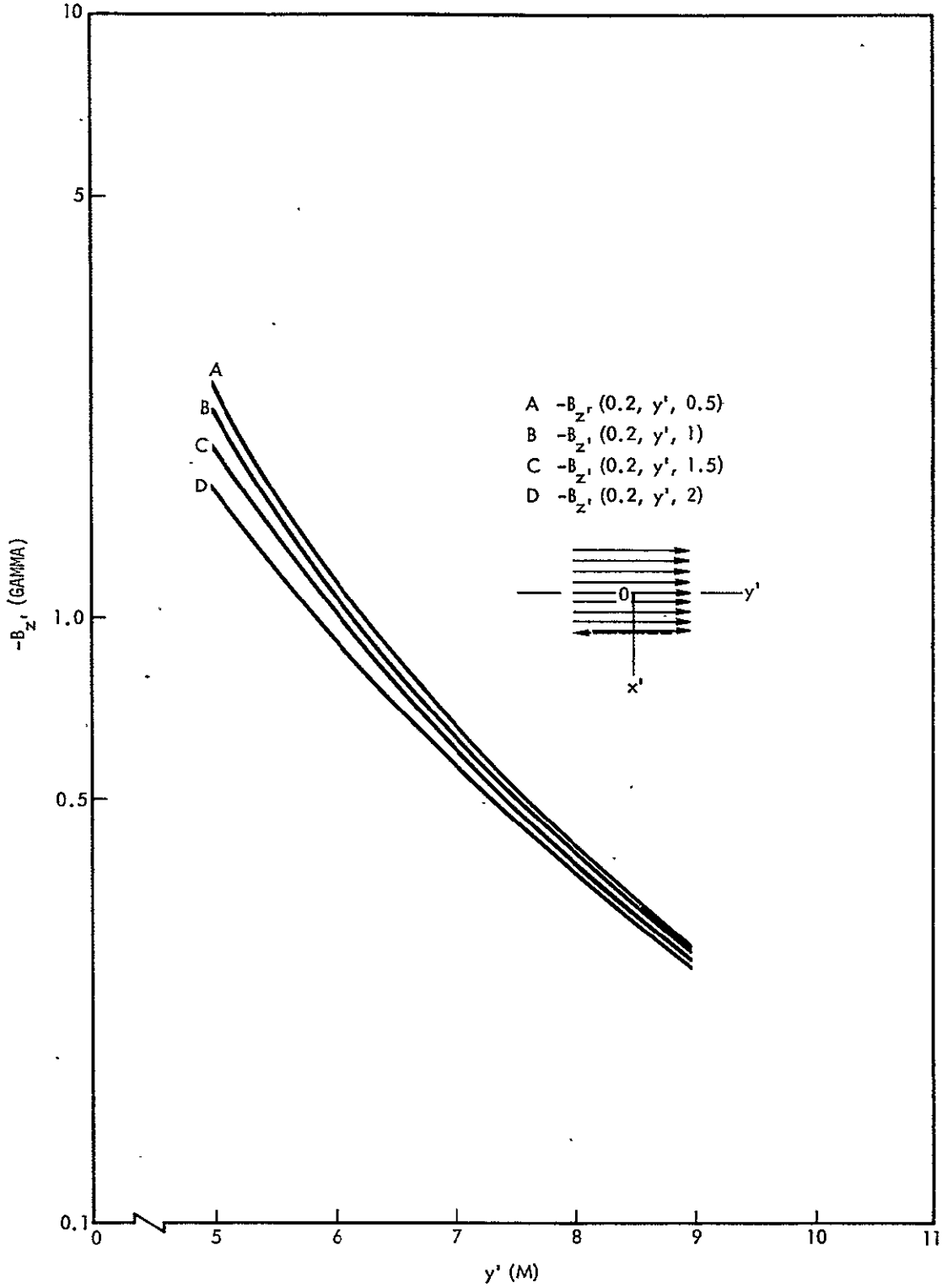

Figure 15. Magnetic field for single string for a single offset backwire at x' = 0.20 m.

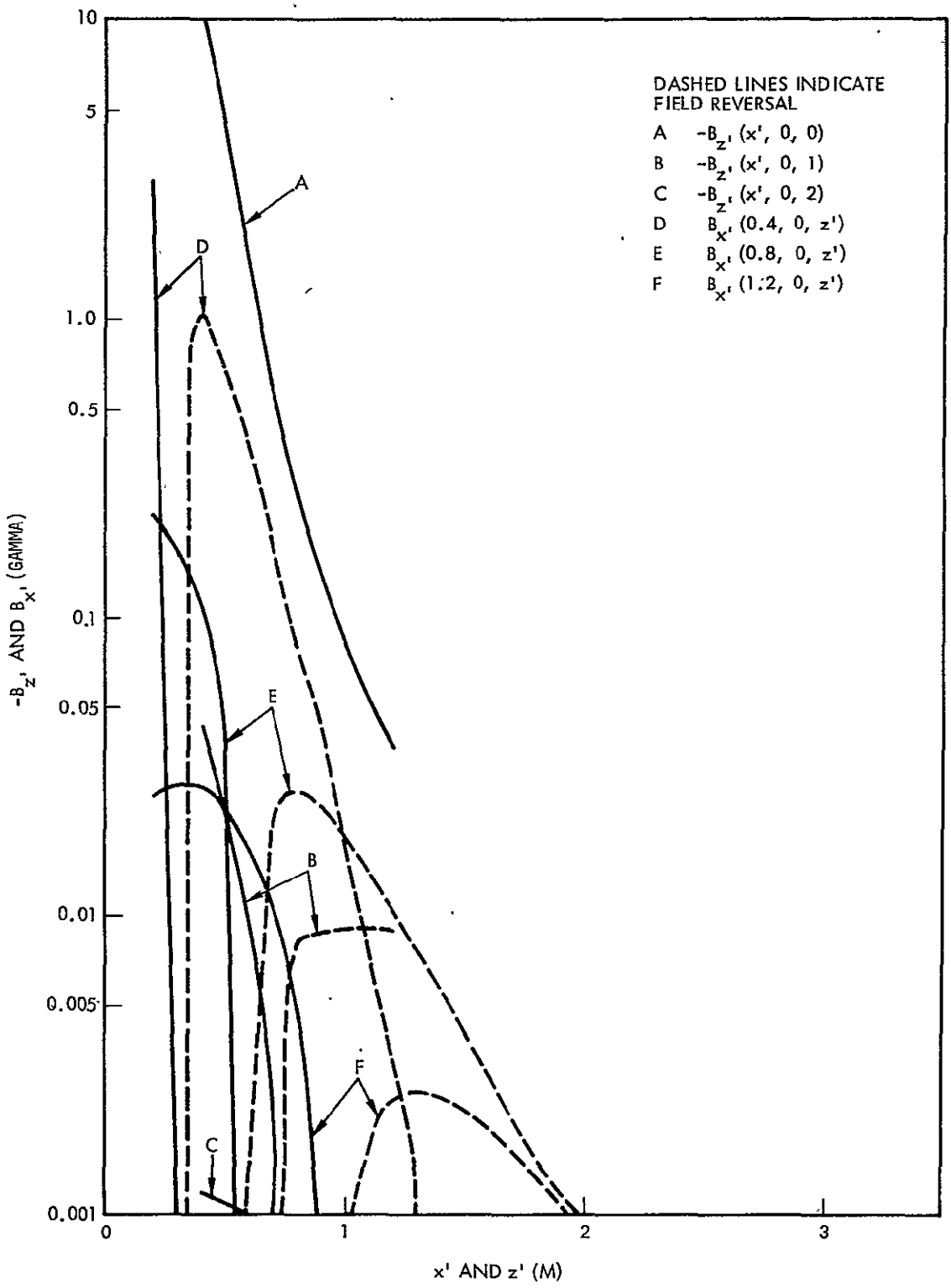

Figure 16. B_z as function of x', B_x as function of z' for two backwire quadrupole null. Wires positioned such that x' = λ = ±0.129 m.

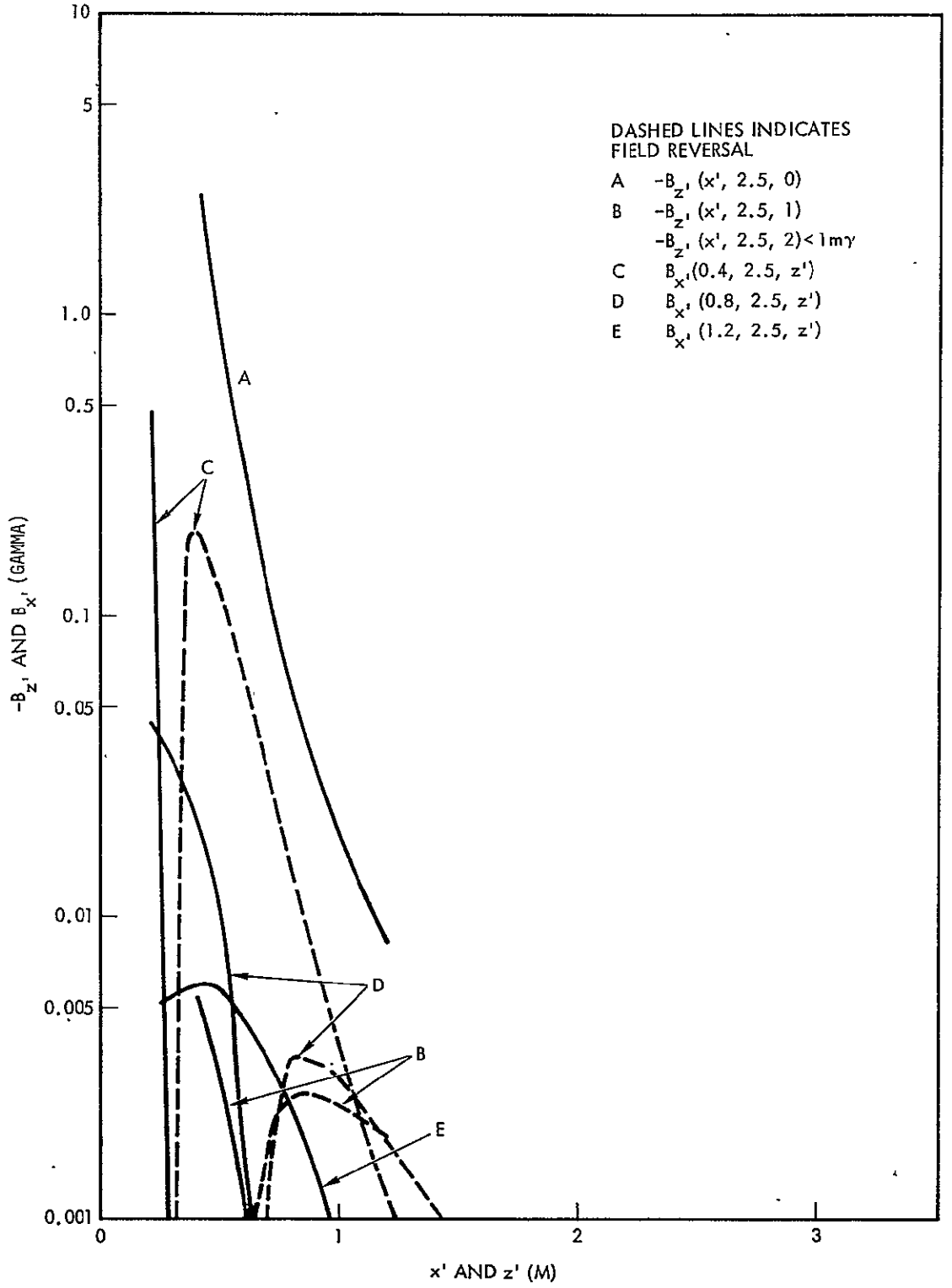

Figure 17. $B_{Z'}$ as function of x', $B_{X'}$ as function of z' for three backwire quadrupole null. Wires positioned such that $x' = \lambda = 0, \pm 0.158$ m.

The injection and collection currents for a single string (in Arm II) utilizing a single balanced backwire are illustrated in Figure 18a. Three aspects of these currents should be noted. First, for central injection, there is a reversal of current direction over comparatively small distances, leading to diminution of contaminant fields. Second, the flow of current into the various solar cell strings results in the decrease of current flowing in the injection busbar for movement away from the central point of the bar. Third, the distant location of the collection busbar (5 meters) from the injection busbar does not permit effective use of the reversal of current flows in these two members as a means of contaminant field reduction. For this reason, contaminant field calculations will consider only the single collection or injection busbar.

The magnetic field from the injection may be calculated by Equation (1), and by a quadrupolar approximation over opposing current elements. Assuming a total injection current magnitude of I which decreases linearly in moving out the two directions of the busbar, the magnetic field in polar coordinate system of Figure 18b is given by

$$B_\phi = \frac{\mu_o I D^2 \sin 2\theta}{16\pi r^3} \qquad \text{MKS} \qquad (8)$$

where D is the half-length of the injection busbar. For $\theta = \frac{\pi}{4}$, I = 1.6 amperes, D = 0.2 meters, and r = 1 meter, $B_\phi = 1.6\gamma$, a value which is comparable to the interplanetary field. For distances r of the order of 2 meters, B_ϕ has decreased to $\sim .2\gamma$. The magnitude of B_ϕ suggests that the single injection point configuration is not desirable, even for central injection.

If the injection point is offset, as illustrated in Figure 19a, the contaminant fields are greatly increased in magnitude. Figure 19b illustrates a polar coordinate system in which the contaminant field is

$$B_\phi = \frac{\mu_o I \hat{D} \sin\theta}{8\pi r^2} \qquad \text{MKS} \qquad (9)$$

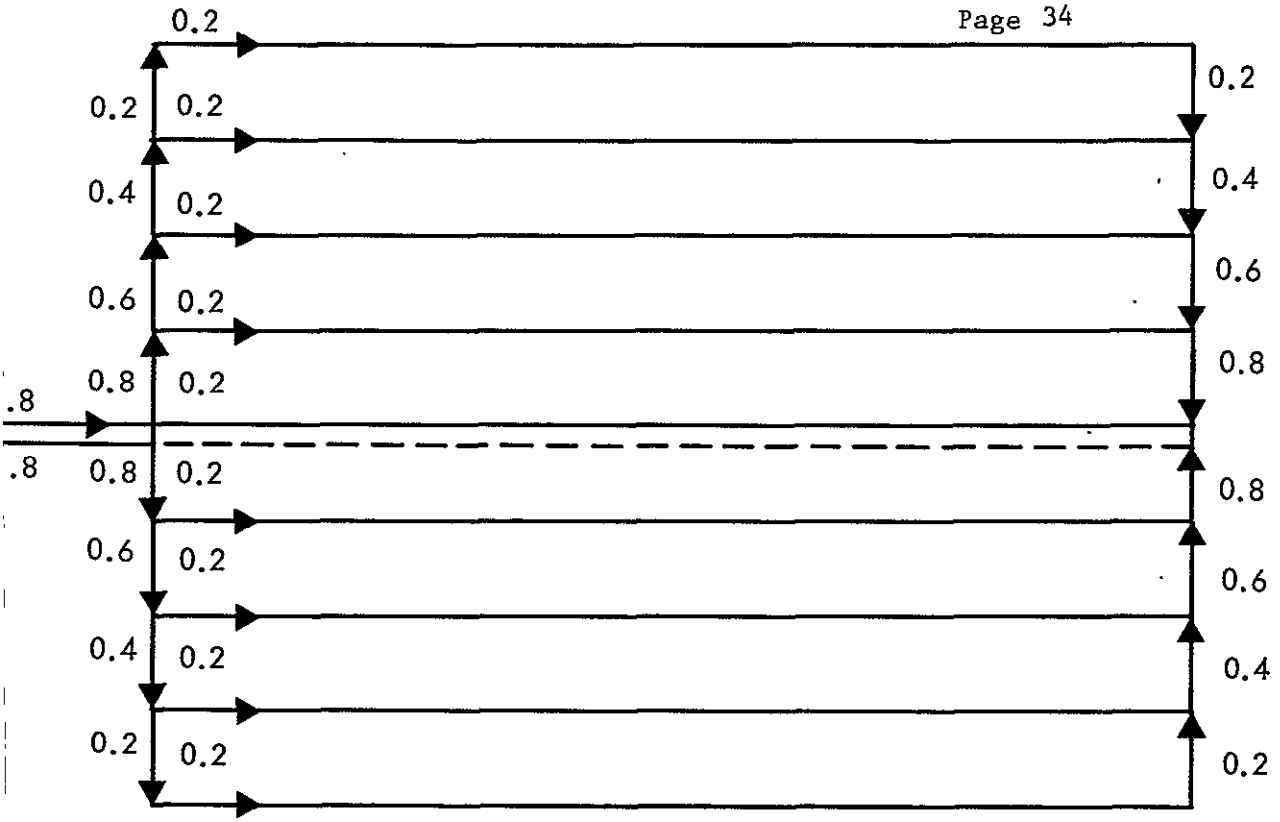

18a. Central injection and collection currents for signle string and single balanced
re.

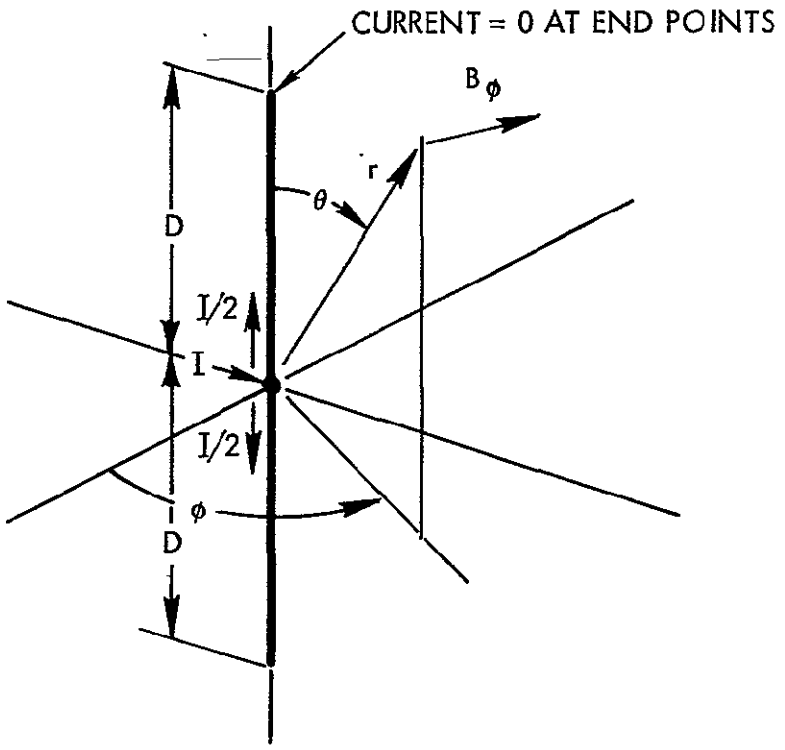

b)

ure 18b. Magnetic field due to central injection and collection of string currents.

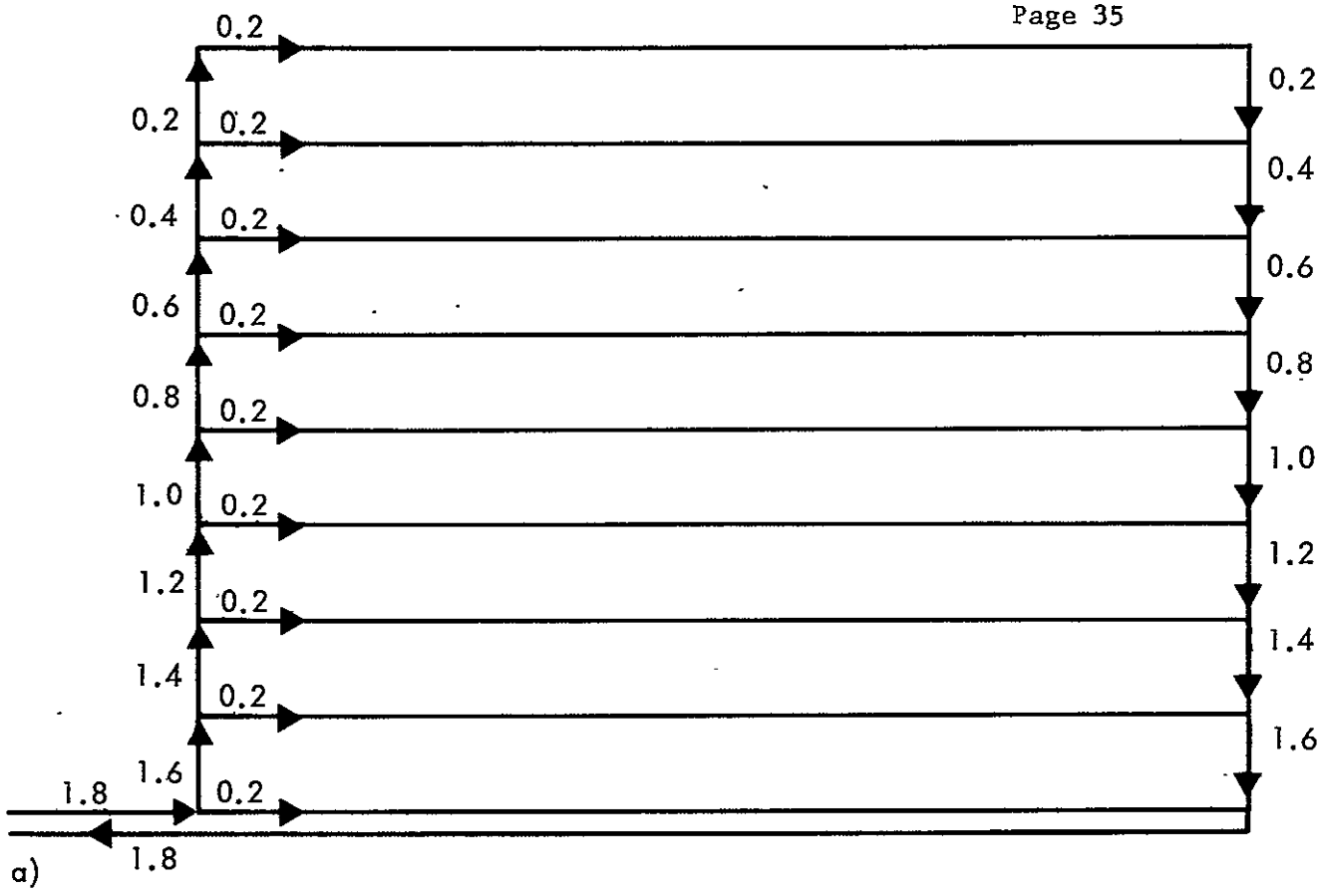

Figure 19a. Offset injection for single string.

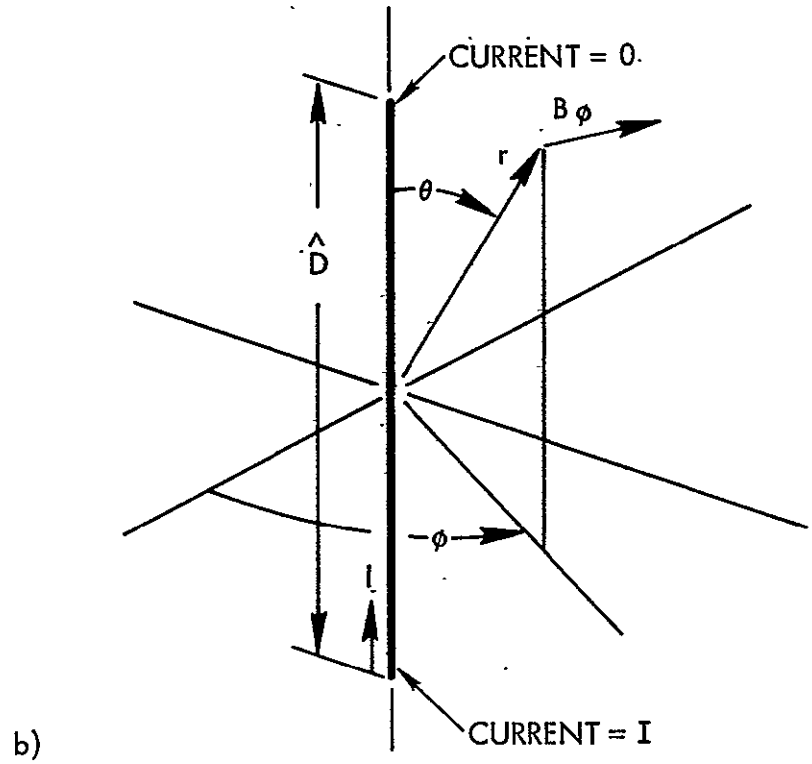

Figure 19b. Magnetic field due to offset injection.

It is assumed that I, the total injection current, diminishes linearly in moving away from the injection point. The term $\hat{D}$ is the total length of the injection busbar (.4 meter) rather than the half-length as in Equation (8). For I = 1.8 amperes, $\theta = \pi/2$, and r = 1 meter, $B_\phi = 36\gamma$, almost an order of magnitude larger than the interplanetary field at 1 AU. At distances of r = 6 meters, B_ϕ has diminished to 1γ. Thus, an injection busbar on the near side of an outboard string would create magnetic fields near the central axis of the array which are of sufficient magnitude to seriously perturb measurements of the interplanetary field. The field magnitudes indicate that injection (and collection) of currents must be central, even for outboard strings of the array.

The formula for central point injection fields (Equation 8), has revealed that substantial perturbations from this source could result from those elements on the near side of the inboard strings, so that, at least for these members, further field reduction is necessary. Such reduction is obtained if multiple backwires are utilized. Figure 20 illustrates the injection and collection currents for a system of three equally spaced backwires and nine forward wires. Figure 20a illustrates the actual current flow and Figure 20 b the equivalent circuit. The quadrupolar fields from the three quadrupole elements are additive. The half length of the quadrupoles is now reduced by a factor of four from that obtained with a single current return and the current flow in each quadrupole is also reduced by a factor of ~ 4. The net reduction is $\sim \frac{43}{3}$ or ~ 20. Thus, for a total string current of 1.8 amperes, a string width of .4 meters and three equally spaced backwires, r = 1 meter and $\theta = \pi/4$, the B_ϕ from all injection busbar (and corresponding backwire-connected busbars) is $.075\gamma$, a value reduced sufficiently so as not to perturb the measurement of the interplanetary field.

The principal point of emphasis from these results is that multiple backwiring acts to reduce contaminant fields from injection and collection busbars to acceptable levels, as was also obtained for the fields generated by the solar cell and backwire currents.

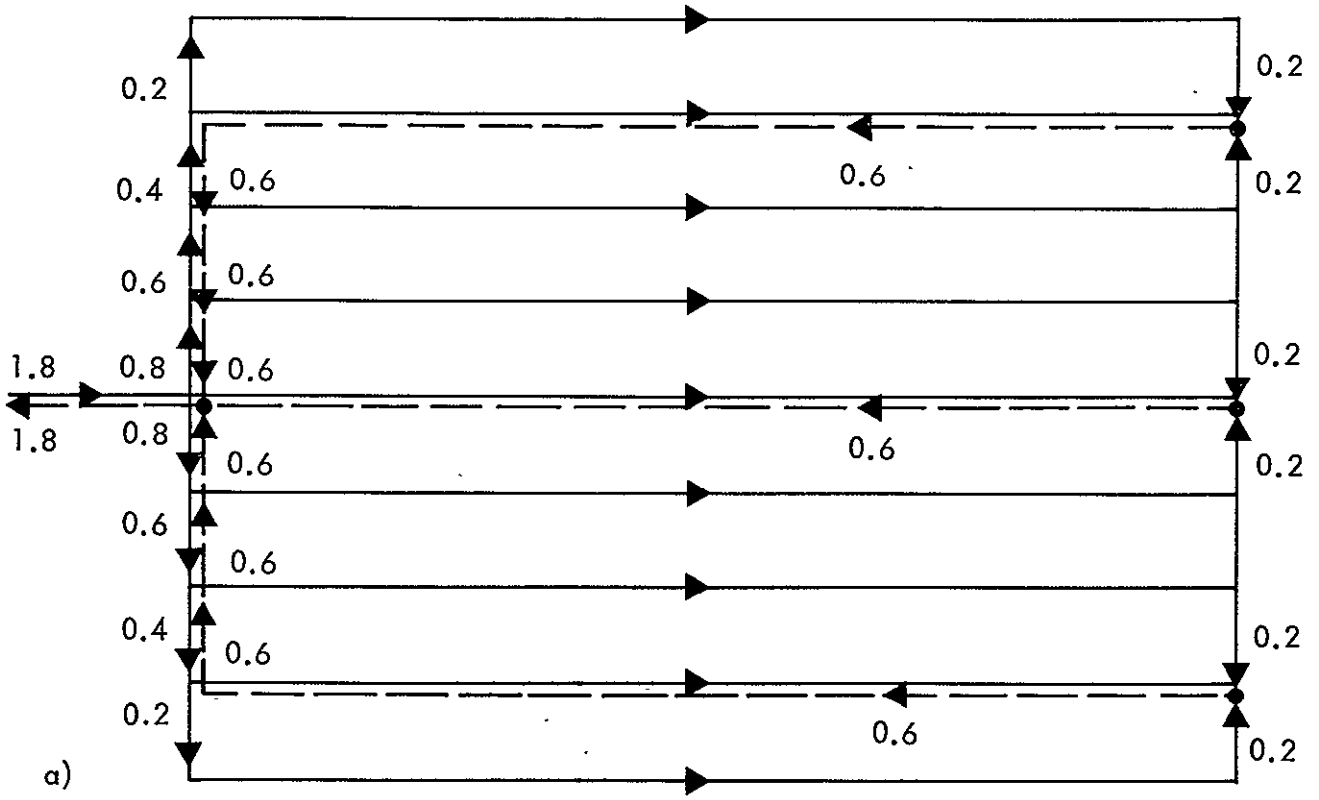

Figure 20a . Injection and collection for single string and for three balanced backwires.

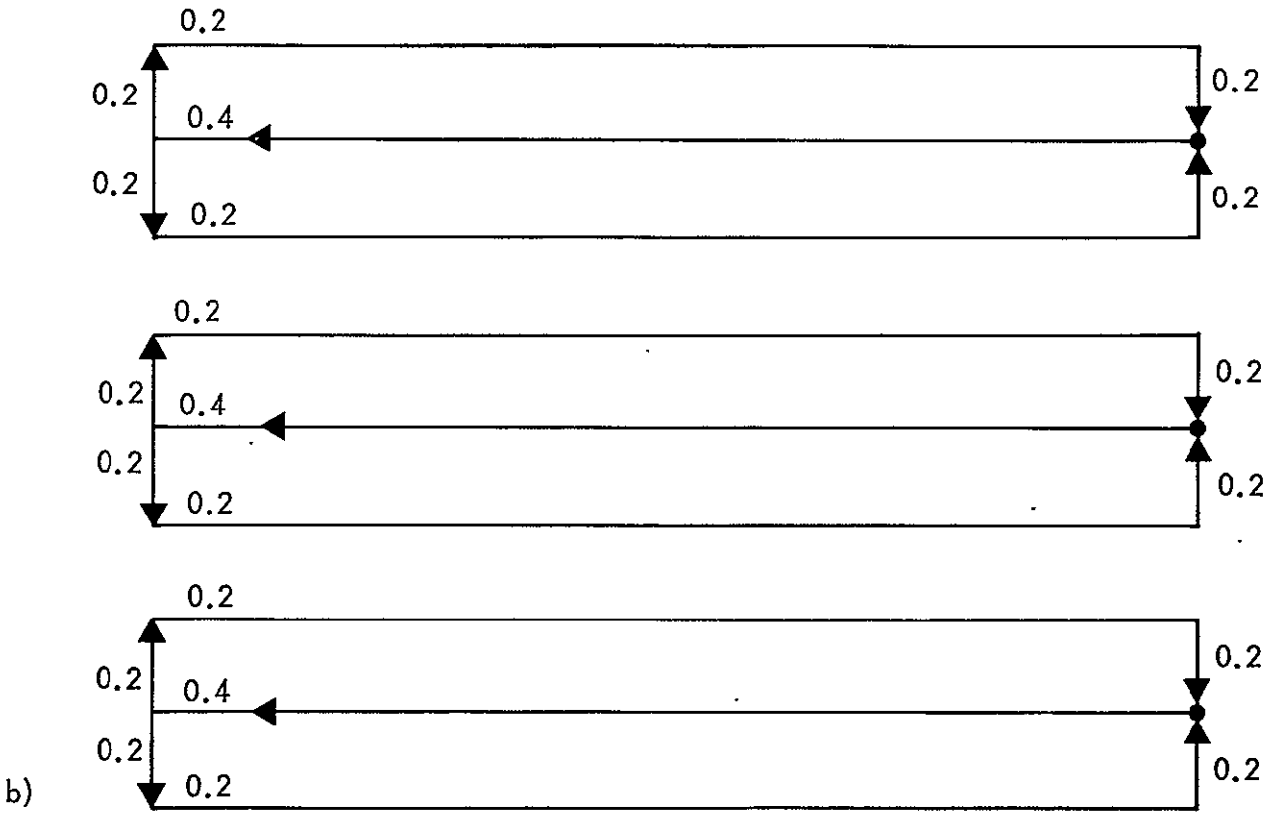

Figure 20b. Equivalent circuit for three balanced backwires.

D. Failure Mode Contaminant Field Levels

The discussion of previous sections has noted that mirror properties and equality of currents in all strings leads to complete cancellation of all field components along the central axis of the array and that B_z, vertical component of the field, vanishes everywhere in a series of some eight planes. If a single string should fail (for example, through an open circuit backwire for single backwiring) the magnitude of the perturbation field at the central axis is that of a single normally operating string, since the field of the total array minus one string can be generated by superposing the working array and a "hole" current string at the location of the interrupted string. At points away from the axis of the array, the failure mode field is that of the initial ideal array plus whatever perturbation fields arise from the appropriate hole currents.

The magnetic field at the point $x = 0$, $y = 1.2$, $z = 2$ meters is given in Figure 21 for an ideal array whose currents (See Figure 6) mirror about both the $x = 0$ and $y = 0$ planes, and which possess single balanced backwires. This point is exactly over the edge of the solar array and is 1.2 meters from the central axis.

Figure 21 illustrates the failure modes for the mirror-mirror current condition of Figure 6. For no failures, the magnetic field is only in the x-direction and has magnitude $B_x = -0.37\gamma$. Should one of the strings fail due to an open circuit backwire the magnetic field would shift in magnitude and direction. For example, if one of the two inner strings fails (case a) the magnetic field would shift from $B_x = -0.37\gamma$ to $B_x = 0.02\gamma$ and $B_z = \pm 0.11\gamma$. More serious perturbations would result, however, if one of the other strings open circuits as indicated in case b and c. Calculations have neglected fields generated by injection and collection busbar currents.

If the mirror-anti-mirror current condition (Figure 4b) is utilized, the x-component of $\vec{B}$ vanishes at (0, 1.2, 2), and non-zero B_z is obtained. Figure 22 illustrates the value of B_z at the indicated point. Also shown are the fields resulting from the failure of any one of the six inboard strings. Failure of outboard strings does not produce significant perturbation fields at the indicated position if balanced backwiring is utilized, for either the present or previous case (Figure 21).

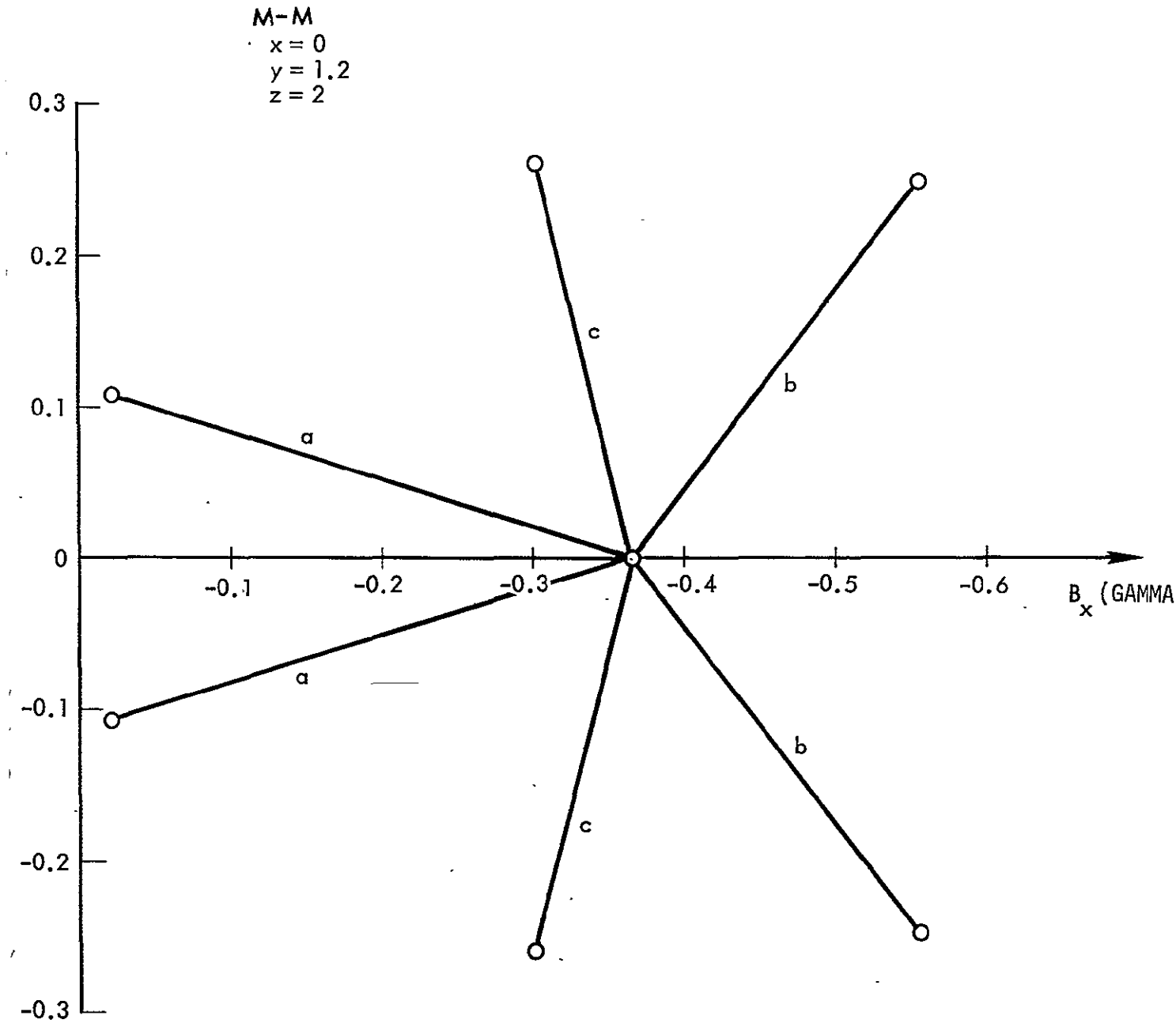

Figure 21. Failure modes for mirror-mirror configurations. Magnetic field is calculated at x = 0, y = 1.2 m and z = 2 m; a) failure of one inner string, b) failure of adjacent string, c) failure of one of the outer strings.

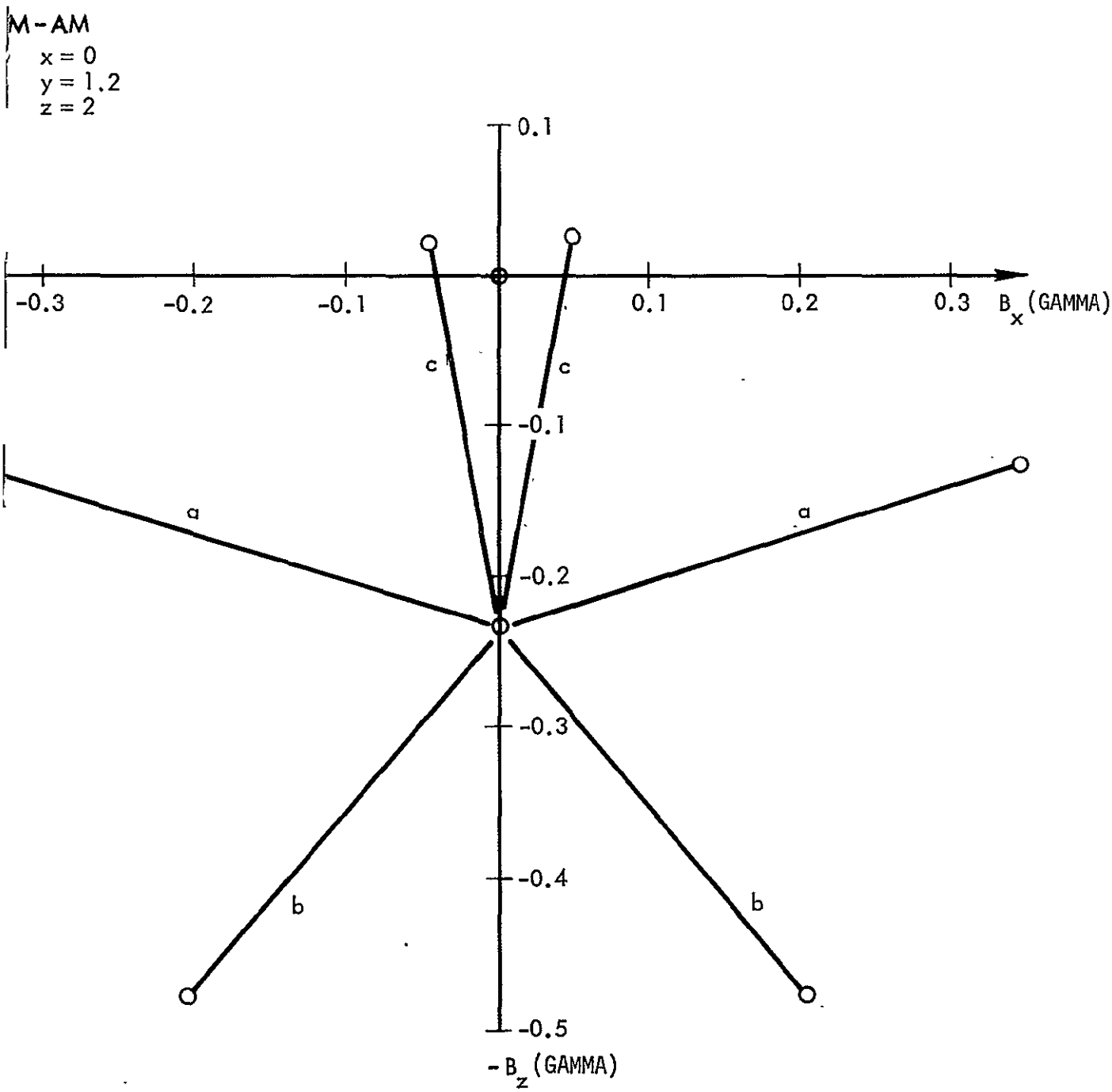

Figure 22. Failure modes for mirror-anti-mirror configuration. Magnetic field calculated at z = 0, y = 1.2 m, and z = 2m; a) failure of one inner string, b) failure of adjacent string, c) failure of outer string.

From Figure 21 and Figure 22 it may be concluded that perturbation fields are somewhat higher for the M-M configuration than the M-AM, both for zero failures and for the failure of a single string. The root mean square of the field magnitude for all M-AM cases is $\sim$ 0.85 that of all M-M cases. This is not considered as significant in view of possible manufacturing advantages in the identical blanket construction allowable for the mirror-mirror configuration. Both configurations utilizing single backwires are above the .1γ level, and use of multiple backwires is viewed as the appropriate method of field reduction.

A final area of concern is the field generated under the failure mode of an open circuit in a backwire for a multiply backwired string. The concern here is that certain failure modes lead to remaining backwires which are not balanced and which possess appreciable dipolar fields. Figures 23 and 24 illustrate fields resulting from the failure of a central backwire of a three-backwire string and an "outside" backwire of that same configuration. The failure of the middle backwire leaves the string in operation with a balanced backwiring configuration, albeit with increased quadrupolar fields. Failure of an outside backwire leaves the central and other outside backwire remaining. This configuration produces dipolar fields of increased magnitude. Of principal concern in failure mode evaluation is the possibility of open-circuit failure in a backwire when considered against the perturbation field reduction obtainable with multiple backwiring.

IV. SUMMARY

The discussion of the previous sections has shown that particular current configurations lead to field cancellation along particular axes and, for certain field components, in a variety of planes. The mirror-mirror configuration (Figure 6) provides $B_z = 0$ through a large number of planes and at the central axis of the array.

The perturbation fields off the central axis of the array and for conditions of various failure modes are determined by the sum of perturbation fields from various strings. The contribution to the total perturbation field of a single string may be reduced to several tenths of a gamma by appropriate physical separation from the string if balanced backwiring is employed. Multiple backwiring

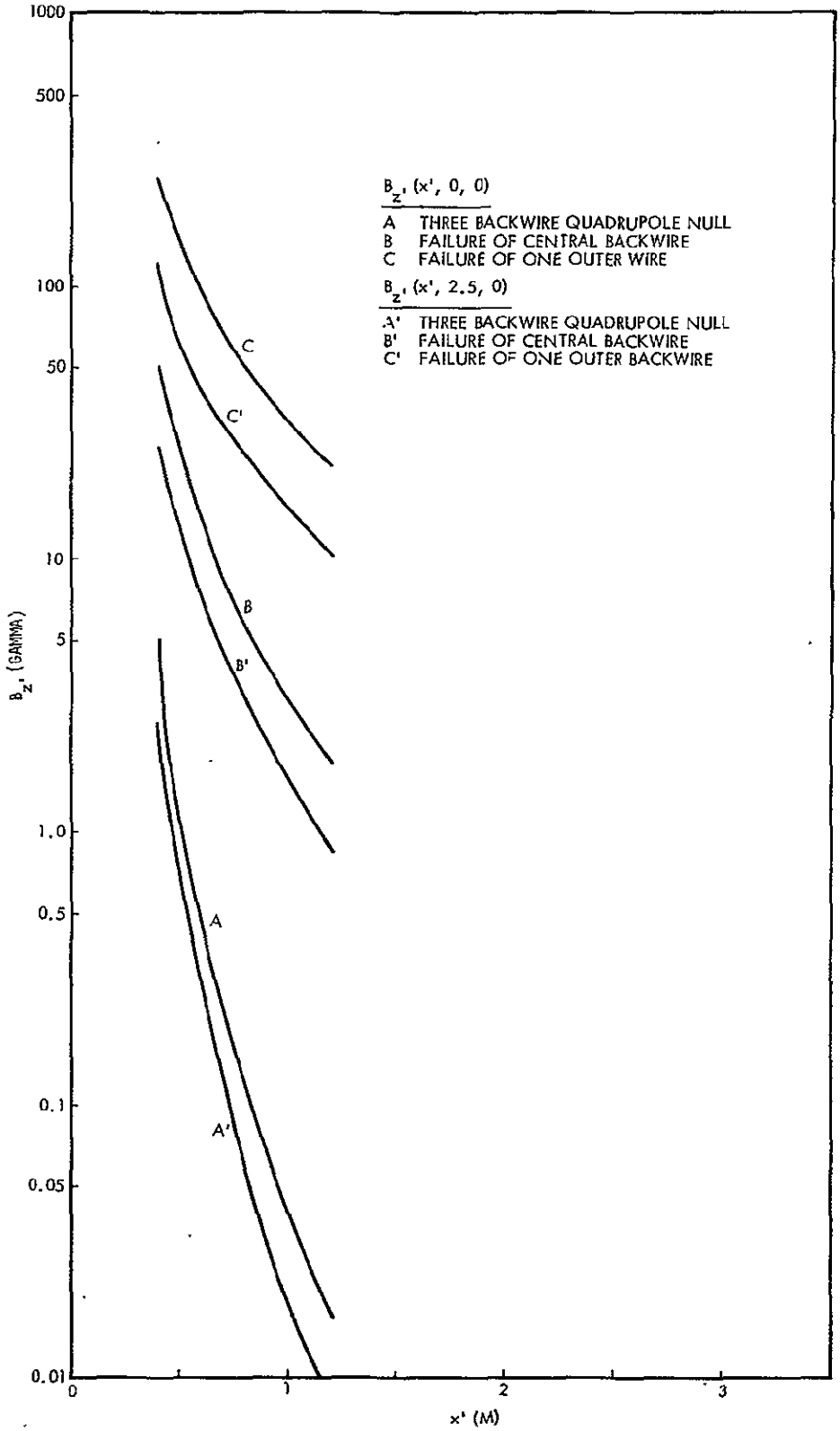

Figure 23. Effect of one backwire failure in the three backwire quadrupole null configuration. $B_{z'}$ as function of x' for $y' = 0$, 2.5 m, $z' = 0$.

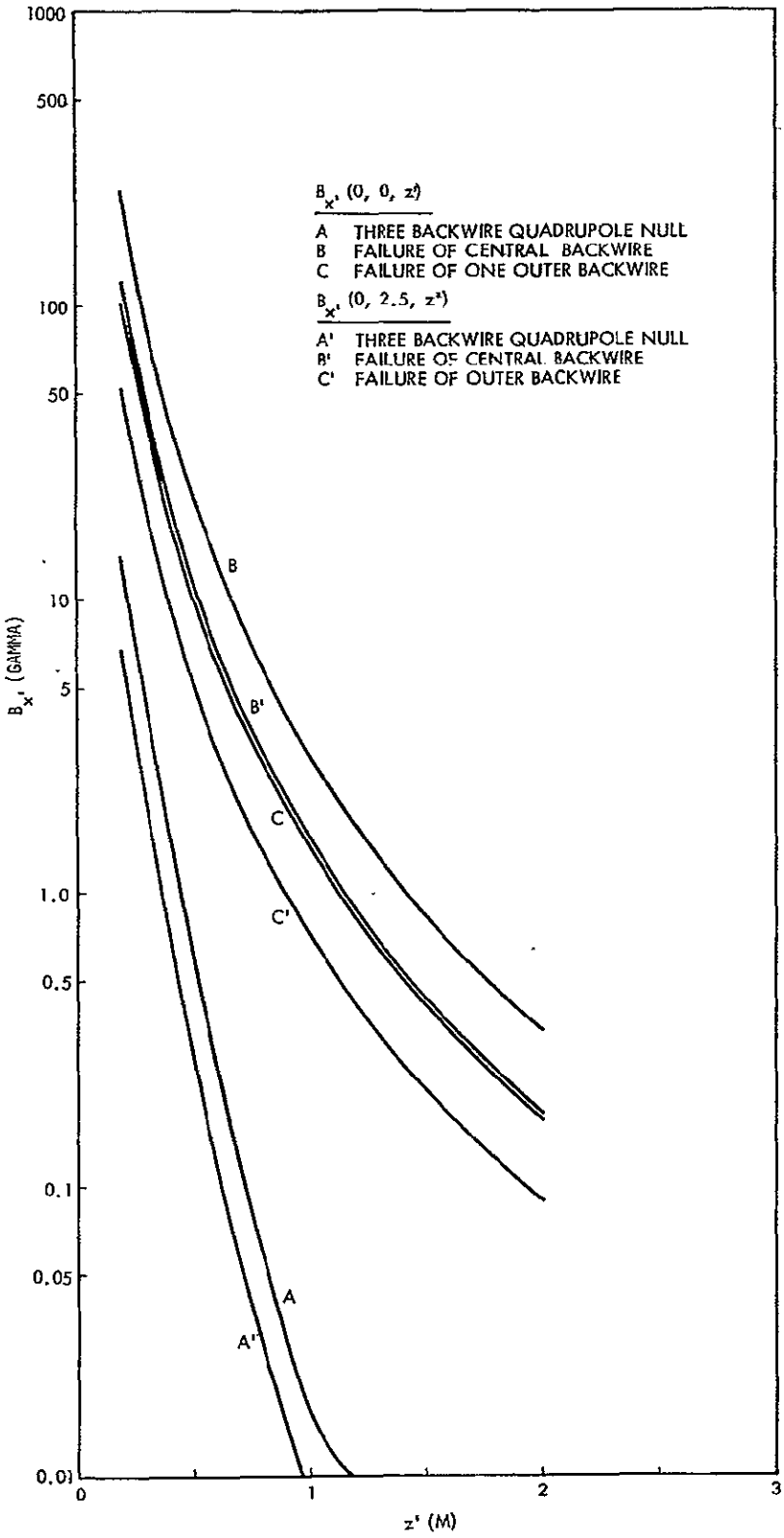

Figure 24. Effect of one backwire failure in the three backwire quadrupole null configuration. $B_{x'}$ as function of z' for y' = 0, 2.5 m, x' = 0.

is required to reduce perturbation fields below .1γ, assuming reasonable limits to isolation distances. Offset backwiring produces high level (several γ) contaminant fields and would appear to be excessive if measurement of interplanetary fields by the spacecraft payload is to be attempted. Similar conclusions exist relative to injection and collection busbar currents.

Quadrupole nulling conditions are possible for multiple backwiring circuits. For these backwire spacing contaminant fields at possible magnetometer locations may be reduced to the order of milligamma.

From these several features, a desirable array condition is considered to be a mirror-mirror current configuration, with multiple balanced backwiring set such as to yield a quadrupole null.

ACKNOWLEDGEMENTS

We wish to thank Dr. A. V. Haeff, Dr. R. K. Cole, Dr. G. T. Inouye, and Mr. C. C. Thorpe for their aid and suggestions in preparing this manuscript.

REFERENCES

1. McMinimy, W. R., "Pioneer Second Flight Spacecraft Magnetic Properties Determination" NAS 2-1700, TRW 2515-6005-R0000, July 1966.

2. Ness, N. F., C. S. Scearce, J. B. Seek, Initial results of the IMP 1 magnetic field experiment, J. Geophys. Res., 69, 3531, 1964.

3. Coleman, P. J., E. S. Smith, L. Davis, and D. E. Jones, Measurements of magnetic fields in the vicinity of the magnetosphere and in interplanetary space: preliminary results from Mariner 4, Space Res, 6, 907, 1966.

4. Scarf, Fred, "Characteristics of the solar wind near the orbit of Jupiter," Planetary Space Sci., 17, 595, 1969.

5. Meissinger, H. F., R. A. Park, H. M. Hunter, Presented at AIAA Joint Electric Propulsion and Plasmadynamics Conference, Colorado Springs, Colorado, AIAA Paper Nò .67-711, Sept. 1967.

6. Kerrisk, D. J., D. R. Bartz, "Preliminary Electric Propulsion Technology - Toward Flight Programs for the Mid-1970's," Astronautics and Aeronautics, 6, 48, June 1968.

7. Barker, T. A., J. V. Goldsmith, and J. R. Edberg, "Spacecraft Electric Propulsion - Now?," Astronautics and Aeronautics, 6, 38, June 1968.

8. "Feasibility study 30 watts per pound roll-up solar array," NAS 7-100, General Electric Report No. 68 SD 4301, June 1968.

SECTION IV. B.

BACKWIRE AND BUSBAR PLACEMENT FOR MAGNETIC CLEANLINESS ON LARGE AREA SOLAR ARRAYS

BACKWIRE AND BUSBAR PLACEMENT FOR MAGNETIC CLEANLINESS ON LARGE AREA SOLAR ARRAYS

J. M. Sellen, Jr.

Physical Research Center

TRW Systems

Redondo Beach, California

30 June 1969

BACKWIRE AND BUSBAR PLACEMENT FOR MAGNETIC CLEANLINESS ON LARGE AREA SOLAR ARRAYS

J. M. Sellen, Jr.

I. INTRODUCTION

The contaminant magnetic fields generated by current flows in a large area solar array have been examined by Sellen and Ogawa.[1] This present report will review and apply the findings of Ref. 1 with particular regard to the array configuration advanced in Feasibility Study -- 30 Watts per Pound Roll-up Solar Array.[2] The technical areas to be discussed include the choice of current flow direction in the separate "strings" of the solar array, the number and placement of backwires to the strings, the geometry of the injection and collection busbars to the strings, and the geometry of the busbars collecting overall solar array arm currents. The outer physical dimensions of the array and of the separate strings will be that utilized in Ref. 2 as will also be the total number of strings and the magnitude of the individual string current. Recommended backwiring and busbar placement will differ from that utilized in Ref. 2.

II. CURRENT FLOW DIRECTION IN SOLAR ARRAY STRINGS

The factors involving contaminant magnetic fields and current flow direction in solar arrays have been treated in II in Ref. 1. It has been shown there by appropriate "mirror properties" to the currents above specific planes in the solar array, that contaminant field cancellation occurs along selected lines, and components of the contaminant field vanish everywhere in certain planes. This field cancellation is exact provided that identical currents flow in all strings and that physical dimensions of the string are identical. In practice, variations will occur among the string currents, and string placement will only be realized within some, as yet, unspecified accuracy. However, current flow choices based on mathematically ideal models are still of value as initial conditions. Following the specification of the current flow direction, the contaminant fields resulting from variations in string current and string placement must be examined. If the initial condition is sensitive to various possible failure modes (large resulting contaminant fields), then other initial choices may be necessary.

The preferred current flow configuration from Ref. 1 is such that currents mirror about both the x = 0 and y = 0 planes, where the z axis is normal to the plane containing the solar array and the arms are centered about and directed along the x and y axes. The mirror-mirror condition necessitates that all blankets of the solar array are identically constructed, considered here as a generally desirable condition. The second desired property to the current flow is reversal of current direction between inboard and outboard strings of a solar array blanket. As shown in II and Fig. 6 of Ref.1 (Figure 1 of present manuscript) this condition creates four additional axes along which all components of the magnetic field vanish and four additional planes in which the z-component of magnetic field vanishes. A final desired property of the current flow is that there be a reversal of current direction between the exterior strings of a blanket (those at the edge of the blanket) and the neighboring interior string. This reversal of current causes diminution of the overall contaminant fields for points away from the various axes and planes previously described and is considered desirable in order to reduce magnetic field produced reorientation of charged particles in their movement from the space plasma to (assumed) particle detectors in the scientific payload.

The final assigned current flow condition is illustrated in Figure 1 (Figure 6 of Ref. 1). This configuration differs significantly from that utilized in Ref. 2. Figure 2 illustrates one arm of the array for the recommended current configuration and for the array advanced in Ref. 2. Indicated on the figure (Table I) are contaminant fields in the plane z = 2 meters and at selected points in x and y. Field values given there have utilized a single balanced backwire. (Note that Ref. 2 has utilized offset backwires for outboard strings. Discussion of and recommendations against such offset backwiring are given in Section II of this report). As may be noted, contaminant fields in excess of 2γ are still present at distances of 2 meters above the plane of the solar array for the Ref. 2 configuration. The recommended configuration has more points for which field cancellation occurs and reduced field levels (.7γ maximum) where cancellation has not occurred.

A final consideration here is the susceptability of a given current configuration to possible failure modes. The possible "failure" to be considered here is variation of the total current flowing in a string and its associated backwires. The contaminant field of all strings may be stated as

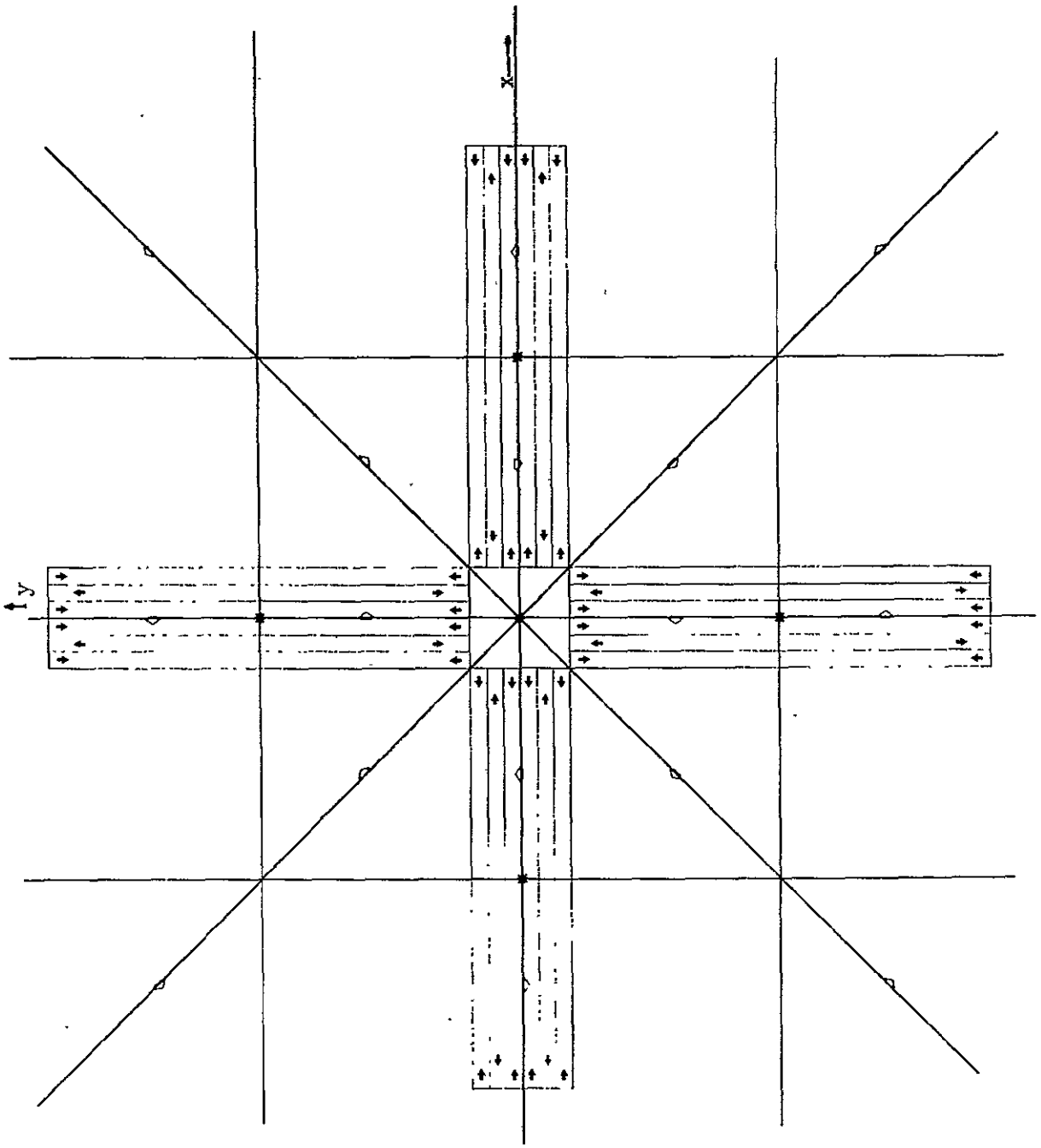

Figure 1. Solar array indicating string currents mirroring about x = 0, y = 0, x = y, and x = -y planes. $B_z = 0$ in these planes, and, y = ±(L+d) and x = ±(L+d) planes. All field components vanish on central axis of array and on central axes (*) of each arm. B_x and B_y vanish throughout z = 0 plane. Field directions at x = 0, y = 0, x = y, and x = -y planes indicated by open arrows (field does <u>not</u> connect from arrow to arrow but circulates through z = 0 plane).

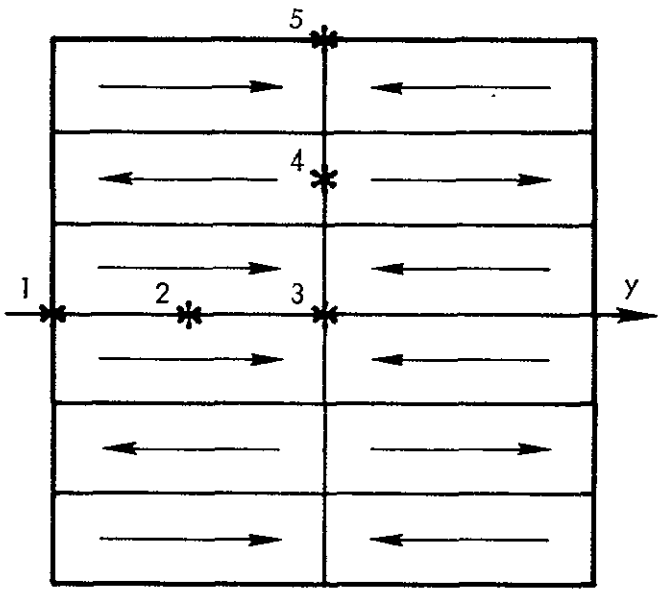

a) PROPOSED CURRENT FLOW CONFIGURATION

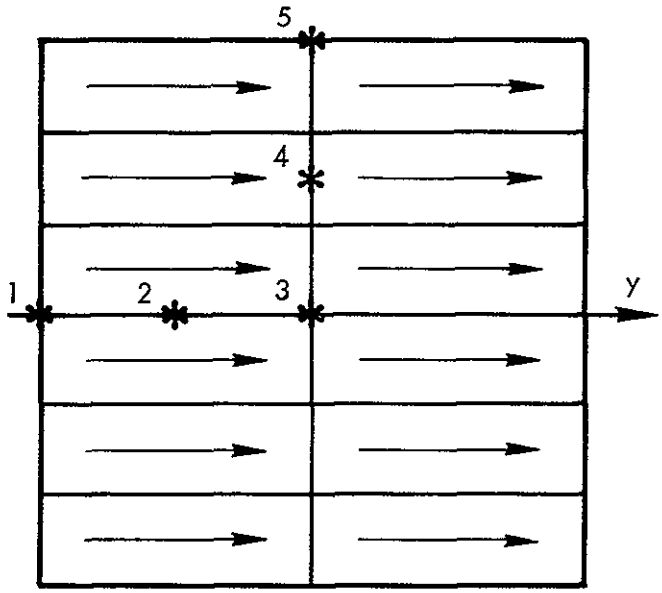

b) CONFIGURATION OF REFERENCE 2

TABLE I

B_Z	B_X	POS	B_Z	B_X
0	-0.380	1	0	-1.220
0	-0.642	2	0	-2.318
0	0	3	0	-2.412
0	0	4	-1.308	-1.956
0	0	5	-1.978	-0.732

CONTAMINANT FIELD FOR a CONTAMINANT FIELD FOR b

Figure 2. One arm of the solar cell array illustrating proposed current flow configuration and configuration advanced in Ref. 2. Table I demonstrates the effectiveness of reverse current flow with single balanced backwire as opposed to undirectional flow with single balanced backwire. Field points are indicated by (*) and 2 meters above plane of the array. B-field are in units of γ.

$$B_i = \sum_j B_{ij} \tag{1}$$

where B_i is the i^{th} component of the magnetic field, B, at a particular point in space and B_{ij} is that contribution due to the j^{th} string. The term B_{ij} may be written as

$$B_{ij} = B_o\Big|_{ij} + \frac{\partial B_{ij}}{\partial I_j} \delta I_j \tag{2}$$

where $B_o\Big|_{ij}$ occurs for I_j, the string current, at its assigned value and δI_j represents the variation away from assigned value in the j^{th} string current in the assumed failure mode. The use of a current configuration as in Figure 1 results in a condition along the z axis

$$\sum_j B_o\Big|_{ij} = 0 \text{ for all } i$$

where it is assumed that all $B_o\Big|_{ij}$ derive from equal string currents. It follows that

$$B_i = \sum_j \frac{\partial B_{ij}}{\partial I_j} \partial I_j \tag{3}$$

for that failure mode of string current variations. If the various δI_j's are independent of each other, then possible values of B_i are not demonstrably sensitive to any one particular configuration of current flow. Configurations of current flow leading to geometrically "frequent" conditions of field cancellation may be selected, then, without regard to overlying judgment on failure mode behavior for the indicated failure conditions given here.

III. BACKWIRING GRANULARITY AND PLACEMENT

A principal recommendation of Ref. 1 was that backwiring be "balanced"...i.e., that the backwire (or wires) be symmetrically located with respect to the solar cell chains carrying current in a string. If a single backwire is utilized and is centrally located, then (III.B of Ref. 1) the solar cell and backwire currents represent a series of line current quadrupoles. If the backwire is offset, the solar cell and backwire currents represent a series of line current dipoles. The dipolar contaminant field is substantially greater than that from the quadrupole configuration. Since the drop-off of fields for line current dipoles proceeds approximately with the square of the distance from a string, contaminant fields from such strings continue to distances of many meters. Offset backwiring may lead to contaminant fields on the central axis of the array of the order of the interplanetary field even for the case of the outboard strings (note that offset backwiring is utilized for outboard strings in Ref. 2). Table II gives values of $\frac{\partial B_{ij}}{\partial I_j}$ for the various field components and string placements for both balanced and offset backwires. Balanced backwiring is recommended in order to reduce contaminant field generation.

A second feature of the backwiring is the granularity of the return current circuit. By increasing the number of backwires, a more finely grained current flow configuration is generated, with consequent reduction in the contaminant field. Field reduction generally proceeds as N^{-2}, where N is the number of backwires. However, with multiple backwiring circuits it is possible, through appropriate backwire placement, to produce a nulling of the quadrupolar field. The remaining octupolar fields may be reduced by several orders of magnitude from the first condition of a single balanced backwire. Table II also lists values of $\frac{\partial^B ij}{\partial Ij}$ for a three-backwire string with backwires arranged to produce a quadrupole null.

A possible disadvantage in multiple backwiring is that the open circuit failure of a single backwire may lead to an "offset" current return condition for the remaining backwires. Contaminant fields generated as a result of such an offset, are dipolar, as noted, and large values of contaminant fields for such failure modes are given in III.D of Ref. 1. A proper failure mode analysis must consider the likelihood of such open circuits in the backwiring. However, the failure of a backwire for a string

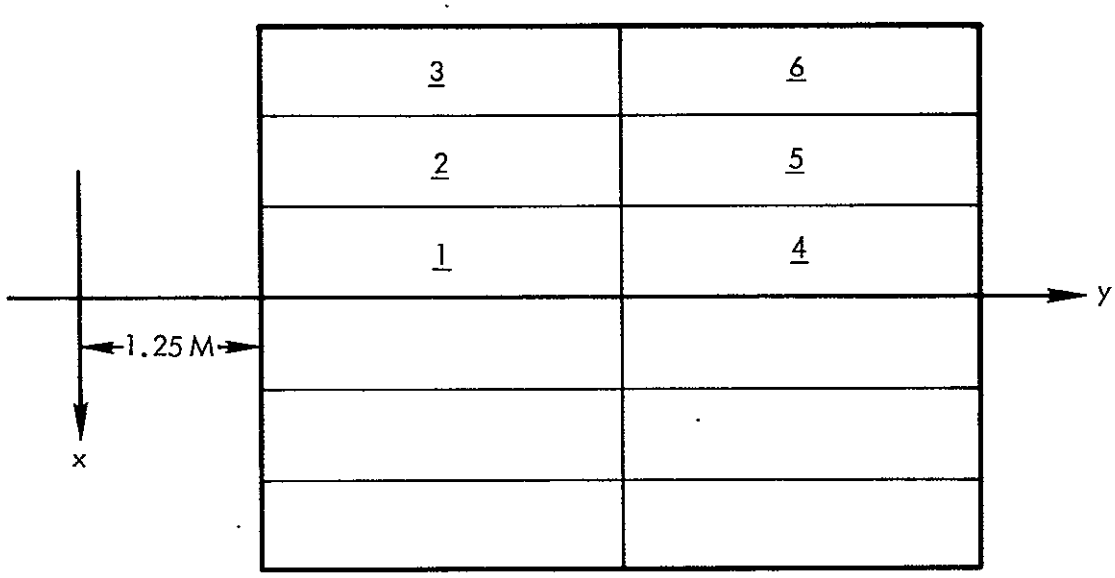

TABLE II

	SINGLE WIRE BALANCED		SINGLE WIRE OFFSET		THREE WIRE QUADRUPOLE NULL	
STRING	$\frac{\partial B_z}{\partial I}$	$\frac{\partial B_x}{\partial I}$	$\frac{\partial B_z}{\partial I}$	$\frac{\partial B_x}{\partial I}$	$\frac{\partial B_z}{\partial I}$	$\frac{\partial B_x}{\partial I}$
1	-0.0167	-0.0551	2.081	-0.192	-5×10^{-6}	-4×10^{-5}
2	-0.0427	-0.0402	1.824	-0.677	-2×10^{-5}	-4×10^{-5}
3	-0.0523	-0.0195	1.373	-0.992	-4×10^{-5}	-4×10^{-5}
4	-0.0002	-0.0006	0.160	-0.002	-2×10^{-7}	-8×10^{-7}
5	-0.0005	-0.0006	0.157	-0.008	-7×10^{-7}	-8×10^{-7}
6	-0.0009	-0.0005	0.151	-0.014	-1×10^{-6}	-7×10^{-7}

Table II. $\frac{\partial B_{ij}}{\partial I_j}$(γ/ampere) given to various field components and string placements for single balanced backwire, single offset backwire and three backwire quadrupole null. These values were calculated at x=0, y=0, and z=2 meters.

utilizing a single backwire also results in appreciable contaminant fields since it produces a total interruption in the I_j of the particular string (and loss of power). A second possible aspect of the failure mode in a multiple backwire string is a variation in resistance causing reorientation of current flow into or away from other backwires. While the two possible conditions are separately described here, they are both portions of a single failure mode condition ... i.e., current reorientation from a balanced to an offset condition in the backwires.

IV. INJECTION AND COLLECTION BUSBAR GRANULARITY

The contaminant fields discussed thus far result from currents in the solar cells and backwires. For Arm II and Arm IV these currents are "y-directed" (See Figure 1, Ref. 1) and lead to fields in the x and z directions. For Arm I and Arm III the solar cell and backwire currents are "x-directed" and produce y and z magnetic fields. The coefficients in Table II may be used for $\partial B_z/\partial I$ and $\partial B_y/\partial I$ for solar cell and backwire currents in Arms I and III. Care must be exercised in adding contaminant fields due to string current variations in the overall array.

The injection and collection busbars in Arms II and IV have currents which are x-directed and which produce y and z magnetic fields. The interest of this present section will be the magnitude of the contaminant fields for this portion of the overall current flow as a function of granularity and placement in the backwiring circuit. As will be noted, contaminant fields from current flow in these elements of the array are comparable to or in excess of the fields from solar cell and backwire currents, and appropriate treatment of injection and collection busbar geometry will be required to produce magnetic cleanliness levels suitable for interplanetary field determinations.

Equation (8) of Ref. 1 provides the quadrupolar fields due to a total current I injected centrally into a busbar with a linear decline to zero current at distance D as

$$B_\phi = \frac{\mu_o I D^2 \sin 2\theta}{16\pi r^3} \qquad \text{MKS} \qquad (4)$$

at distance r, for polar angle θ in the (θ, ϕ, r) spherical coordinate system (See Figure 18b, Ref. 1). The value of $\frac{\mu_o D^2}{16\pi} = 1\gamma$ for D = 0.2 meters, the value resulting from central injection into a string of 0.4 meters total width. Thus $\partial B\phi/\partial I = 1.0\gamma$/ampere at r = 1 meter, $\theta = \frac{\pi}{4}$. To express B_ϕ in terms of B_x and B_z in the Cartesian coordinate system of Figure 1 will require specific detail of the busbar placement on the solar array. However, overall values of 1γ/ampere at 1 meter=distance (reduced to .125 γ/ampere at 2 meters) may be considered as too large for spacecraft hoping to determine interplanetary fields. For example, the open circuit failure of a backwire leads to a δI of $\sim$ 2 amperes leading to δB_ϕ of 2 γ at 1 meter and .25 γ at 2 meters. These contaminant fields are comparable to the interplanetary fields and their appearance (upon the open circuit backwire failure) would enact severe perturbation to interplanetary field measurements.

The use of multiple backwiring results in current flows in the injection and collection busbars which produce field cancellation. Figure 20 of Ref. 1 illustrates how a three backwire (balanced) array leads to currents in backwire collection busbar which cancel or reduce fields generated by currents in the injection busbar to the solar cells. Here it is assumed that the injection busbar to the solar cells and the backwire collection busbar are similarly located in the x, y plane are separated in the z direction by only the thin layer of insulator. For the example of Figure 20, Ref. 1, the field B_ϕ at $\theta = \pi/4$, r = 1 meter and a total string current of 1.8 amperes is $.075\gamma$. The $\partial B\phi/\partial I \simeq .04$ γ/ampere at 1 meter and $\theta = \pi/4$ and .005 γ/ ampere at 2 meters and $\theta = \pi/4$. These contaminant fields are sufficient reduced to avoid perturbations to interplanetary field measurements. Finally, the collection of currents from the solar cells and the injection of these currents into the backwire system leads to a similar series of small quadrupolar fields. The significant feature here is that multiple backwiring, which serves to reduce contaminant fields from the solar cell and backwire elements, also serves to reduce the contaminant fields from the current flow in injection and collection busbars.

If the backwiring is offset, as is utilized in the outboard strings of Ref. 2, then the currents in the injection and collection busbars produce dipoler fields with magnitudes considerably increased relative to those produced with central injecion and collection. Figure 19 of Ref. 1 illustrates the current flow and resulting fields from the injection busbar with offset injection. The field is given by

$$B_\phi = \frac{\mu_o I \hat{D} \sin\theta}{8\pi r^2} \qquad \text{MKS} \qquad (5)$$

where $\hat{D}$ is the total length of the injection busbar, I is the busbar injection current (which diminishes linearly to zero at distance $\hat{D}$) and ϕ is the aximuthal coordinate in a (θ, ϕ, r) system. For 1.6 amperes and $\hat{D}$ = .4 meters, $B_\phi = \frac{32 \sin\theta}{r^2}$ where B_ϕ in γ and r in meters. It may be noted that fields of the 1 γ level result here even from separation distances of 5-6 meters (inboard end of the outboard strings) from the central axis of the array. The term $\frac{\partial B_\phi}{\partial I}$ is 20 γ/ampere at 1 meter and is 0.8 γ/ampere at 5 meters. At the central axis, these contaminant fields are comparable to the interplanetary field for even the outboard location of a string, and offset injection or collection is not recommended if interplanetary magnetic field measurements are to be perfórmed by the spacecraft. It should be noted that balanced backwiring, which substantially reduces the contaminant fields from the solar cells and backwires from the level produced with offset backwiring, also leads to a condition of balanced injection and collection of currents.

V. SOLAR ARRAY BLANKET INJECTION AND COLLECTION BUSBAR CURRENTS

The currents from the several strings of a blanket of the array are brought to and injected from a pair of busbars located on the inboard edge of the inboard strings. Since this edge of the array is in close proximity to the spacecraft and its scientific payload, and since the level of current flow is large (summing the various strings), the geometrical disposition of the current flow is of particular concern. If the busbar geometry and current flow leads to dipolar fields, then contaminant fields from these busbars may reach levels many times larger than the interplanetary field. In the configuration utilized

in Ref. 2, such high level contaminant fields will result. The essential aspects of the currents and geometry of the Ref. 2 injection and collection busbars are given in Fig. 3 of this report. The dipolar field from one of the bars is approximately $B_\phi \sim \frac{200\gamma}{r^2}$ and the location of an oppositely directed current at a distance of h introduces a factor of h/r in the resulting total field. Since h $\sim$ .08 meters (see Ref. 2), the general level of the contaminant field from the busbar pair is $\sim 16\ \gamma/r^3$. For r = 2 meters, this contaminant field is still in excess of 2 γ and is a severe perturbation to interplanetary field measurements. (Note that the geometry utilized in Ref. 2 does <u>not</u> produce a mirror-mirror current configuration for current flow in these elements and field cancellation on the central axis of the array does not result, even for mathematically exact current flows in all strings of the array.)

A modification of the busbar placement for the busbars collecting and injecting the string currents is shown, together with backwiring curcuits, in Fig. 4. The arrangement is "balanced" in the flow of current on the solar array blanket. Elements A-A′ produce a quadrupolar field while elements B-B′ produce a quadrupole field of reversed polarity. Taken together, A-A′ and B-B′ produce an octupolar field. A corresponding result obtains for C-C′ and D-D′, and C-C′, D-D′ comprise an octupole whose polarity is the reverse of the A-A′-B-B′ octupole. The longer length of C-C′-D-D′ does result in a larger octupole moment than A-A′-B-B′ so that elimination of the octupole moment does not occur. Note, however, that the balanced withdrawal of current from the array blankets does result in a mirror-mirror current configuration which produces total field cancellation along the central axis of the array for mathematically exact current flows in all strings.

VI. RECOMMENDATIONS

The discussion of the previous sections leads to the following recommendations:

1) Construction of the overall array should yield current flows which have a mirror-mirror configuration about the x = 0 and y = 0 planes (see Fig. 1). This requires identical construction of all array blankets and "balanced" construction on each blanket (for example, see the backwiring and busbar placement of Fig. 4).

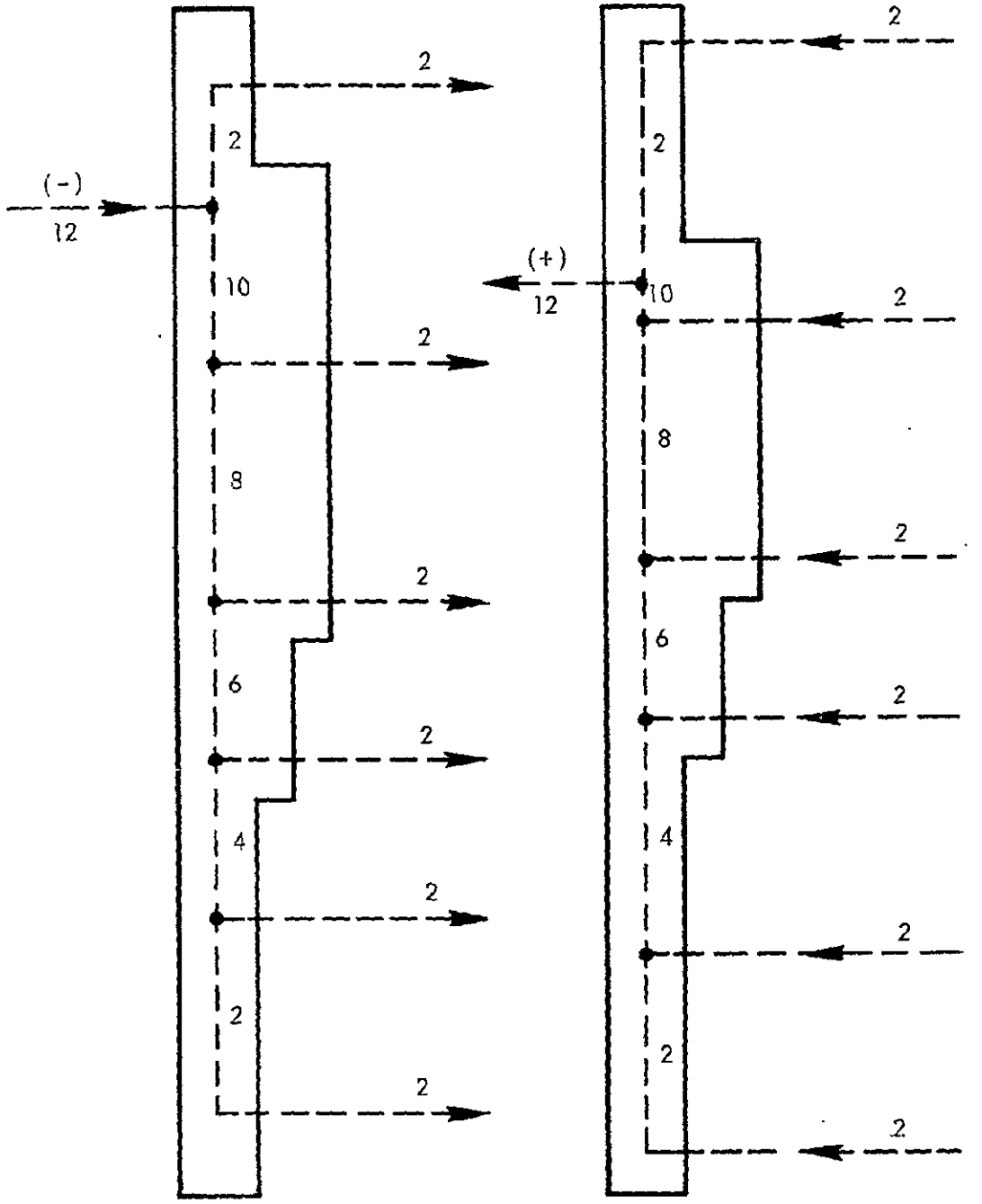

Figure 3. Collection and injection busbars for blanket of solar array. (Not to scale). Busbar length is ∿ 1.2 meters and busbar separation is ∿ 0.08 meters. Figures indicate approximate current in amperes. (Ref. 2)

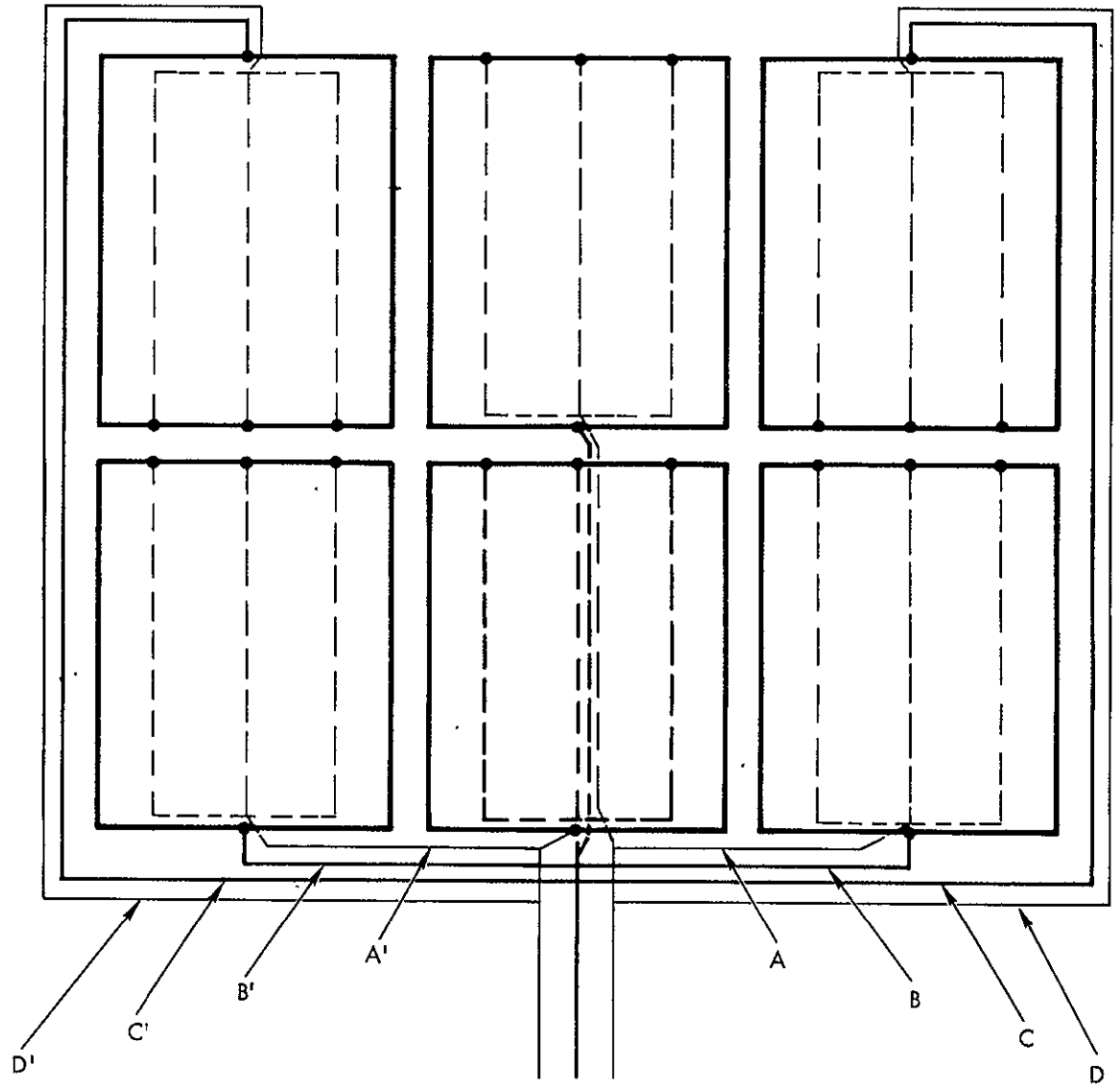

Figure 4. Recommended collection and injection busbar configuration. Multiple backwiring (3 balanced backwires) is utilized. Thin lines represent collection current path, and thick lines represents injection current path. Collection currents A-A′ and injection currents B-B′ produce octupole fields. Similarly collection currents D-D′, and C-C′ produce octupole fields of reverse polarity, however, of slightly larger magnitude.

2) Solar cell current flow direction should reverse between the inboard and the corresponding outboard string of a solar array blanket (see Fig. 4).

3) Solar cell current flow direction should reverse between the exterior (blanket edge) strings and the corresponding interior strings of a solar array blanket (see Fig. 4).

4) Backwiring for the solar cells of a string should be balanced (Fig. 4). Offset backwiring should not be utilized. Injection and collection of solar cell currents on a string should be central. Offset injection and collection should not be utilized.

5) Multiple backwiring should be used for the various strings, both inboard and outboard. Three wire backwire systems with spacing such as to produce a "quadrupole null" are recommended.

6) Busbars collecting the string currents for a solar array blanket should be balanced on the blanket. Arrangements to produce opposing quadrupoles reduce the overall moment of these busbars to that of opposing octupoles are illustrated in Fig. 4.

7) An engineering failure mode analysis should be made for the failure mode of an open circuit backwire condition.

REFERENCES

1. Contaminant Magnetic Fields from Large Area Solar Arrays, J. M. Sellen, Jr. and H. S. Ogawa, TRW 12738-6006-R000, 16 June 1969.

2. "Feasibility Study -- 30 watts per pound Roll-up Solar Array" NAS7-100, General Electric Report no. 68 SD 4301, June 1968.

SECTION IV. C.

MEASUREMENTS OF EQUILIBRATION POTENTIAL BETWEEN A PLASMA "THRUST" BEAM AND A DILUTE "SPACE" PLASMA

AIAA Paper
No. 69-263

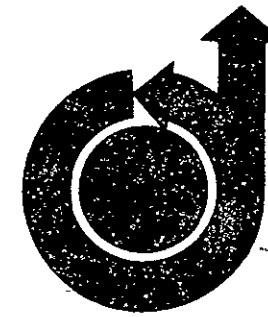

MEASUREMENTS OF EQUILIBRATION POTENTIAL BETWEEN A PLASMA "THRUST" BEAM AND A DILUTE "SPACE" PLASMA

by

H. S. OGAWA, R. K. COLE
and
J. M. SELLEN, JR.
TRW Systems
Redondo Beach, California

AIAA 7th Electric Propulsion Conference

WILLIAMSBURG, VIRGINIA/MARCH 3-5, 1969

MEASUREMENTS OF EQUILIBRATION POTENTIAL BETWEEN A PLASMA "THRUST" BEAM AND A DILUTE "SPACE" PLASMA*

ABSTRACT

Equilibration potentials of a dense "thrust" beam coupled to a dilute "space" plasma have been measured. Thrust beams were 5.0-mamp Cs^+ ion beams at 200 eV ion energy, 2 μpervs perveance, source aspect ratio ~ 22, initial beam densities $> 10^9$ ions/cm^3, with immersed unipotential hot wire neutralization. Space plasmas were Cs^+ plasma wind tunnel streams uniform in density over the total interaction volume of the two plasmas. Space plasma density was varied from 10^6 to 10^7 ions/cm^3 for the experiments. Length of thrust beam in equilibration with space plasma was limited to 40 cm for present wind tunnel geometries. Thrust beam axis was transverse to wind tunnel flow. Tests of simple equilibration models were provided. Measured potentials were in agreement with this model for density ratio of $\sim 10^2$ between dense and dilute plasmas but were in disagreement for density ratios of $\sim 10^3$. Plasma beam-space plasma conductances have been determined.

I. INTRODUCTION

The plasma thrust beam from an electrically propelled spacecraft is released into a space which already contains, in general, a dilute ambient plasma. At distances far from the spacecraft, the density of the plasma thrust beam diminishes to levels which are small compared to the space plasma and conditions in the space are, essentially, unperturbed. For regions near the spacecraft, thrust beam densities in general greatly exceed local plasma densities. Interaction between these two plasmas occurs from the spacecraft, through the near regions and to the "merge" point at which beam densities have diminished to ambient densities.

*This work was performed for the Jet Propulsion Laboratory, California Institute of Technology, sponsored by the National Aeronautics and Space Administration under Contract NAS7-100 and NAS7-564.

The electric field structure through the two plasmas influences charged particle motion and sets up particle interchange currents. In steady state, if such conditons exist, the particle densities are constant and surfaces may be defined along which net current densities everywhere vanish.

The interest of this paper will be the electrical equilibration between the plasma thrust beam and an ambient plasma. The potential structure through the two plasmas will be derived for a simplified equilibration model. Particle currents resulting from perturbations away from the equilibrium potential structure will be related to a resistance model of the plasma-plasma system. Experiments in plasma wind tunnels of the equilibration between a "thrust" beam and "space" plasma will be described and results will be related to equilibration models.

II. THRUST BEAM DENSITY AND POTENTIAL STRUCTURE

Density measurements in initially cylindrical neutralized high perveance ion thrust beams[1,2] have shown such beams to be essentially "conical"--that is, straight line ion trajectories directed from an apparent focal point--and to possess approximately a "uniform core-exponential wing" radial density distribution. These features are illustrated in Figure 1 where $z = 0$ is the point of release of the accelerated ions, and $z = -z_o$ is the apparent point of origin for the ion rays. The density distribution for the ions is given by

$$(1)\quad \rho_b(r,z) = \rho_{bo}\left(\frac{z_o^2}{(z+z_o)^2}\right) \qquad 0 \le r \le r_{co}\left(\frac{z+z_o}{z_o}\right)$$

$$(2)\quad \rho_b(r,z) = \rho_{bo}\left(\frac{z_o^2}{(z+z_o)^2}\right)\exp\left\{-\frac{r - r_{co}\left(\frac{z+z_o}{z_o}\right)}{a_o\left(\frac{z+z_o}{z_o}\right)}\right\} \quad r \ge r_{co}\left(\frac{z+z_o}{z_o}\right)$$

The radius of the core region at $z = 0$ is r_{co} and the exponential fall-off distance at $z = 0$ is a_o and ρ_{bo} is ion density at $r = 0$, $z = 0$.

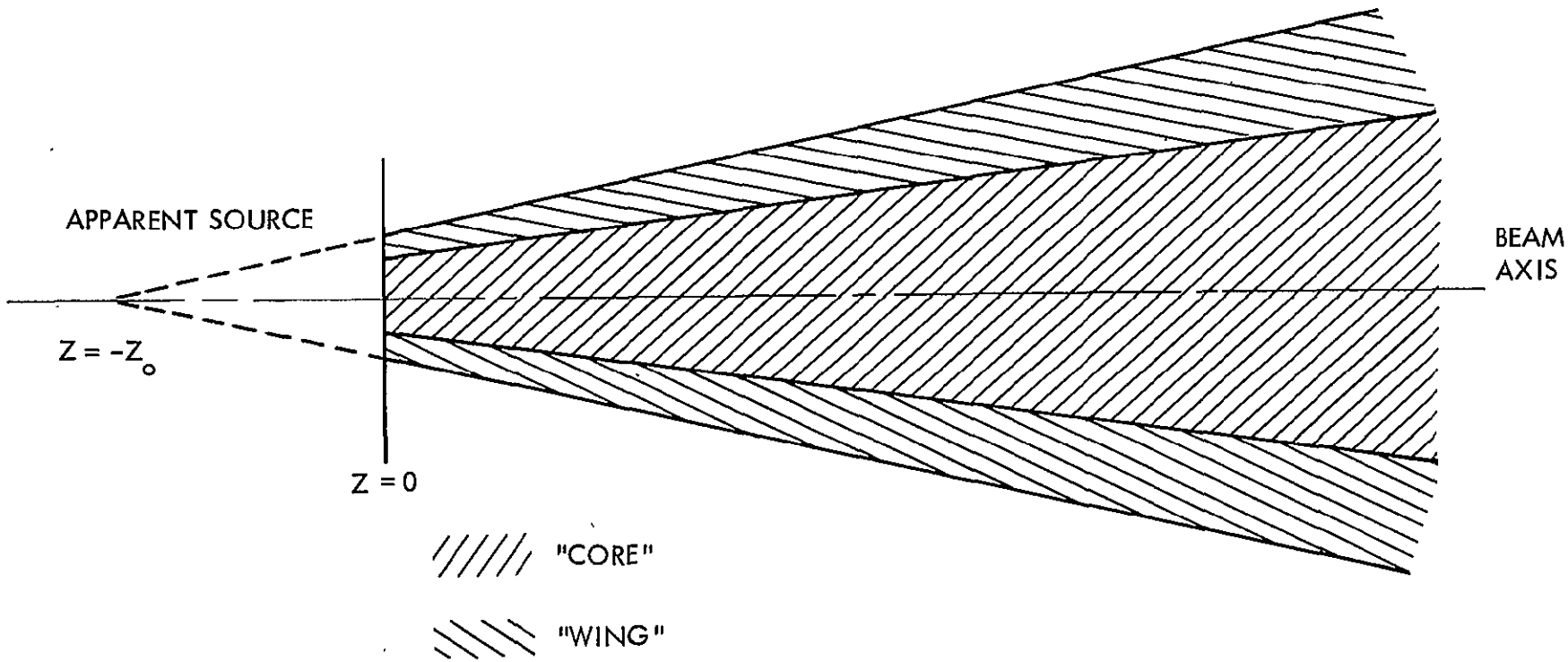

Figure 1. Ideal "Uniform Core-Exponential Wing" Model of Conical Plasma Beam.

For high perveance ion thrust beams, the Debye length, λ_D, in the neutralized plasma is small compared to the beam diameter D_b. Electron densities must be, then, substantially equal to ion densities on a point by point basis. If the ion density were perfectly uniform over distances of a great many Debye lengths, then exact charge neutrality between ions and electrons would occur throughout any region of at least a few Debye lengths in extent. Ion densities in actual beams are not perfectly uniform, even in the core region. The core region, moreover is of limited extent, and, outside of it there exist substantial particle density gradients. These particle density gradients and the existence of a finite temperature of the neutralizing electrons necessarily lead to potential gradients in the plasma column. The quasi-neutrality relationship allows a statement of potential in the plasma relative to particle density and electron temperature. From it

$$\rho_b = \rho_{bo} \exp\left(-\frac{eV}{kT_e}\right) \tag{3}$$

where ρ_b is particle density and V is potential at a point (r,z), e is the electron charge (= - 1.6 x 10^{-19} coulombs), k is Boltzman's constant, and T_e is electron temperature. Here V = 0 at (r,z) = 0, by definition. Note that V < 0 for $\rho_b < \rho_{bo}$. Thus, in moving from the high density region at the origin of the beam to the outer, low density regions, a negative excursion in potential is realized. This negative potential may also be viewed as the self-consistent mechanism which prevents electrons, with their high mobility, from escaping the confines of the plasma stream and which requires, moreover, that electrons everywhere exist in substantially equal densities to the ions. The effects of this potential on ion motion have not been taken into account in the ion density distribution. The assertion of a "conical" beam neglects ion divergence through "electron pressure" effects. Such assertions are reasonable if kT_e is $<<< \frac{M_+ v_+^2}{2}$, the ion acceleration energy.

Equation 3 is the electrostatic equivalent of the barometric equation for neutral particle density in a gravitational field. Conditions for the validity of such an equation are that net diffusion is everywhere zero. In the plasma thrust beam this condition is only partially upheld. Electron diffusion in the radial direction is zero at any fixed axial location. However, axial diffusion of electrons in thrust beams exhausted into space (or against floating collectors in laboratories) must be such that the average electron z velocity, $\langle v_e \rangle_z = v_+$, the ion streaming velocity. In a series of experiments on potential structure in neutralized thrust beams (Ref. 1), Eq. 3 was verified for both radial and axial excursions in the plasma column. A possible explanation is, since average electron thermal velocities $\langle v_e \rangle$ are >> than v_+, that $\langle v_e \rangle_z = v_+$ is, essentially, a condition of zero diffusion and that the potential structure is not greatly altered by the requirement that average electron axial velocity, instead of being zero, must equal ion axial velocity.

From Eq. 3 the equidensity contours in the plasma column are also equipotential contours, provided that T_e is uniform throughout the beam. This constancy of T_e may not occur in practice. Experiments on neutralized beams in large chambers have indicated downstream cooling of the neutralizing electrons.[2] For present purposes, however, T_e will be assumed constant throughout the beam.

A final point here is that Eq. 3 is not dependent upon the specific form of the density distribution. Equidensity contours remain equipotential contours, whatever the exact shape of the equidensity contours may be.

III. THRUST BEAM DIRECTED INTO A DILUTE SPACE PLASMA

From (1) and (2), for sufficiently large r or z, arbitrarily small values of ρ_b may be encountered in the plasma beam. Also, the potential excursion between (r,z) = 0 and (r,z),

$$V = \frac{-kT_e}{e} \ln\left(\frac{\rho_b}{\rho_{bo}}\right) \qquad (3')$$

is not limited to any maximum value, but may increase arbitrarily for sufficiently small values of ρ_b. While such conditions might occur in a perfect vacuum, the thrust beam released into space is in the presence of a dilute ambient plasma. For sufficiently large r or z the level of beam density, ρ_b, diminishes to the space plasma densities, ρ_{sp}. The axial point at which $\rho_b = \rho_{sp}$ has been previously referred to as the "merge" point, although, indeed, "merging" occurs along the entire equidensity contour $\rho_b = \rho_{sp}$.

The presence of the space plasma introduces a lower bound to the particle density which may exist in the plasma-plasma system. This lower bound, in turn, would appear to set an upper limit on the potential difference between (r,z) = 0 and points throughout the whole of the space plasma. For conditions in which T_e is the same in both space and beam plasmas, this potential difference would be

$$\hat{V} = \frac{-kT_e}{e} \ln\left(\frac{\rho_{sp}}{\rho_{bo}}\right) \qquad (3'')$$

From this limiting potential it can be seen that electric fields in the plasma-plasma system would essentially vanish along the merging contour and everywhere outside of it. Potential gradients would exist inside the merging contour from the particle density gradients in these "beam" regions.

Beyond the merging contour the beam particles become less and less dense compared to space plasma particles, and, inside the merging contour, beam particles predominate, so that, although there is interpenetration of the two plasmas, separate regions may be identified as "beam" and "space" plasmas. This regional distinction is, for the better part, limited to ions. Interchange reactions make it difficult to assign "beam" or "space" to electrons in regions downstream from the neutralizer at distances greater than the electron interchange length.

Electron interchange along the merging contour will differ somewhat from one point on the contour to another. At small axial distances the equidensity contour contains the ion trajectory and consequently the ion current density across the contour is zero. Here the radially outward diffusion of "beam" electrons provides an electron flux density of $\frac{\rho_b \langle v_e \rangle}{4}$ (assuming random orientation of the radial electron velocities). These outward diffusing beam electrons interchange with inward diffusing space plasma electrons whose flux density is $\frac{\rho_{sp} \langle v_e \rangle}{4}$. Since $\rho_{sp} = \rho_b$ along the merging contour (and $\langle v_e \rangle$, electron thermal velocities, are assumed everywhere equal), then outward and inward fluxes of electrons balance. Interchange processes occur, but with zero net flux.

The electron interchange between beam and space plasmas may be considered to be essentially complete when 50% of those electrons initially injected into the thrust beam from the neutralizer have interchanged with space plasma electrons. Derivations of this interchange length are given in Ref. 3. Sample calculations, also Ref. 3, for typical thrust beams in the lower ionosphere and in interplanetary space reveal interchange lengths of ~ 6.5 meters and ~ 2.35 KM. In each instance, interchange occurs at axial distances small compared to the axial position of the merge point.

Along the merging contour at axial positions near the axial merge point, ion trajectories do result in a net ion flux across the contour. Here, electron flux in the outward direction must balance the inward diffusing electron flux and also provide an extra component to current neutralize the ion flow. If this condition can, indeed, occur, then the net current vanishes on a point-by-point basis along the entire merging contour. The simplified equilibration model presented here assumes such a point-by-point balance. Experimental evaluations of such "large geometry" plasma interactions have not been carried out, being subject to the limitations of laboratory facilities, Sec. VI.

The vanishing of the net current density everywhere along the merging contour satisfies the condition of an electrically isolated plasma beam source--that ion and electron currents from this system balance. It should be noted that balance of total currents might occur without having a

point-by-point balance along any closed contour. The possibility of recirculating current loops through the beam and space plasma regions is present. Variations of electron temperature along the plasma thrust beam or variations in temperature between beam and space electrons could result in electron diffusion patterns locally non-zero, and only satisfying charge and current neutralization requirements when summed over large interaction regions.

Finally, it should be noted that the potential defined in Eq. 3" is a statement of the potential difference from the space plasma to the origin of the thrust beam. The equilibration potential of the spacecraft relative to the space plasma involves other potential increments. To determine this equilibration potential, a knowledge of the neutralizer injection potential, V_{inj}, is required. Further, a knowledge of neutralizer bias potential, V_{bias}, relative to the spacecraft is required. The proper summation of $\hat{V} + V_{inj} + V_{bias}$ allows the equilibration potential of the spacecraft, V_{eq}, to be determined. This equilibration potential need not be zero. In general, some value of potential difference will exist between the spacecraft and the space plasma. Depending upon geometrical factors, insulating surfaces, and equilibration potentials, currents of charged particles will flow from the space plasma to the vehicle. These currents impose perturbations on the equilibrium condition. To estimate the perturbation which such currents impose on the equilibration, a knowledge of resistances of the return path from the spacecraft to the space plasma via the thrust beam is required. The following section will detail identifiable elements of the resistive chain for the return to the space plasma of perturbation currents.

IV. CONDUCTIVITIES IN THE SPACECRAFT PLASMA-PLASMA SYSTEM

This section will discuss the effects on the potential difference between the spacecraft and the space plasma due to currents to the spacecraft and variations in these currents.

If the spacecraft is somehow electrically insulated so that no currents may flow from the plasma to the spacecraft except through the propulsion system, then the magnitude of the neutralizer current must equal the positive ion current. Under this equilibrium condition a potential difference, V_{eq}, exists between the spacecraft and the space plasma. A current from the ambient space plasma to the spacecraft will cause a corresponding change in the neutralizer current and will change the potential between the craft and the space plasma. We will assume in the following discussion, unless otherwise stated, that the current to the spacecraft is small compared to the thrust beam current, and its effect will be considered as a perturbation on the neutralizer current. The change in potential, δV, between the spacecraft and space environment produced by this perturbation current involves the conductivities or resistivities of this spacecraft-plasma-plasma system. Such conductivities are complicated by geometric factors, properties across various sheaths, and particle density gradients, and there are no a priori assurances of linearity. The resistance chain for a perturbation current from the spacecraft to the space plasma is illustrated in Fig. 2. For this chain some five elements of resistance have been denoted. The first of these is R_{sc-n}, the resistance from the spacecraft to the neutralizer. The second term, R_{n-tb}, is the neutralizer sheath resistance to the thrust beam. This is a dynamic resistance term, $\frac{\delta V_{inj}}{\delta i}$, where V_{inj} is the potential difference from the neutralizer to the thrust beam plasma and δi is a perturbation current flow. A similar dynamic resistance term, R_{tb-mc}, exists for the thrust beam plasma to the merging contour. Potentials are uniform along the boundaries of the neutralizer sheath and along the merging contour, under normal conditions. It will be assumed that equipotential surfaces remain unchanged in shape for the perturbation current flow δi. The dynamic resistances defined by $\frac{\delta V}{\delta i}$ are taken between equipotentials and are not dependent on reference to specific points on these surfaces. R_{mc} defines the resistance from the thrust beam to the space plasma across the merging contour and R_{sp} the resistance from the merging contour to the spacecraft sheath. Only the first resistance, R_{sc-n}, is of the conventional linear form.

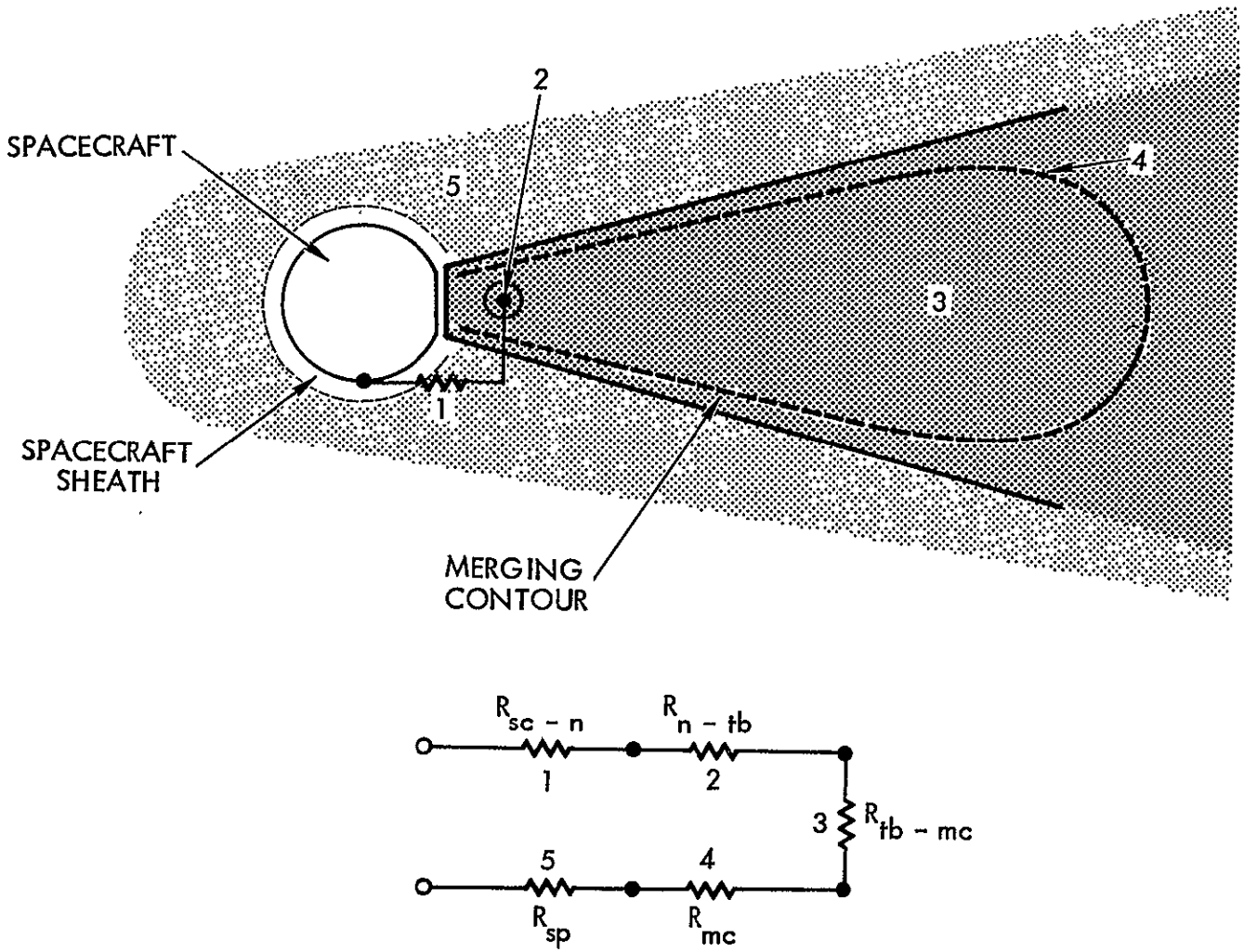

Figure 2. Spacecraft-Thrust Beam-Space Plasma System. Resistive Chain for Perturbation Current from Spacecraft to Space Plasma Shown.

Some indications of R_{n-tb} for various methods of electron injection are given in Ref. 4 and Ref. 5. Experimental values relative to this term are described in Sec. V and VI. R_{tb-mc} is not subject to simple description. It must be emphasized that this quantity is determined from $\frac{\delta V}{\delta i}$ considerations, here being the variation in the potential at the merging contour relative to the potential at the thrust beam origin for a perturbation current flow. Note that under normal beam operating conditions the flow of neutralizing electrons moves from the origin to distant regions at potentials which are negative with respect to the beam origin. A resistance defined in terms of steady state values would be a negative resistance. However, the particle flow under normal conditions is governed by electron mobility and by particle density gradients and is not the quantity of concern for perturbation currents for which the resistance term $\frac{\delta V}{\delta i}$ is relevant and is positive.

The resistance across the merging contour is discussed further in Sec. VI. R_{sp} will not be treated further here.

The total resistive chain in Fig. 2 can be used, in principle, to measure the shift in the spacecraft equilibration potential relative to the space plasma for a specified perturbation current flow, $\delta V = R_{chain}\ \delta i$.

A second system which simulates some of the aspects of the plasma-plasma system in Fig. 2 is illustrated in Fig. 3. Here, a "thrust" beam is allowed to couple to the "space" plasma of a plasma wind tunnel stream. R_{n-tb} is, again, the neutralizer sheath resistance, R_{tb-mc} is the resistance from the thrust beam origin to the merging contour, R_{mc} is the resistance across the merging contour, R_{sp} is the resistance from the merging contour to the beam origin of the plasma wind tunnel, and R_{sp-n} is the sheath resistance of the plasma wind tunnel neutralizer. $R_{tbn,meas}$ and $R_{spn,meas}$ are small measuring resistors to determine current flow as a function of potential shift across the terminals of the resistance loop.

An estimate of the resistance across the merging contour may be obtained from the following simple model. The current density of outward diffusing electrons is $\frac{e\rho\langle v_e\rangle}{4}$ where ρ is the electron particle density at

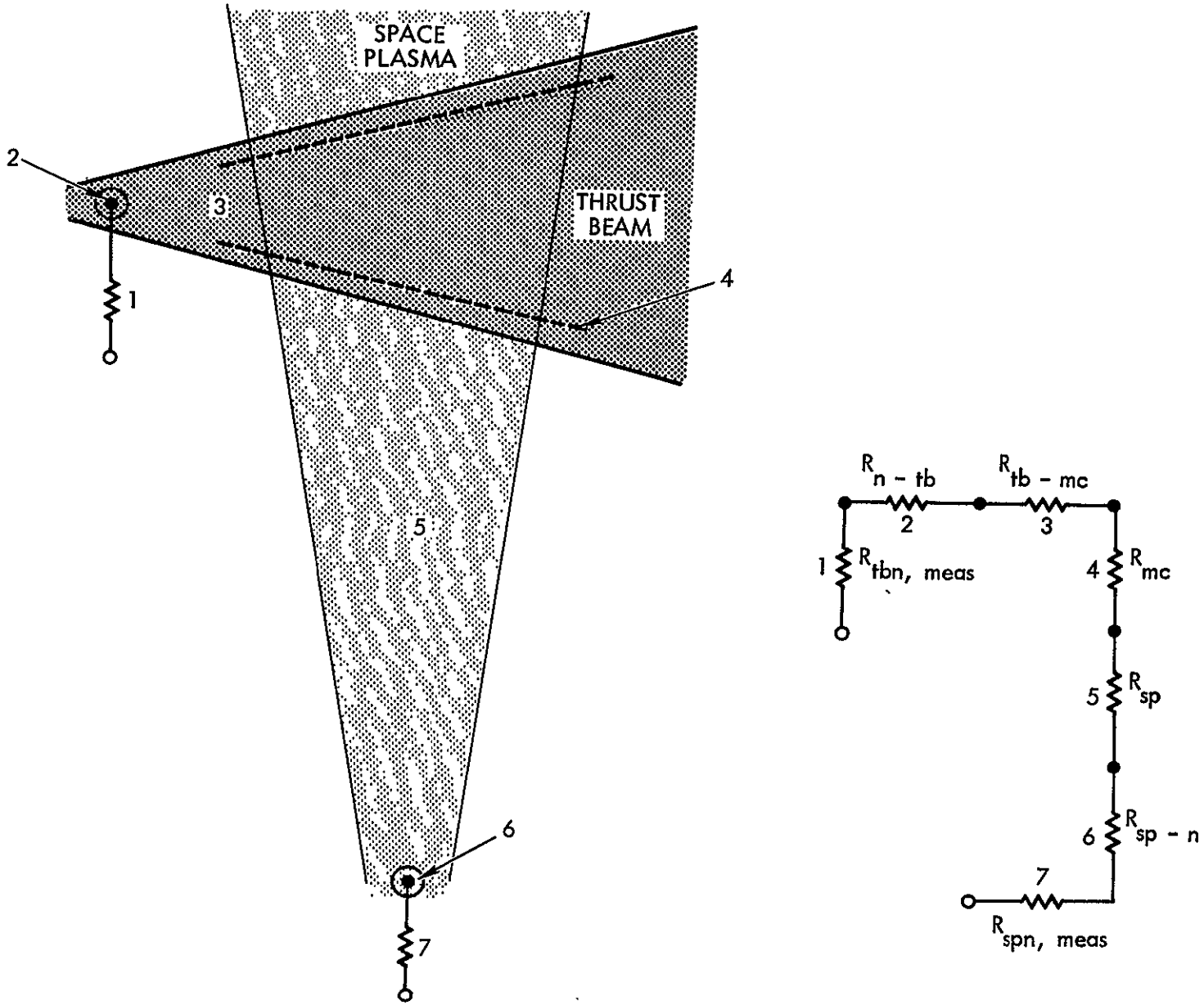

Figure 3. Experimental Configuration for Spacecraft Thrust Beam-Space Plasma System. Resistive Loop Shown.

the merging contour ($= \rho_{sp}$). The functional dependence on this outward current upon an incremental change in potential, V', across this merging sheath is

$$j_-\Big|_{out} = \frac{e\rho_{sp}\langle v_e\rangle}{4} \exp\left(-\frac{eV'}{kT_e}\right) .$$

The inward diffusing electron current density is also $\frac{e\rho_{sp}\langle v_e\rangle}{4}$, (thus, balancing outward diffusion in the absence of potential increments across the sheath). The dependence of this inward current flow to changes in V' across the merging sheath is set here as

$$j_-\Big|_{in} = \frac{e\rho_{sp}\langle v_e\rangle}{4} \exp\left(\frac{eV'}{kT_e}\right) .$$

The net current density outward is $j_-\Big|_{out} - j_-\Big|_{in}$ and is

$$j_-\Big|_{net} = \frac{e\rho_{sp}\langle v_e\rangle}{4}\left\{\exp\left(-\frac{eV'}{kT_e}\right) - \exp\left(\frac{eV'}{kT_e}\right)\right\} .$$

The $$\frac{\partial j_-\Big|_{net}}{\partial V'} = \frac{e\rho_{sp}\langle v_e\rangle}{4}\left(-\frac{e}{kT_e}\right)\left\{\exp\left(-\frac{eV'}{kT_e}\right) + \exp\left(\frac{eV'}{kT_e}\right)\right\}$$

For $V' \to 0$, $\frac{\partial j_-}{\partial V'} \to \frac{e\rho_{sp}\langle v_e\rangle}{4}\left(\frac{-2e}{kT_e}\right)$. Expressed as a resistance

$$\frac{\partial V'}{\partial j_-}\Big|_{net} \simeq \left(\frac{2kT_e}{-e}\right)\left(\frac{1}{e\rho_{sp}\langle v_e\rangle}\right) . \qquad (4)$$

The resistance here given is negative (increasing negative current across the sheath for a positive potential increment, V'), but this is a conventional resistive term. As an example of resistive values, for $\rho_{sp} = 10^6$ electrons/cm^3, $v_e = 4 \times 10^7$ cm/sec, and $\frac{kT_e}{e} = .25$ electron-volts, this resistance is $\approx 80{,}000\ \Omega\ \text{cm}^2$. The area of the merging contour between a thrust beam of an ion engine and a space plasma of 10^6 ions/cm^3 is of the order of 10^5 cm^2, and since these resistive elements are in parallel, the resistance across the entire merging contour may be $\approx 1\Omega$. Smaller values of total contact area, as imposed by plasma wind tunnel geometries, lead to larger resistance values.

The experiments described in Sec. V and discussed in Sec. VI, allow some determination of the resistive terms illustrated in Fig. 2. Since large variations in geometry and plasma density may exist between the real space condition and these laboratory tests, present results can only be considered as qualitative descriptions of the space interactions.

V. PLASMA-PLASMA EQUILIBRATION EXPERIMENTS

Experimental studies of electron interchange between a "spacecraft thrust beam" and a "dilute space plasma" were conducted to determine equilibration potentials, plasma-plasma resistance, and to verify, if possible, the predictions of the simple equilibration model. The streaming Cs^+ plasma (simulated space plasma) was generated in the 4' x 8' plasma wind tunnel and emerged through a 40 cm circular aperture into a cylindrical extension chamber (1.25' diameter by 4' length). The plasma terminated on collector #1 which was 3.5 m downstream from its source. The four outer collector rings which formed the aperture in the 4' x 8' chamber and the wall liners of the extension chamber were electrically isolated in order to minimize electric field perturbations on the beam. A "spacecraft" ion engine was mounted on the extension chamber such that the axis of the thrust beam was perpendicular to the axis of the streaming space plasma. The intersection of the two plasma axes was 3.25 m from the space plasma source and 32 cm from the spacecraft ion engine. The thrust beam terminated on collector #2, 63 cm downstream and outside the ambient space plasma. See Fig. 4.

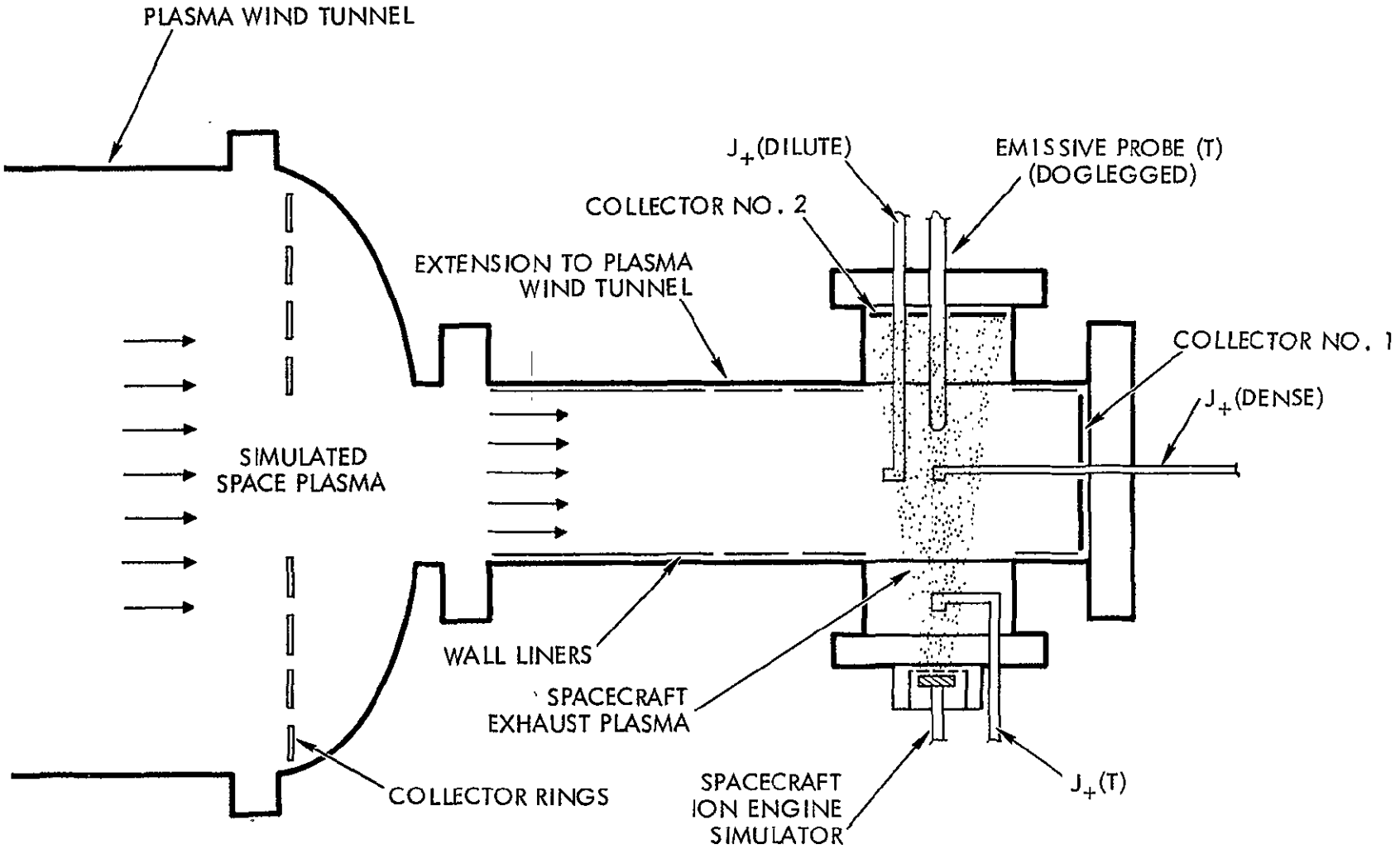

Figure 4. Test Geometry for the Plasma-Plasma Equilibration Experiments Showing Plasma Wind Tunnel, Extension Chamber, Simulated "Space Plasma", and "Spacecraft Thrust Beam Plasma" and Plasma Diagnostic Instruments.

The schematic diagram showing the electronics and the interacting plasmas is given in Fig. 5. The electrical systems for both plasma sources were essentially the same. However, the spacecraft common or ground was electrically isolated from the vacuum chamber wall or Earth ground. By opening a single switch the spacecraft could be electrically isolated, interacting only with the space plasma. Both neutralizers were heated to the same temperature (2500°K) by identical half wave rectified power supplies which were in phase. By doing so the electron temperature in both plasmas would be approximately equal in the interaction region. The pulse width of the acceleration potentials were identical and were out of phase with the neutralizer heating cycle so that both neutralizers were unipotential during the plasma "on" time. By varying the timing of the trigger to the pulsed acceleration voltage power supplies, the two plasma beams could be separated or overlapped in time.

The experiments were performed with both source voltages V_{S1} and V_{S2} equal to +200 V. The pulse width of each source was 2 ms; the grid voltages were both equal to -100 V. The neutralizer bias potential of source #1, V_{N1}, was set equal to +10 V, and the bias on the neutralizer of source #2 was adjusted so that the emission current from each neutralizer remained constant whether the beams were separated or overlapped in time. There is, thus, no net flow of electrons from one plasma to another, satisfying the required conditions of balanced electron interchange for electrically isolated plasma thrust beams in space. This condition occurred when V_{N2} = +10.25 V. This does not mean that the potentials of the two plasmas are only separated by approximately .25 V. The potential of the dense thrust beam is approximately the neutralizer potential. However, the long path length and the density dimunution from the beam source to the interaction region for the dilute plasma beam results in potential increments of approximately 1.5 V, in keeping with the quasi-neutrality relationship, and thus the condition of balanced interchange actually occurs with a potential separation between the interior of the dense plasma thrust beam and the dilute space plasma of approximately 1.5 V. Further discussion of these potential differences will be given in a following paragraph.

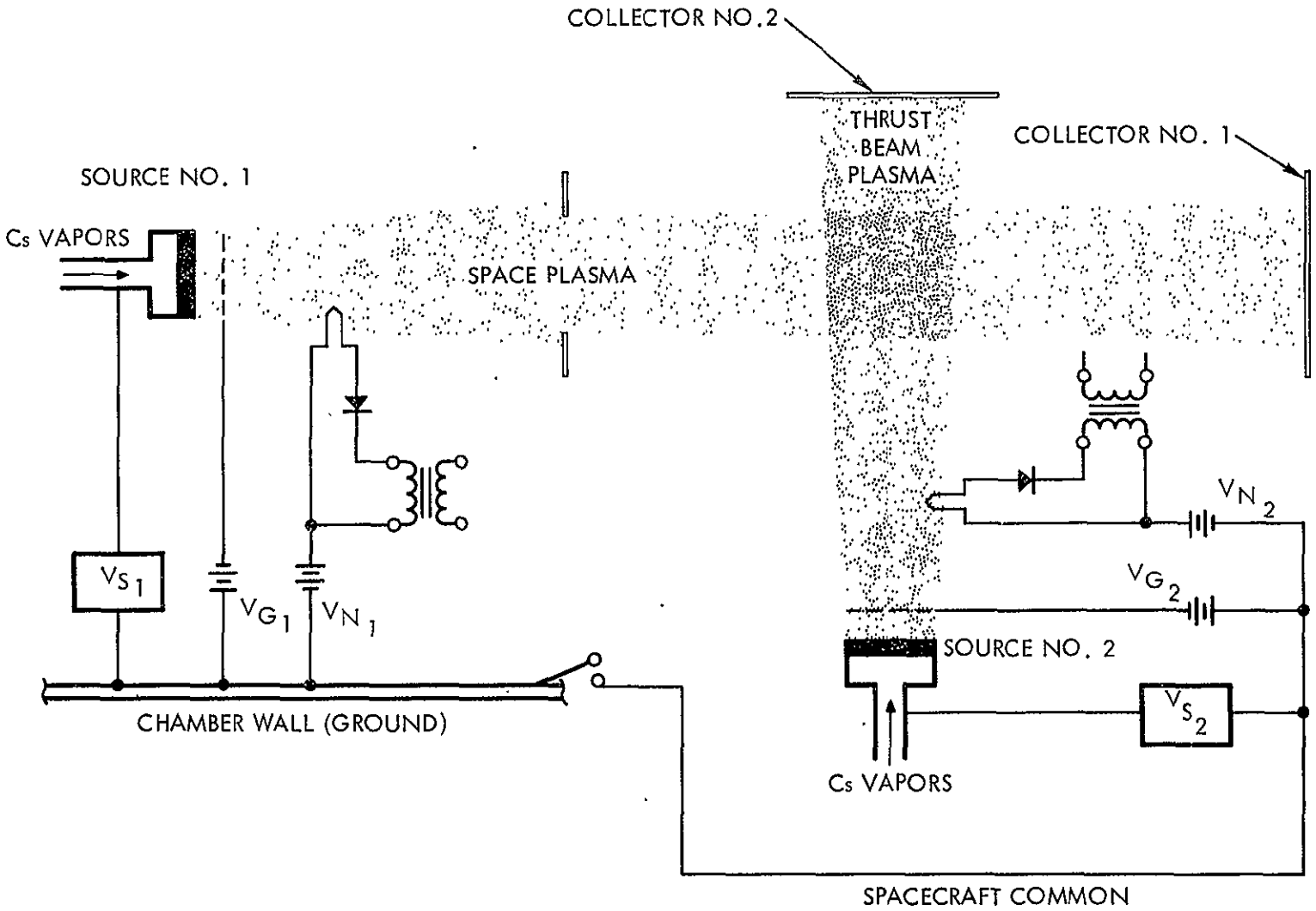

Figure 5. Schematic Diagram for Plasma-Plasma Interaction Showing Electronic System for Both Plasma Sources.

A first series of experiments were conducted with the spacecraft common grounded to the chamber walls. For this condition the density profiles of the thrust beam plasma and the streaming space plasma were measured with the beams separated and overlapping in time. Fig. 6 shows the thrust beam plasma density profile along the axis of the chamber hence, across the diameter of the plasma thrust beam). The center density was equal to 5.3×10^8 ions/cm^3. The space plasma density profile in the interaction region along the x axis was measured by probe J_+ (dilute) and is shown in Fig. 7. This plot indicates a relatively uniform incident space plasma with a density of $\approx 7 \times 10^6$ ions/cm^3.

Measurements of the potential distribution of both beams are shown in Fig. 8. Emissive probe (T), used as a floating emissive probe, was used for these plasma potential measurements in the region of the interaction. Measurements were made with the plasma both separated and overlapped in time. Curve A is the radial distribution across the thrust beam location of the space plasma potential with the beams separated in time. Curve B is the radial distribution of the thrust beam potential along the same path with the beams separated in time. Curve C shows the potential distribution along the same path with the beams interacting. These results show that for a condition of balanced electron interchange the plasma potential in the dilute outer portion of the plasma thrust beam must equal the potential of the space plasma. In the view of the simple model of Sec. II, the balanced electron interchange should occur when the potential in the plasma thrust beam, at that point at which the thrust beam density is equal to the space plasma density, equals the potential of the space plasma.

Emissive probe measurements of the potential of the separated and interacting plasmas are shown in Fig. 9 and indicate that the potential of the incident space plasma was 8.6 V, the potential of the thrust plasma (not interacting with the space plasma) was 9.9 V, and the potential of the interacting beams was 9.9 V. Relative potential measurements by means of emissive probe techniques (not floating emissive probe measurements) are considered more reliable than the corresponding floating emissive

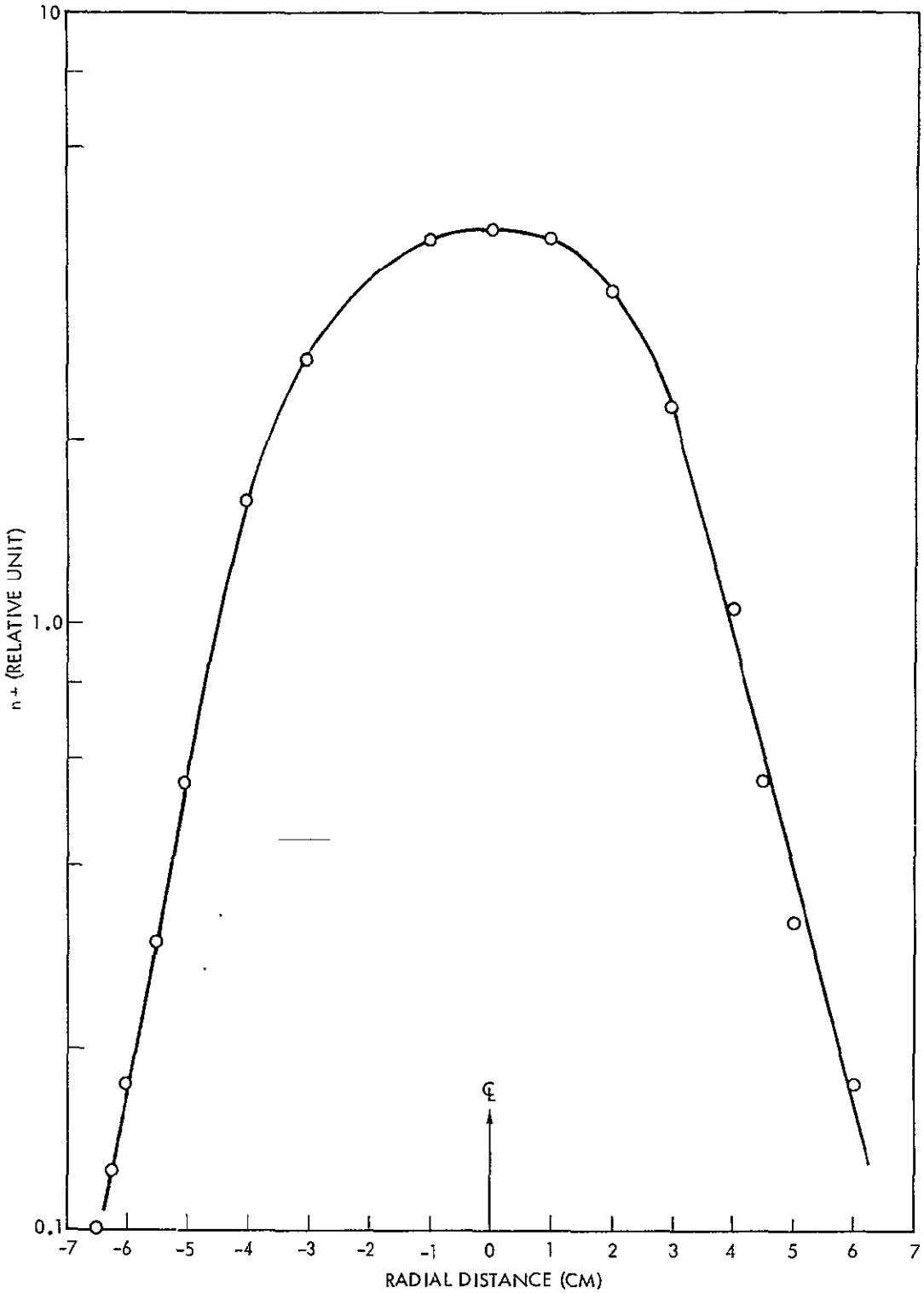

Figure 6. Thrust Beam Plasma Ion Density Distribution Along Axis of Space Plasma Beam Using J_+ (Dense).

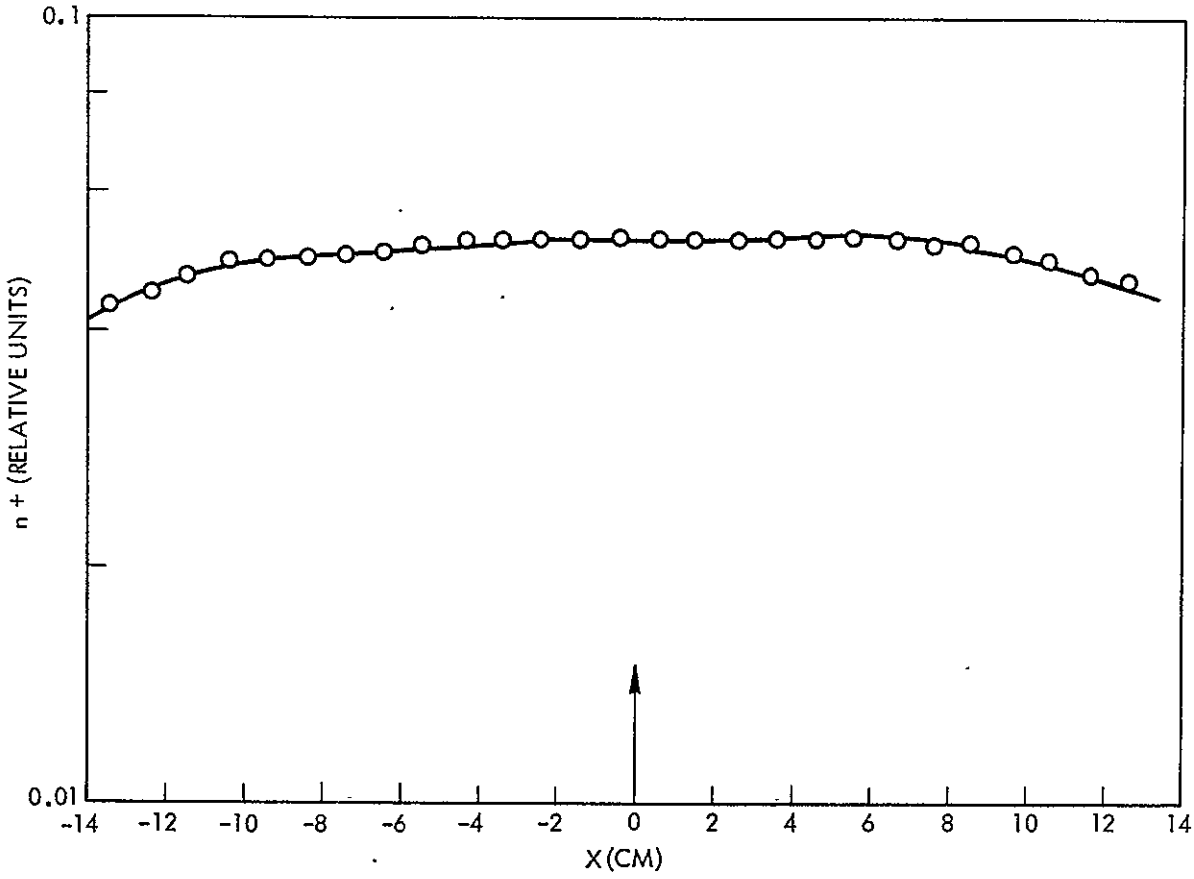

Figure 7. Space Plasma Ion Density Distribution Along X-Axis Using J_+ (Dilute) Probe.

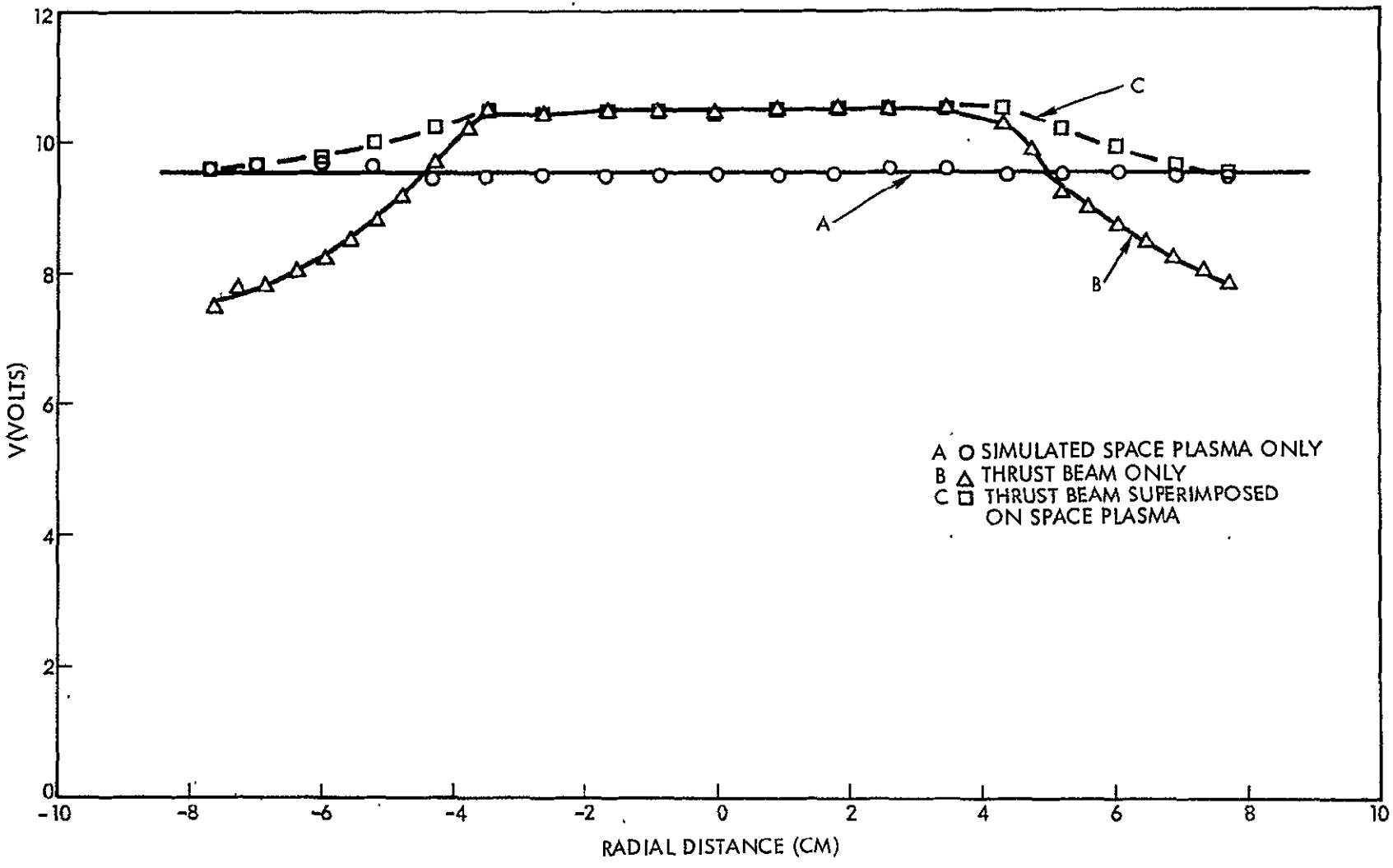

Figure 8. Radial Plasma Potential Distribution Across Thrust Beam Using Emissive Probe (T).

A. Simulated Space Plasma Only
B. Simulated Thrust Beam Plasma Only
C. Thrust Beam Interaction with Space Plasma

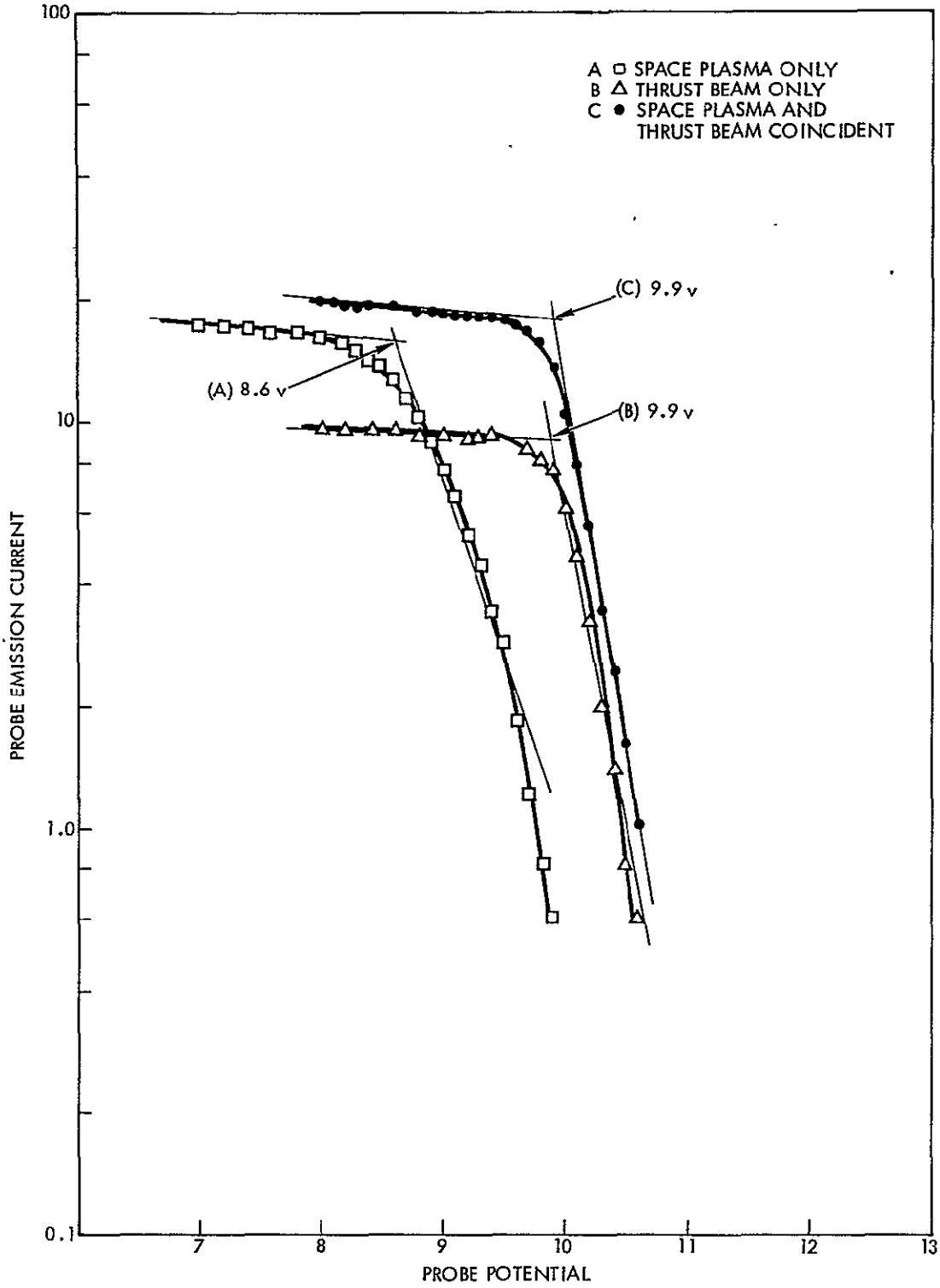

Figure 9. Emissive Probe Measurements at the Intersection of Both Beam Axes.

A. Space Plasma Only
B. Thrust Beam Plasma
C. Space Plasma Interacting with Thrust Beam

probe measurements which are somewhat influenced by density differences. With a balanced electron exchange between the two beams, the thrust beam potential was about 1.3 volts (or about $\frac{5kT_e}{e}$) above the space plasma potential . This is consistent with the relative neutralizer potentials and the expected potential drops along the plasma wind tunnel.

To obtain a measure of the electron interchange and the coupling between the two plasmas, the neutralizer emission currents from both sources were measured as a function of the relative potential between the two plasmas. The results are shown in Fig. 10. The two plasmas were made to interact with each other with neutralizer #1 fixed at +10 V. The emission currents of both neutralizers were measured as a function of V_{N2}. The data indicate that net electron interchange does occur. When the neutralizer bias potential of the spacecraft was increased, electrons for neutralization of the thrust beam were provided by the space plasma. As V_{N2} was decreased, the spacecraft neutralizer provides electrons to neutralize the space plasma. If the electron temperatures of the two plasmas were equal, as in this case, no significant problems would arise in the electron temperature measurement of the space plasmas. However, if the temperatures were different, diagnostic measurements of the space plasma might be perturbed due to electron interchange.

The density of the space plasma was then decreased by a factor of 10 to $\sim 5 \times 10^5$ ions/cm^3. For this condition the coupling between the two plasmas was very weak and the electron interchange was not pronounced. This behavior, however, may have occurred because of the method in which the density was lowered. This was done by placing an attenuator (floating metal plate with several holes) in front of the space plasma source. The attenuator may have hampered the coupling between the two beams.

A final experiment attempted was to simulate a spacecraft floating in a space plasma. As a first step in this simulation, however, the neutralizer biases were adjusted so that a condition of balanced electron interchange was obtained. This occurred at V_{N2} at a potential of 10.25 V with respect to the chamber ground. Note that for this condition the

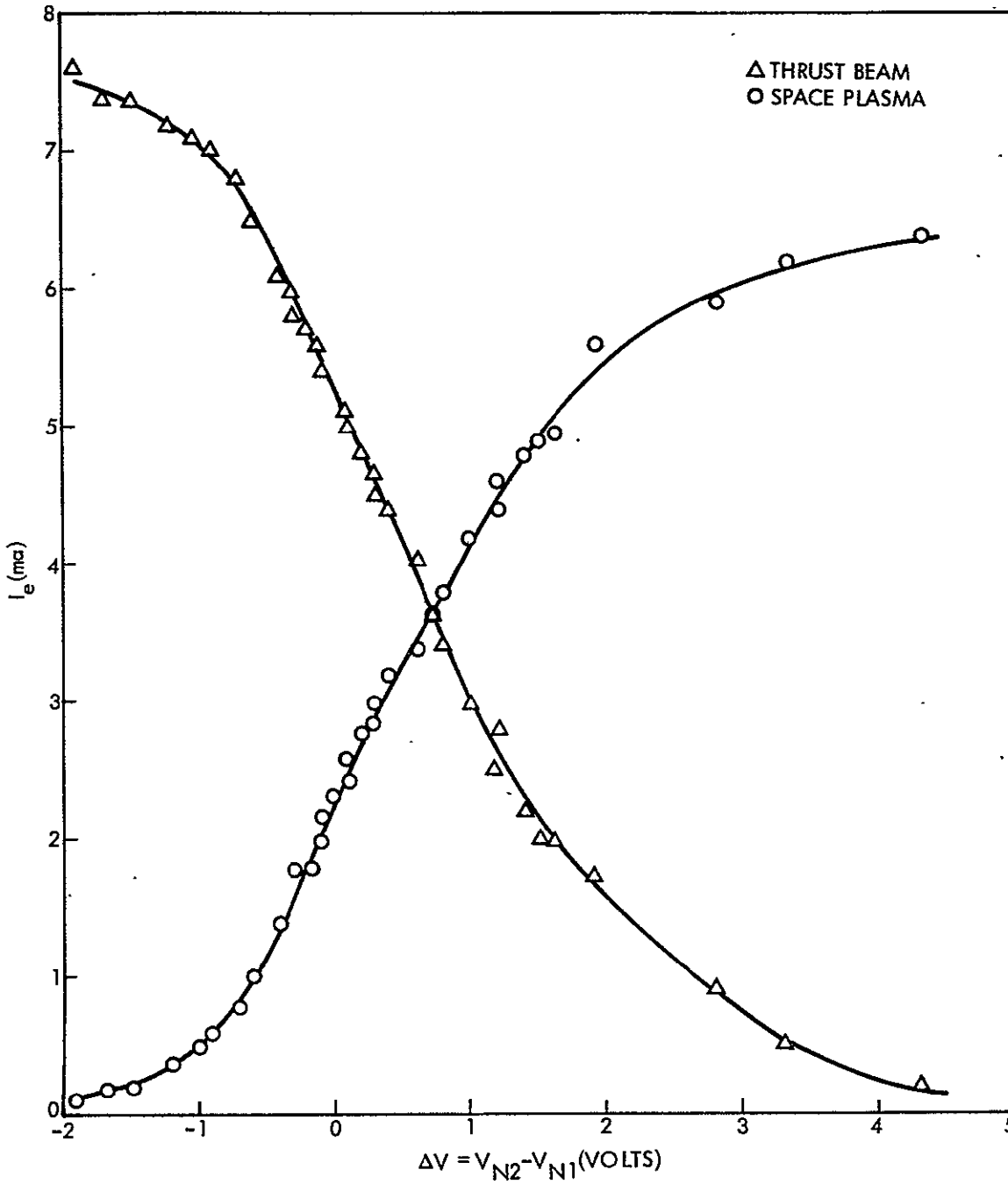

Figure 10. Neutralizer Emission Current vs. Relative Neutralizer Potential of Thrust Beam Plasma and Space Plasma. Note: Thrust Beam Plasma Potential Is Approximately Equal to V_{N2}; Space Plasma Potential in Interaction Region Is 8.6 V when V_{N1} = +10 V. I_{e1} = 2.45 ma for Space Plasma Only, I_{e2} = 5.00 ma for Thrust Beam Only, ΔV = 0.25 V for Balanced Electron Condition.

spacecraft ground and the chamber ground are connected so that a bias of 10.25 V also exists between the spacecraft neutralizer and the spacecraft ground. When the spacecraft ground is opened, thus electrically isolating the plasma thrust beam in the dilute space plasma, the relative bias between the neutralizer and the spacecraft ground remains fixed at 10.25 V. However, the potential of the neutralizer relative to the chamber ground may not stay fixed if it is found necessary to vary this potential in order to maintain an algebraically zeroed current (ion current equal to electron current) from the now electrically isolated spacecraft. When this experiment was performed it was found that the spacecraft tended to shift in the negative direction by ~ 0.20 V upon opening the ground connection from the spacecraft to the chamber walls. From the previously described transfer characteristics of electrons from one plasma to another, a negative shift in the thrust beam relative to the space plasma results in a flow of electrons from the thrust beam into the space plasma. Using the curves shown in Fig. 10 one may estimate that an electron current of ~ 0.5 milliamperes was flowing from the plasma thrust beam into the space plasma. Since this is not the condition of balanced electron interchange obtained with the spacecraft ground set to the chamber ground, the possibilities of currents to other elements of the testing area must be examined. For example, probes inserted in the plasma beams have comparatively small areas. Nevertheless, these probes are grounded surfaces, not floating surfaces, and particles which strike them need not be balanced by an equal current of oppositely charged particles. Thus, with the spacecraft ground to the chamber ground established, a small fraction of the ions leaving in the plasma thrust beam may strike grounded surfaces. Electron flow from the neutralizer is not required to match this fraction of the ion flow. With the spacecraft ground opened, however, the current of electrons leaving the spacecraft neutralizer must equal all of the ion current ejected by the source and this ion current is slightly in excess of that which the neutralizer was previously required to match. The apparent escape route for these extra electrons is to flow into this space plasma, and this is accomplished by the potential of the thrust beam plasma making a negative movement with respect to the local space.

To verify this hypothesis, additional experiments were performed in which the exposed area of grounded surfaces with which thrust beam particles or space plasma particles may interact was significantly reduced. It was found that by reducing such small grounded surface areas that the difference between the electrically grounded spacecraft (with balanced electron interchange) and the electrically isolated spacecraft became progressively lessened. It would appear, thus, that by exercising more and more stringent controls upon the testing requirement that simulation to space conditions may be improved. In the present instance with density ratios of the order of 100, it is possible to effect a comparatively rigorous simulation of the space conditions. However, as density ratios become larger (10^3, for example) additional requirements, which have not yet been successfully met, must be established.

VI. DISCUSSION OF EXPERIMENTS

The condition of balanced electron interchange occurred for a potential difference of 1.3 volts between the thrust beam and the space plasma.. From Eq. (3"), $\hat{V} = \frac{-kT_e}{e} \ell n \frac{\rho_{sp}}{\rho_{bo}}$, and for $\frac{kT_e}{e} = .25$ volts and $\rho_{sp} \simeq 10^{-2} \rho_{bo}$, $\hat{V} \cong 5 \frac{kT_e}{e} \simeq 1.3$ volts, in agreement with the measured result. This indicates that the simple model is, at least, qualitatively correct for density rations of $\sim 10^2$.

For higher density ratios, $\sim 10^3$, balanced electron interchange appeared to occur for potential separations well in excess of the predictions of Eq. (3"). Two possible explanations for the discrepancies in the regime of density ratio may be made. The first is that Eq. (3) may be of only limited validity. The experimental measurements to verify Eq. (3) were carried out through only two orders of magnitude in plasma density. For excursions into more dilute regions of the beam, the plasma potential structure may be influenced by boundary effects. A second possible perturbation is that the electrons in the thrust beam may contain a small fraction which is not representative of T_e. For example, electrons leaving the ion accelerator electrode and entering the plasma thrust beam

have large kinetic energies. A small quantity of such high energy thrust beam neutralizing electrons would not be a serious perturbation for density ratios of $\sim 10^2$ between thrust beam and plasma, but could exercise considerable influence on the equilibration at density ratios of 10^3 or higher.

A second feature of interest in the experiments is the resistance around the plasma-plasma loop. From Fig. 10, this $\frac{\partial V}{\partial i}$ indicated a loop resistance of $\sim 450\Omega$. The measuring resistors, $R_{spn,meas}$ and $R_{tbn,meas}$ are small (10Ω) so that $\sim 430\Omega$'s results from $R_2 + R_3 + R_4 + R_5 + R_6$. R_2 and R_6 are similar but may not be exactly equal since the plasma densities at the thrust beam origin and the space plasma (plasma wind tunnel) beam origin differ by a factor of ~ 2. Using earlier experiments[5] it is possible to estimate $R_2 + R_6 \simeq 200\Omega$. The value of R_4 (R_{mc}), the merging contour resistance can be estimated at $\sim 10\Omega$ (using $\rho_{sp} = 7 \times 10^6$ ions/cm^3 and an estimated contact area of $\sim 10^3$ cm^2). If this resistance is, indeed, of this magnitude, its determination in this plasma wind tunnel experiment is not possible in view of other, and larger resistances.

From the measured loop resistance and the estimates of various elements of this loop, only qualitative conclusions may be drawn. First, there are no overt discrepancies between the equilibration model and the measured resistances. For a spacecraft operating under the conditions of the plasma wind tunnel tests, the resistance chain between the spacecraft and the ambient plasma (see Fig. 2) would be about 300Ω.

One of the questions on laboratory tests of plasma-plasma equilibrium is the effect of limited physical extent to the testing configuration. This "truncation" necessarily restricts the total contact area between the plasmas to values less than would obtain in the space environment. A previous estimate of 10^5 cm^2 along the merging contour between an ion engine beam (initial diameter 10 cm, 6° half angle divergence, 10^{10} ions/cm^3 at beam origin) and an (ionospheric) space plasma of 10^6 ions/cm^3 is some two orders of magnitude larger than obtained in the plasma wind tunnel tests. Thus, the resistance across the merging contour should be less in the space configuration. The resistance values from the thrust beam origin to the merging contour should also be reduced in the space geometry compared to the laboratory test because of the increased volumetric path in space.

The various resistances noted in the plasma-plasma chain are density dependent. As space plasma density is lowered the resistance from the beam origin to the equidensity contour along which merging occurs should increase. Simple models of the equilibration indicate that resistance across the merging contour should be invariant to density changes. The resistance, R_{mc}, is inversely proportional to ρA where ρ is plasma density and A is the total contact area of the merging contour. This contact area, however, is inversely proportional to ρ so that ρA is invariant to density changes. Finally, the resistance in the space plasma should increase with diminishing density. From these several factors, the resistance of the total chain (in Fig. 2) should increase as ρ_{sp} diminishes. Since the space plasma has a maximum value (in the F2 layer) of $\sim 10^6$ ions/cm^3 and may diminish to levels of ~ 10 ions/cm^3 (in the interplanetary space), the possible chain resistances may become large enough to merit concern for spacecraft equilibration as it is affected by perturbation currents. The shift in spacecraft equilibration potential, δV, will be $\delta i \, R_{chain}$ where δi is the perturbation current and R_{chain} is the resistance of the relevant perturbation current path. It should also be emphasized, in conclusion, that resistance values have only limited regions of linearity and excessively large perturbation currents may act to place the entire spacecraft-plasma-plasma configuration into high effective resistance conditions.

VII. CONCLUSIONS

A simple model of the equilibration between a plasma thrust beam and a space plasma has been developed. Plasma wind tunnel tests of a dense "thrust" beam in a dilute "space" plasma have determined the equilibration potential of these two plasmas for a condition of balanced electron interchange. Measured equilibration potentials agree with the predictions of the simple model for density ratios between dense and dilute plasmas of $\sim 10^2$. At density ratios of $\sim 10^3$ measured equilibration potentials do not agree with predictions of the model. Causes for this disagreement have not yet been determined.

The resistance elements in the thrust plasma-space plasma chain have been identified. Values of total loop resistances for the bi-plasma system have been determined at several hundred ohms for the experimental configuration employed. Knowledge of these resistances allows an estimate of variations in equilibration potential resulting from perturbation current flows.

Finally, truncation effects in plasma wind tunnel experiments result in differences between laboratory tests of equilibration and actual behavior in space. Present laboratory tests may hope, however, to qualitatively describe spacecraft-thrust beam-space plasma equilibration.

VIII. ACKNOWLEDGMENTS

The authors gratefully acknowledge the assistance of Edward C. Ashwell and G. K. Komatsu in the performance of the plasma wind tunnel experiments.

REFERENCES

1. Sellen, J. M., Jr., Bernstein W., and Kemp, R. F., "The Generation and Diagnosis of Synthesized Plasma Streams," Rev. Sci. Instr. 36, 316-322 (1965).

2. Sellen, J. M., Jr., Kemp, R. F., and Hieber, R. H., "Observations of Neutralized Ion Thrust Beams in the 25-Meter NASA Testing Chamber," TRW #8603-6039-KU-000, July, 1964.

3. Sellen, J. M., Jr., "Thrust Beam Equilibration Models," Section IV.D., Study of Electric Spacecraft Plasmas and Field Interactions, TRW #07677-6013-R000, May, 1968.

4. Kemp, R. F., Sellen, J. M., Jr., and Pawlik, E. V., "Beam Neutralization Tests of a Flight Model Electron Bombardment Engine," AIAA Preprint 2663-62 (November, 1962).
"Neutralizer Tests on a Flight-Model Electron Bombardment Ion Thruster," NASA TN-D1733, July, 1963.

5. Sellen, J. M., Jr., "Ion Beam Neutralization," TRW #8939-SU-000, March, 1962.

SECTION IV. D.

INTERACTION OF SPACECRAFT SCIENCE AND ENGINEERING SUBSYSTEMS WITH ELECTRIC PROPULSION SYSTEMS

AIAA Paper
No. 69-1106

INTERACTION OF SPACECRAFT SCIENCE AND ENGINEERING SUBSYSTEMS WITH ELECTRIC PROPULSION SYSTEMS

by

J. M. SELLEN, JR.
TRW Systems Group
Redondo Beach, California

AIAA 6th Annual Meeting and Technical Display

ANAHEIM, CALIFORNIA/OCTOBER 20-24, 1969

INTERACTION OF SPACECRAFT SCIENCE AND ENGINEERING SUBSYSTEMS WITH ELECTRIC PROPULSION SYSTEMS*

ABSTRACT

The operation of solar-electric spacecraft may impact upon the validity of scientific data obtained by the vehicle. Errors in scientific measurements may result from alterations in spacecraft conditions under thruster operation or through direct perturbation of the space environment. Magnetic contamination, electrostatic contamination, space plasma contamination, and electromagnetic contamination are under a quantitative examination for solar-electric spacecraft measuring properties of the near (1 AU) to distant (5 AU) interplanetary regions. Studies, by other investigators, of material deposition and spacecraft material alteration resulting from thruster operation are in process. Achievement of acceptable levels of cleanliness for the various contaminants impacts upon spacecraft configuration and upon the design and construction of spacecraft subsystems. System and technology requirements for acceptable levels of vehicle cleanliness are discussed. Studies of effects on spacecraft configuration from propellant deposition and interaction with spacecraft surfaces are reviewed.

I INTRODUCTION

A series of recent studies[1-11] have examined the possible performance capabilities of "solar electric spacecraft." The power for the operation of the craft and its electric thrusting units would be derived from large area solar arrays. Primary emphasis for the propulsive units, beyond the chemical boost phase, has been directed toward the "electrostatic" thruster - or ion engine. These studies have revealed capabilities in solar electric spacecraft which make the application of such craft to scientific missions appealing. Principal aspects of these capabilities are in ranges of excursion (both in space and time), in available payload, and in available power for payload and craft operation (both during and subsequent to thruster operation).

*This work was performed for the Jet Propulsion Laboratory, California Institute of Technology, sponsored by the National Aeronautics and Space Administration under Contract NAS7-100.

The application of electric propulsion systems to scientific spacecraft, however, must not violate the desired context of such missions -- the unimpeded and unaltered collection and transmission of scientific data. Previous studies[12,13] have examined the (electrical) equilibration of both passive and active spacecraft with the ambient plasma of space and possible plasmas and fields interactions between electric spacecraft and the space plasma. The possible effects which such interactions may have upon the collection and interpretation of scientific data have been examined in these previous studies, and this present discussion will continue that examination, with, however, additional emphasis upon required system configurations and system constraints to minimize or eliminate any impact upon the scientific exercise of the spacecraft which might be imposed by the operation of the thrusting units.

The approach of this study of subsystem interactions with electric propulsion systems is illustrated in Figure 1. The "data pool" indicated there is the total body of information on the various properties of the space. The operation of the spacecraft science subsystem in collecting information from the data pool and the processing, transmission and recording of this information comprise a "data chain." The expulsion of a plasma thrust beam from the electric thrusting unit may impact upon the data pool or upon one or another elements or subelements in the data chain. When the thrusting units are not in operation, the spacecraft is "passive" and the impact of the overall craft upon the data pool and data chain must be considered. Discussion of possible interaction effects for the passive spacecraft will be given. Primary emphasis, however, will be upon active spacecraft with thrusting units in operation.

II IMPACT OF THRUSTING UNIT OPERATION ON DATA POOL

A. Data Pool Elements

The total body of information on the properties of the space has been designated as the data pool. These properties include the mass, number density, energy, charge, and direction of single particles and of aggregates of particles. Electric and magnetic fields, both steady state and time varying are also properties of the space. Frequencies for the time varying electromagnetic fields range from VLF to optical. The 'electron content' which

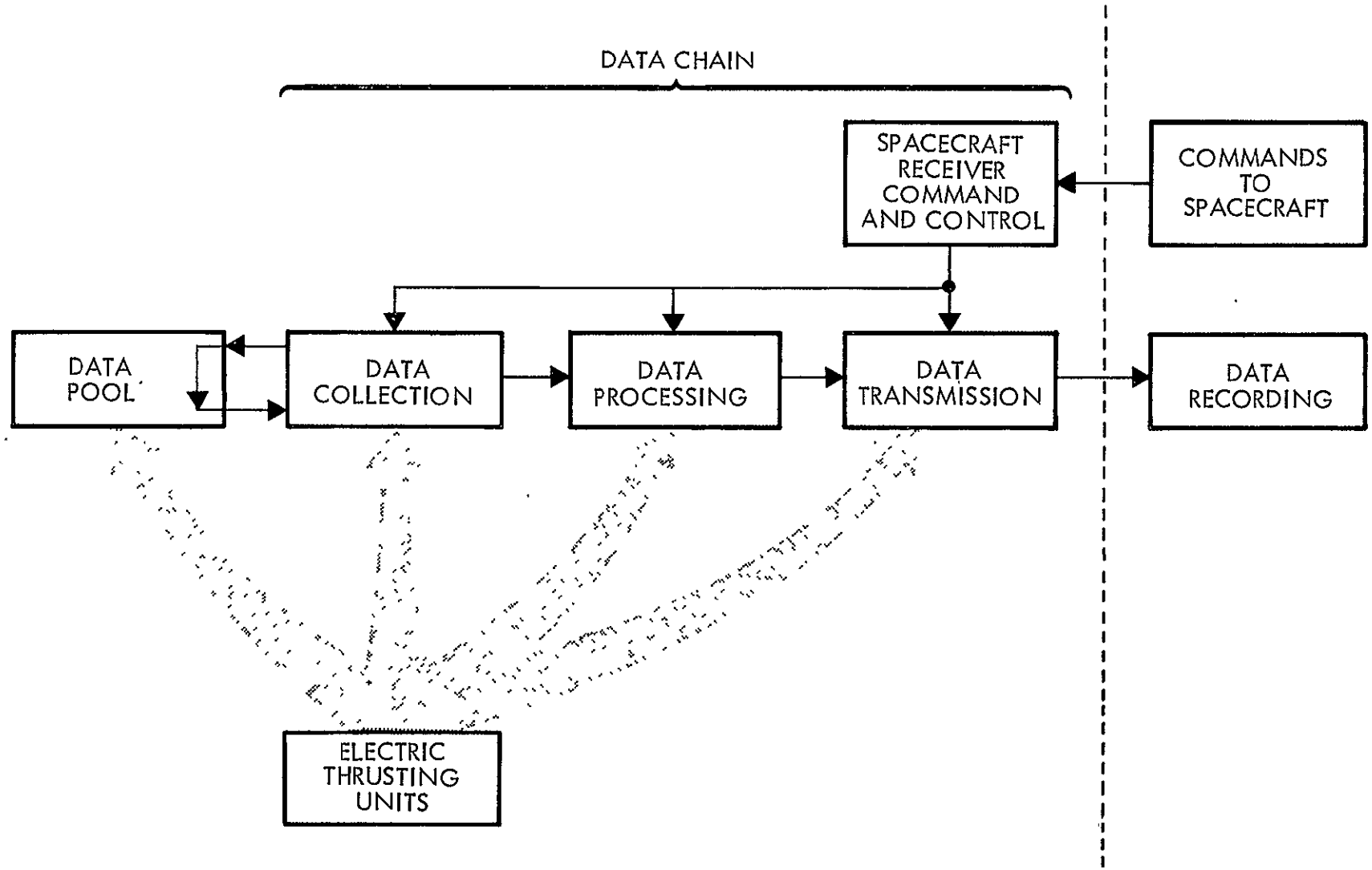

Figure 1. Data pool and data chain elements. Large arrows indicate possible processes through which the operation of the electric thrusting units may impact upon the data pool or upon the data chain.

describes the total number of electrons in a column extending from Earth to the spacecraft is an integral rather than a differential property of the space, but remains of interest in interplanetary scientific measurements and will be considered as an element of the data pool. Particular scientific missions may concentrate upon one or another elements of this total pool with reduced or no interest in other elements. For generality, however, this present discussion will consider all of the measurable properties of the space.

Some of the properties of the space are beyond any possible influence from the operation of the thrusting units. Since the particles released in the thrust beam are of the order of several kilo electron volts at most, energetic particles (for example, solar protons of multi-MeV energies) will be, when observed, a genuine occurrence and not the result of an injection of matter from the thrust beam into the local space. Meteoroids, if observed, must be similarly genuine events. Only for the range of particle energies encompassed by the particles in the thrust beam are there possibilities of a "space plasma contamination" by the thruster exhaust, and, even here, the kinetics of the ion acceleration and release prevent the appearance of thrust beam ions in the greater part of the total region surrounding the spacecraft. Lower energy "charge exchange" ions emerge from the thrust beam to traverse more extensive regions of the space around the vehicle, and electrons, inter-changing between the thrust beam and the space plasma may, under the influence of the interplanetary magnetic field, occupy, to some extent, all of the region around the spacecraft. Features of these particle releases are illustrated in Figure 2, and the possible contamination of the space plasma by <u>low</u> energy charged particles must be examined further.

An important component of the data pool is in electromagnetic waves whose frequencies range from VLF to optical. Emissions from the ion thruster cover a similarly broad spectrum so that "electromagnetic contamination" of the space is, in principle, a possible condition. Some avenues of relief are present here in a manner similar to the relief through "kinetics" in space plasma contamination. Radiation from the ion thruster operation ranging from ultaviolet through infrared will be present but is released into a limited range of directions from the spacecraft and moves through an essentially transparent space. Emission from neutral atoms in the thrust beam exhaust will occur in an amount determined by total neutral efflux and by the temperature of the thrust beam neutralizing

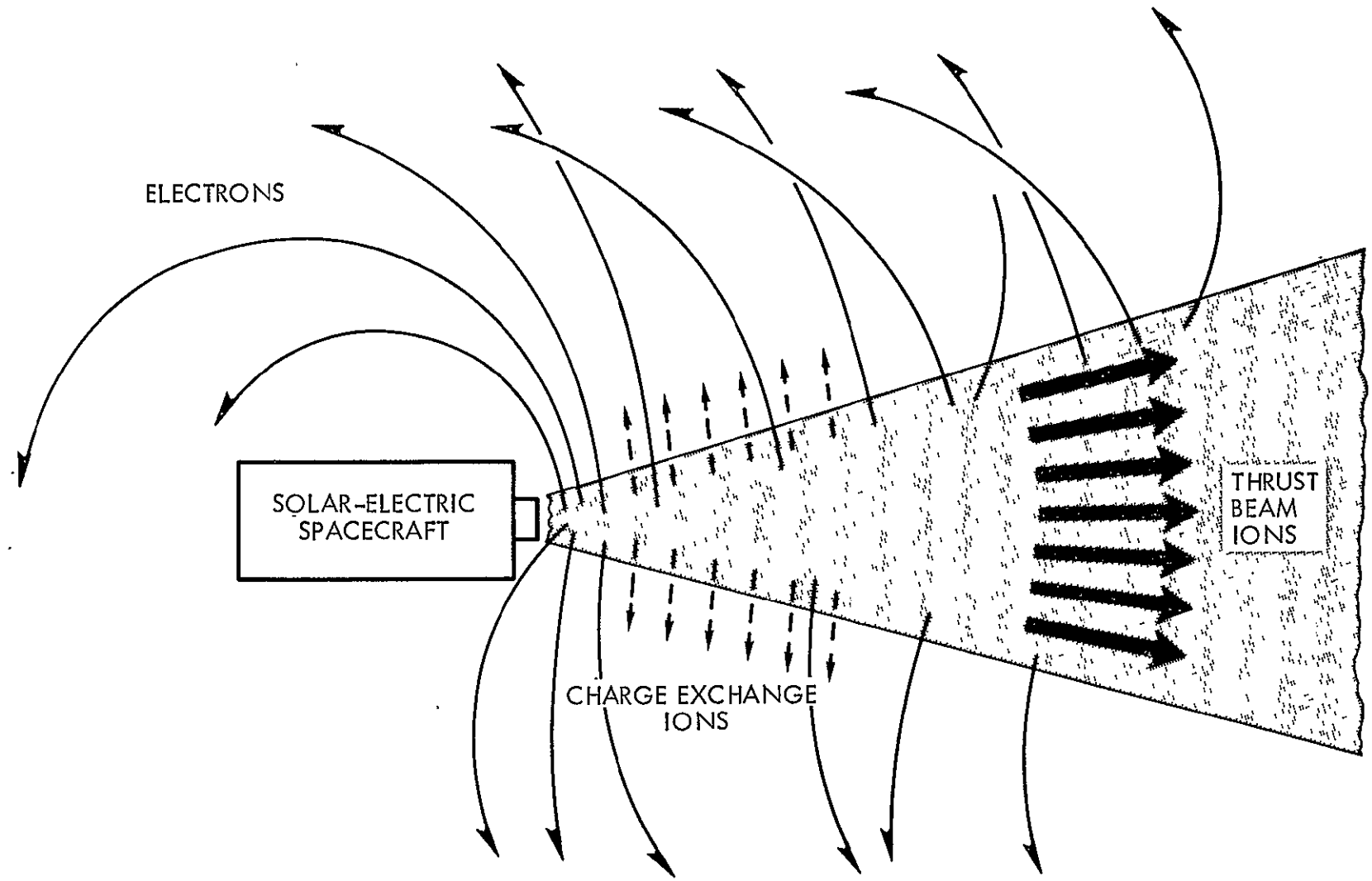

Figure 2. Particle releases from thrust beam of solar electric spacecraft. (Solar array not shown). Heavy arrows indicate thrust beam ions (Group 1, III.C), dashed arrows indicate charge exchange ions (Group 4, III.C) and light arrows indicate thrust beam electrons interchanging with space plasma electrons. Curvature of electron trajectories results from magnetic field in space.

electrons which create the neutral atom exitation. Other elements of wave emission may occur at frequencies ranging from 1 GHz ($=10^9$Hz), which represents the electron plasma frequency in the discharge of an electron bombardment thruster, to VLF, ranging downward to 10-100 Hz, from the electrical equilibration of the plasma thrust beam with the interplanetary plasma. Features of these several sources of electromagnetic waves are illustrated in Figure 3. Of principal concern are emissions in the VLF range, since this would appear, from present experimental evidence, to be the most prevalent wave-particle interaction regime for the interplanetary plasma. Possible relief from an electromagnetic contamination of the local space may derive from appropriate system configurations and/or constraints and from the demonstration that the (largely conjectural) low-frequency fluctuations in thrust beam-space plasma equilibration are, if present at all, of negligibly small magnitude.

Another element in the data pool is the magnetic field. In the interplanetary space near 1 AU this field is of the order of several γ ($1\gamma=10^{-5}$ gauss), and its measurement, both in magnitude and direction, has comprised one of the most important aspects of space science in the "near" interplanetary region. For increasing heliocentric distance, the magnitude of this field diminishes, with expected values of $\sim 1\gamma$ in the region of 5 AU. The radial component of the field at these high heliocentric distances may be as small as $.1\gamma$, so that requirements of magnetic cleanliness on the spacecraft for operation in these distant regions will be, at the least, as demanding as for those scientific spacecraft which have obtained the presently available measurements of this field. The possibility of a "magnetic contamination" of the space by the operation of a spacecraft has several features for the solar electric craft which were not present in the previous (and passive) spacecraft. The first of these is in the general context of solar-electric operation which may be expected to be at a multi-kilowatt power level - some one to two orders of magnitude in excess of the power of spacecraft used in these earlier explorations. The generation and utilization of this power involves current flows which will create magnetic contamination unless appropriate structuring and compensation is utilized. Here, all systems of the solar electric craft must be considered, solar array, electric thrusting units, and spacecraft electronic circuitry. In addition there is the electrical equilibration of the plasma thrust beam with the space

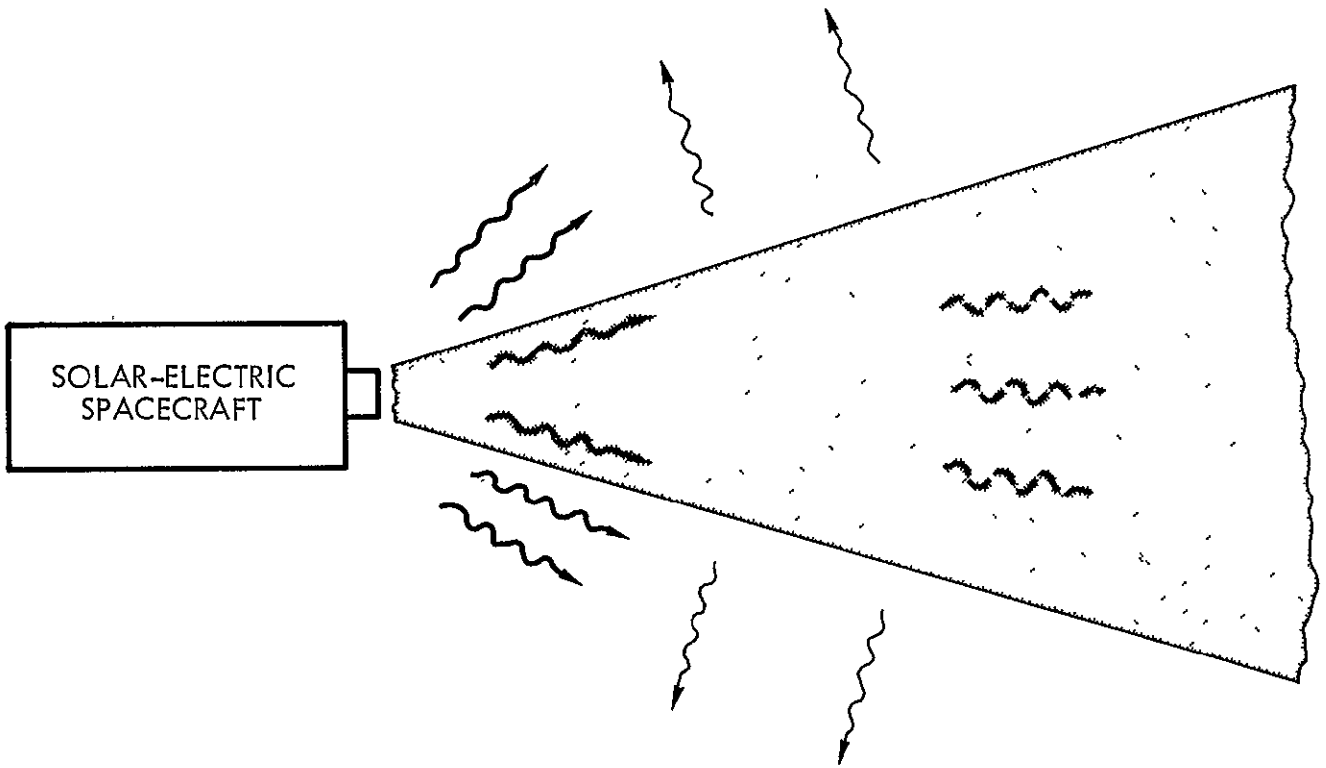

Figure 3. Possible wave releases from thrust beam of solar-electric spacecraft (Solar array not shown). Heavy wave lines indicate optical radiation (ultraviolet to infrared) from operation of ion engine. Dashed wave lines indicate radiation at electron plasma frequency in discharge region of electron bombardment thruster. Thin wave lines indicate postulated low frequency plasma waves in electrical equilibration of thrust beam with space plasma.

plasma. Conditions in this equilibration which yield current loops in the bi-plasma system have been postulated. Figure 4 illustrates some of these possible equilibration states. The generation of a magnetically clean electrical equilibration in the thrust beam-space plasma system, and the configuration of spacecraft and electric thruster currents to eliminate magnetic contamination of the local space will be an important requirement for scientific spacecraft determining the properties of distant interplanetary regions.

A final element to be considered in the data pool is the electric field. The presence of a material body in a plasma results, in general, in the build-up of surface charges on that body, and electric fields from this surface charge to charged particles in the plasma restructure the electric field away from that value possessed in the unperturbed space (material body absent). Charged particles traversing the "sheath" region which separates the distant plasma from the spacecraft are altered in both their energy and direction. For low energy charged particles, such as the electrons in the interplanetary space, these energy and directionality perturbations are severe, resulting in major alterations in the properties of these particles. This "electrostatic contamination" of the space derives from the mere presence of a material body, so that spacecraft, both active and passive, may lead to perturbations in measurements of electric fields and low energy charged particle properties. There is, however, some possibility that this electrostatic contamination may be reduced or eliminated by active spacecraft, and the solar electric craft may possess capabilities of electrostatic cleanliness that are not present in passive craft.

B. Magnetic Contamination

The elements of the data pool which may be affected by the operation of the electric thrusting units have been detailed. To reduce or eliminate an impact upon the data pool under "thrust" conditions will require appropriate system configurations and/or constraints. In the area of magnetic contamination three system elements will be considered - the solar array, the electric thruster, and the bi-plasma equilibration. Large area solar arrays with power levels to the multi-kilowatt level are presently under design and development.[14,15] The cell stack and current flow levels of a 30' roll-out solar array[14] have been utilized in studies of magnetic cleanliness of such large area arrays.[16,17]

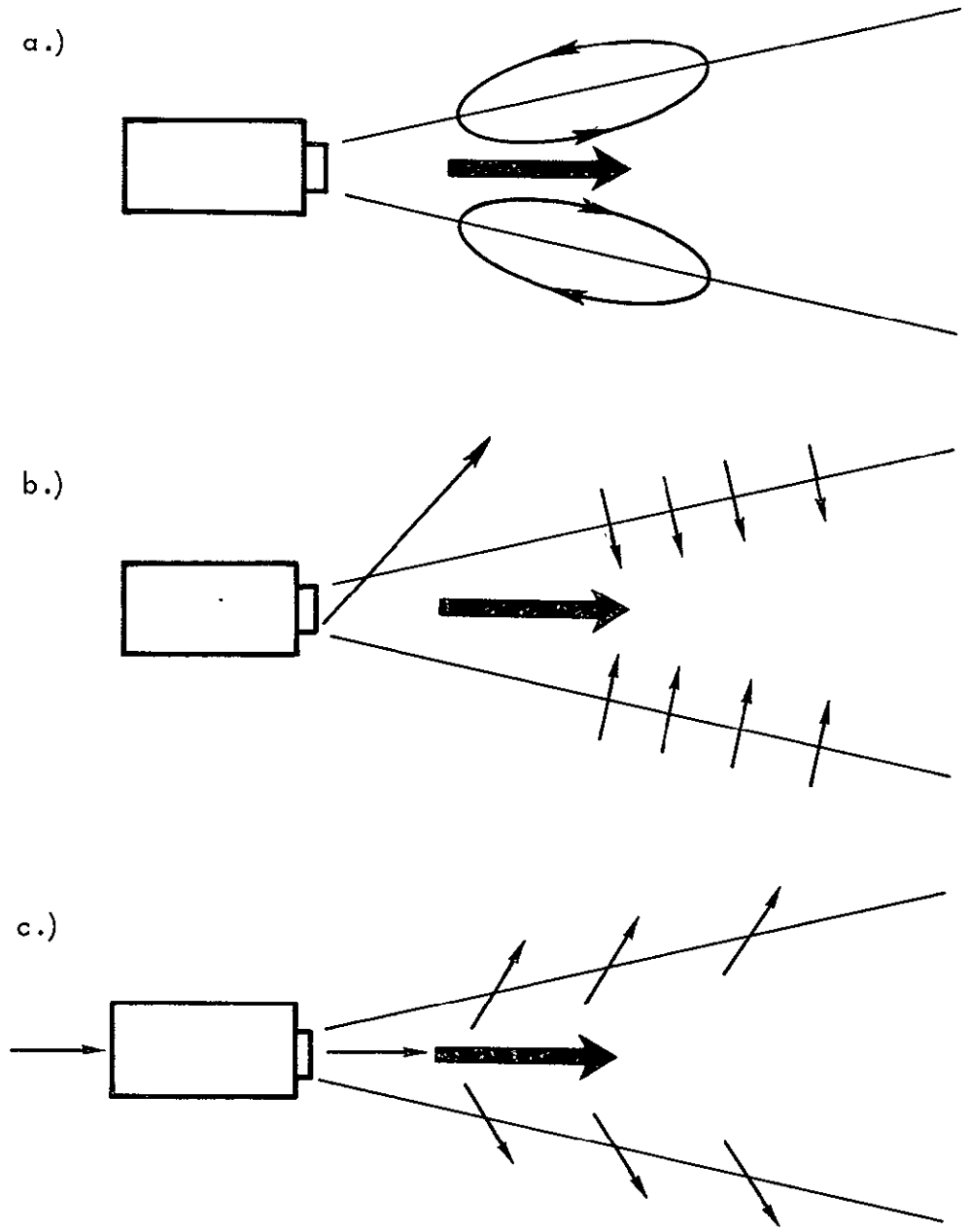

Figure 4. Possible current flows in thrust beam-space plasma equilibration of solar electric spacecraft. Large arrows indicate ion flow. Light arrows indicate electron flow. a. Inward diffusion of space plasma electrons exceed outward flow of thrust beam electrons at upstream points with opposite conditions at downstream points. b. Energetic beam neutralizing electrons not retained in thrust beam whose neutralization proceeds by inward diffusion of space plasma electrons. c. Electrons drainage current to spacecraft returning to space plasma via the neutralizer-thrust beam-space plasma coupling.

Considered in these studies are the current flow configuration for the overall array, back-wire placement, back-wire granularity, and current injection and collection bus bar geometry. It has been demonstrated that magnetic cleanliness levels of .1γ or less may be realized for separation distances from the array of ∿2 meters. These levels of cleanliness may be realized without the imposition of penalties in array weight or in complexity in the backwiring circuits. Further gains in magnetic cleanliness below the .1γ level may be achieved by particular backwiring configurations which provide a null for dipolar and quadrupolar magnetic fields from the separate "strings" of the cell stack.

The thruster to be considered here will be of the electron bombardment type. Three current flows in this thruster are possible sources of contaminant fields. These are the current flow in the electron bombardment discharge, the current loop from ion generation to thrust beam neutralization, and the current flow in the solenoids which produce the discharge magnetic field. It is assumed that the remaining currents (in boiler, discharge cathode, and neutralizer heaters) yield sufficiently reduced dipole fields or allow for field reduction by appropriate coaxial configurations. The possible generation of contaminant fields through current flows in the discharge and in the ion generation to ion neutralization loop is illustrated in Figure 5. For the worst case condition of discharge structure (Fig. 5a), the magnetic moment is of the order of $100\gamma m^3$. (gamma meter^3), and withdrawal from the thruster in excess of 5 meters is required to release a reduction of contaminant field levels to .1γ. If the discharge current is axially symmetric, (Fig. 5b), then magnetic field lines become entirely enclosed within the discharge region and acceptable levels of magnetic cleanliness will be present at comparatively modest separation distances from the thruster. Similar considerations apply to the ion generation to ion neutralization current loop (Figures 5c and 5d). Since it is likely that electron injection into the plasma beam will be carried out by a single neutralizer, some loss of axial symmetry must result in the current configuration. The multiple wire pattern illustrated in Figure 5d, however, may be expected to diminish contaminant field levels in excess of one order of magnitude, (relative to Figure 5c), which would appear to be a sufficient reduction. The technology requirements for acceptably small contaminant field generation from these first

a.)

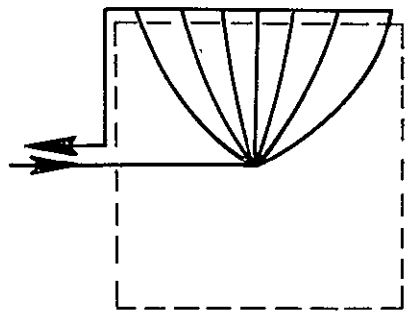

5a. Asymmetrical discharge condition producing net magnetic moment and contaminant magnetic field.

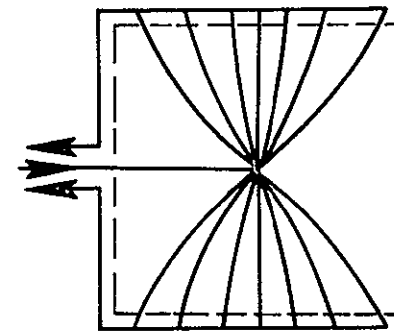

b.)

5b. Axially symmetric discharge condition with zero net magnetic moment. Magnetic field lines contained in discharge region.

c.)

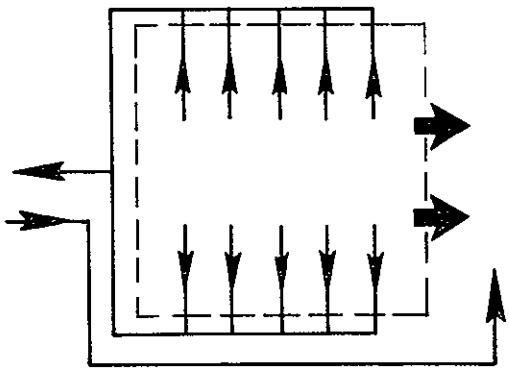

5c. Symmetric discharge with neutralization current through HV supply to asymmetric current return to neutralizer. Contaminant magnetic field generated.

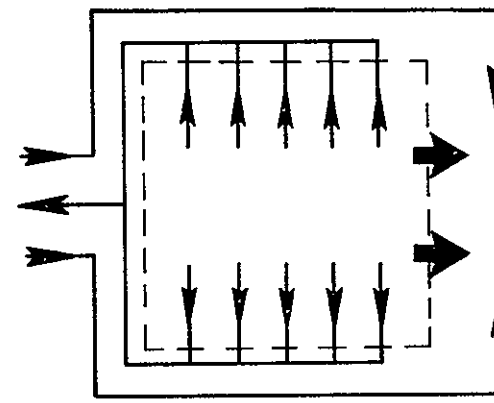

d.)

5d. Symmetric discharge with neutralization current through HV supply to axially symmetric current return to neutralizer. Magnetic field lines confined to thruster.

Figure 5. Discharge and neutralization current flows in electron bombardment thruster. Dashed lines indicate discharge region. Solid lines indicate electron flows. Large arrows indicate ion flow in neutralization current loop.

two current flows are in the axial symmetry of the current pattern, which may be determined in actual thrusting systems through Langmuir probing of the discharge and through appropriate current lead configuration from the discharge region to the neutralizer.

The contaminant field level from the operation of the solenoids which provide the discharge region magnetic field will depend upon the means of this field generation. If the discharge utilizes an air core solenoid then typical values of magnetic moment for this current flow will be $\sim$30,000γ m^3, and withdrawal in excess of 50 meters would be required to realize the .1γ levels of contaminant field. Such separation distances may be considered to be excessive, so that some means of contaminant field reduction should be utilized. Three possible approaches are, 1) reversal of current direction for solenoids in adjoining thrusters if an even numbered multi-thruster system is utilized, 2) solenoid current return through a larger area single turn whose magnetic moment is equal and opposite to the thruster magnetic moment, and 3) use of a magnetic shielding cavity for thruster emplacement. Process 2) above would result in some minor penalties to the system weight and power, but does provide direct and exact cancellation of the contaminant fields at all distances large compared to the diameter of the return loop and is not dependent upon the operation of adjoining thrusters.

While extensive use has been made of air core solenoids in the electron bombardment thruster, more recently developed ion engines have utilized magnetic materials in the production of the field. If the discharge region magnetic field is provided by a series of small solenoids with external flux concentrators,[10] then contaminant field levels about the spacecraft will be considerably reduced. This occurs in that the return path for magnetic field lines through the discharge region is now in the flux concentrator material. Exact expressions for contaminant field fall-off for this thruster configuration cannot be given as for the air core solenoid. System testing to assure that contaminant fields are sufficiently reduced would be required for the thruster configuration to be used on a particular mission. If the contaminant field were to need further reduction, one or another of the three processes previously outlined could be applied to the system.

The remaining system element which may generate contaminant magnetic fields is the electrical equilibration of the thrust beam with the space plasma. The reduction or elimination of current loops in the bi-plasma system and from the space plasma to the spacecraft to the thrust beam and returning to the space plasma will be by appropriate coupling of the neutralizer to the thrust beam and by appropriate bias potentials between the neutralizer and the spacecraft. The reduction of electron release other than through the neutralizer also appears as a requirement for magnetic cleanliness. These actions in the "tailoring" of the beam neutralization process will affect not only the area of magnetic contamination but also the areas of electrostatic and space plasma contamination. Discussion of this neutralization requirement will be given in the following section.

C. Electrostatic and Space Plasma Contamination

Factors affecting the electrical equilibration of the plasma thrust beam with the space plasma have been examined[12,13] under the condition that the temperature of the electrons neutralizing the thrust beam is equal to the temperature of the electrons in the space plasma. While the assumption of equal temperatures simplifies the model of the bi-plasma equilibration and provides for a condition of electron interchange which does not result in changes in the temperature of either medium, it is not likely to occur in an actual vehicular case. There are, first, temporal variations in the temperature of the space plasma electrons even for a fixed position in space. For missions ranging to high heliocentric distances there will be an expected cooling of solar wind electrons compared to temperatures in the 1 AU region. Finally, temperature variations for the electrons neutralizing the thrust beam have been observed as a function of axial position in the beam plasma.[18] These several factors lead to the conclusion that, in general, electron temperatures in the two plasmas will not be equal, and that interchange of electrons will result in variations in the properties of both media. Under this condition configurations and constraints in the neutralization system must be established so as to yield minimum effects in magnetic, electrostatic, and space plasma contamination.

A first neutralization condition to examine is that of a "low conductance" injection system. (Figure 4b). Here the required increment of potential from the neutralizer to the plasma thrust beam in order to extract electrons from the neutralizer is large, and electrons moving from the neutralizer into the thrust beam acquire significant injection energies. These electrons are not necessarily retained in the thrust beam and, indeed, for sufficient injection energies, the function of the electrons leaving the neutralizer is solely for the current neutralization of the spacecraft. Charge neutralization of the thrust beam does occur, but is carried out through an inward diffusion of electrons from the space plasma to the thrust plasma. Flow patterns of electrons within the space plasma-thrust beam system eventually yield current and charge neutralization on a point-by-point basis, but the region in which this occurs may be distant from the spacecraft, while near the spacecraft net ion or electron streaming current density conditions exist. The magnetic fields resulting from these currents cannot be neglected if measurements of the interplanetary field are to be conducted. In the configuration of 4b, and for thrust beam current levels of 1 ampere, contaminant fields of $\sim 100\gamma$ result at a distance of 1 meter, and separation distances of 10-20 meters are required to obtain enough fall-off in contaminant field to permit interplanetary field measurements. The further penalties of the low conductance electron injection system are in overall thruster efficiency, in electrostatic contamination, and in space plasma contamination. If an increment of potential of 100 volts from neutralizer to thrust beam is required to extract the neutralization electron current, then an efficiency penalty of ~ 100eV per ion is imposed on the thruster, since the bulk of the electron injection energy is non-recoverable as the fast electrons stream outward into the space plasma. For the same assumed condition of injection potential and for a neutralizer placed at the spacecraft potential, conditions of severe electrostatic contamination may be expected to result, since inwardly diffusing electrons provide a comparatively effective coupling between the thrust beam and space plasma and the spacecraft attains a negative potential relative to the space plasma of, essentially, the magnitude of the injection voltage. Finally, the release of large currents of comparatively high energy electrons into the space plasma results in a particle contamination of that medium.

For a high conductance coupling between neutralizer and thrust beam significant diminutions of each of the contaminant effects may be expected. Electron injection energy is lowered, improving overall system efficiency. Electrons moving from the neutralizer to the thrust beam may interchange with the space plasma electrons, but have prolonged periods of residency before interchange, thus avoiding the magnetic contamination and space plasma contamination effects resulting from a bulk outward streaming of thrust beam electrons. Finally the condition of reduced required potential difference between neutralizer and thrust beam results in generally reduced potential difference between the spacecraft and the space plasma. Under these conditions, the application of only modest bias potential between the neutralizer and the spacecraft may reduce or eliminate the potential difference between spacecraft and space plasma. This condition of electrostatic cleanliness is a possible property of active spacecraft, as distinct from passive craft, and, by its presence, opens up possibilities for low energy charged particle measurements aboard solar-electric vehicles that have not been previously realized.

The technology requirements for a neutralization system would now appear to place a premium upon a high conductance coupling between neutralizer and plasma. Injection energies of neutralizing electrons should be at minimum possible values. Quantitative estimates cannot yet be set, but, qualitatively, injection potentials less than 10 volts appear as a design goal. Electron temperatures for these initially injected particles should be as low as is possible. The total electron interchange process between the two plasmas must balance, of course, but if local imbalances must exist, these should be at minimum possible levels. Electrostatic conditions which lead to the thrust beam as a local <u>sink</u> for space plasma electrons and a distant <u>source</u> of electrons moving into the space plasma provide an overall balanced interchange as required but do not result in the deposition of thrust beam electrons near the craft, thus reducing or eliminating any contamination of the space plasma. The circulating current levels in such a local sink - distant source condition are very small as the inward diffusion rate of space plasma electrons is small, thus reducing magnetic contamination effects. Furthermore this interchange may be expected to possess a comparatively symmetric pattern about the axis

of the thrust beam, the presence of axial symmetry being effective in containing contaminant magnetic field lines to the near neighborhood of the thrust beam. Finally, the neutralization system should possess a capability for applying a variable bias between neutralizer and spacecraft to yield a condition of spacecraft electrostatic cleanliness. This final system property also requires the use of surface field sensing devices on the spacecraft and appropriate feedback and control loops.

D. Electromagnetic Contamination

Several possible sources of electromagnetic contamination of the data pool from the operation of electric thrusting units have been described (II.A., Fig. 3). Radiation at optical frequencies has not been considered as a contaminant in that these emissions emerge in a comparatively narrow cone of directions and move through essentially non-reflective media. Possible exceptions here are resonance radiation lines of cesium, or mercury, which might appear in the "backward" direction (opposite to beam direction) through excitation of neutral atoms by electron impact or through charge exchange reactions. Even if such radiation were to be present in measurable quantities, sensors measuring optical radiation from the data pool may avoid contaminant effects from the thrust beam with only minor restrictions on "look angles."

The discharge region of an electron bombardment thruster is a plasma of 10^{10} to 10^{11} ions/cm^3. Characteristic frequencies of plasmas of this density are in the range of GHz (10^9Hz), and detectable quantities of such radiations are to be found in bombardment engine exhausts. It is not considered likely, however, that this radiation will act as a contaminant to the data pool. First, although the radiation is detectable to sensors within the plasma thrust beam, antennae of the spacecraft science payload examining the electromagnetic component of the data pool are well removed from the thrust beam. Coupling from the electron bombardment discharge to the thrust beam through the dilute space plasma is ineffective at best. Second, the relevant electromagnetic frequencies in the data pool are those characteristic of the dilute plasmas in the interplanetary space. For these reduced densities, characteristic frequencies are in kilo Hz, or less (electron cyclotron frequencies are in the region of several hundred Hz). Thus, antennae and possible sensing devices

and electronics are adapted to frequencies of the VLF range, and detection of bombardment discharge radiation is unlikely. Radiation from the thrust beam in the GHz range will be of concern to the spacecraft transmission and reception systems (III.B.), but will not be considered further here.

The remaining element of concern in electromagnetic contamination is for frequencies in the VLF range. A variety of thrust beam-space plasma equilibration modes which might lead to fluctuations in this frequency regime have been postulated.[13,19] These modes have not been verified in laboratory tests of bi-plasma equilibration. Experimental tests of equilibria are underway, however, and, subject to the geometrical limitations of laboratory testing systems, may reveal which, if any, of these very low frequency oscillatory modes are present, and, if present, under what circumstances. Since the relevant geometry for the bulk of the postulated modes is the unbounded geometry of space, the most direct tests for possible sources of VLF contamination would be conducted in situ.

E. Radio Wave Absorption and Refraction

One further area of possible impact upon the data pool through electric thruster operation should be examined. Of interest here are the radio propagation determinations of the total 'electron content.' Through measurements of phase and group velocities of radio waves of two different frequencies moving from Earth to the spacecraft, a determination of the integral of the electron density along the propagation path is obtained. This electron content measurement (in electrons/area) may be affected if the propagation path from the Earth transmitter to the spacecraft receiver passes through the plasma thrust beam. Two effects must be considered. The first of these is that an additional electron colony now exists in the space because of the presence of the thrust beam, and the integral of the electron density along the propagation path will now possess an additive perturbation. For a propagation path along the axis of the thrust beam from the thruster to infinity (maximum possible perturbation content) and for realistic values of initial thrust beam electron density and thrust beam divergence angles, perturbation contents of $\sim 5(10)^{15}$ electrons/m^2 are obtained.[20] For spacecraft at distances of 1 Gm(10^9m) from Earth, total electron contents (ionospheric plus interplanetary) range from

$2(10)^{17}$ electrons/m^2 for "quiet" conditions to $2(10)^{18}$ electrons/m^2 for "burst" conditions.[21] From these results, the perturbation introduced by the presence of the plasma thrust beam would range from .1 to 1%, and would not appear to be of concern. There is, however, an additional effect relating to the absorption of the propagating waves in the plasma thrust column in regions of that column which become "overdense" (plasma electron frequency in excess of radio wave frequency).

Frequencies utilized in radio propagation measurements have been 50 and 425 MHz[21] and 40 and 430 MHz.[22] Comparatively extensive portions of the plasma thrust beam are overdense to the lower of these frequencies, and more limited portions of the plasma are overdense for 400-500 MHz propagation. Calculated attenuation factors of the waves along selected propagation paths reveal severe attenuation for the lower frequencies and modest attenuation of upper frequencies.[20] Since the radio propagation measurement necessarily utilizes both frequencies, the loss of one component results in the loss of experimental data. For propagation paths through other regions of the plasma thrust beam in which plasma electron frequency is less than wave frequency, absorption of the wave does not occur but refraction of the wave front through large angles may occur. Such large angle scattering of the radio waves also leads to loss of signal loss for the bulk of those propagation paths linking the (finite) area of the receiver to the transmitted signal.

Corrective action here lies in receiving antenna placement and spacecraft configuration such that the propagation path does not lie through the plasma thrust beam. Alternatively, measurements of total electron content could proceed during periods when the thrusting units are inactive and during periods when the line of sight from Earth to the receiving antenna does not encounter the dense (upstream) portions of the plasma exhaust.

III IMPACT OF THRUSTING UNIT OPERATION ON DATA CHAIN

A. Spacecraft Collection and Processing of Data

Figure 1 has indicated elements of the data chain for the collection of data from the pool and its subsequent processing. These functions may be affected by operation of the thrusting units. Emphasis here will be directed

toward "internal" processes as distinct from the "external" processes in the interaction of telemetered data and commands with the thrust beam plasma (III.B.) or material deposition from the thrust beam on the surfaces of the spacecraft (III.C.).

An example of an internal process through which thrusting unit operation may impact upon the data chain is in thermal loading. This is not a unique process for solar-electric spacecraft, but the levels of power generated and dissipated on this type of spacecraft will introduce new dimensions to this problem. For a multi-kilowatt solar-electric craft, the bulk of the power is in the thrust beam. However, the power dissipated in the conversion units between the solar array and the thruster and in the generation of ions in the thruster may be at the kilowatt level, even for electrically efficient power conversaion and thrust units. The steady state release into the spacecraft of power at this level will require appropriate insulation of those systems which are more sensitive to temperature variations and passive or active thermal control of those regions of the spacecraft with significant power dissipation. There are no apparent major difficulties in this thermal control. It does, however, merit inclusion as a design problem for solar-electric spacecraft.

A second internal process of concern here is electromagnetic interference - either of the radiated or conducted form. Some insight into this potential problem area may be gained from the Snap 10A Test Flight (Vehicle 7001) which included an electrostatic thruster in its secondary payload.[23] The post flight analysis of ion engine operation[24] contains an extensive investigation into problems associated with EMI from the thrusting unit system. For convenience a brief review of observed behavior and subsequent analysis will be given here. At revolution 18 of Vehicle 7001, the ion engine secondary payload was commanded on for approximately one hour. During pass acquisition, telemetry data indicated many anomalies in SNAP 10A and electrical system performance. At revolution 19 it was observed that an abnormal amount of gas in the attitude control system had been expended, and tape recorded data indicated severe vehicle slewing had occurred. Engine shutdown was commanded and all other system performances returned to normal. Recorded data also revealed

that the ion engine high voltage supply cycled on and off repeatedly during revolution 18. This cycling indicates an overload created by arcing at the high voltage terminals of the thruster.

Analysis of flight data and subsequent EMI tests led to the conclusion that arcing at the high voltage terminals was established with the initiation of cesium flow in the thruster and that arcing induced EMI introduced false error signals in the Agena horizon sensors (creating severe vehicle attitude perturbations), upset the synchronization of submultiplexers on one telemetry link and amplitude modulated the data wave train and otherwise affected data on another telemetry link. Laboratory tests of a high voltage power supply and ion thruster identical to the flight unit were conducted with conditions of both intermittent and steady state shorting of the high voltage electrodes of the thruster. Measurements of radiated EMI, both broad and narrow band (from 15 KHz to 40 MHz) were obtained with pickup antennae near the thruster, and measurements of conducted EMI (broad and narrow band from 14 KHz to 25 MHz and broad band from 30 Hz to 15 KHz) were obtained with the thruster system operating through circuitry elements similar to those in the spacecraft wiring layout. It was found that cycling of the high voltage supply resulted in both radiated and conducted EMI substantially above specified design levels. Analysis of test data led to the conclusion that the effects observed in flight were probably the result of low frequency (below 1 MHz) conducted EMI from the cycling of the high voltage supply.

The cited flight evidence should not be considered as a general and unavoidable feature of electric thruster operation. Arcing during ion engine startup was observed on SERT I, but there was no apparent loss of data channels or inadvertent changes in spacecraft circuitry.[25] The evidence does indicate some of the problems of thruster system integration into specific spacecraft, and points out an area for additional emphasis in system integration and testing.

B. Spacecraft Transmission of Data and Reception of Commands

A previous section (II.E.) has treated problems in measurements of total electron content when the propagation path from Earth to the spacecraft receiver passes through the plasma thrust beam. Similar, but less severe,

problems exist for the radio waves used for the transmission of data and the reception of commands. For these radio waves and assuming the use of the 2.3 GHz Deep Space Network, frequencies are in excess of the electron plasma frequency at any point in the plasma thrust beam, so that wave absorption will not occur although refraction of the waves may take place. For a "uniform core-exponential wing" density model of the plasma thrust beam with total ion current of 1 ampere at 5000 seconds specific impulse and a core divergence angle of 6° (total cone angle = 12°), the refraction of 2.3 GHz waves has been calculated as a function of the position of wave encounter with the plasma beam and for wave motion both in the exponential wing region of the plasma and at the boundary of the uniform core.[26] These calculations have determined that the principal refraction of the wave is in the encounter with the boundary of the dense, uniform core, region. Refraction of the wave in its motion through the exponential wing region depends upon the extent of this wing. For a comparatively broad wing, refractive effects here are similar to but somewhat smaller than the refraction at the core boundary. Taken together, total refraction of the wave front in excess of 1° may occur for encounter of the propagation path with the thrust beam within, approximately, the first five meters of the plasma column. Figure 6 illustrates these wave refractions for both the transmitted waves and for waves reaching the spacecraft from Earth.

Other calculations of wave refraction have been performed with a somewhat different beam density model than used above.[8] Angles of refraction for this second density model were somewhat less than those given above, but were considered sufficiently large to merit further study.

The concern over comparatively small diffraction angles derives from the required pointing accuracy in the transmitted beam and in the antennae for the received signal. For deep space communication the required pointing effects cannot be neglected. Relief from possible problems of loss of signal strength (either transmitted or received) through refraction in the plasma thrust beam would appear to be in antenna placement such that encounter of the propagating waves with the thrust beam does not occur within a predetermined minimum axial downstream position. Such a condition may impose a constraint on spacecraft configuration for particular missions.

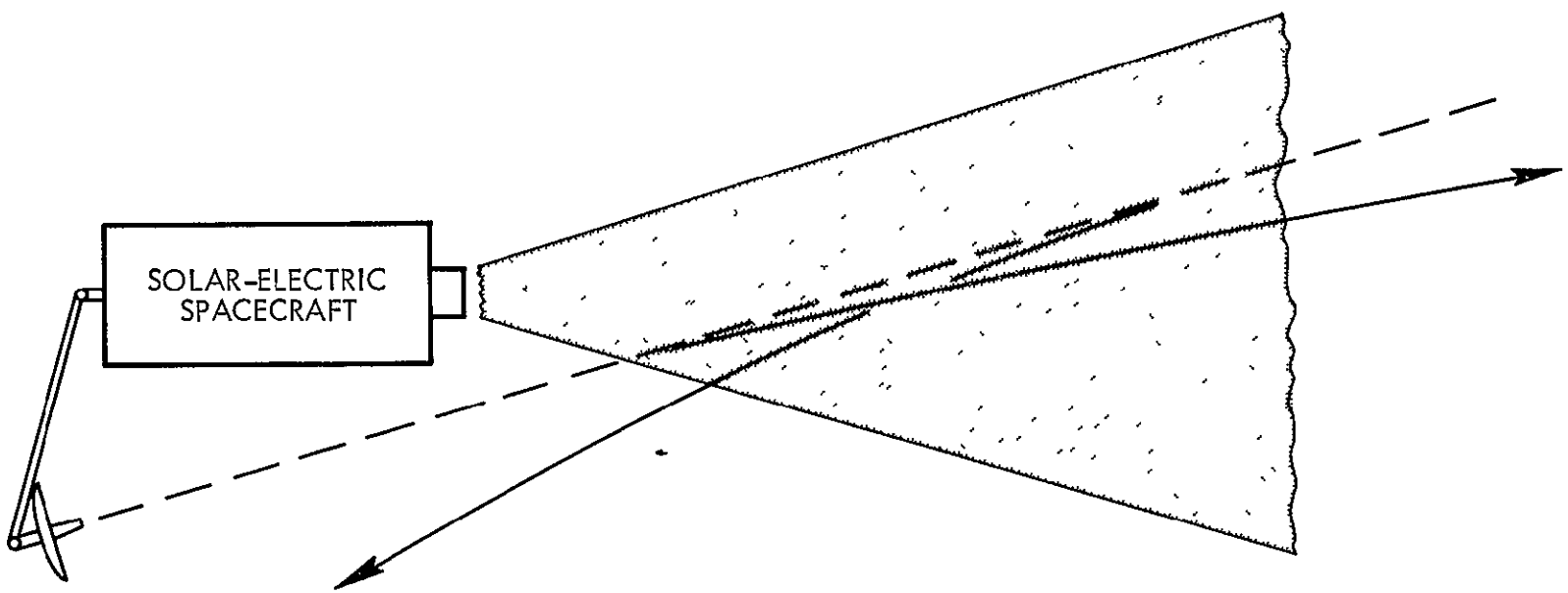

Figure 6. Wave refraction for propagation path through plasma thrust beam of solar electric spacecraft. Dashed line indicates line-of-sight between Earth and spacecraft antenna. Solid lines indicate propagation direction for transmitted waves and received waves.

C. Material Deposition on Spacecraft Components

The operation of electric thrusting units releases both neutral and charged particles, some fraction of which may intercept the surfaces of the spacecraft, depending on craft configuration. The most energetic particles in the thrust beam exhaust are the primary ions, and their impact on surfaces may cause erosion through sputtering and may also enter into a variety of chemical and metallurgical reactions with the spacecraft materials. Charge exchange ions possess less energy and their impact upon surfaces will not result in significant sputtering although they may participate along with deposited neutrals in chemical and metallurgical processes in a manner similar to that of the energetic ions. Other physical processes resulting from the deposition of layers of propellant material on spacecraft surfaces include variations in absorptance and emittance of the surface. Electrons will not possess energies which lead to significant surface erosion. Their presence, however, may determine the charge state of the surface which, in turn, may govern the dynamics of other charged particles moving in the vicinity of the surface.

The dynamics of the various types of particles released in the thrust beam have been examined in a series of recent studies. The distribution of atoms and charge exchange ions downstream from a 15cm diameter mercury electron bombardment thruster has been calculated using an analytical model of the ion flow in the ion acceleration and neutralization region.[27] The first group of charge exchange ions considered are denoted "Group 2" (to distinguish from the primary ion beam, or Group 1) and result from charge exchange reactions occurring in the ion acceleration and deceleration regions of the thruster. Because these particles do not follow the more carefully tailored ion optical paths of the primary beam, their dispersion angles relative to the thrust beam axis encompass a larger range than the primary beam. Some of these ions may emerge at right angles to the thrust axis and intercept surfaces there if the spacecraft is so configured. The lower bound to the permissible mesh size in the computer program, however, limits application of the results for these charge exchange ions to the range of dispersion angle within 45° from the beam axis. A second group of charge exchange ions (denoted Group 4) are formed downstream from the ion thruster and emerge from the thrust plasma at essentially 90° from the axis of the beam.

While energies of some of the Group 2 ions may range upward to the primary ion beam energy, ions of the Group 4 category are uniformly low in energy. This first study indicated that charge exchange ions and neutral particle fluxes from the cited mercury ion thruster would be negligible in the region outside the primary ion beam and at least .75 meters from the axis of the beam.

In a second study of the propellant deposition, the treatment was broadened to include neutral and charged states of both cesium and mercury.[28,29] Here the possible mechanisms which might degrade spacecraft components included propellant condensation, chemical and metallurgical reactions, sputtering erosion, and radiation damage from the deposition of energy within solids by high energy ions. The spacecraft components in the study included thermal control coatings, optical elements and coatings (solar cell cover glass and lenses), structural materials, insulators, conductors, adhesives, moving joints and solid state components. Initial emphasis in the study was to isolate possible problem areas for future experimental examination. Application of a developed propellant condensation theory to a large area solar array for an electrically propelled Jupiter flyby spacecraft revealed the possibility of mercury condensation on the front surface of inboard solar array panels as the spacecraft proceeded beyond heliocentric distances of ∿3AU. Analysis here did not include secondary factors of range in surface thermal properties, heat loading of the spacecraft to the array, and the dynamics of layer growth under varying array temperatures. The possibility of partial loss of array power through mercury condensation on the front of the array is sufficiently developed, however, to warrant more detailed treatment in the event of an established mission.

Two additional studies have been made on the condensation of propellant on surfaces near the ion thruster exhaust. In the first of these,[30] a mercury electron bombardment thruster is utilized. Arrival rates of neutral propellant have been calculated for primary surfaces (those within the cone of line-of-sight directions from the thruster) and for secondary surfaces (accessible, via line-of-sight, from primary surfaces). These calculations indicate that neutral efflux rates are sufficiently high and interplanetary flight times sufficiently long that substantial quantities of propellant may impinge on surfaces nearby and downstream from the thruster exhaust and that reflection and re-evaporation of propellant from primary surfaces will be sufficient to yield impingement of

propellant on secondary surfaces. For these latter impingements, however, more refined calculations will be required to establish magnitudes. An application of the calculations to a Jupiter flyby solar-electric spacecraft indicated that condensation may occur on the regions of the solar array near the thruster during the latter part of the mission. These conclusions are similar to those in the previously cited study[28] in predictions of possible condensation. Also, both studies indicate a need for improved analytical treatment of the thermal dynamics of the solar array in condensation problems.

The final study[31] for review here has examined the effects of propellant condensation from the thrust beam of a cesium ion thruster upon the aluminum thermal control shutters and the radiation cooler of an ATS configured spacecraft. The analysis includes both neutral and charged particles from the thruster exhaust. For the reference configuration utilized, the analysis indicated that condensation upon the thermal shutters would not impact upon the operation of that system. Build-up of cesium of several monolayers thickness is predicted, but alteration of thermal radiation characteristics would not appear as likely. Operation of the radiation cooler, however, would appear to be severly perturbed by condensation of exhaust particles for the spacecraft configuration utilized. The principal source of difficulty in condensation was considered to be the low energy charge exchange ions, and electrostatic approaches to the rejection of this component of the thruster exhaust were proposed.

In addition to analysis, experimental examination of selected condensation materials problems is in process. From previously indicated problem areas,[28,29] experimental studies of chemical and metallurgical interactions, surface thermal properties and ion erosion have been initiated.[32] These experiments have revealed major and comparatively rapid changes in the (xenon simulated) solar absorptance of spacecraft surface materials under mercury ion bombardment. Materials showing increases by factors of 2 to 4 in absorptance were RTV-41, and Z-93, PV-100, and S13G white paints. Ion dosage to produce these marked alterations in absorptance were $\sim 10^{17}$ ions/cm^2 at energies of $\sim$3KeV. Comparatively minor changes in absorptance and hemispherical emittance were observed for mercury ions impacting on Microsheet, quartz, 3M and Cat-a-lac black paint, and gold. Exposure of a variety of surfaces (gold, polished aluminum, Microsheet, quartz, RTV-41, 3M, PV-100,

Z-93, S13G, and Cat-a-lac) to mercury neutrals revealed only minor variations in absorptance and emittance. Neutral dosages were in excess of that possible deposition for extended interplanetary missions, while ion dosages which created variations in solar absorptance were at "possible" levels for interplanetary missions and for configurations allowing such impact. The deterioration of materials observed in these tests would indicate restructuring of spacecraft systems to prevent ion interceptions at this level. Neutral interception, for the present conditions of sample temperature which do not allow condensation to occur, have not demonstrated chemical alterations to material properties sufficient to produce any reconfiguration of spacecraft systems.

The evaluation of the total impact of material deposition on spacecraft surfaces is still in process. From analyses, which have indicated possible problem areas, and from experimental tests, which are establishing tolerance limits, the restraints on spacecraft configuration to avoid materials deposition problems will be derived.

IV. SUMMARY

A series of possible processes have been detailed through which the operation of electrical thrusting units may impact upon the data pool or upon the operation of the data chain. System configurations and constraints to reduce or eliminate various possible contaminants have also been detailed. These include appropriate placement and granularity in the backwiring of solar cell arrays, field cancellation configurations for ion thruster operation, neutralizer coupling and bias properties to yield minimized electrostatic, magnetic and space plasma contamination in the thrust beam-space plasma electrical equilibration, constraints on antennae placement and "look angles," system integration and testing limits on both radiated and conducted EMI, and tolerance limits on material deposition on spacecraft surfaces.

While possible problem areas have been defined, these problems do not appear to be beyond solution. Rather there are encouraging prospects that electrically propelled spacecraft may provide a more hospitable environment for the collection and processing of scientific data than has previously been possible for purely passive craft. The possibility of electrostatic cleanliness

is a particular example of this promise. Beyond these factors are increased excursion capabilities in space and time, increased payloads for scientific subsystems, and increased power levels for the conduction of experiments and the maintenance of auxiliary systems to provide a contaminant free condition of spacecraft operation.

REFERENCES:

1. "Potentials of Solar Power for Electric Propulsion," D. Ritchie, R. Toms, and W. Menetrey, Presented at the AIAA Fifth Electric Propulsion Conference, San Diego, Calif., March 1966. AIAA Preprint 66-210.

2. "Design of a Solar-Electric Propulsion System for Interplanetary Spacecraft," J. H. Molitor, D. Berman, R. L. Seliger, and R. N. Olson, Presented at the AIAA Fifth Electric Propulsion Conference, San Diego, Calif., March 1966. AIAA Preprint 66-214.

3. "Solar Powered Electric Propulsion Systems - Engineering and Applications," J. W. Stearns and D. W. Kerrisk, Presented at the AIAA Fourth Aerospace Sciences Meeting, Los Angeles, Calif., June 1966. AIAA Preprint 66-576.

4. "Solar Powered Electric Propulsion," Program Summary Report SSD 60734R, Space Sciences Division, Hughes Aircraft, JPL Contract 951144, Dec. 1966.

5. "Photographic Exploration of Mars with Solar-Electric Propulsion," L. H. Wood, W. P. Prasthofer, and R. I. Vachon, Journal of Spacecraft and Rockets 5, 503-509, May 1968., also Presented at the AIAA Fifth Aerospace Sciences Meeting, New York, New York, Jan. 1967. AIAA Preprint 67-88.

6. "A 3KW Solar-Electric Spacecraft for Multiple Interplanetary Missions," H. F. Meissinger, R. A. Park, and H. M. Hunter, Presented at AIAA Joint Electric Propulsion and Plasmadynamics Conference, Colorado Springs, Colorado, Sept. 1967. AIAA Preprint 67-711.

7. "Use of Electric Propulsion for Exploring the Distant Regions of the Geomagnetic Tail," H. F. Meissinger and E. W. Greenstadt, Presented at the AIAA Sixth Aerospace Sciences Meeting, New York, Jan. 1968. AIAA Preprint 68-120.

8. "1975 Jupiter Flyby Mission Using Solar-Electric Propulsion," JPL Report ASD 760-18, March 1968.

9. "Spacecraft Electric Propulsion - Now?" T. A. Barber, J. V. Goldsmith, and J. R. Edberg, Aeronautics and Astronautics, Vol. 6, No. 6, 38-47, June 1968.

10. "Primary Electric Propulsion Technology - Toward Flight Programs for the Mid-1970's," D. J. Kerrisk and D. R. Bartz, Aeronautics and Astronautics, Vol. 6, No. 6, 48-53, June 1968.

11. "Future Missions for Libration Point Satellites," R. Farquhar, Aeronautics and Astronautics, Vol. 7, No. 5, 52-57, May 1969.

12. "Spacecraft - Space Plasma Equilibria for Passive and Active Spacecraft," J. M. Sellen, Jr., Presented at the AIAA Electric Propulsion and Plasmadynamics Conference, Colorado Springs, Colorado, Sept. 1967. AIAA Preprint 67-702.

13. "Study of Electric Spacecraft Plasmas and Field Interactions," J. M. Sellen, Jr., Presented at the AIAA Seventh Electric Propulsion Conference, Williamsburg, Va., March 1969. AIAA Preprint 69-276.

14. "Feasibility Study - 30 Watts per Pound Roll-up Solar Array," General Electric Missile and Space Division Report 68SD4301, JPL Contract 951970, June 1968.

15. "Final Report. Phase II. Large Area Solar Arrays," Boeing Co. Report D2-113355-7, October 1968.

16. "Contaminant Magnetic Fields from Large Area Solar Arrays," J. M. Sellen, Jr. and H. S. Ogawa, TRW 12738-6006-R000, June 1969.

17. "Backwire and Busbar Placement for Magnetic Cleanliness on Large Area Solar Arrays," J. M. Sellen, Jr., TRW 12738-6007-R000, June 1969.

18. "Investigations of Ion-Beam Diagnostics," J. M. Sellen, Jr., Sect. III.G, TRW 8603-6037-SU-000, April 1964.

19. "Study of Electric Spacecraft Plasmas and Field Interactions," Robert K. Cole, H. S. Ogawa, and J. M. Sellen, Jr., TRW 07677-6013-R000, Contract NAS7-564, May 1968.

20. "Plasma Thrust Beam Total Electron Content and Possible Perturbations to Radio Propagation Measurements," J. M. Sellen, Jr., TRW 9884-64-3, Sept. 1969.

21. "Radio Propagation Measurements of Pulsed Plasma Streams from the Sun Using Pioneer Spacecraft," Richard L. Koehler, Journal of Geophysical Research, 73, 4883-4894, August 1968.

22. "Measurements of the Electron Content of the Interplanetary Medium Between Earth and Venus," D. B. Campbell and D. O. Muhleman, Journal of Geophysical Research, 74, 1138-1143, March 1969.

23. "Engineering Analysis Report," Lockheed Missile and Space Corporation, Contract AF04(695)-136, Undated.

24. "Ion Engine Flight Test Analysis - Snapshot," Lockheed Missile and Space Corporation, LMSC/A748484, Contract AF04(695)-136, May 1965.

25. "Results from SERT I Ion Rocket Flight Test," R. J. Cybulski, D. M. Shellhammer, and J. T. Kotnik, NASA TN D-2718, 1965.

26. "Plane Wave Refraction at the Boundary of a Plasma Thrust Beam," J. M. Sellen, Jr., TRW 9884-64-1, Aug. 1969.

27. "Distribution of Neutral Atoms and Charge-Exchange Ions Downstream of an Ion Thruster," John F. Staggs, William P. Gula, and William R. Kerslake, Journal of Spacecraft and Rockets 5, 159-164, February 1968.

28. "Electrostatic Rocket Exhaust Effects on Solar-Electric Spacecraft," David F. Hall, Brian E. Newnam, and James R. Womack, Presented at the AIAA Seventh Electric Propulsion Conference, Williamsburg, Va., March 1969. AIAA Preprint 69-271.

29. "Evaluation of Electric Propulsion Beam Divergence and Effects on Spacecraft," Final Report JPL Contract NAS7-575, TRW 08965-6013-R0-00, Sept. 1969.

30. "Propellant Condensation on Surfaces Near an Electric Rocket Exhaust," Thaine W. Reynolds and Edward A. Richley, Presented at the AIAA Seventh Electric Propulsion Conference, Williamsburg, Va., March 1969.

31. "A Study of Cesium Exhaust from an Ion Engine and Its Effect upon Several Spacecraft Components," Hittman Associates, HIT-399, June 1969.

32. "Propulsion Beam Divergence Effects," David F. Hall, JPL Contract 952350, Report Period Aug. 31 - Sept. 26, 1969.

SECTION IV. E.

FACTORS IN THE ELECTROSTATIC EQUILIBRATION BETWEEN A PLASMA THRUST BEAM AND THE AMBIENT SPACE PLASMA

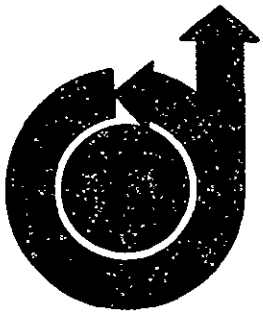

AIAA Paper
No. 70-1142

FACTORS IN THE ELECTROSTATIC EQUILIBRATION BETWEEN A PLASMA THRUST BEAM AND THE AMBIENT SPACE PLASMA

by
HOWARD S. OGAWA, ROBERT K. COLE
and
J.M. SELLEN, JR.
TRW Systems Group
Redondo Beach, California

AIAA 8th Electric Propulsion Conference

STANFORD, CALIFORNIA/AUGUST 31-SEPTEMBER 2, 1970

FACTORS IN THE ELECTROSTATIC EQUILIBRATION BETWEEN A PLASMA THRUST BEAM AND THE AMBIENT SPACE PLASMA*

ABSTRACT

Factors in the electrostatic equilibration between a plasma thrust beam and the ambient space plasma have been investigated both analytically and experimentally. Plasma models, utilizing an electrostatic equivalent of the barometric relationship, provide a specification of thrust beam neutralizing electron temperature for a given electron injection energy. Limitations on the barometric relationship must be invoked unless energy transfer occurs between thrust ions and neutralizing electrons. Plasma wind tunnel tests have extended previous studies of thrust beam-space plasma interactions. Neutralizing electron injection potentials have ranged from 0 to $\sim$ 100 volts. Conditions were observed for moderate injection potentials in which partial thermalization of electrons occurred. Other conditions of neutralization yielded an electron temperature not simply related to injection energy. Experimental results are detailed with application to possible equilibration conditions of electrically propelled spacecraft.

I. INTRODUCTION

In the production of thrust by an electrically propelled spacecraft, a plasma beam is released from the craft into the ambient plasma of space. The flow of charged particles in the thrust beam, the presence of charged particles in the ambient space, and the conductivities and particle mobilities of both of these media result in conditions of electrostatic equilibration that are not, in general, prevalent for conventional passive spacecraft in the space plasma.[1] This paper will examine various contributing factors in the electrostatic equilibration of this bi-plasma system.

*This work was performed for the Jet Propulsion Laboratory, California Institute of Technology, sponsored by the National Aeronautics and Space Administration under Contract NAS7-100.

Previous analytical studies of the thrust beam-space plasma interaction have treated a simplified equilibration model in which electron temperature is everywhere constant.[2,3] Plasma wind tunnel experiments to test the simplified model have utilized neutralization conditions of equal beam and space plasma electron temperatures.[3] In the vehicular case, however, there are both temporal variations in the space plasma and spatial variations in the thrust beam which make constancy of electron temperatures unlikely. The treatment of this more general interaction, including electron temperature gradients, is considerably more difficult than for the earlier simplified model.

To gain further understanding of the generalized bi-plasma interaction, extensions of earlier analytical treatments have been made. Plasma wind tunnel studies have also been carried out through a wider range of neutralizing electron injection conditions. The interpretation of "bounded geometry" laboratory results in terms of "unbounded geometry" space equilibrations is necessarily limited. However, both analyses and experiments have provided insight into actual beam-in-space interactions.

The interactions of the thrust beam with the space plasma relates, in turn, to the performance of scientific spacecraft in the acquisition and interpretation of scientific data. Previous studies[4,5] have examined the possible impact on scientific experiment operation from magnetic contamination, electrostatic contamination, and space plasma contamination produced by the expulsion of a thrust beam from the spacecraft. The analyses and experiments here presented allow the development of, at least, qualitative specifications on neutralization system performance to provide conditions of "cleanliness" appropriate for scientific spacecraft operation.

II. PLASMA MODELS

A. General Features

In the description of the thrust beam and space plasma, the quantities of primary interest are the plasma density, the electron temperature, and the potential. For thrust beams with even moderately well-coupled neutralization systems, the electric fields in the plasma system do not cause

any substantial alteration of thrust beam ion trajectories. The existence of straight line thrust ion trajectories and the common occurrence in electrostatic thruster beams of an apparent common point of origin for these trajectories leads to the description of such beams as "conical." The outward divergence of the ion beam trajectories leads eventually to vanishingly small thrust ion densities. The boundary along which thrust ion density has diminished to ambient space plasma density has been termed the "merging contour."

Because of the magnitude of thrust ion energy in comparison to potentials throughout the bi-plasma system, the plasma density is determined by the beam dynamics (current densities, divergence angles) at the thruster, and, beyond the merging contour, by the ambient plasma. Laboratory tests of thruster performance are sufficient to determine these beam dynamics, and significant differences between laboratory and space would not be expected. A somewhat different circumstance may exist relative to electron temperature and the potential structure throughout the bi-plasma system.

The occurrence of electric fields in the thrust beam-space plasma is the result, principally, of two parameters. The first of these is the comparatively large magnitude, in general, of electron thermal speeds relative to the ions. The second is the existence of plasma density gradients. For the plasma densities involved, the interaction of electrons with ions through single particle collisions is comparatively infrequent, and the plasma is considered "collisionless." There are, however, collective effects in which, through the Coulomb interaction, the charge colonies of ions and electrons do relate, in a self-consistent fashion, with each other. The manifestation of this collective interaction is the potential structure in the plasma, and the following portions of this section will be concerned with the form of this potential and its relation to electron temperature.

B. Single Thrust Beam

1. Barometric Relationship

The thrust beam to be considered here will be axially symmetric and "conical," in the matter of straight line ion flight and an

apparent source point for all trajectories. Measurements of such beams[6,7] have been described by a "uniform core-exponential wing" density model. The density distribution, ρ_b (r, z), for such beams is given in Reference 3. Measurements of potential and electron temperature in beams neutralized by immersed unipotential hot wire neutralizers have revealed[6]

$$\rho_b = \rho_o \exp\left(\frac{-eV}{kT_e}\right) \tag{1}$$

where ρ_b is particle density, V is potential at (r, z), e is electron charge (-1.6×10^{-19} coulombs), k is the Boltzmann constant, and T_e is electron temperature. For (r, z) = (0, 0), V = 0 by definition. Under the Maxwellian energy distribution, characterized by T_e, it may be noted that potential increments resulting from a non-zero electron temperature and density increments in the plasma are given by

$$dV = \frac{-kT_e}{e} \frac{d\rho}{\rho} \tag{2}$$

Thus, potential gradients become smaller for decreased electron temperature or decreased density gradients. Magnetic fields which can alter the forms of Eq. (1) and (2), will be assumed to be absent throughout the discussion. This assumption is justified in view of the magnitude of magnetic fields in the space environment.

Eq. (1) is an electrostatic equivalent of the barometric relationship, and its appearance would indicate an equilibrium state between a Boltzmann gas (electrons) and a potential structure, generated in a self-consistent fashion by the interaction between electrons and ions. For beams with immersed hot wire neutralizers ($T_e \sim 2500°K \sim T_{wire}$) the relationship would appear to hold through at least a variation of two orders of magnitude in plasma density. There are, however, limitations to the use of "barometric" conditions if a steady state transport of electrons must take place in the presence of this potential structure.

2. Limitations on Potential Structure

Equation (1) is an exact statement of an equilibrium between a Boltzmann gas at T_e and a potential and density structure in which electron diffusion velocity is zero. For electrons in an ion thrust beam, the electron diffusion velocity in the radial direction is zero (here neglecting ion radial velocity through beam divergence) so that barometric conditions should be expected to be obtained for radial density and potential scans. For the axial direction, the conditions of current and space charge neutralization require an electron drift velocity equal to the ion velocity. Retarding potentials (for electron motion) should be expected to be "relaxed" somewhat from barometric values to allow a net electron drift in this potential structure. However, for the examined cases of immersed hot wire neutralizers, Equation (1) was observed to hold for both radial and axial potential scans. Previous explanations for this behavior centered about the consideration that for electron drift velocities which are small compared to electron thermal speeds, the potential structure should be essentially that of the diffusion-free condition.

Of further concern, however, are the energy requirements of a steady state electron drift in the presence of such retarding potentials. For an electron to move from the beam origin (ρ_o, V = 0) to a downstream point at ρ and V (given by (1)) requires an energy input of $eV = kT_e \ln \frac{\rho_o}{\rho}$. Such an energy input might occur through the conversion of kinetic energy (T_e) to potential energy, and some cooling of electrons has been observed[7] for electron temperature scans in the axial direction. However, such cooling could not account for the continued motion of electrons from the neutralizer wire into retarding potential regions of the order of 6 kT_e as reported in Reference 3. Other possible explanations for an energy transfer to the electrons to allow their motion against the retarding potential include interactions between the electron colony and the neutralizer wire (preferential absorption of lower energy plasma electrons and preferential retention and axial transmission in the plasma of the tail of the emitted neutralizing electrons) and non-conservative plasma processes which selectively transfer energy from the ions (which possess large streaming energies) to the electrons.

Since the overall quantities of energy transfer required to explain the observations of immersed wire beams are only of the order of one electron-volt per electron, the determination of the source and method of such an energy flow would be considered to be difficult.

For a thrust beam neutralized with more energetic electrons, the growth of a potential structure with retarding potentials of several kT_e would require an even larger energy input to the electron colony. For beams neutralized with a withdrawn wire, the electrons are produced at a potential which is negative with respect to the beam origin by the magnitude of the injection potential, $|V_{inj}|$. For an energy flow to the electrons to be required, $kT_e \ln \frac{\rho_o}{\rho}$ must be larger than eV_{inj}. For conditions of injection, beam density, space plasma density, and electron temperature considered to have been present for the SERT I test flight, it was possible to conclude, using a simple equilibration model, that retarding potentials in the thrust beam did exceed the electron injection potential, and that the equilibration potential of the neutralizer wire (and spacecraft) relative to the space plasma would have been positive (perhaps by as much as 20 volts).[3,8,9] Evidence from the spacecraft surface electric field strength meters would appear to confirm such a positive spacecraft equilibration potential.[9] An energy transfer, through some unspecified mechanism, would be required to transport the current of electrons from the neutralizer to the space plasma. A central question is whether, in fact, such energy transfers occur. The SERT I evidence cited may only be considered as indirect, and a principal point of emphasis in the laboratory studies to be described will be a search for conditions of possible energy transfer to the electron flow in the thrust beam. If such transfer processes cannot be verified, then clear limitations exist in the permissible amount of potential excursion in the plasma thrust beam. This, in turn, will determine the magnitude and sign of possible electrostatic contamination of electrically propelled spacecraft. For the present discussion, the consideration of energy transfer does present possible limitations to the application of Equation (1).

A final factor limiting the application of the barometric equation is the possible non-Maxwellian character of the electron energy

distribution for conditions of increased injection potential. These features will be treated further in the sections detailing laboratory experiments.

3. Relation of Electron Temperature to Injection Energy

a. Thermalization Mechanisms

This section will consider the injection of electrons from a withdrawn unipotential hot wire into the thrust beam. The extent of the separation between the wire and the plasma column establishes a required potential difference to transport the neutralization current and electron injection energies ranging from 0 to $\sim$ 100 electron volts per electron may be obtained, covering a range which is of direct interest to operational thrusting systems.

Electrons entering the thrust beam will interact with the potential structure in the plasma column. If this interaction is strictly conservative, then the kinetic energy of an electron at a point (r, z, V) will be given by the difference in potential between V and the wire potential, V_{inj}. Such electrons would be single valued in their speed. If electrons move about in the potential structure with conservative scattering from the electric field in that structure, then, in principle, the electrons at (r, z, V) would possess a single speed, but with random orientation. The almost randomized motion of electrons in the plasma column (but with an average axial velocity which matches the ion axial velocity) is a conventional situation in neutralized plasma beams, and the scattering of electrons from the potential structure has been termed, "L'iouville trapping," and/or "electrostatic bottle." It should be emphasized, and later sections will discuss in detail, that considerable variations from this behavior may be obtained. For the present, it will be assumed that the average dwell time of an electron in any particular incremental axial region is identical to the dwell time of an ion moving through this same region and, since electron thermal speeds are large compared to ion speeds, electrons would move in semi-randomized paths. From these considerations, at a point in the plasma, random orientation of a single valued electron speed should be the desired condition of a conservative interaction of the electrons with the plasma column.

The observations of Langmuir probes in these plasma columns are, in general, contrary to the above conclusion. The probes reveal an electron distribution which is essentially Maxwellian; which is, in turn, consistent with observations of a barometric relation in ρ, V, and T_e. The existence of a Maxwellian distribution in energy, rather than "single valued," does not necessarily lead to a non-conservative interaction of electrons in that a redistribution from a single valued to a broadly distributed energy spectrum may occur through a conservative interchange of kinetic energy between members of the distribution. In an earlier series of measurements[10] in which thermalization was observed, the simultaneous occurrence of oscillations at the electron plasma frequency was taken to indicate that interactions between newly injected electrons and resident plasma electrons through the electron two-stream instability were responsible for the thermalization. Experiments to be described in later sections would now make it appear that such two-stream instabilities, while capable of generating electron plasma frequency oscillations, may not be an effective thermalization mechanism if the dwell time of freshly injected electrons is not sufficiently prolonged. For the present, then, the mechanism of thermalization, for those beams in which it is obtained, remains in question. A likely explanation is that thermalization occurs as a result of collective interactions and under conditions in which electrostatic trapping of freshly injected electrons in and near the injection region provides a sufficient period (and electron path length) for such interactions to become effective.

b. Injection of Electrons into Single Slab of Beam

This calculation will examine the allowable electron temperature for electrons injected conservatively into a narrow slab of beam at the beam origin, as shown in Figure 1. It will be assumed that thermalization occurs and the kinetic energy of an electron will be $\frac{3}{2} kT_e$ (here assuming three-dimensional thermal motion). The electrons originate at a wire at V_{inj} and the core region of the thrust beam is specified at V = 0. The barometric equation will be assumed to hold. The core and wing regions of the plasma are indicated in Figure 1, where r_{co} is core radius and a_o is the density exponential drop-off distance at the beam origin. From conservation of energy

$$eV_{inj} \int_o^\infty 2\pi r\rho(r)\, dr = \int_o^\infty [\tfrac{3}{2} kT_e + eV(r)]\, 2\pi r\rho(r)\, dr \qquad (3)$$

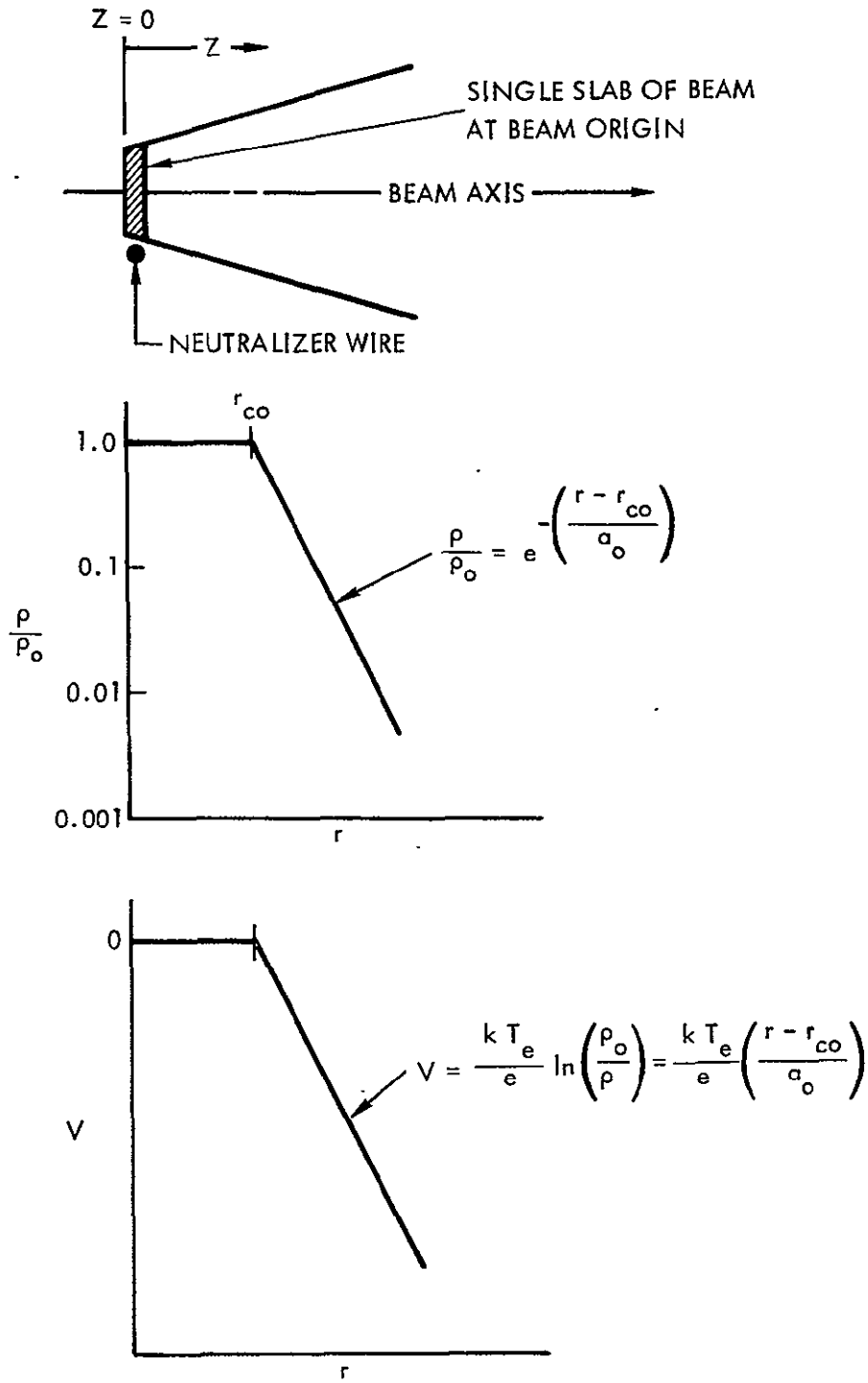

Figure 1. Model utilized in calculations of allowable electron temperatures for electrons injected into a single slab of beam near origin. Uniform core-exponential wing radial dependence on charge density and quasi-neutrality relation assumed.

Using

$$\rho = \rho_o \qquad r \leq r_{co}$$

$$\rho = \rho_o e^{-\left(\frac{r-r_{co}}{a_o}\right)} \qquad r > r_{co}$$

and $eV = 0 \qquad r < r_{co}$

$$eV = kT_e \ln \frac{\rho_o}{\rho} = kT_e \left(\frac{r-r_{co}}{a_o}\right) \qquad r > r_{co}$$

equation (3) may be evaluated and yields

$$eV_{inj} = kT_e \left(\frac{3}{2} + \frac{2a_o^2 + a_o r_{co}}{a_o^2 + a_o r_{co} + \frac{1}{2} r_{co}^2}\right) \tag{4}$$

Equation (4) may be examined for several conditions of "core-wing" ratio. These conditions are 1) "core" only ($a_o = 0$), 2) "wing" only ($r_{co} = 0$), and 3) "core" content $\simeq$ "wing" content ($r_{co} \sim 3a_o$). For these conditions:

1) $kT_e = \frac{2}{3} eV_{inj}$ "core" only

2) $kT_e = \frac{2}{7} eV_{inj}$ "wing" only

3) $kT_e \simeq \frac{1}{2} eV_{inj}$ "core" content ≈ "wing" content

In the earlier experiments[6] in which T_e was examined as a function of V_{inj}, it was found that $kT_e \sim 0.3\ eV_{inj}$, a result in general agreement with the calculations above [(2) and (3)]. This agreement may be, to some measure, fortuitous, but it does illustrate that comparatively simple models with conservative injection are capable of yielding electron temperatures of the general magnitude of those observed.

c. Injection of Electrons into Column of Finite Length

The calculation in b. above was restricted to the slab of beam at Z = 0. However, electrons do move back and forth along the axis of the plasma column, and it is of interest to calculate the electron temperature for the finite length of beam from Z = 0 to Z = Z. Figure 2 illustrates the beam region to be examined. To simplify, only the core region will be utilized. Following the notation of Reference 3, in the core

$$\rho(Z) = \rho_o \left(\frac{Z_o}{Z + Z_o}\right)^2 \tag{5}$$

where Z_o is the distance separating Z = 0, the beam origin, from the apparent origin of the ion trajectories. From the barometric equation, $eV(Z) = kT_e \ln \left(\frac{Z_o + Z}{Z_o}\right)^2$. For a conservative injection

$$eV_{inj} = kT_e \left\{\frac{3}{2} + \frac{1}{Z} \int_o^Z \ln \left(\frac{Z + Z_o}{Z_o}\right)^2 dZ\right\} \tag{6}$$

where the first term on the right hand side is the average kinetic energy and the integral provides the average potential energy. Completing the integration in Equation (6) yields

$$eV_{inj} = kT_e \left\{\frac{3}{2} + 2 \left[\left(\frac{Z + Z_o}{Z}\right) \ln \left(\frac{Z + Z_o}{Z_o}\right) - 1\right]\right\} \tag{7}$$

For $Z \to 0$, the condition becomes that of injection into a thin slab ("core" only case) and $kT_e = \frac{2}{3} eV_{inj}$, the result obtained in the previous section. For large Z, the potential energy term becomes of increasing importance with Equation (7) becoming

$$eV_{inj} = kT_e \left\{\frac{3}{2} + 2 \ln \frac{Z}{Z_o}\right\} \qquad Z >> Z_o \tag{8}$$

For example, consider a length of column in which, through beam divergence, the density has diminished by two orders of magnitude from the value at Z = 0. From (5), this requires $(Z + Z_o) = 10\ Z_o$, and inserting this value in Equation (7) yields $kT_e = 0.22\ eV_{inj}$, a value somewhat lower than that observed experimentally.

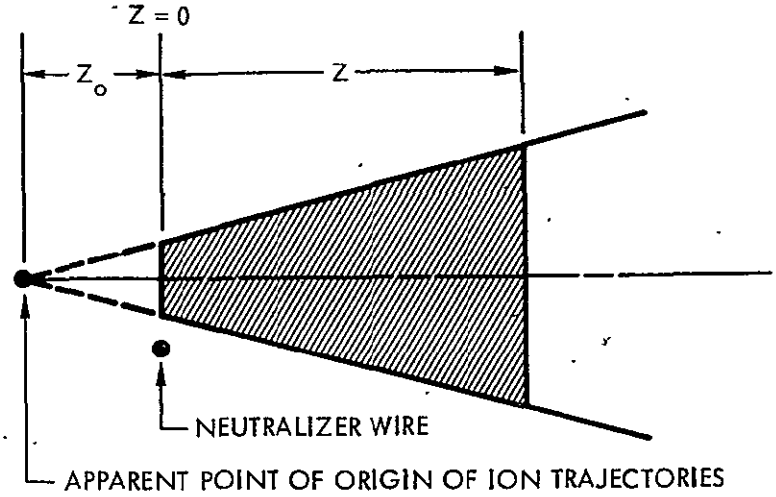

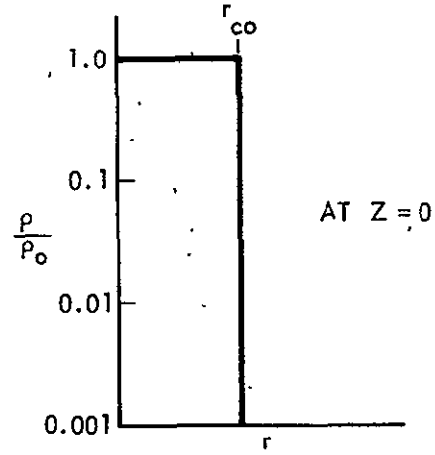

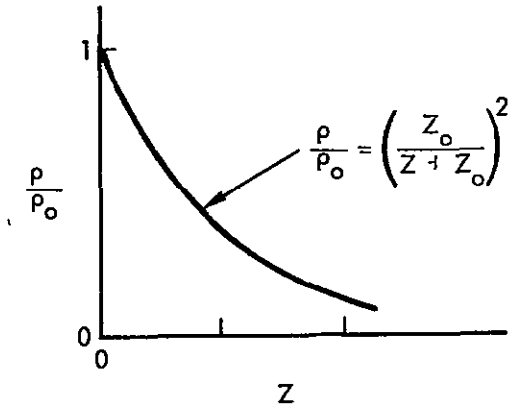

Figure 2. Model utilized in calculations of electron temperatures for a plasma column of finite length. Column assumed to be uniform in cross section and with an axial dependence on charge density characteristic of a conical beam.

Two considerations should be emphasized here. First, the restriction of the evaluation of the integral to the "core" only condition has placed a lower bound on the average potential energy. The consideration of a substantial fraction of the beam population in a "wing" region, whose densities are diminished from the adjoining core, requires from the barometric equation, larger energy inventories in the potential energy term. Thus, the evaluation of a more realistic core-wing model would further diminish the allowable magnitude of kT_e relative to eV_{inj}. Second, in the example, considered, only a comparatively short length of plasma column was utilized ($Z = 9Z_o$). If a longer column length had been utilized, the values of allowable kT_e would be further reduced and even more variant from observed values. These results, and those of the previous section, suggest that a conservative injection and thermalization is possible provided that some (unspecified) mechanism limits the distances over which an effective thermal communication of electrons may take place. The electron temperature gradients that have been observed in axial scans of large chamber beam tests[7] have similarly implied some mechanism which "localizes" electron thermal properties. A possible cause of such "localization" of electron properties could be the presence, in the testing environment, of (even) weak magnetic fields. However, such possible inhibitions of electron motion (and thermal communication) remain conjectural. The calculations of the present simple model which yield electron temperatures, for a conservative injection into an extended column length, less than those observed experimentally, suggests that such a model is not appropriate.

d. Injection with Conservative Electron Cooling

In II.B.2., it was noted that, if the potential in the downstream regions of the plasma column diminishes to values which are negative with respect to the potential of the electron source, a steady state energy flow (from some unspecified source) will be required to transport the electron current from the neutralizer to these regions of the plasma. In II.B.3.b., an assumption of conservative thermalization of electrons over extensive column lengths was shown to produce electron temperatures of less magnitude than are observed. A mechanism for the "localization" of electron properties would alleviate this discrepancy, and there is some experimental basis for believing that localization

processes do exist. The discussion of this section will assume such processes, acknowledging that there is, thus far, only an experimental suggestion of their existence. The discussion will also utilize a completely conservative interaction between the electrons and the potential structure, thus avoiding the difficulties of a required energy flow. In the model to be used, the diffusion of electrons along the (Z) axis of the beam results in the transfer of electrons into regions of more negative potential, and the inventory in potential energy is allowed to increase through diminutions in the kinetic energy. Considering a slab of electrons now in a net motion along the Z-axis, the conservation of energy requires that

$$\frac{3}{2} kT_e (Z) + \langle eV(Z) \rangle_r = \text{Constant} = eV_{inj} \tag{9}$$

where $\langle eV(Z) \rangle_r$ is the average, over the radial direction of the column of the potential energy of electrons at position (Z). The barometric relationship between V, ρ, and T_e will be assumed to hold with, however, the additional consideration that $T_e = T_e(Z)$. Taking the derivative of Equation (1) yields

$$\frac{3}{2} k\, dT_e (Z) + d\langle eV(Z) \rangle_r = 0 \tag{9'}.$$

Utilizing

$$eV(Z) = kT_e (Z) \ln \frac{\rho_o}{\rho(Z)} ,$$

allows an evaluation of dV(Z) which, because of the conical nature of the beam, will be equal to $d\langle V(Z) \rangle_r$. Thus

$$\frac{3}{2} k\, dT_e (Z) = -\left(k\, dT_e (Z) \ln \frac{\rho_o}{\rho(Z)} - kT_e (Z) \frac{d\rho(Z)}{\rho(Z)}\right) . \tag{10}$$

For the conical beam $\rho(Z) = \rho_o \left(\frac{Z_o}{Z + Z_o}\right)^2$ which specifies the term $d\rho(Z)/\rho(Z)$. Collecting terms and rearranging leads to

$$\frac{dT_e(Z)}{T_e(Z)} = - \frac{2\, dZ}{(Z + Z_o)\left[\frac{3}{2} + \ln \frac{\rho_o}{\rho(Z)}\right]} \tag{11}$$

The integration of Equation (11) is complicated by the ln term on the right hand side. However, through limited regions of Z, this term is essentially constant, allowing an approximate form for $T_e(Z)$. For the region near Z = 0

$$T_e(Z) \cong T_e(0) \left(\frac{Z + Z_o}{Z_o}\right)^{-4/3} \tag{11'}$$

which is a more rapid variation in Z than has been observed.[7] Correct inclusion of the ln term will result in a less rapidly diminishing temperature. Finally, from Equations (9) and (11), it may be seen that

$$V(Z) \to V_{inj} \text{ for large Z while } T_e(Z) \to 0.$$

The phenomenological model given here illustrates possible behavior for a conservative injection and thermalization and a conservative and self-consistent conversion of electron kinetic energy to potential energy in the subsequent diffusion along the axis of the beam.

4. Dynamic Resistance Effects

a. Injection Resistance

In order for the current of electrons to be conducted from the neutralizer to the plasma, a potential difference of magnitude $|V_{inj}|$ is required. If the injected electron current varies, then $|V_{inj}|$ may be expected to vary. Variations in required beam current may result either from variations in thrust ion current or from the use of the neutralizer-thrust beam-space plasma coupling as a release path, back to the space plasma for particles collected by the spacecraft.

The quantity $\frac{dV_{inj}}{di_e}$ has the dimensions of a resistance, and is the dynamic resistance element from the neutralizer to the thrust beam for the variations in the neutralization current. For practical purposes, it is desirable that this dynamic resistance be maintained at comparatively low values. For example, for a dynamic injection resistance of 10^3 Ω, a perturbation current of 1 milliampere creates variation in the neutralizer to beam potential of 1 volt. Such perturbation voltages are of sufficient magnitude

to create concern relative to their effect on electrostatic contamination of spacecraft scientific measurements. There are, however, compensating effects.

In II.B.3., relationships between electron temperature and injection energy were discussed. For withdrawn wire neutralizers, $kT_e \sim .3\ eV_{inj}$ is observed and is in agreement with simple models of the injection process. From this, it may be estimated that

$$dT_e \sim \frac{0.3e}{k}\ dV_{inj}$$

would be the result of a variation in injection potential. The potential structure in the beam is, in turn, related to electron injection temperature. This establishes a dynamic resistance quality in the plasma stream which may act to compensate for the injection resistance.

b. Negative Dynamic Resistance in Beam

If the temperature of electrons is increased in the injection region, then there will be an increase in the magnitude of the retarding potentials between the injection region and downstream regions. Figure 3A illustrates the potential from neutralizer to injection region to downstream region for an established current (case A) and with a perturbation current imposed (case B). The beam origin has been defined to V = 0 in all cases. From an increase in retardation potential for increased electron current flow, the dynamic resistance of the plasma column, for the length considered, is negative. This negative resistance will counteract the effect of the positive dynamic injection resistance. In Figure 3B, three conditions are considered, negative dynamic beam resistance a) less than, b) equal to, and c) greater than the positive injection dynamic resistance. Condition a) is non-conservative with a net loss of electron injection energy, condition b) is conservative with a complete recovery of the electron injection energy, while condition c) is non-conservative requiring a net energy flow from some (unspecified) source into the electrons. Condition a) is stable, b) is non-determined, and c) is unstable. In a bi-plasma system equilibration, the existence of condition c) would lead to a perturbation current flow which engages in unstable growth until limited by other, perhaps non-linear, factors.

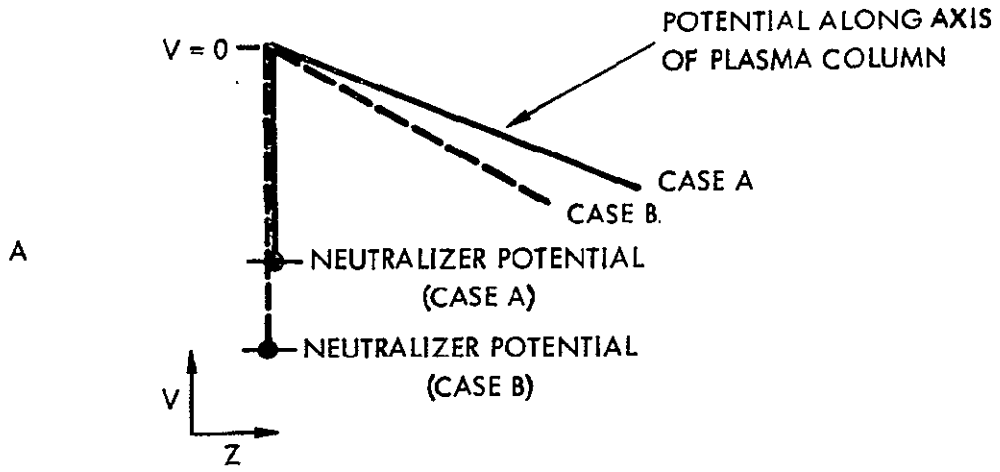

EXTRA CURRENT FLOW PRESENT IN CASE B RESULTS IN INCREASE IN REQUIRED MAGNITUDE OF INJECTION POTENTIAL

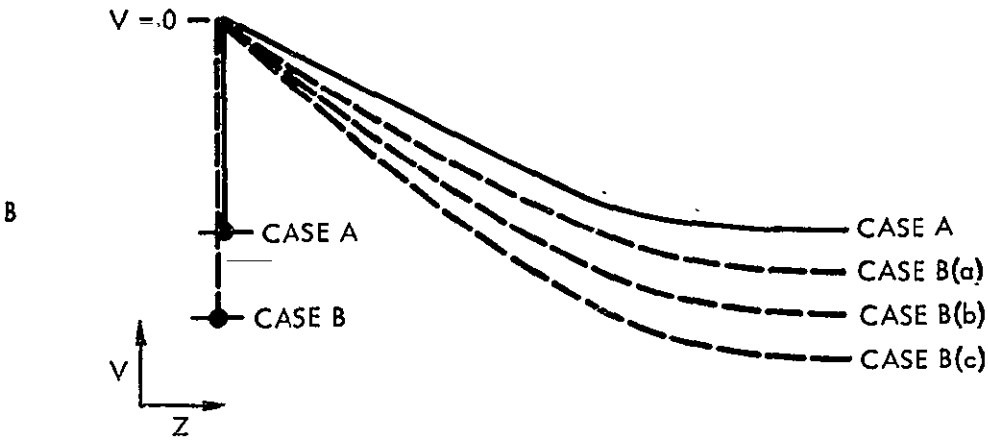

IN CASE A POTENTIAL IN DOWNSTREAM REGION OF PLASMA COLUMN IS ASSUMED TO LIMIT TO VALUE OF NEUTRALIZER POTENTIAL (COMPLETE RECOVERY OF INJECTION ENERGY)

Figure 3. Potential along axis of plasma beam. Neutralizing electrons are injected by withdrawn wire.

A) Case A: $i_- = i_+$
Case B: Perturbation current present (behavior suggests column to have negative dynamic resistance).

B) Case A: $i_- = i_+$
Case B: Negative dynamic beam resistance (a) less than, (b) equal to, and (c) greater than positive dynamic resistance of injection regio

The present discussion should not be interpreted as prediction of any one particular condition, but rather as an outlining of possibilities against which experimental results may be compared.

A final consideration in beam dynamic resistance relates to "electron pressure" effects. Normally, the influence of electrons upon ion trajectories is neglected. However, the radial potential gradients resulting from radial density gradients and T_e do produce divergence forces on the ions which are of sufficient magnitude to cause some reorientation of trajectories.[6] An increase of electron injection temperature, thus, may lead to increased radial electric fields which creates increased ion beam divergence and increased density gradients in the axial direction. The increased axial density gradients and increased electron temperature create, in turn, increased axial potential gradients. The combination of these effects is an increase in the negative dynamic resistance of the beam.

C. Bi-Plasma System

The previous sections have considered only the processes of a single thrust beam released into an ideal vacuum. For a thrust beam released into space, the actual condition is that of a bi-plasma system whose regions interact electrically with each other. From the magnitude of the electric fields in the interaction, the motion of electrons may be significantly altered from conditions that would prevail if only one or the other plasma is present.

In the earlier equilibration model,[2,3,4] it was assumed that electron temperatures in the beam and in space were equal and were everywhere constant. In the "interchange" process at the merging contour of the beam-space plasma system, an outwardly diffusing beam electron is interchanged with an inwardly diffusing space electron. The energies of the two electrons are equal, but velocities are oppositely directed. For such an interchange, the electron properties of both media are unaltered. The difference in potential from the origin of the thrust beam to the space plasma is given by

$$eV_{b-sp} = kT_e \ln \frac{\rho_o}{\rho_{sp}}$$

where ρ_{sp} is the space plasma density.

If the electron temperatures for the beam and the space are not equal, then the equilibration process of the beam-in-space plasma may lead to profound alterations of the properties observed for the single thrust beam in vacuum. The extent of this alteration may depend upon the "dwell time" of the electrons back diffusing from the space plasma to the thrust beam. If these electrons are retained for sufficiently long periods, then the electrons in the thrust beam may become predominantly determined by the properties of the ambient space plasma. If, on the other hand, space plasma electrons, having back diffused into the beam are, through some "ejection" process, returned to space, and if the period before ejection is suitably reduced, then the electron properties in the thrust beam may be comparatively unaltered from the bi-plasma condition to the single beam in vacuum condition. Of primary importance is the density of the space plasma, with a dense space plasma providing large currents of back diffusing electrons and a dilute space plasma providing reduced back diffusion currents.

The process of electron interchange between plasmas with dissimilar electron temperatures creates a possible range of conditions which will now be examined for two conditions. It will be assumed that comparatively large injection potentials are required for thrust beam neutralization and that electrons in the space plasma possess energies which are very much less than eV_{inj}. For the first condition to be discussed, the back diffusing electrons will be considered as a minor perturbation to the thrust beam. Under these various conditions, the electron temperature in the thrust beam will be determined by the injection potential with proportionality constants as given in II.B.3.b. For these "hot" thrust beam electrons, there will be electron pressure effects which create divergence forces on thrust beam ions. The combination of particle density gradients and hot neutralizing electrons will yield strong electric fields in the regions in and near the injection region. Retarding potentials from the thrust beam origin to the merging contour will essentially recover the injection potential (here there is no assumed energy flow from ions to electrons). The equilibration potential of the neutralizer, then, is very near to the space plasma potential. The electrostatic contamination of the spacecraft would be reduced. Magnetic contamination effects through gross outward streaming of beam neutralizing electrons would not be

present. The overall electrical efficiency of the thrusting process would be enhanced because of the recovery of the neutralizing electron injection energy.

The conditions discussed above, and illustrated in Figure 4A, contrast greatly with those which might be established if strong back diffusing currents of cold space plasma electrons are retained in the thrust beam. The conversion from that of Figure 4A to that of Figure 4B could, in concept, occur in the following manner. The interchange of "cold" space plasma electrons with "hot" thrust beam electrons results in a decrease in electron temperature in the thrust beam. This, in turn, reduces the potential gradients (and total potential increment) from the merging contour to the origin of the thrust beam. The required injection potential to conduct the neutralizing current from the neutralizer to the thrust beam remains fixed, however. Thus, the cooling of electrons in the thrust beam results in a negative going movement of neutralizer potential relative to space plasma potential. Since electrons entering the thrust beam with eV_{inj} now are confronted with diminished retarding potentials from that point to the space plasma, the direct escape of such electrons becomes more probable. This may also be termed "reduced L'iouville trapping." The result is that the electron injection energy is less effectively transformed into a thrust beam electron temperature and even further diminutions of T_e are obtained. Under continued conditions such as these, the configuration might be expected to collapse unstably until reaching the situation of Figure 4B. Here, T_e in the beam is no longer related to injection potential but is determined by the space plasma electron temperature. Potential gradients in the beam are reduced because of the low resulting T_e. The extraction potential from neutralizer to thrust beam remains at V_{inj} to conduct the required current, but the freshly injected energetic electrons are not retained in the beam and stream directly into the space plasma. This electron streaming sets up magnetic contamination effects. Electrostatic contamination is also obtained since the neutralizer equilibration potential relative to the space plasma becomes essentially V_{inj}. Electrical efficiency penalties are also present, since the electron injection energy, eV_{inj}, is lost to space rather than recovered in the thrust beam. In this final configuration, a stagnant colony

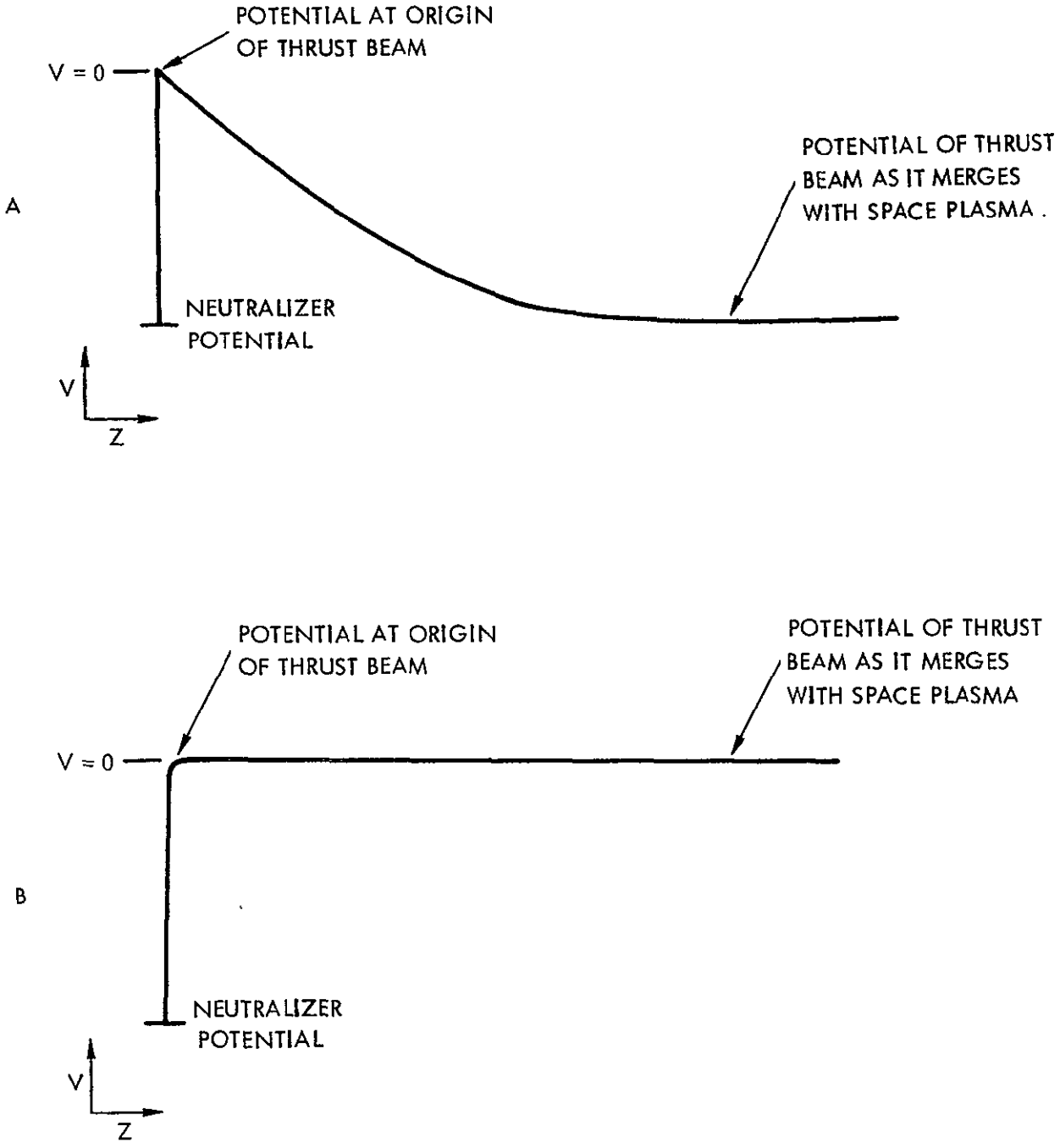

Figure 4. Potential along axis of plasma thrust beam
A) Back diffusion of cold space plasma electrons acts only as minor perturbation. Injected electrons thermalize and produce strong retarding electric fields near origin.
B) Strong back diffusion of cold space plasma electrons charge neutralizes thrust beam. Injected electrons stream directly to space and provide only current neutralization. Electron temperature in thrust beam is diminished and potential gradients of thrust beam are reduced.

of back diffused space plasma electrons provides the space charge neutralization for the thrust beam ions, while the current from the neutralizer merely acts to current neutralize the spacecraft.

Inasmuch as the equilibration behavior of 4A is widely variant from that of 4B, it would be desirable to be able to predict which configuration a given thrust beam-space plasma might generate. It is not likely, however, that this can be done quantitatively. In the sections which follow, various aspects of thrust beam and thrust beam-space plasma behavior will be inferred from laboratory experiments. From these experiments and the factors discussed in this present section on plasma models, it is hoped that, at least, qualitative regimes of behavior in the bi-plasma system may be established.

III. EXPERIMENTAL APPARATUS

The Cs^+ beam system utilized for experimental measurements is illustrated in Figure 5. Three beam configurations are possible with this array. For single beam studies, either the long beam or the short beam may be used separately, while for "beam-space plasma" experiments, the beam along the 12' direction of the tank provides the dilute "space" plasma, with the shorter cross beam providing the dense "thrust" plasma.

Neutralization of either beam is achieved through unipotential tungsten hot wire neutralizers. Both beams possess an immersed wire (fixed position) neutralizer and a variable position neutralizer which may move from complete immersion to complete withdrawal. Injection potentials may be varied from 0 to $\sim$ 100 volts, depending upon neutralizer position, or, in some instances, depending upon bias potentials applied to the wire. To prevent spurious drainage of electrons from the plasma beams to the walls of the vacuum chamber, the neutralizer wires are biased positively with respect to the walls by small potentials ($\sim$ 7 to 10 volts). Potentials in the plasma columns, thus, are no longer at the V = 0 level which was convenient for use in the analysis of Section II. Relationship of experimental data to analytical models may be made, however, by simple shifts in the reference potentials.

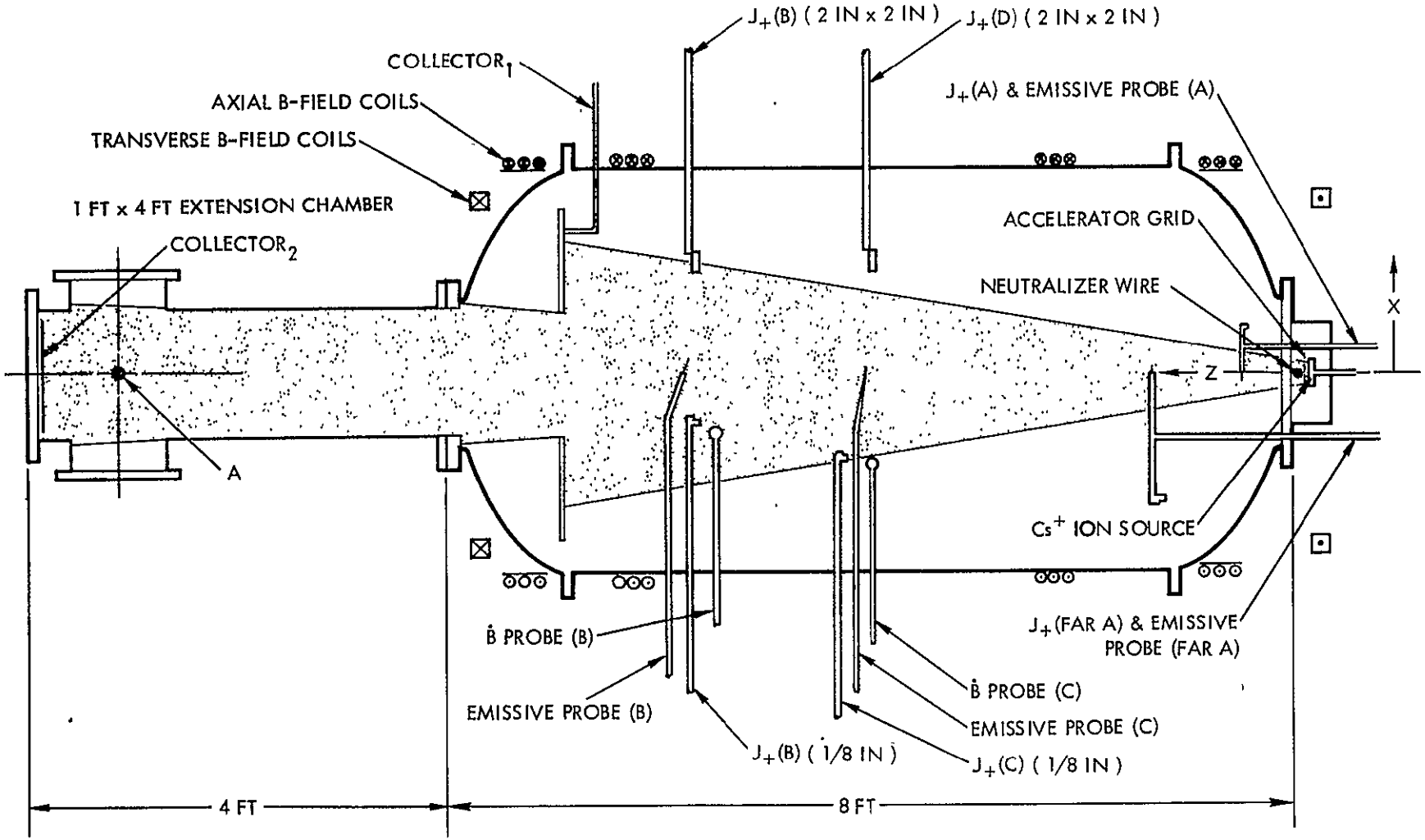

Figure 5. Experimental configuration showing 4' x 8' plasma wind tunnel, 1' x 4' extension chamber, degaussing coils, and plasma diagnostic probes. Long beam, short beam, and bi-plasma (details shown in Figure 6) experiments performed with this test geometry. Position A is intersection of beam axes.

Plasma densities depend upon total accelerated ion current and upon position in the beam. Near the ion source, typical beam densities are of the order of 10^9 to 10^{10} ions/cm^3. For the dilute space plasma in bi-plasma equilibration experiments, beam densities range from 10^6 to 10^7 ions/cm^3 in the regions for which observations are conducted. Figure 6 shows additional details of the apparatus for the bi-plasma studies.

The plasma beams are pulsed with a repetition rate of 60 pulses/second. Data is taken during the steady state period which is obtained after the plasma fronts have reached the various collectors. Timewise variations in plasma beam behavior do not occur following this initial time-of-flight period except for some cases in which larger injection potentials are utilized. Discussions of these time-varying cases are given in Section VII.

IV. SINGLE BEAM STUDIES: SINGLE AND DUAL WIRE INJECTION

This section will describe experiments on single beams with unipotential hot wire neutralizers. Both single and dual wire injection was utilized. For the single wire condition, complete immersion was maintained. For dual wire injection, at least one of the neutralizers was immersed in the plasma stream.

The use of two physically separate sources of electrons allows an injection condition in which different species of electrons are realized. Thus, by applying a bias potential between the wires, the injection energy of one group of electrons may be varied relative to the other. By varying the emission capabilities of the wires, the relative magnitudes of the two species may be varied.

Figure 7 illustrates the injection conditions for a single wire and dual wire injection, with a bias applied between the wires for the two wire condition. In the first condition, the beam has the conventional properties of beams neutralized with unipotential hot wires. In the second condition, the negatively biased wire was emission limited to a value of half the total ion current. For neutralization to occur, the plasma potential must adjust to extract the remaining half of the neutralization current from the upper wire. This requires a plasma potential approximately that of the upper wire potential, and the upper wire operates space charge limited. Langmuir probe

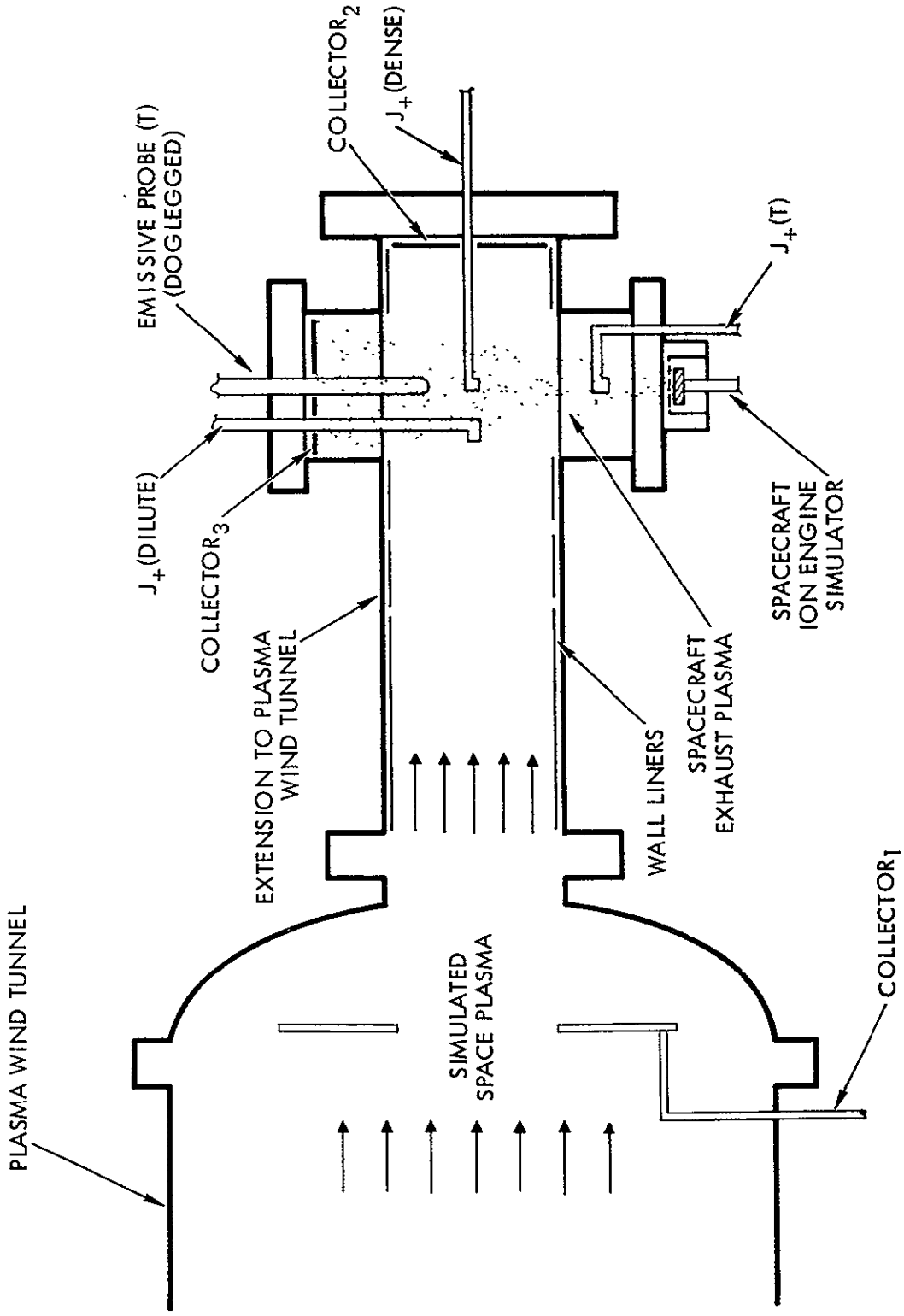

Figure 6. Test geometry for short beam and bi-plasma experiments showing plasma wind tunnel, extension chamber, space plasma, thrust beam-plasma, and plasma diagnostic probes.

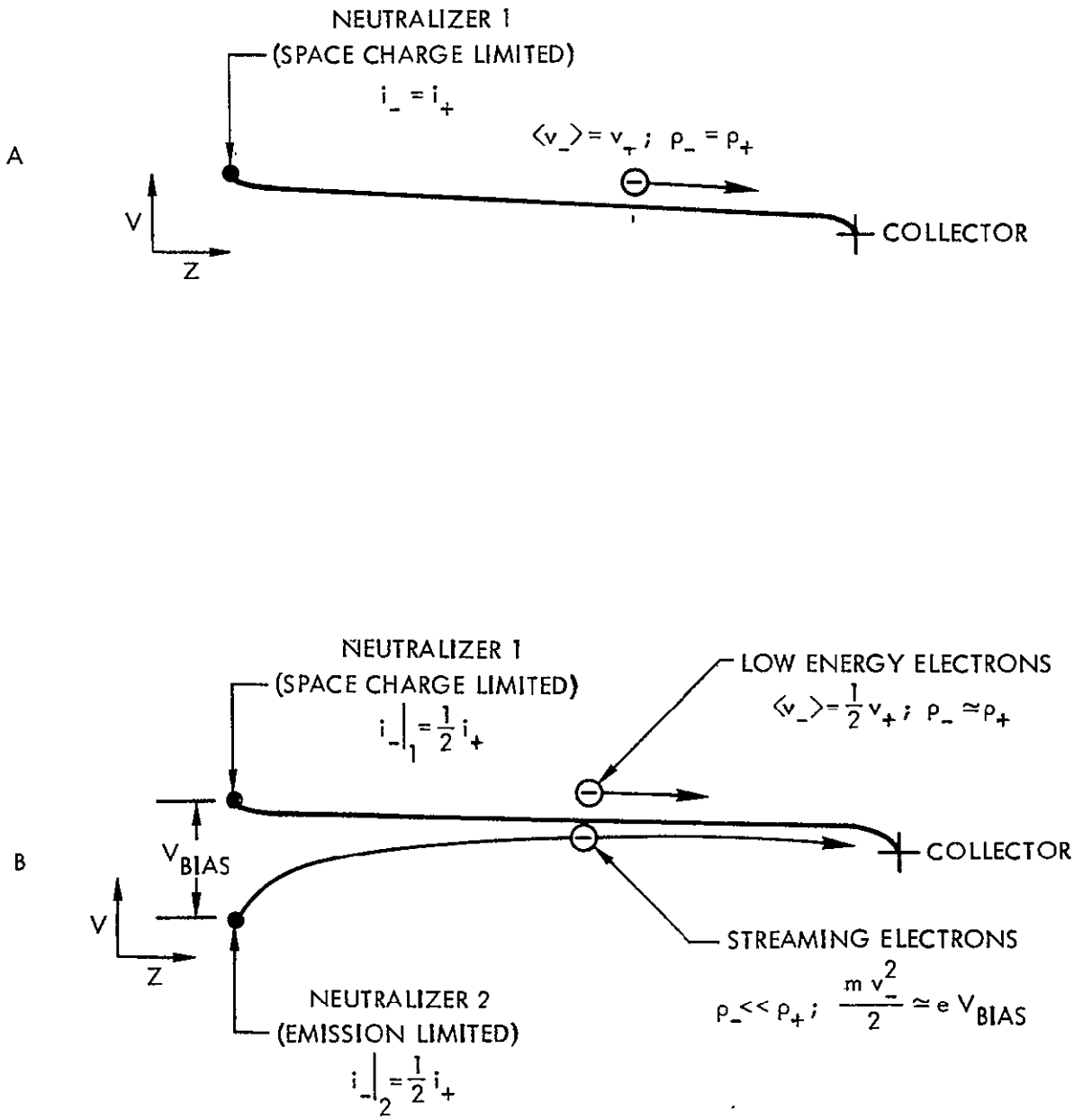

Figure 7. Plasma potential along axis of plasma beam.
A) Single space charge limited neutralizer.
B) Dual wire neutralization. Bias potential applied between two wires with lower wire emission limited to emit $i_- = 1/2\ i_+$.

traces taken in the two beams are given in Figure 8*. From the slope of curve A, the electron temperature is ∿ 3000°K, which is approximately the wire temperature. Collector floating potential is approximately the wire potential. This behavior is typical of immersed hot wire neutralized beams. Curve B is the Langmuir probe trace for an injection condition with half of the neutralization current possessing ∿ 5 eV of injection energy. The electron temperature in this beam is, however, virtually unchanged from the previous single wire case. There is a small downward shift of plasma potential resulting from the fact that the neutralization current through the space charge sheath around the upper potential wire has diminished by a factor of ∿ 2 from condition A to B. The conventional dynamic resistance of this neutralizer sheath should result in a negative movement in thrust beam potential for a diminution in delivered electron current. For condition B, the floating collector potential remained, as before, near the potential of the upper wire.

For condition A, the electron kinetic energy at injection is ∿ .25 eV, while for condition B, average injection energy is ∿ 2.5 eV. However, despite an order of magnitude increase in electron injection energy from A to B, electron temperature in the thrust beam (and associated density and potential gradients) remained virtually unaffected. This clearly demonstrates that the injection energy of the energetic electrons is not being retained within the thrust beam. This condition, termed electron streaming (as it applies to the energetic electrons) has been discussed earlier (II.C.) as a possible occurrence for the bi-plasma system.

From the observed electron temperatures and potentials, the behavior of the two species of electrons may be deduced. Figure 7B illustrates the potential configuration and electron streaming patterns. The energetic electrons enter the plasma with ∿ 5 eV, encounter only weak electric fields within the beam and stream to the collector, providing a current neutralization

*(The fixed position neutralizer is denoted "N" and a variable position "NF" for either immersed or withdrawn conditions. In Figure 8, the variable position neutralizer is immersed.)

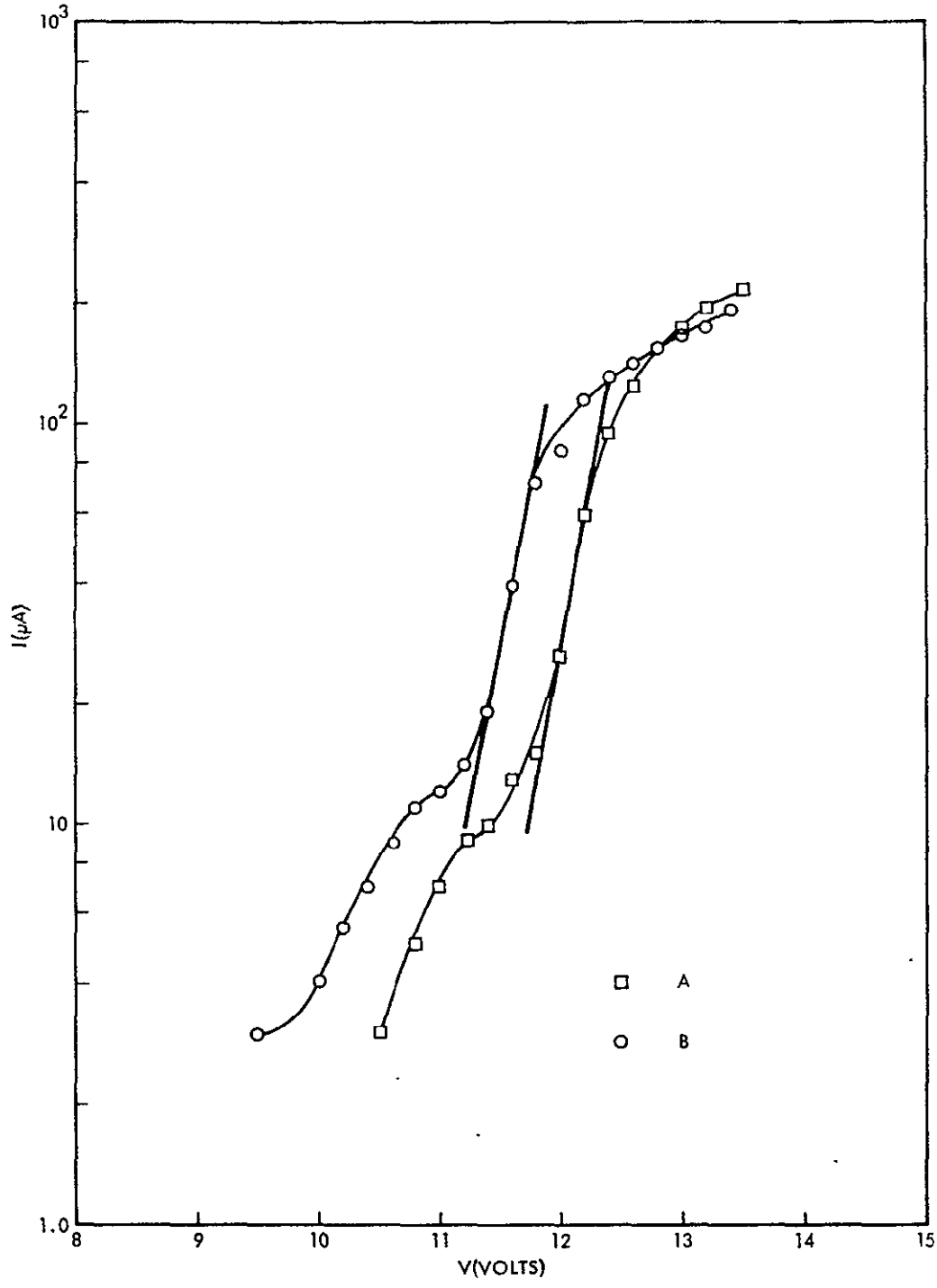

Figure 8. Langmuir probe traces for two neutralization conditions:
A) Single wire, space charge limited, $V_{N1} \approx 12.0V$, plasma potential $V_p = 12.0V$.
B) Dual wire injection, upper wire space charge limited with $V_{N1} = 12.0V$.
lower wire emission limited with $V_{NF1} = 7.0V$. $V_p \approx 11.5V$. $V_{inj} = 4.5V$.
Slopes indicate electron temperatures in both conditions to be identical and ∿3000°K (∿ neutralizer wire temperature).

for half of the ion current arriving there. (The energetic electrons may also move to the upper potential wire, but the area for exit through this point is very much less than the area of the collector so that only a very small fraction of electrons emitted by the lower potential wire will move to the other neutralizing wire). The electrons emitted from the upper potential wire must act in two capacities. First, they must provide the colony of electrons which space charge neutralizes the ion flow from the source to the collector. Second, they must provide a current neutralization at the collector for the remaining half of the ion current to that boundary. From these two conditions, it may be shown that these lower energy electrons now possess a dwell time in the source to collector region which is twice the ion time-of-flight across this space. Thus, average electron axial drift velocity for the low energy electron species is 1/2 v_+, where v_+ is ion acceleration velocity.

For the experimental conditions described, the low energy species cannot be described as stagnant, since their dwell time has only been increased by a factor of two over that normally realized by a neutralizing electron. A degree of stagnation has, however, been demonstrated. Also demonstrated in this experiment is that electron two stream instabilities, while they may occur between the two species, do not result in a significant coupling of injection energy from the "hot" to the "cold" species. In previous discussions of processes which thermalize injection energy, the importance of "L'iouville trapping," combined with collective interactions was advanced. The present experimental evidence would tend to suggest that, in the absence of "L'iouville trapping," which prolongs the dwell time of an electron in the plasma, coupling of injection energy through collective effects may not result in any significant retention of this injection energy in the plasma. The buildup of a stagnant colony of low temperature electrons in the beam could, thus, result in conditions for which freshly injected energetic electrons stream directly through the plasma.

A question of interest is the degree to which the low energy electron colony may be stagnated. By increasing the emission of electrons from the lower potential wire, the current from the upper wire is diminished and the average axial drift velocity of low energy electrons is diminished. In

principle, this velocity could approach zero as the current from the upper wire approaches zero. In practice, this limit has not been obtained. As the plasma dependence upon the upper wire is reduced toward zero, the potential structure around the wire acting to retard emission from the wire also acts as a collecting force for those electrons now retained in the plasma. The competition of emission and collection (here of both low and high energy electrons) does not produce a quiescent equilibrium, but rather one given to considerable sensitivity to minor fluctuations in any of the systems parameters. Experiments, thus, were not able to explore the condition of complete stagnation where the cold stagnant colony is produced by emission from an immersed wire. Even if such an experiment were possible, the extrapolation to the bi-plasma equilibration in space is uncertain. There the factors of the coupling between the two plasmas, which yields the possible magnitude of back diffusing space plasma electrons, and the retention time in the thrust beam of such back diffused electrons (which depends upon whatever possible ejection processes may exist) will materially affect the equilibration, and such factors are not adequately represented in the laboratory configuration.

Two other features of this "electron streaming" experiment were examined. The first of these was to investigate whether additional column length would alter the "short beam" result. Using the "long beam," identical results were obtained; i.e., that the electrons from the lower potential wire streamed to the collector with no measurable increase of electron temperature in the colony acting to charge neutralize the thrust beam. Second, the placement of the lower potential wire was moved from an immersed to a withdrawn position. Withdrawal was limited here to distances such that current from the wire continued to be emission rather than space charge limited. Streaming of the energetic electrons, with no measurable energy deposition in the plasma, was obtained for the withdrawn condition in the same manner as had been observed for the immersed condition. This latter experiment indicates that the observed streaming is not the consequence of a particular point of injection for these electrons or of the particular form of the electric fields in the regions from the neutralizer to the plasma.

V. BEAM-IN-PLASMA

A. Experimental Configuration

For these experiments, the "short" beam is utilized as the dense, "thrust," plasma, and the "long" beam is the dilute, "space," plasma. See Figure 6. The "thrust" beam is neutralized by a variable position unipotential hot wire. The "space" plasma is neutralized by an immersed unipotential hot wire so that electrons in this plasma have a temperature approximately that of the wire. For the thrust beam, electron temperatures move over a broader range because of the variations of injection potential obtained for varying degrees of neutralizer withdrawal.

B. Single Beam Properties

In examining the behavior of the dense beam immersed in a dilute plasma, it is instructive to establish some properties of a single beam in the absence of an ambient plasma.

Figure 9 illustrates emissive probe traces on the axis of the beam (at Point A, Figure 5) as the neutralizer wire is moved from an immersed position to withdrawn positions. The withdrawal of the wire results in an increase of plasma potential in the injection region and portions of this increased potential are still evident at Point A. Figure 10 shows Langmuir probe traces at Point A for these same neutralizer positions. The straight line characteristics indicate Maxwellianization of the injected electrons with a temperature which increases for increased injection potential. The relationship between injection potential and electron temperature (II.B.3.) cannot be accurately assessed from the data of Figures 9 and 10 since these measurements are not performed at the injection point.

A third feature of the single beam is illustrated in Figure 11, with ion current density scans across the diameter of the beam at Point A for the given neutralizer conditions. These current densities display "uniform core-exponential wing" characteristics which radially enlarge, with consequent diminutions of centerline density, as the electron temperature is increased, Features of this beam divergence through "electron pressure" have been previously discussed (II.4.b.).

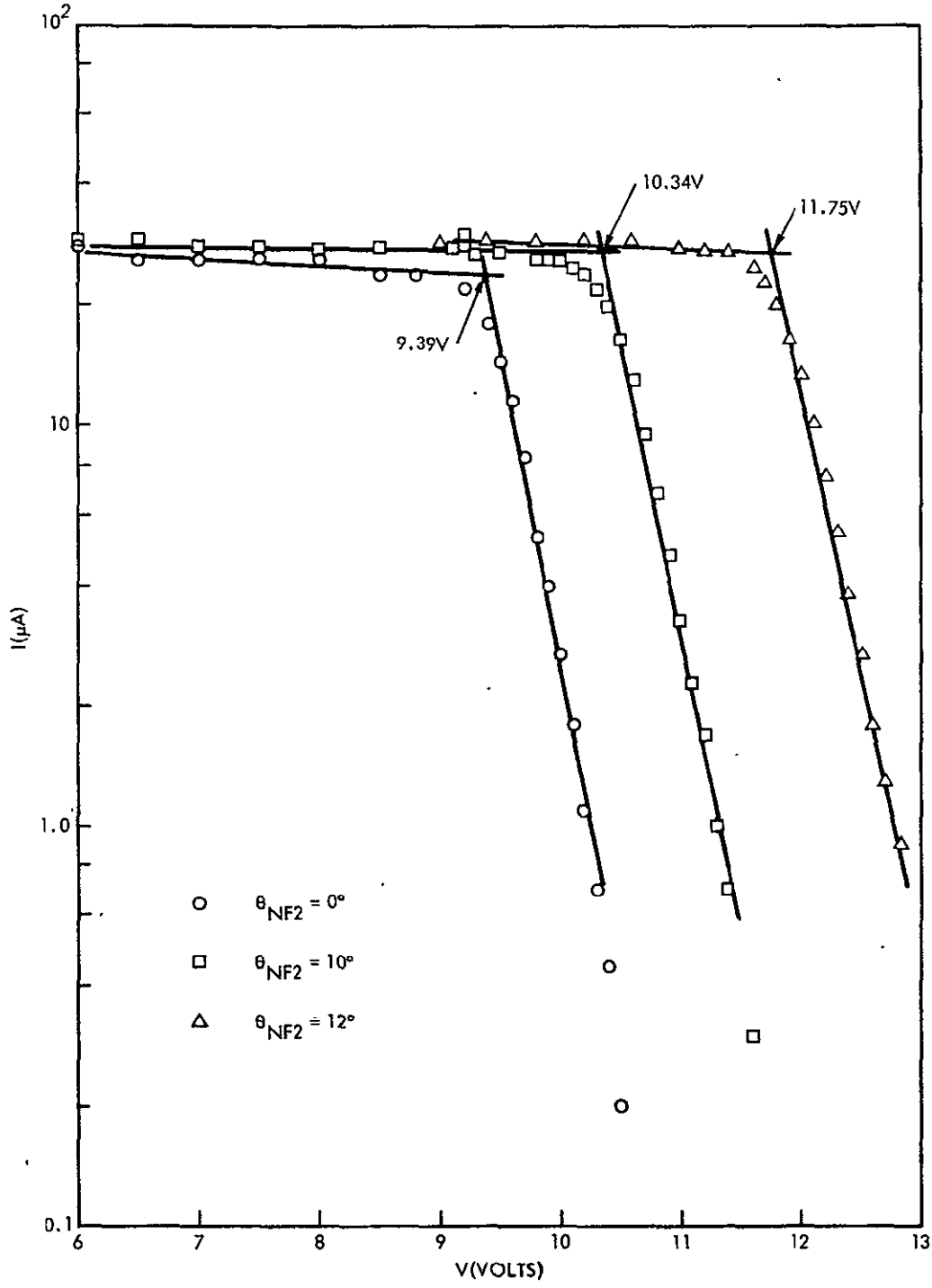

Figure 9. Emissive probe traces at position A of Figure 5. Neutralizer wire biased with V_{NF2} = 10.00V.
θ_{NF2} = 0° (immersed position), V_p = 9.39V
θ_{NF2} = 10° (source edge), V_p = 10.34V
θ_{NF2} = 12°, V_p = 11.75V
Plot demonstrates increasing injection potential as neutralizer wire is withdrawn.

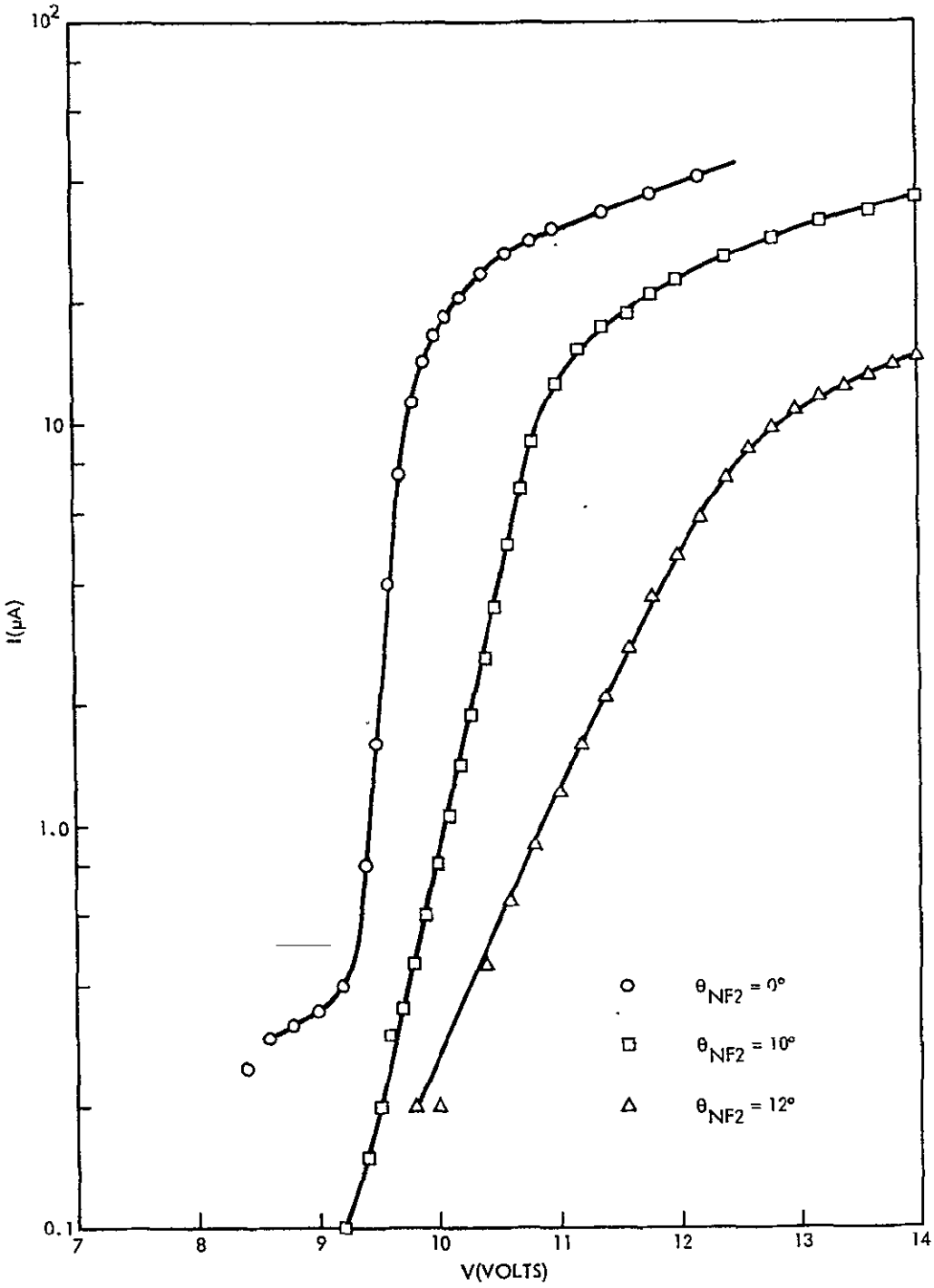

Figure 10. Langmuir probe measurements at position A of Figure 5. Neutralizer wire biased with V_{NF2} = 10.00V.

θ_{NF2} = 0°, $T_e \sim$ 1500°K
θ_{NF2} = 10°, $T_e \sim$ 2700°K
θ_{NF2} = 12°, Te $\sim$ 8800°K
Plot demonstrates increasing electron temperature as neutralizer wire is withdrawn.

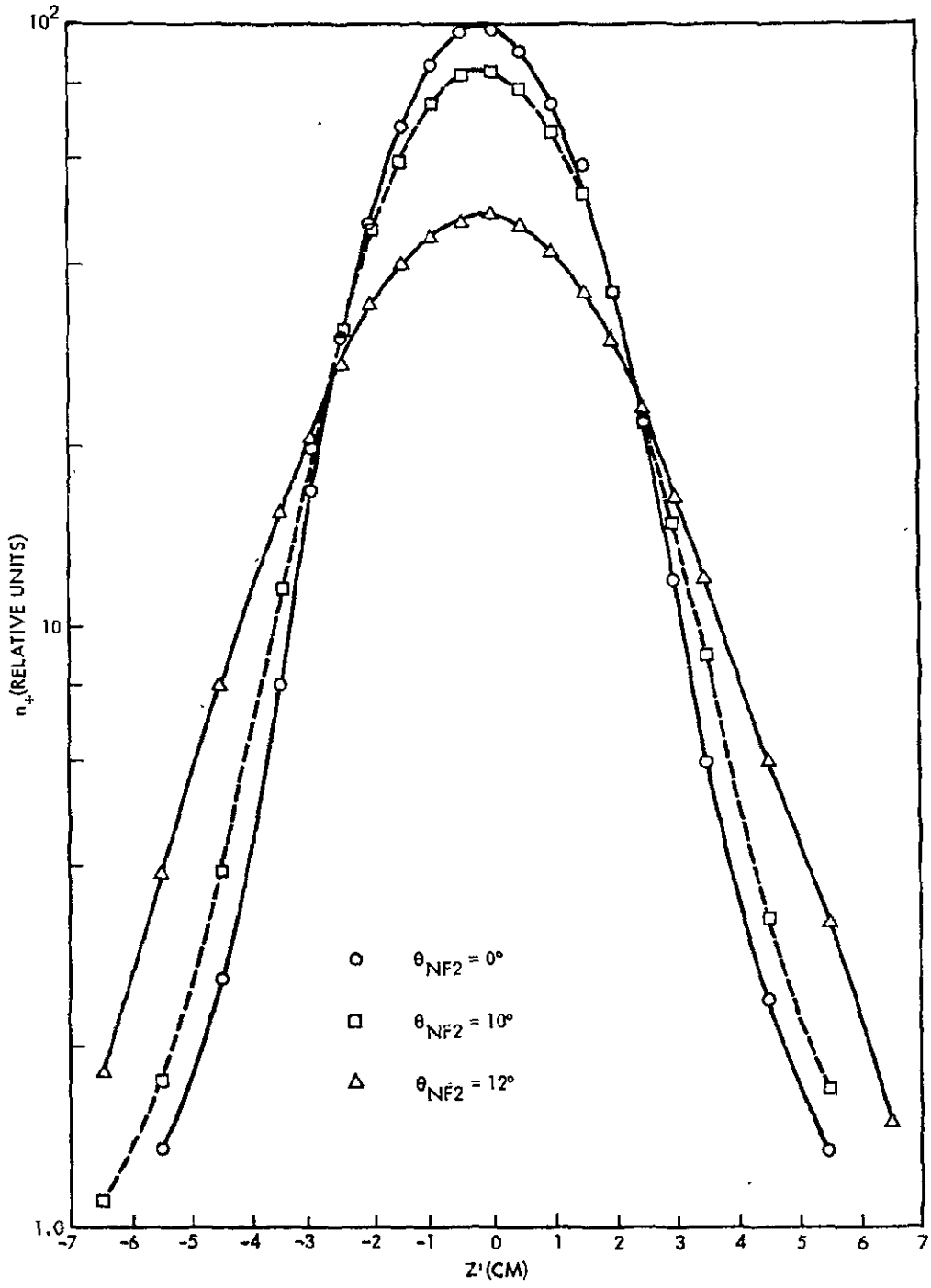

Figure 11. Ion density profiles of thrust beam about position A of Figure 5 (Z' = 0) for three neutralizer wire positions: $\theta_{NF2} = 0°$, $\theta_{NF2} = 10°$, $\theta_{NF2} = 12°$. Plot demonstrates electron pressure effects.

C. Bi-Plasma Interactions

For these experiments, both plasmas are present. By appropriate variations of the potentials on the neutralizer wires for the two plasmas, a condition of balanced electron interchange (zero net electron current flow) may be obtained, or a net electron current flow from one to the other plasma may be obtained. Figure 12 illustrates floating emissive probe measurements of plasma potential along the axis of the thrust beam as these interchange conditions are varied. The thrust beam neutralizer wire is placed in a fixed withdrawn position. By lowering the potential of the thrust beam neutralizer, additional electrons are extracted from this wire and move, essentially, into the dilute plasma (and to the floating collectors for this plasma stream). The positive dynamic resistance of the sheath region between the withdrawn neutralizer and the dense thrust beam is such that a net increase of plasma potential is obtained for the additional flow of electrons (note that net increase in injection potential includes the positive potential increment realized at the plasma beam and the negative potential increment imposed at the neutralizer wire). Also to be noted is the increased slope of the potential contour as additional electron current moves along the thrust beam. Such an increase in retarding potential is the negative dynamic resistance property treated earlier (II.4.b.). Combining both the positive (sheath) and negative (beam) dynamic resistances, however, still leads to a positive overall resistance characteristic at the Point A. Such an overall positive resistance is important, since it provides for stable equilibration in the bi-plasma system.

Figures 13, 14, and 15 detail these dynamic resistances with somewhat greater precision. For these figures, a somewhat larger separation of the wire from the plasma beam was utilized than for condition of Figure 12. Figure 13 gives emissive probe traces for plasma potential measurement in the injection region. From the overall shift of 2.12 volts for a 1 milliampere increment of injected electron current, a dynamic injection resistance of 2120 Ω's is obtained. In Figure 14, emissive probe traces for the plasma potential at Point A are given. Here, the overall shift (relative to the neutralizer wire) is 1.27 volts/1 milliampere. Thus, the combined positive

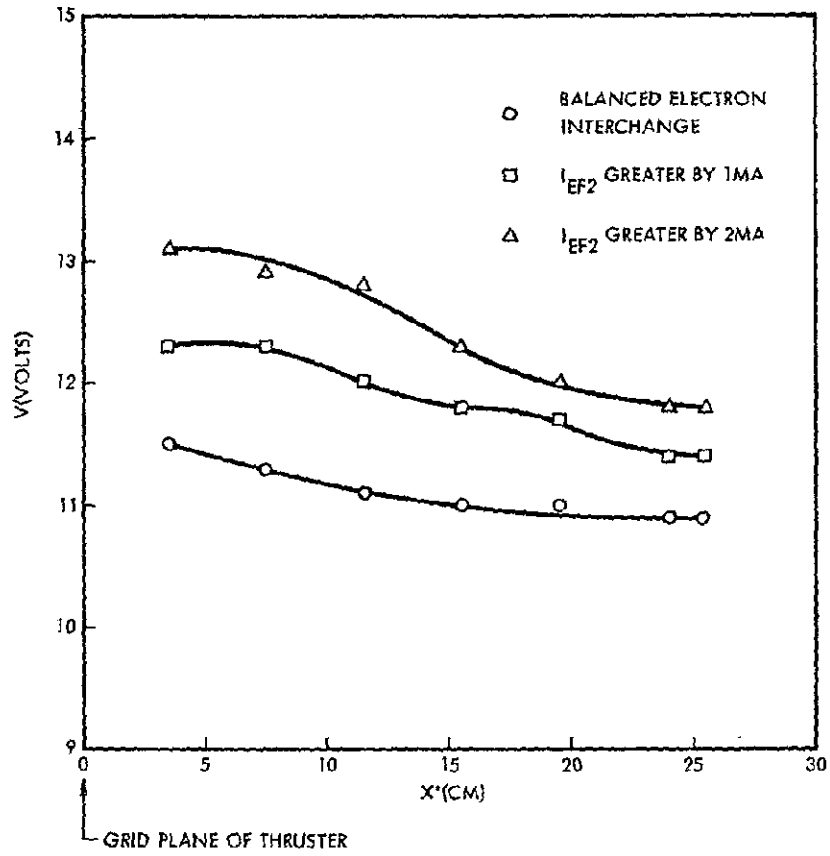

Figure 12. Negative dynamic resistance effect in plasma beam. Floating emissive probe measurements of plasma potential along axis of thrust beam from origin (X' = 0) to position A of Figure 5 (X' = 25.5 cm). θ_{NF2} = 13°. V_{NF2} = 9.35V (balanced interchange), V_{NF2} = 8.67V (I_{eF2} greater by 1 ma), V_{NF2} = 7.90V (I_{eF2} greater by 2 ma). Neutralizer wire bias potential and plasma floating potential illustrates positive dynamic injection resistance. Axis of short beam designated as X' in bi-plasma experiment.

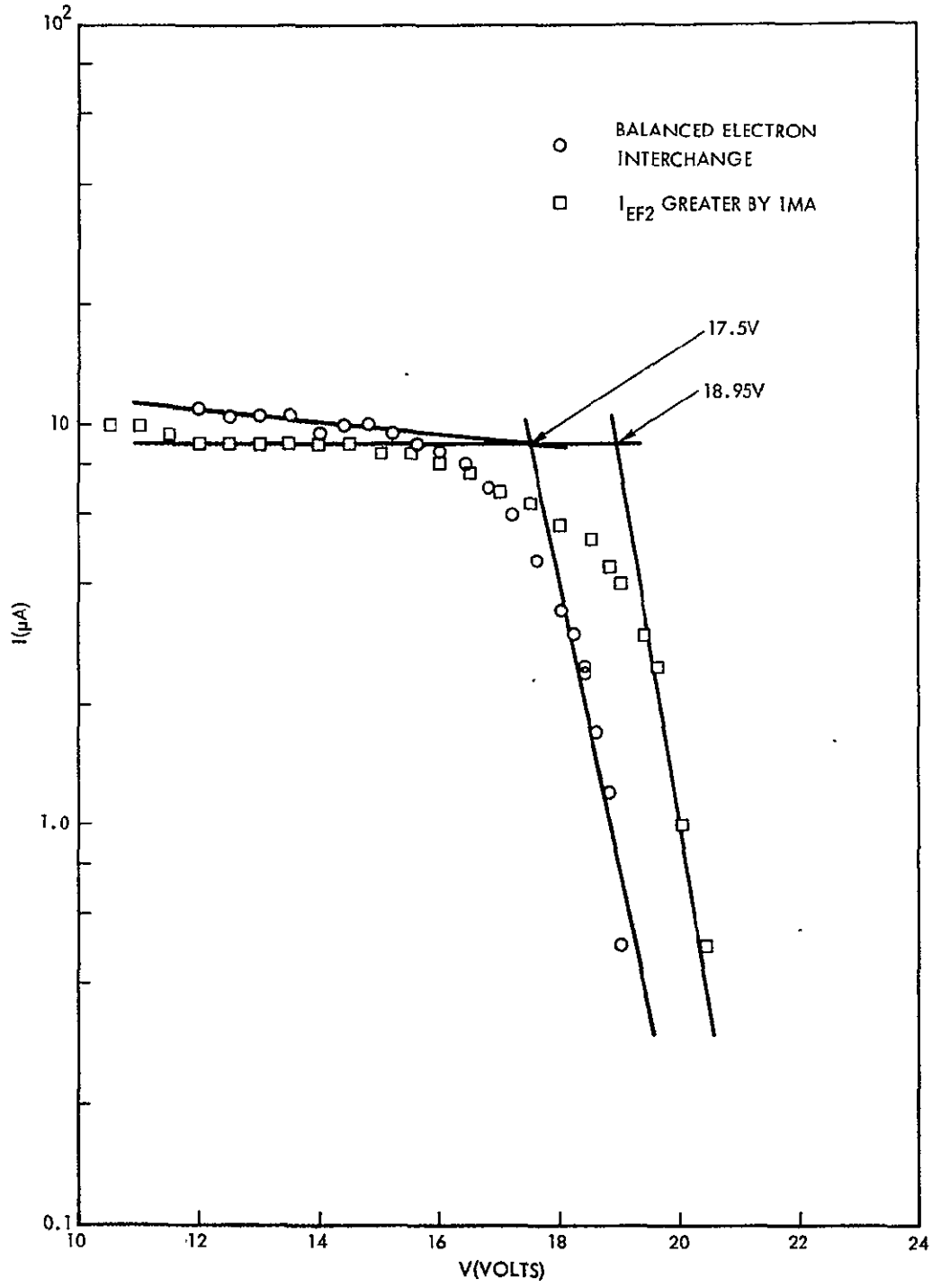

Figure 13. Emissive probe measurements at X' = 3.5 cm. Balanced interchange when V_{NF2} = 8.07V and V_P = 17.5V. For 1 ma extra current V_{NF2} = 7.40V and V_P = 18.95V. Net shift in injection potential is 2.12V. Dynamic resistance of neutralizer sheath is 2120Ω. Neutralizer wire withdrawn to θ_{NF2} = 14°.

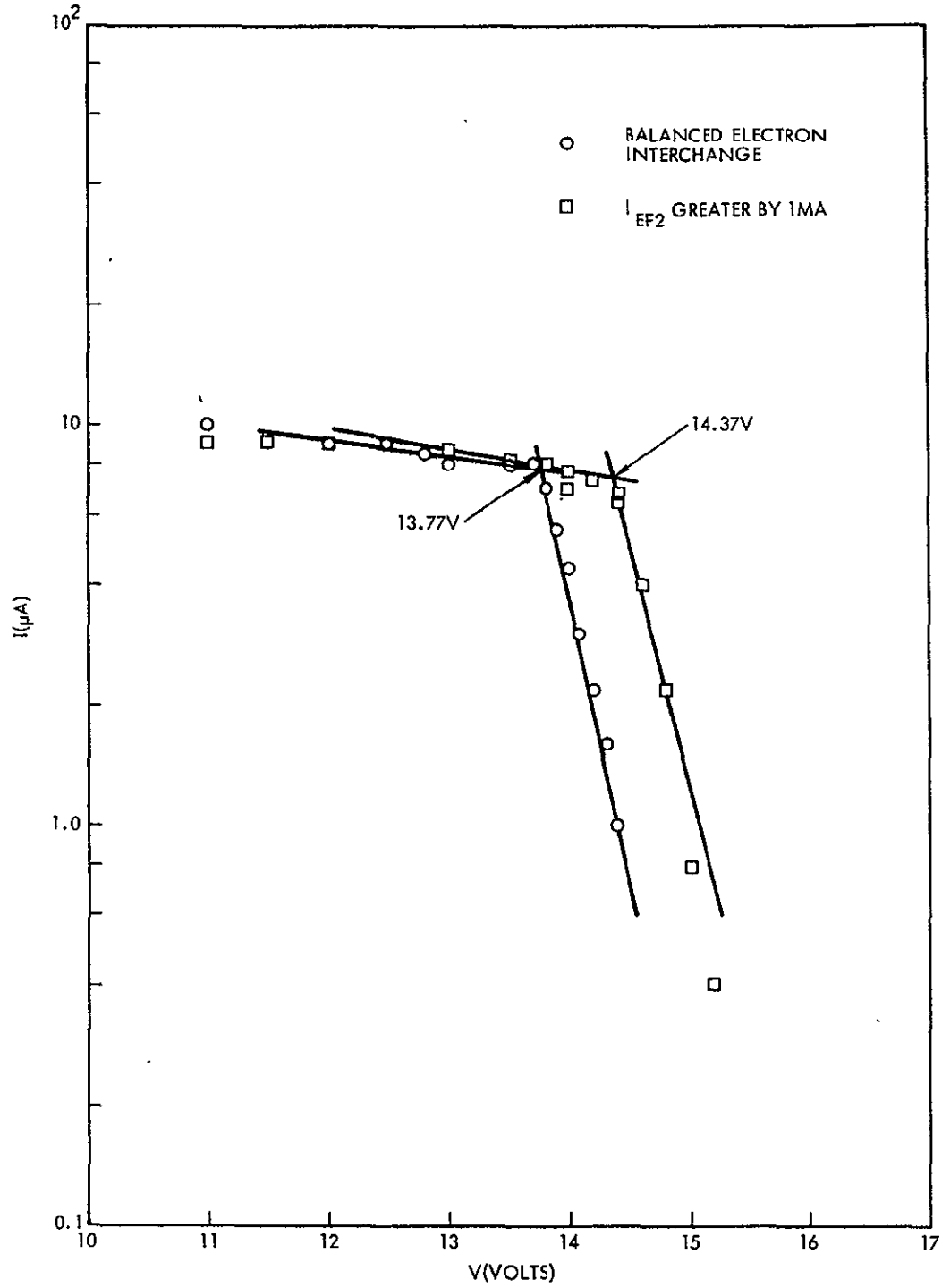

Figure 14. Emissive probe measurement at point A of Figure 5 (X' = 25.5 cm). Balanced interchange when V_{NF2} = 8.07V and V_P = 13.77V. For 1 ma extra current V_{NF2} = 7.40V and V_p = 14.37V. Net shift in potential (relative to neutralizer wire) is 1.27V. Dynamic resistance between neutralizer and point A is 1270Ω - dynamic resistance along indicated portion of thrust beam equals -850Ω. Neutralizer wire withdrawn to θ_{NF2} = 14°.

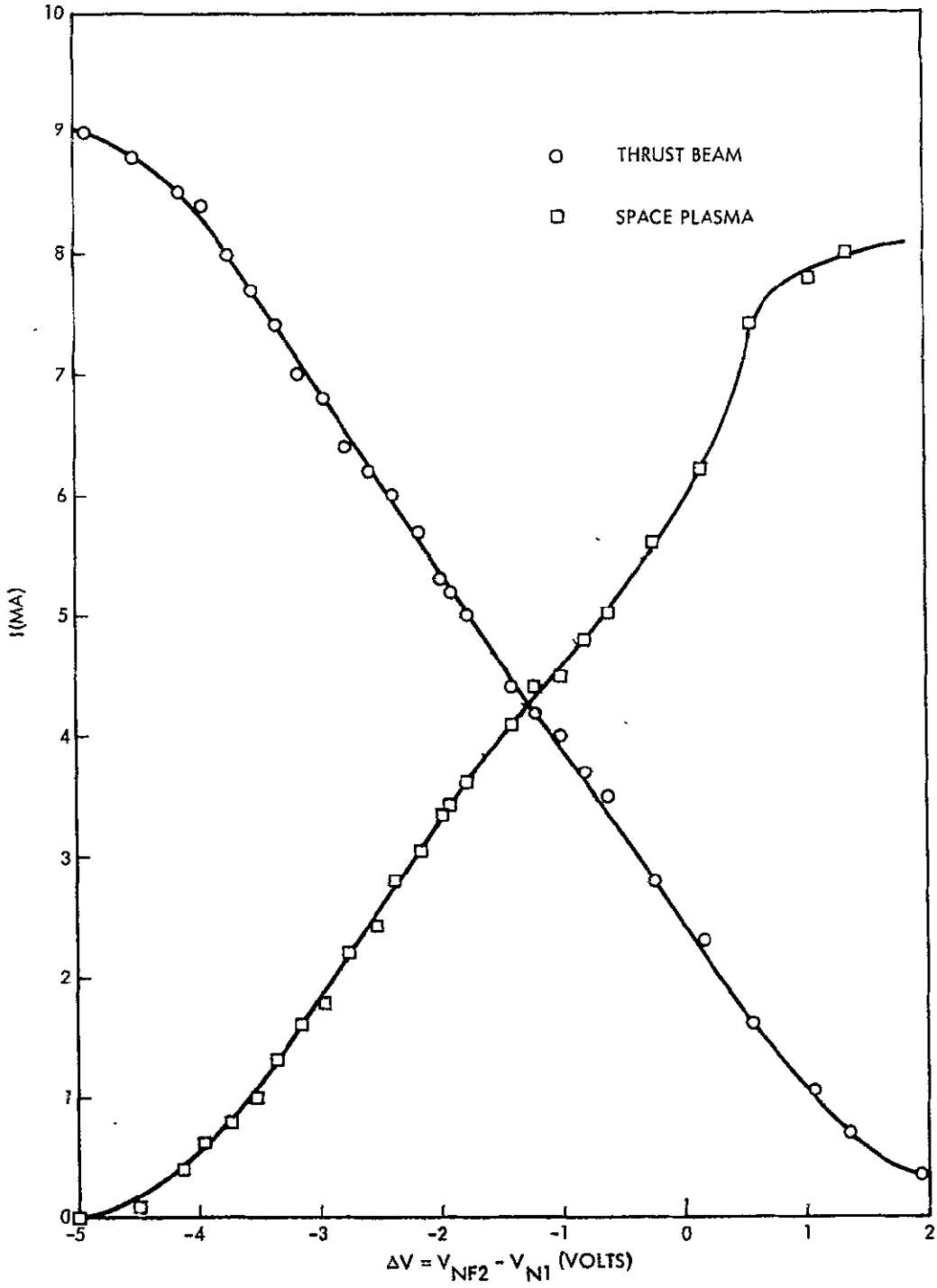

Figure 15. Transfer characteristic emission current vs. relative neutralizer potential of thrust beam and space plasma. Balanced interchange occurs when $\Delta V = -1.9V$, $I_{el} = 3.4$ ma (space plasma) = I_{il}, and $I_{eF2} = 5.2$ ma (thrust beam) = I_{i2}. Neutralizer wire withdrawn to $\theta_{NF2} = 14°$. Plot demonstrates net positive dynamic loop resistance of $\sim 700\Omega$ indicating stable bi-plasma equilibration.

dynamic resistance of the injection sheath and the negative dynamic resistance of the plasma column from injection to Point A is 1270 Ω's, indicating that the dynamic resistance for the portion of the thrust beam presently examined is ∿ -850 Ω's. Now, the complete dynamic resistance around the loop from thrust beam neutralizer to space plasma includes other plasma regions as yet not determined. In Figure 15, the transfer characteristic between the two plasmas is determined (see Reference 3 for further details of this measurement technique). A value of ∿ 700 Ω's is obtained from the slope of the i(V) curves ($dI/d\Delta V = 1.4 \times 10^{-3}$ amperes/volt). Two features are important. First, the overall loop resistance is positive, indicating stable bi-plasma equilibration. Second, much of the effects of the positive dynamic injection resistance have been counteracted by negative dynamic resistance in the plasma column. The comparatively low overall value of the dynamic resistance from thrsut beam neutralizer to space plasma is a desirable result, since it provides for reduced potential excursions in the equilibration in the presence of perturbation current flows.

From the data of Figures 13, 14, and 15, another feature of the equilibration is implied; i.e., that back diffusion of elèctron from the space plasma to the thrust beam has not resulted in the collection of a cold stagnant colony of neutralizing electrons. If this were to occur, then the negative dynamic resistance of the plasma column would be lessened, and the equilibration would be more sensitive to perturbation currents because of the (now) noncounteracted positive dynamic injection resistance. To further examine the effect of the ambient plasma on the electron temperature in the thrust beam, Langmuir probe measurements of electron temperature were made at Point A for both the single beam (withdrawn wire) and the bi-plasma system with balanced electron interchange. These measurements are shown in Figure 16. The presence of the ambient plasma for this examined case has no apparent effect upon the thrust beam electron temperature. There is no appearance of a cold stagnant back diffused colony and no observed tendency for an unstable collapse into a "streaming" situation. A quantitative explanation of this observed behavior cannot be made. However, it would appear that the ability of the cold ambient plasma to alter properties in the thrust beam will be determined by some overall "coupling" between

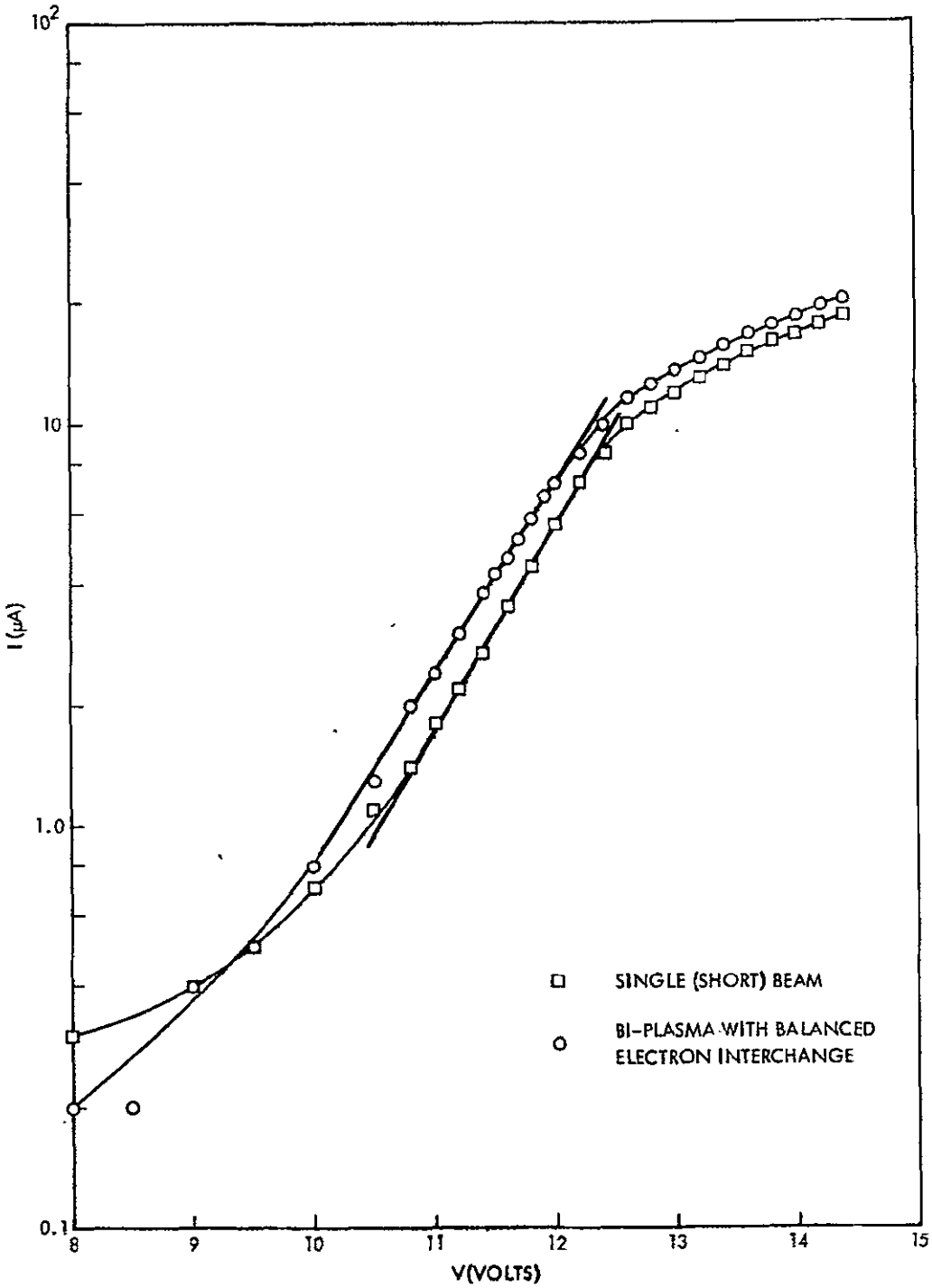

Figure 16. Langmuir probe measurements at position A of Figure 5 for single (short) beam using withdrawn wire, and for bi-plasma (balanced interchange) interaction. For this case, no apparent cooling of electron temperature is provided by ambient space plasma. Thrust beam electron temperature ∿10,000°K, space plasma electron temperature ∿2,000°K.

the two plasmas. This coupling becomes more effective for increased contact area between the two plasmas and, probably, for an increased ambient plasma density. For the present case, this coupling is not sufficient to allow marked alterations of thrust beam properties through the presence of the ambient plasma.

VI. SINGLE BEAM STUDIES: MODERATE INJECTION POTENTIAL

For these studies, the "long" beam was used (Figure 5) and neutralization was achieved with a single withdrawn unipotential hot wire neutralizer. Separation of the neutralizer from the beam was adjusted so that injection potentials ranged from a few volts to $\sim$ 10 volts. Figure 17 illustrates ion current density (and ion number density) contours at various axial locations for a beam with an injection potential of $\sim$ 5 volts. Langmuir probe electron collection current for this beam is given in Figure 18. At the point at which the curve was taken, a separate emissive probe measurement indicated a plasma potential of 11.4 volts. This is 4.4 volts of injection potential, since the neutralizer wire was held at 7.0 volts for these experiments. The Langmuir probe characteristic in the potential regime just negative of the plasma potential is essentially straight line with a slope of 3.0 volts/decade. From this, a Maxwellian distribution is inferred, and with a temperature of $\sim$ 15,000°K. For this case, $kT_e \sim 1.3$ electron volts, and, from the injection potential of 4.4 volts, $kT_e \sim 0.3\ eV_{inj}$. Such values are consistent with those derived from a conservative injection into a single slab of beam with a "wing" content somewhat larger than the "core" content (see II.B.3.b.). The result is also consistent, in general, with conservative inspection into a column of finite length (II.B.3.b.) and with a somewhat higher core-to-wing ratio. Since these earlier models are only phenomenological cases, the present data cannot be interpreted as favoring either one or the other thermalization condition.

Figure 18 also reveals that, for retarding potentials on the probe of larger than 1 to 2 volts (relative to the plasma potential), the current collection is less than should be observed with a truly Maxwellian distribution. This feature is a frequently observed characteristic for neutralization in

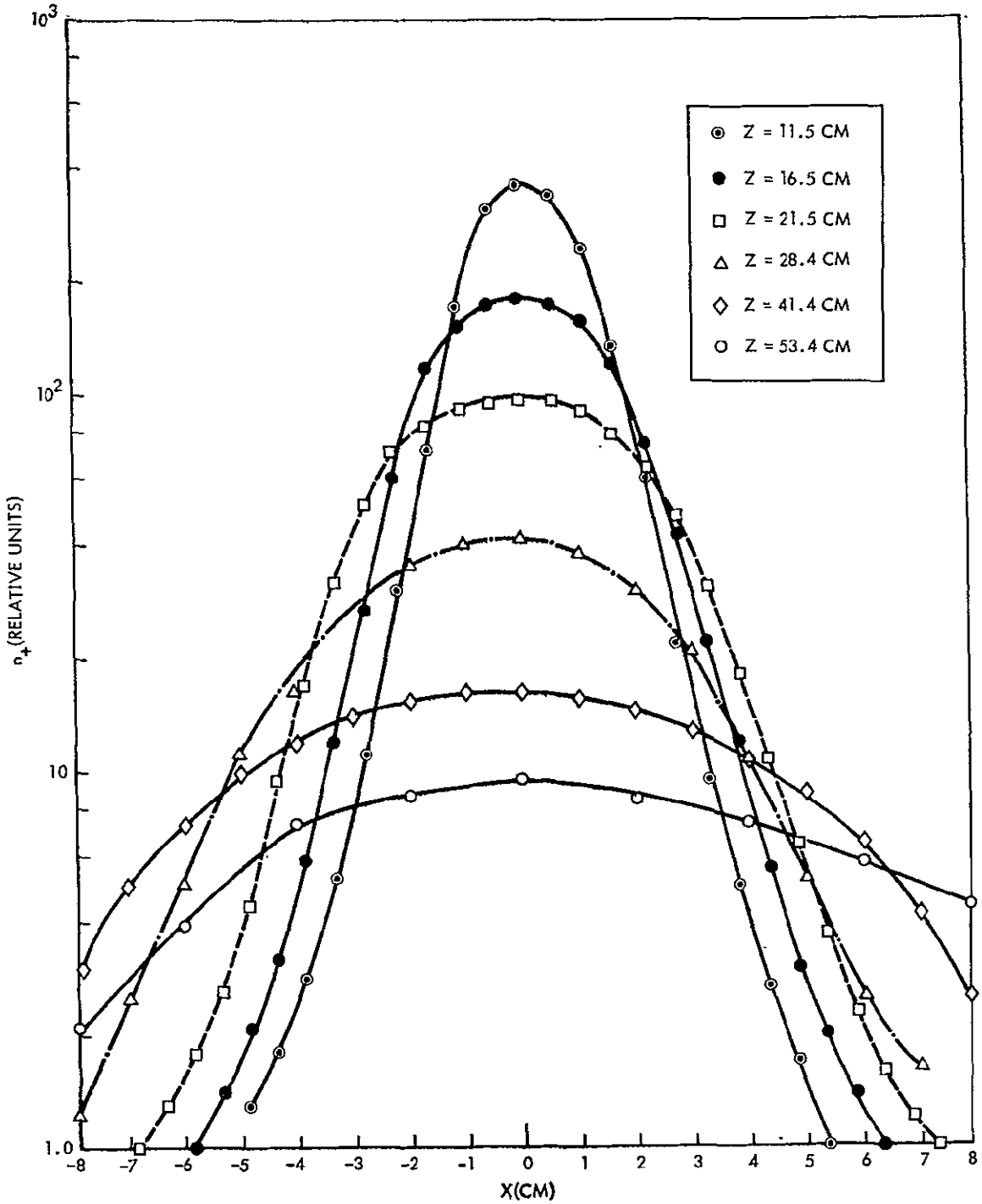

Figure 17. Ion density profiles at various axial locations for $V_{inj} \sim 5V$. Beam origin corresponds to Z = 0, and beam axis to X = 0.

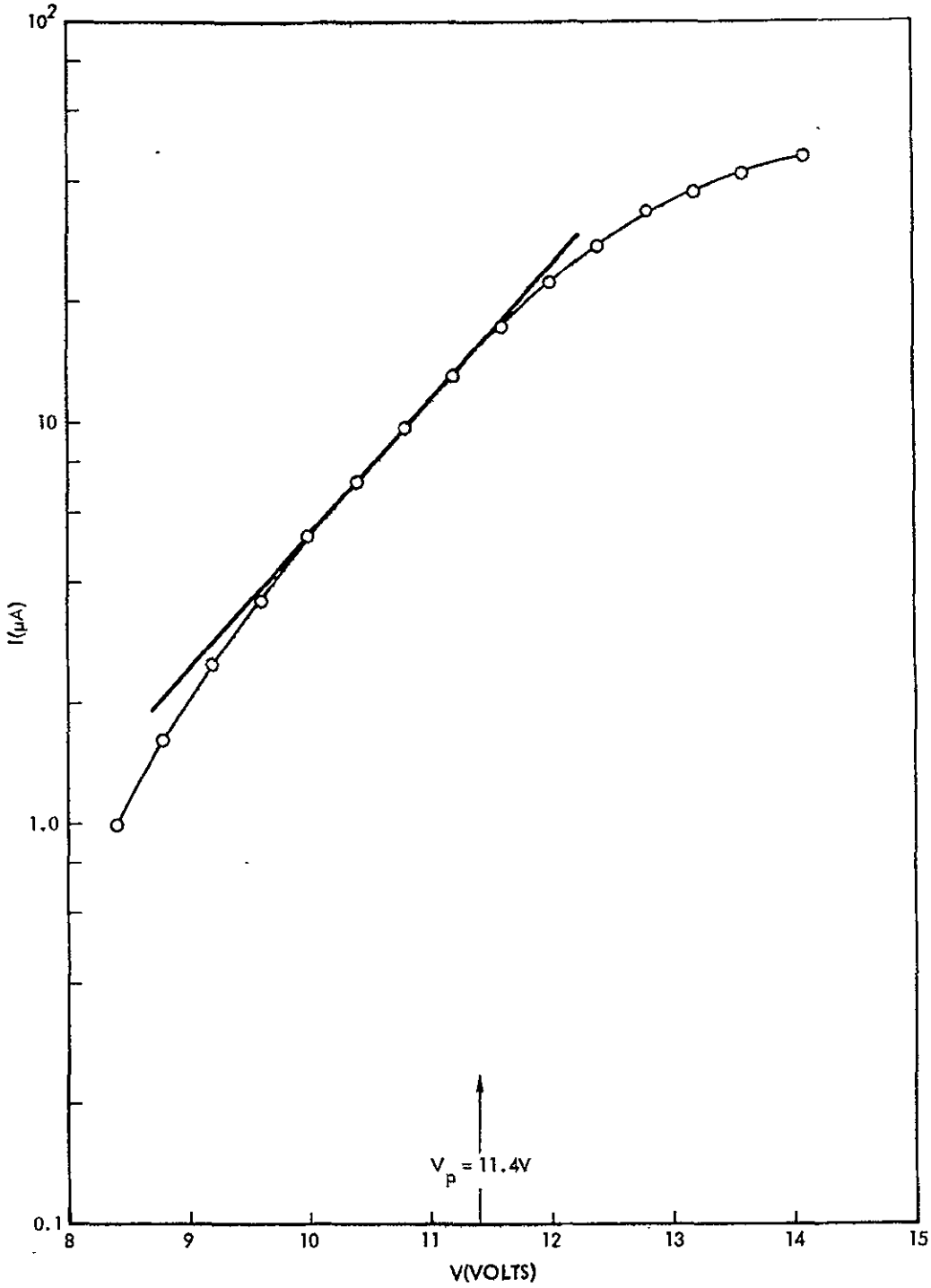

Figure 18. Langmuir probe measurement at X = 0, Z = 11.5 cm, indicates Maxwellian distribution with $T_e \sim 15{,}000°K$. Measured V_p = 11.4V and neutralizer potential V_{N1} = 7.0V. $kT_e \sim 0.3\ eV_{inj}$.

this moderate injection potential regime. Since the collection characteristic at these retarding potentials is a measure of the presence of the more energetic electrons in the distribution, the diminution of current below the Maxwellian line may be interpreted as a preferential escape from the potential structure in the beam of the more energetic electrons in the contained colony. This condition should also lead to a lower value of T_e for probe characteristics taken in the more negative going portions of the plasma potential structure.

Figure 19 is a plot of plasma potential as a function of plasma density for points along the axis of the beam. The slope of the (ρ, V) curve is 2.1 volts per decade in density, which, from the barometric equation yields an electron temperature of $\sim$ .9 electron volts, somewhat lower than the temperature derived for the lower energy portions of the distribution in Figure 18. This is, in general, consistent with the observation that, for the more energetic electrons which populate broader reaches of the plasma (in more negative going portions of the potential structure), electron temperatures are lowered (currents diminished below the Maxwellian line).

Figure 20 is a (ρ, V) plot for a radial scan near the beam origin. The values are barometric with a falloff of 2.3 volts per density decade (1.0 eV electrons). Figure 21 is a similar (ρ, V) radial scan at an axial position further downstream. Here, barometric conditions are obtained, with 2.0 volts per decade of density increment (.87 eV electron temperature). Some cooling of electrons as a function of axial position may be occurring here, but the small amount of the decline weighs against firm conclusion. From the several (ρ, V) plots, it is possible to cross-plot plasma potential for fixed values of plasma density as a function of the axial position at which the density contour is examined. If the plasma potential is essentially barometric, then equidensity contours should also be equipotential contours. Figure 22, which cross-plots this data, indicates that potential along an equidensity contour is essentially constant.

By further increases in the separation from the wire to the plasma, further increases in injection potential may be obtained. Figure 23 is the Langmuir probe characteristic at the origin of the long beam with an

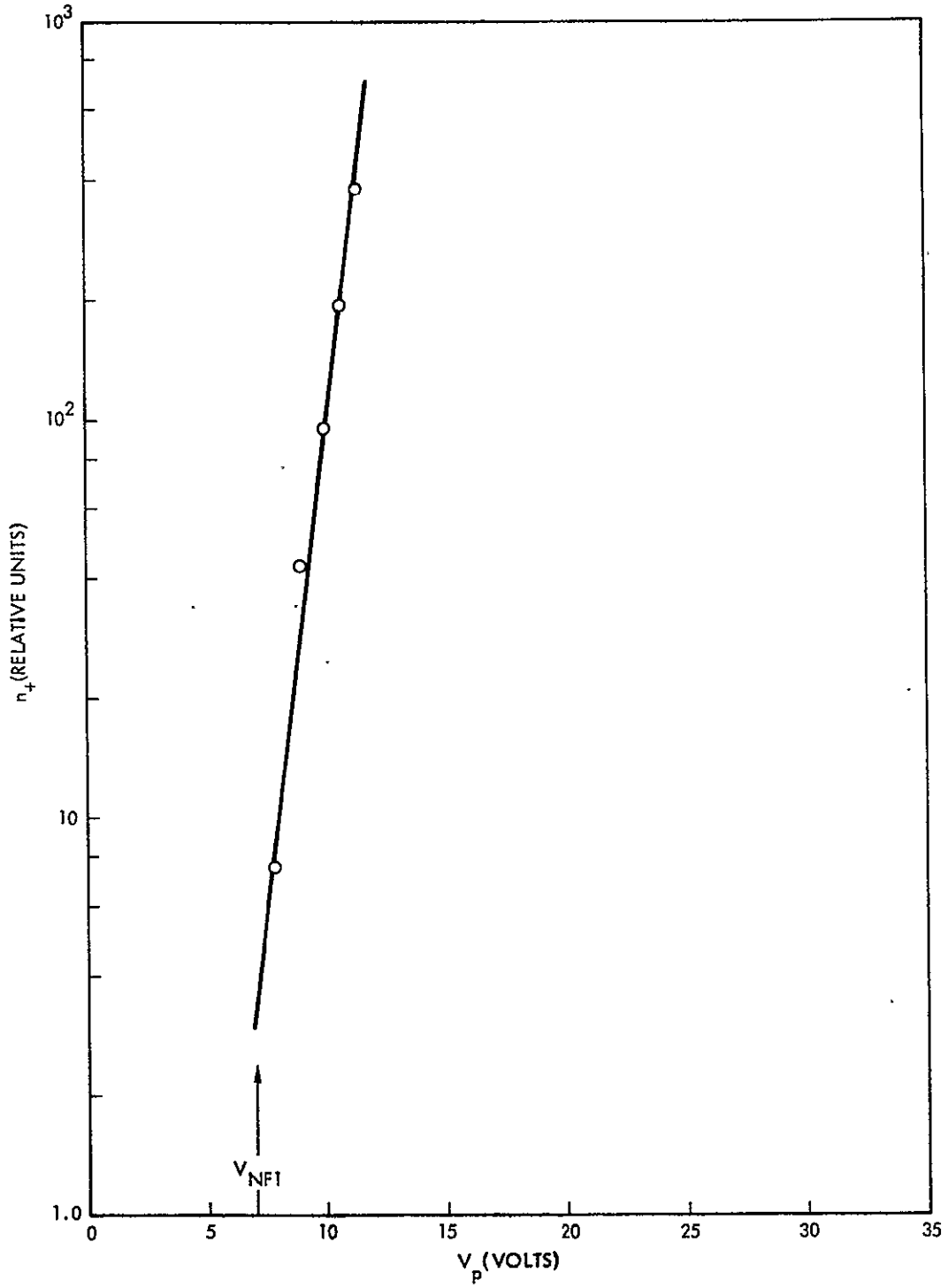

Figure 19. Ion density (n_+) as function of plasma potential (V_P) along axis of beam. Slope indicates electron temperature(T_e)$\sim$10,600°K.

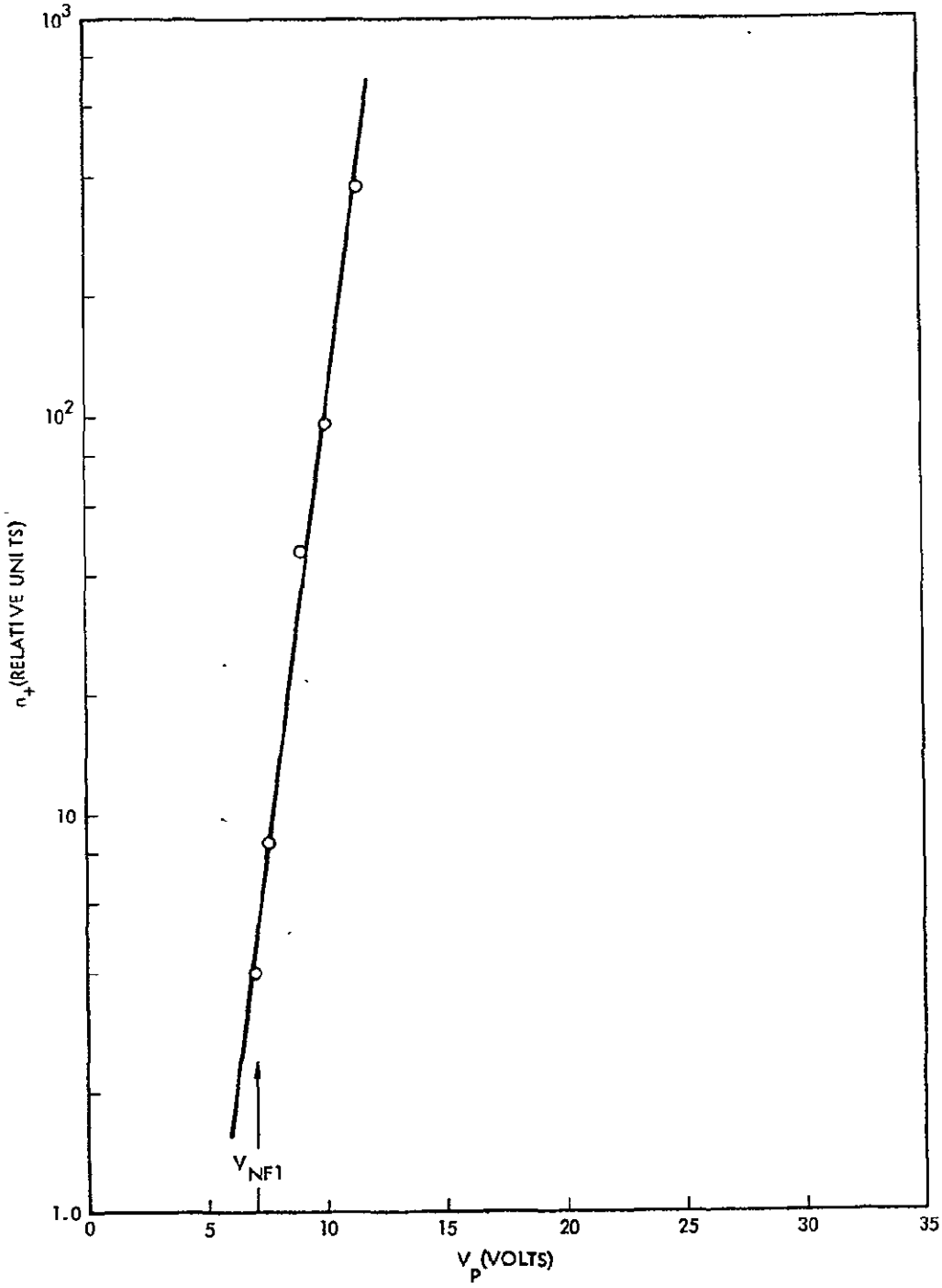

Figure 20. Ion density (n_+) as function of plasma potential (V_p) at Z = 11.5 cm scanned in the radial direction. Slope indicates electron temperature (T_e)$\sim$11,600°K.

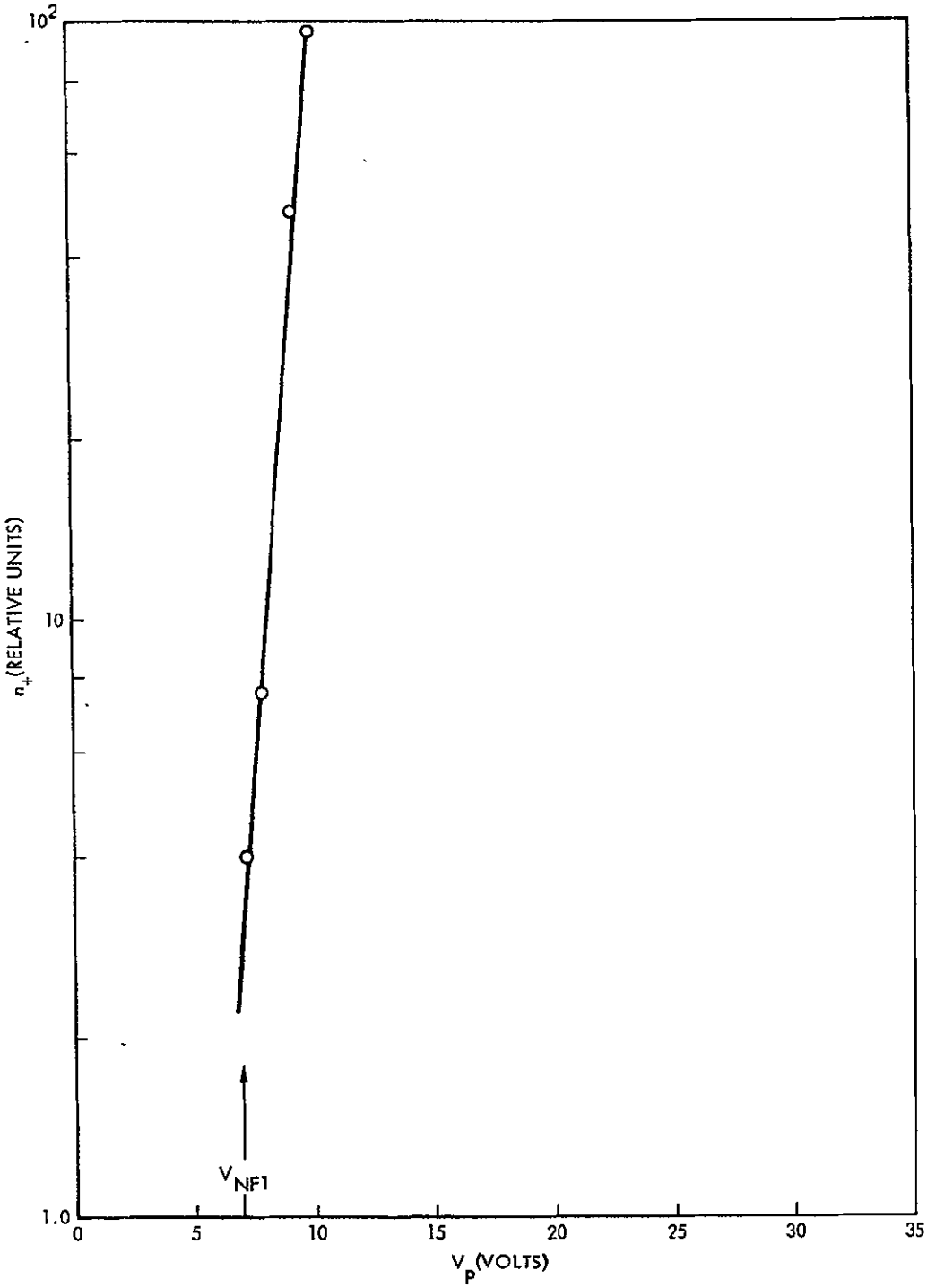

Figure 21. Ion density (n_+) as function of plasma potential (V_p) at Z = 21.5 cm scanned in the radial direction. Slope indicates electron temperature (T_e)$\sim$10,100°K.

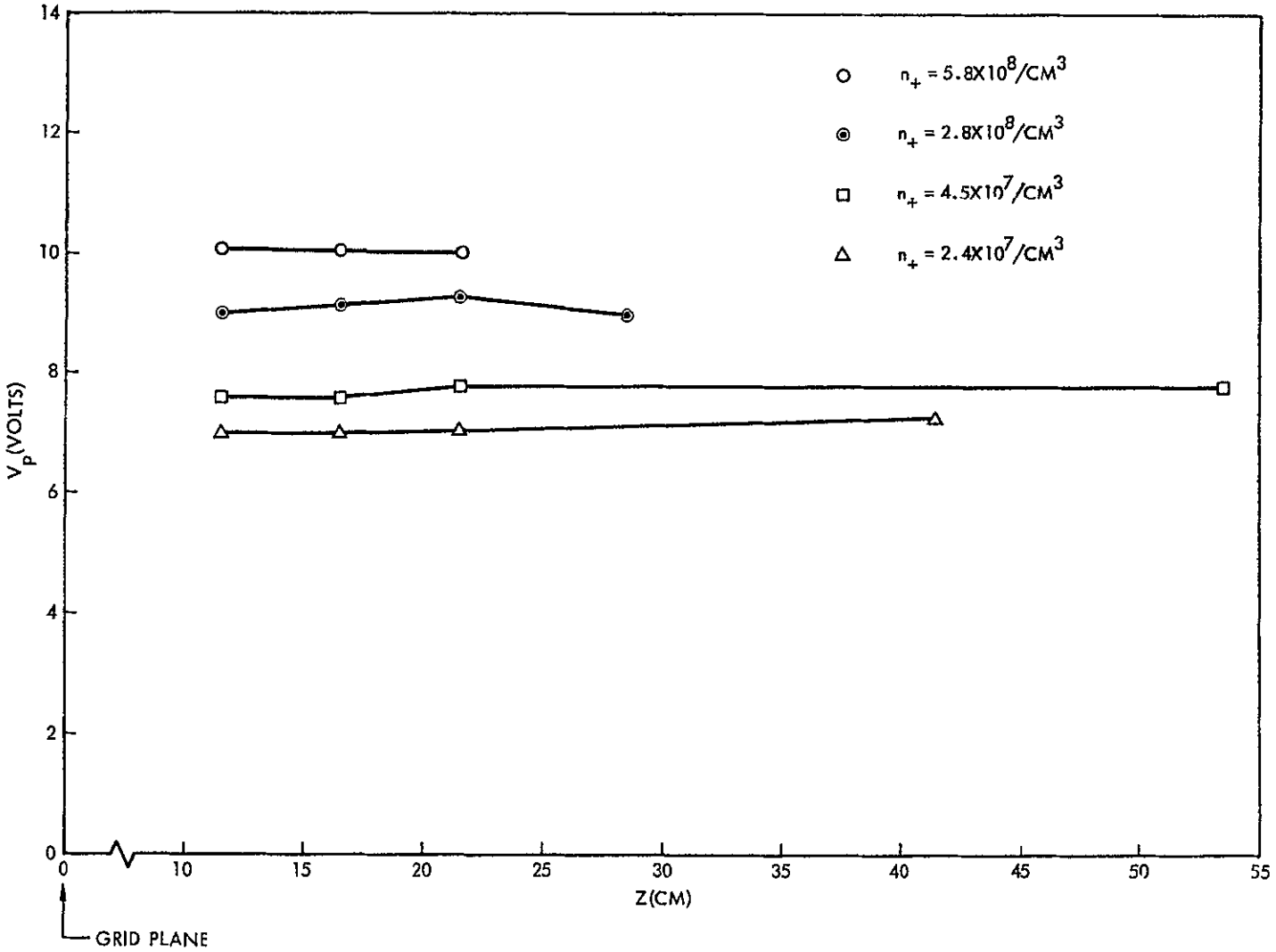

Figure 22. Plasma potential (V_p) measured along equidensity contours. Equidensity contours are equipotential contours. $n_+(0) \sim 4x10^9/cm^3$.

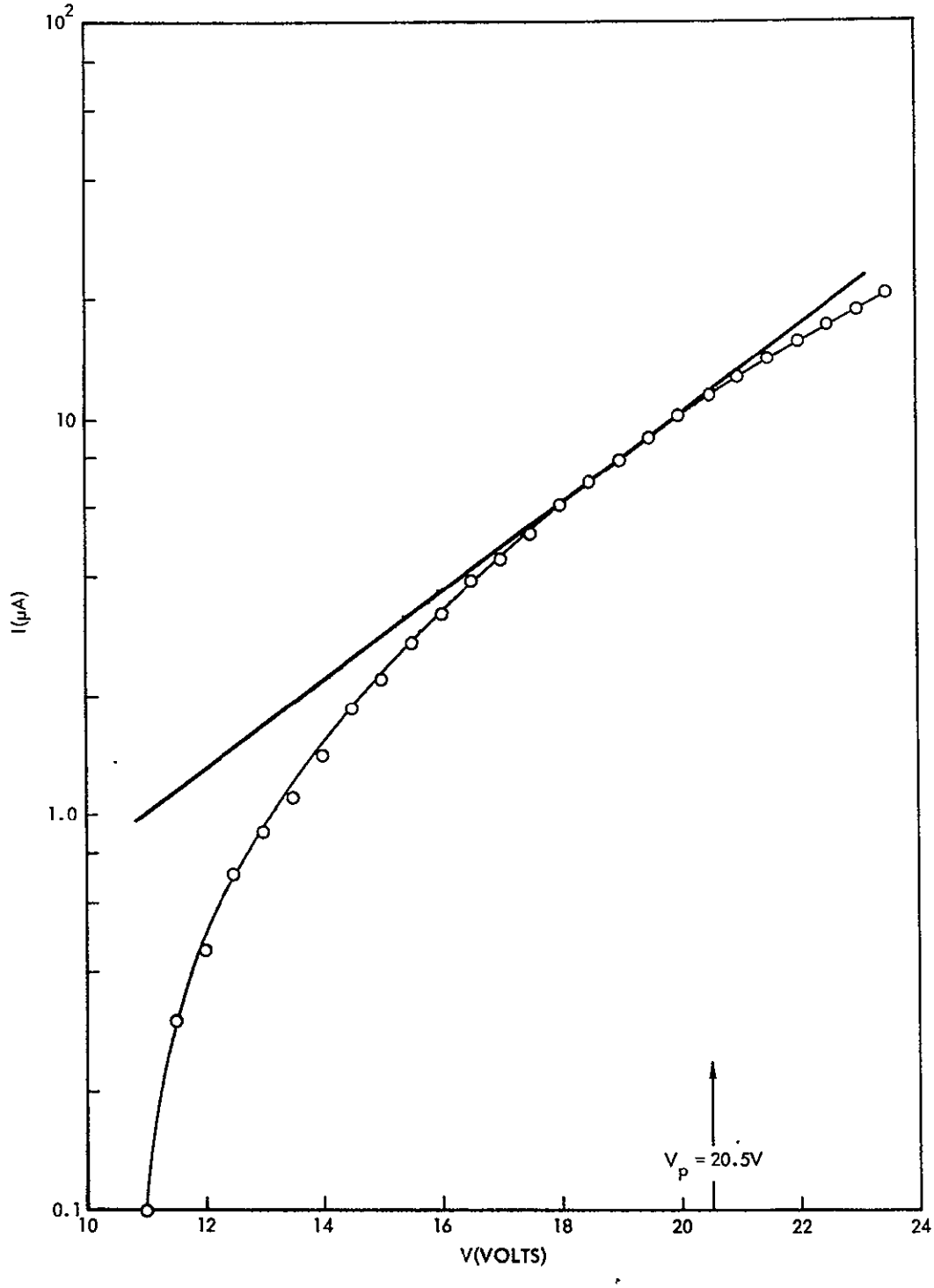

Figure 23. Langmuir probe measurement at X = 0, Z = 5 cm. V_P = 20.5V, V_{NFl} = 10.0V, V_{inj} ∿10.5V, T_e = 45,400°K, kT_e ∿0.37 eV_{inj}. Distribution has only limited range characterized as Maxwellian at T_e.

injection potential of 10.5 volts (20.5 volts plasma potential and 10.0 volts neutralizer wire potential). Near the plasma potential, the slope of the curve is 9.0 volts/decade which yields an electron temperature of 3.9 electron volts. For the measured injection potential, $kT_e = .37\ eV_{inj}$, which is of conventional magnitude. Diminution of current below the Maxwellian line is also present here indicating that electron temperature in more negative going regions of the plasma potential structure will be reduced from that value indicated on axis at the beam origin. Figures 24 and 25 are (ρ, V) plots, radial for axial positions at beam origin and 30 cm downstream, and along the beam axis. For these curves, barometric conditions may be considered to exist on a more localized basis, with values of temperature which are high for points near the beam origin but which diminish for either radial or axial excursions into more negative going regions of the potential structure. A limited cross-plot of (ρ, V) for points along two equidensity contours is given in Figure 26. Here, the equidensity contours are not equipotential to the degree that was obtained for conditions in Figure 22.

For the two cases discussed, measurements have been conducted over a range of $\sim$ two orders of magnitude in plasma density. If the plasma potential structure were purely barometric with a constant value of T_e, then a potential increment of $4.6\ kT_e$ would be encountered for a density increment of 10^2. For the case of $kT_e = .3\ eV_{inj}$, $4.6\ kT_e = 1.4\ eV_{inj}$, which would predict that plasma potential at such a point would be negative with respect to the neutralizer wire by $.4\ eV_{inj}$. For Case 1 (Figures 17-22), $eV_{inj} = 4.4$ volts which predicts that potentials some 2.0 volts negative with respect to the neutralizer should be present. In actuality, the potential at the lowest density contours examined merely moved to near equality to the neutralizer potential. This is probably the result of diminished values of T_e for the less dense regions (more negative going) of the plasma. It would also tend to indicate that an energy flow from ions to electrons does not occur to any substantial degree and that there are limitations on the negative going extent of the plasma potential (see discussion of II.B.2.).

For Case 2 (Figures 23-26), an unqualified application of the barometric equation with the T_e observed on axis at the beam origin should

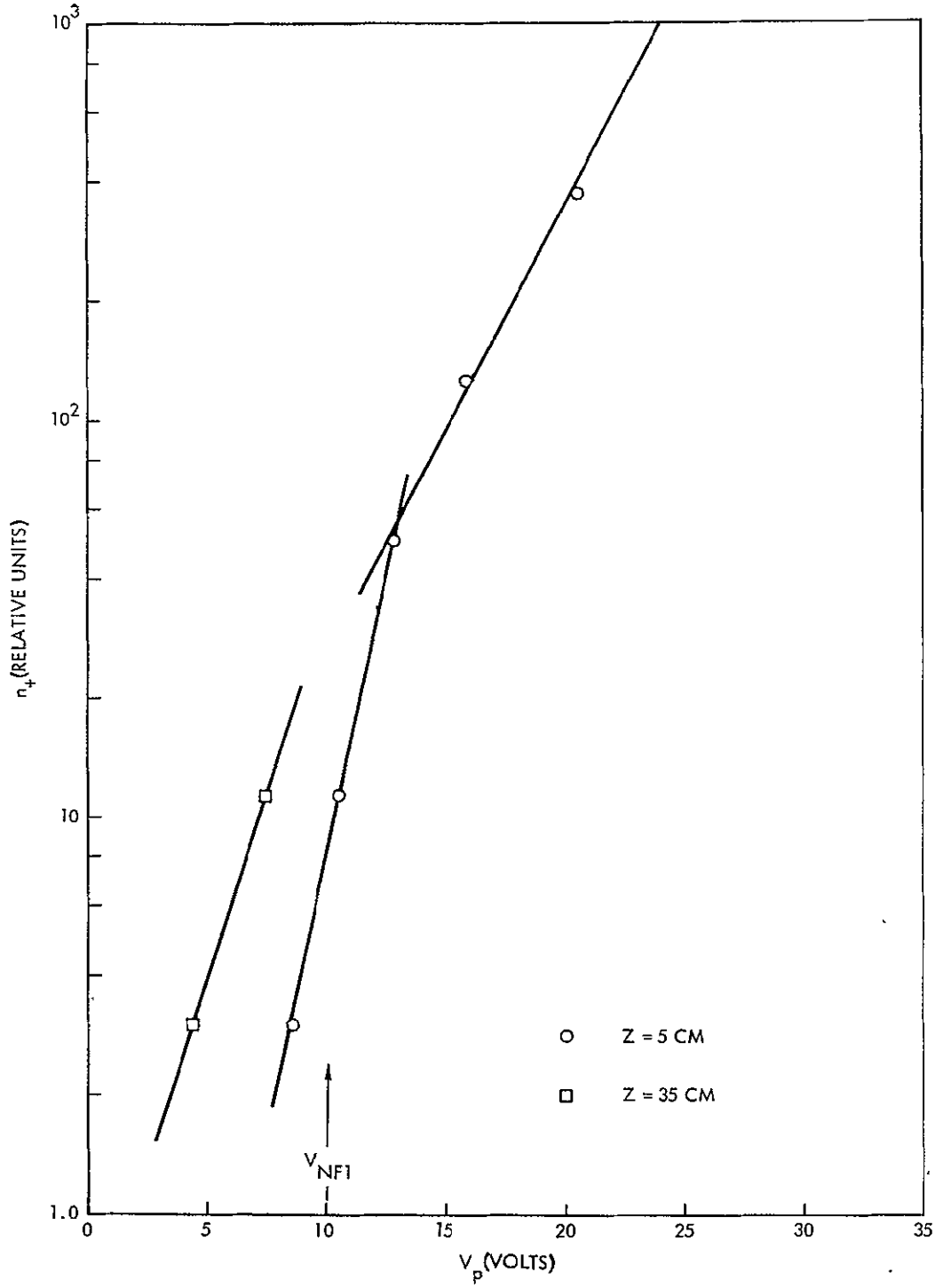

Figure 24. Ion density (n_+) as function of plasma potential(V_p) at Z = 5 cm and Z = 35 cm,scanned in the radial direction. Upstream (Z = 5 cm) electron temperature diminishes in radial excursions away from origin. Slopes of plots indicate T_e = 45,000°K and 18,000°K.

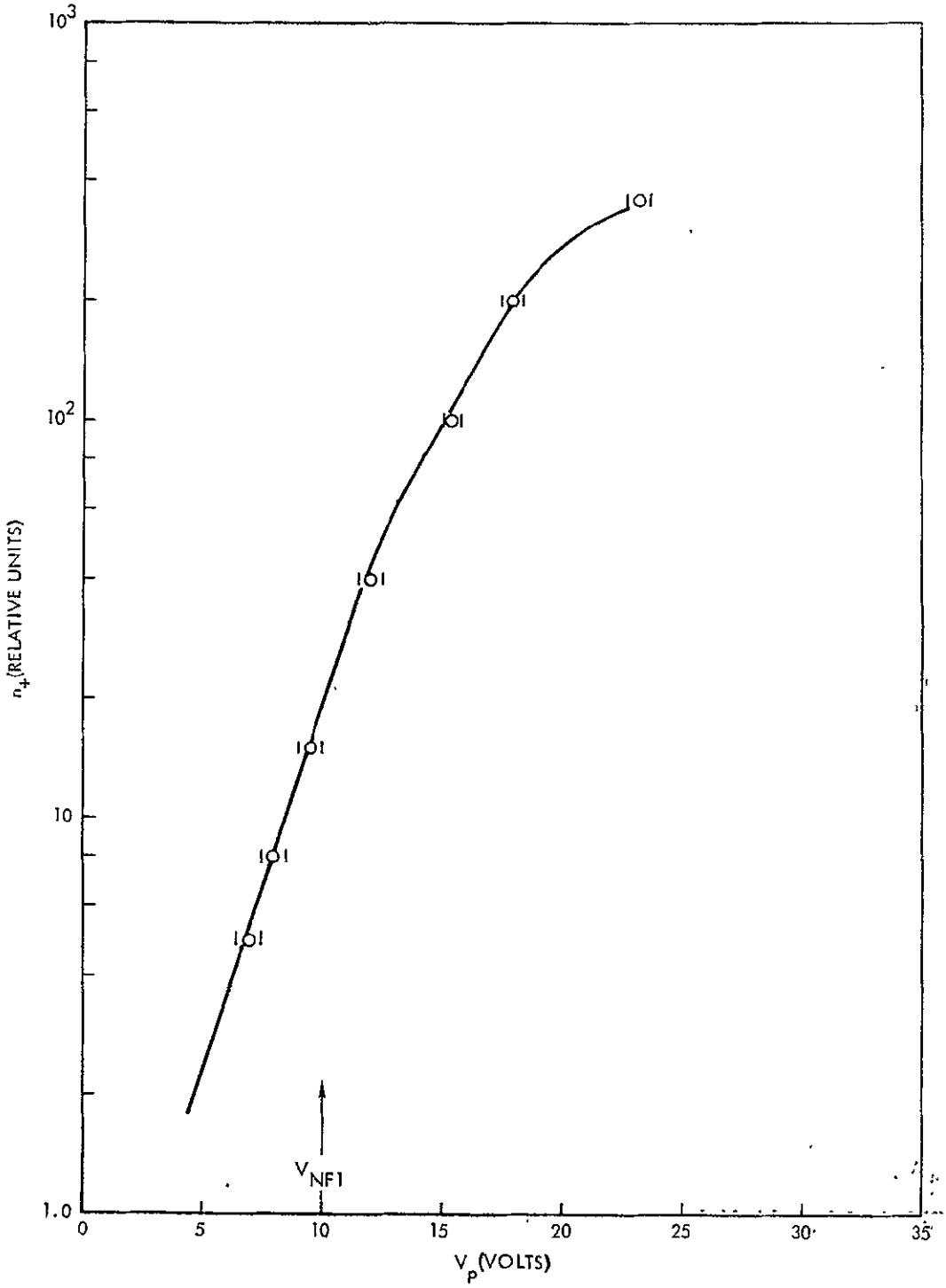

Figure 25. Ion density (n_+) as function of plasma potential (V_p) along axis of beam. Electron temperature diminishes in moving to downstream regions.

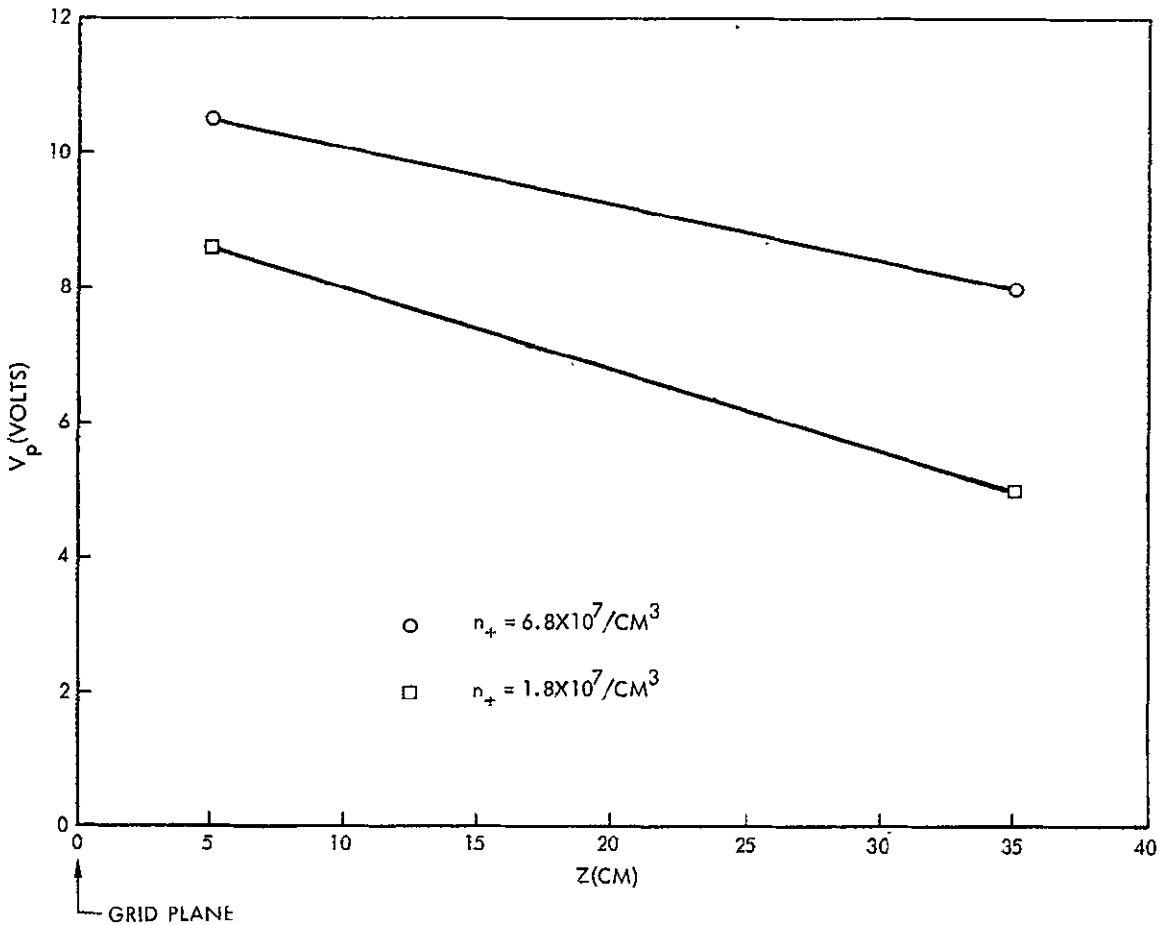

Figure 26. Plasma potential (V_P) measured along equidensity contours. Equidensity contours are not equipotential contours. $n_+(0) \sim 4x10^9/cm^3$.

yield potentials along the lowest examined density contour (10^{-2} ρ_o) which would be 7 to 8 volts negative with respect to the neutralizer wire. The data of Figure 26 does indicate potentials that are negative with respect to the electron source but not of the magnitude indicated from the unqualified use of barometric conditions. Again, limitations on the extent of negative going potentials appear to be present. While Figure 22 does not indicate a required energy flow within the plasma region examined, Figure 26 does. Perhaps, this last result is associated with the difficulties in plasma potential measurement by emissive probes which were observed to be encountered in dilute portions of the plasma column and for increased magnitudes of injection potential. Considerable rounding of probe characteristics are obtained under these conditions making interpretation of plasma potential less precise. The possibility of an energy flow from ions to electrons, then, cannot be completely dismissed. There are, however, clear limitations to the extent of the negative going regions of the plasma potential. Such limitations now make it appear unlikely that SERT I could have existed at the positive potential increment above the space plasma which would derive from a constant temperature, barometric condition[3,4,9] for the injection condition assumed. SERT I may still have been positive with respect to space as inferred from the electric field strength meter data, but, positive voltages would now appear to be small if present at all.

A final observation relative to the two cases presented here relates to the differences obtained for regions of the plasma with negative going potentials (with respect to the neutralizer wire). While differences exist in the data, the principal fact would appear to be that an energy flow from ions to electrons, if present at all, does not scale with injection energy. For the immersed wire, the plasma was barometric to $\sim -6\ kT_e$, while for 10 volt injection potentials and larger values of T_e, negative going potentials are, if present, of order kT_e.

VII. SINGLE BEAM STUDIES: MODERATE TO HIGH INJECTION POTENTIAL

This section will discuss studies in which, through increased separation between neutralizer and thrust beam, injection potentials up to $\sim$ 100 volts were obtained. Because of apparent difficulties in the

measurement of plasma potentials by conventional emissive probe techniques for beams with increased values of injection potentials (Case 2, Section IV), plasma diagnosis for this present series of experiments used floating potentials (of hot wire probes or of the beam collector). There is a loss of accuracy in potential determination where floating potentials are utilized (electron temperature effects and surface work function effects). However, it is not believed that the principal results of the experiments in this moderate to high injection energy regime are compromised by the diagnostic approach.

For these studies, the long beam was utilized. Neutralization was achieved through a unipotential hot wire whose position was variable. Measurements of floating potentials of hot wire probes at the injection region and at various locations in the plasma column were made for varying degrees of neutralizer withdrawal. Beam collector floating potential was also measured, while Faraday cups monitored ion current density in the beam.

Figure 27 illustrates the injection potential obtained as a function of neutralizer placement (withdrawal is achieved through neutralizer support rotation, expressed in degrees). The separate curves illustrate injection potential as a function of time after the ON pulse is applied to the pulsed beam (for a discussion of pulsed beam operation, see Reference 6). For the general degree of neutralizer withdrawal utilized here, timewise variations in injection potential are observed. This is the result of diminutions in the total accelerated ion current which were allowed to occur as a function of time after the beam was pulsed into operation. For those beams, the diminution of current occurs principally at the outer boundary of the beam. Thus, diminished total ion current leads to an effective increase in the withdrawal of the neutralizer wire and increased injection potentials.

Figure 28 illustrates the dependence of the "relative" floating collector potential (collector potential relative to neutralizer wire potential) as a function of injection potential and at various times after the beam ON pulse. For an immersed wire condition ($V_{inj} = 0$), this relative collector potential is ~ -4 volts. For accurately diagnosed plasmas (conventional emissive probe potential measurements), the potential at such downstream points is, typically, ~ -1 volt. Floating potential measure-

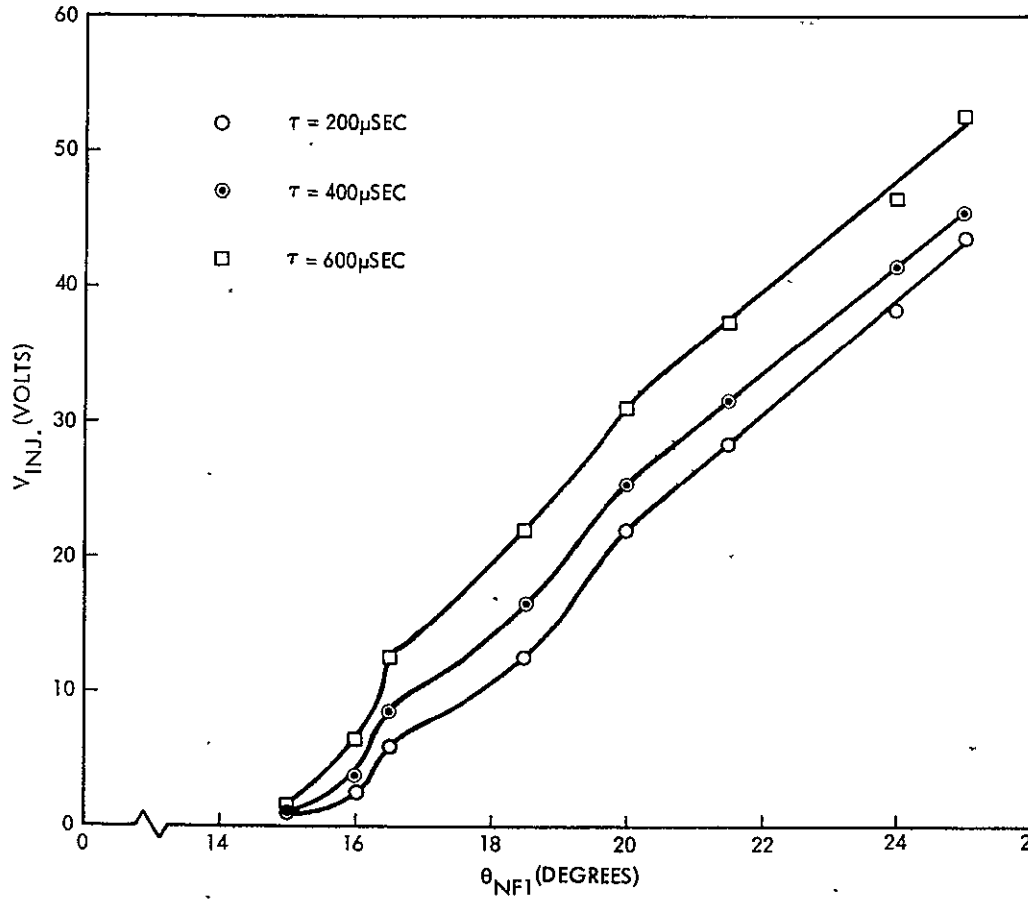

Figure 27. V_{inj} as function of neutralizer wire withdrawal expressed in degrees (θ_{NF1}). Separate curves illustrate V_{inj} as function of time after plasma pulses ON.

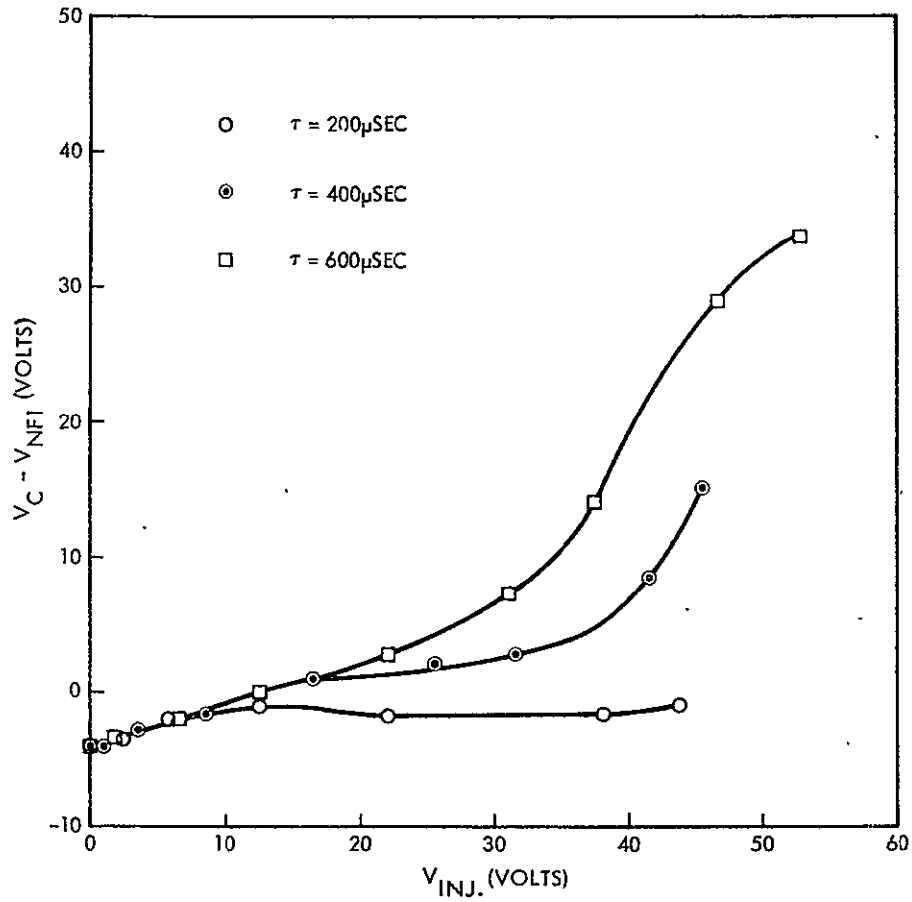

Figure 28. "Relative" floating potential of collector[1], (collector potential relative to neutralizer wire potential) as function of injection potential and for various times after plasma pulses ON. At 200 μs constant collector potential indicates thermalization of electrons. At 400 μs and 600 μs collector potential rises indicating a growth of a cold colony of stagnant electrons with resultant streaming of freshly injected neutralizing electrons.

ments are, however, influenced by surface work functions. For the (possible) low work function cesiated surfaces of the beam collector, contact potential shifts of $\sim$ 3 volts relative to clean tungsten are not unlikely. Thus, the collector floating potential for the immersed wire condition appears to be capable of explanation.

For the "200 μsec" curve on Figure 28, the relative floating collector potential remains virtually unchanged for increases of injection potential to values of almost 50 volts. What is being observed, then, is a high energy injection which produces a large value of electron temperature in the thrust beam. Electron pressure effects cause increased ion beam divergence. Density gradients and electron temperatures combine in an essentially barometric situation to produce strong potential gradients in the plasma, the net effect of which is that all of the injection potential has been "recovered" in the plasma at the axial distance of the collector. If this plasma were to engage in electrical equilibration with another plasma and the geometrical onset of equilibration were to be in this downstream region, it is possible that the equilibration potential of the neutralizer would be very nearly that of the space. The electron injection energy would have been recovered and only minor problems of electrostatic contamination of a spacecraft (of equal potential as the neutralizer) would be present. This overall condition corresponds to a situation discussed in II.C., page 18.

For the time period 400 μsec after the beam is pulsed into operation, some important variations away from 200 μsec behavior may be noted. These variations occur in smaller degrees for the range from 10 to 20 volts injection potential, and are rapid variations for injection potentials above $\sim$ 35 volts. The data show collector floating potentials which are rising reflecting the fact that proportionately less of the injection potential is now being recovered in the plasma. Faraday cup probes reveal that ion beam divergence is now diminished, indicating reduced electron pressure effects. Both beam divergence and collector potential data indicate the growth of a colony of electrons in the plasma column which are of reduced energy relative to the freshly injected electrons and which are, at least, partially stagnated. Because of the now diminished retarding potentials in the downstream regions of the plasma, freshly injected electrons may stream directly from the neutralizer to the

collector providing current neutralization there for the ions. In sum, the electron temperature in the plasma no longer represents a conservative thermalization of injection energy, and the situation previously described as "streaming" is evident.

At 600 μsec after the beam ON pulse, the conditions of streaming are even more thoroughly in evidence. The major part of the injection potential, say at 50 volts injection, is now unrecovered. Assuming the downstream plasma potential to be nearing that of space, if a space equilibration was being enacted, these conditions would produce a situation of strong electrostatic contamination of the spacecraft, loss of electrical efficiency (through failure to recover electron injection energy), and magnetic and space particle contamination of the ambient space through electron streaming.

Figure 29 is one further set of potential measurements in the plasma column. Here the quantity shown is the difference in potential between a floating wire at the beam origin and the beam collector. At τ = 200 μs this potential increment is approximately equal to the injection voltage illustrating that the major portion of the injection potential has been recovered in the plasma thrust beam. At τ = 400 μs the recovery of the injection potential is diminished, and for injection potentials above the order of 40 volts the fraction of the recovery is further diminished. At τ = 600 μs the fractional recovery is of a still smaller magnitude. In addition, the point at which $d(\Delta V)/dV_{inj}$ becomes negative has now moved to $\sim$ 30 volts.

What is apparent in these experiments is the growth and retention, in a laboratory environment, of a colder and (probably) stagnant colony of neutralizing electrons in the thrust beam. There are several processes that may be responsible for the creation of lower energy electrons. Three possibilities are: 1) secondary electron emission from the beam collector under either ion and/or electron bonbardment, 2) release of electrons through ionization of residual neutral particles in the laboratory testing environment, and 3) plasma processes (here unspecified, but included because of observed bursts of high frequency noise at the point in time for which a rapid buildup of lower energy electrons is observed). Of these three possible sources, probably only two

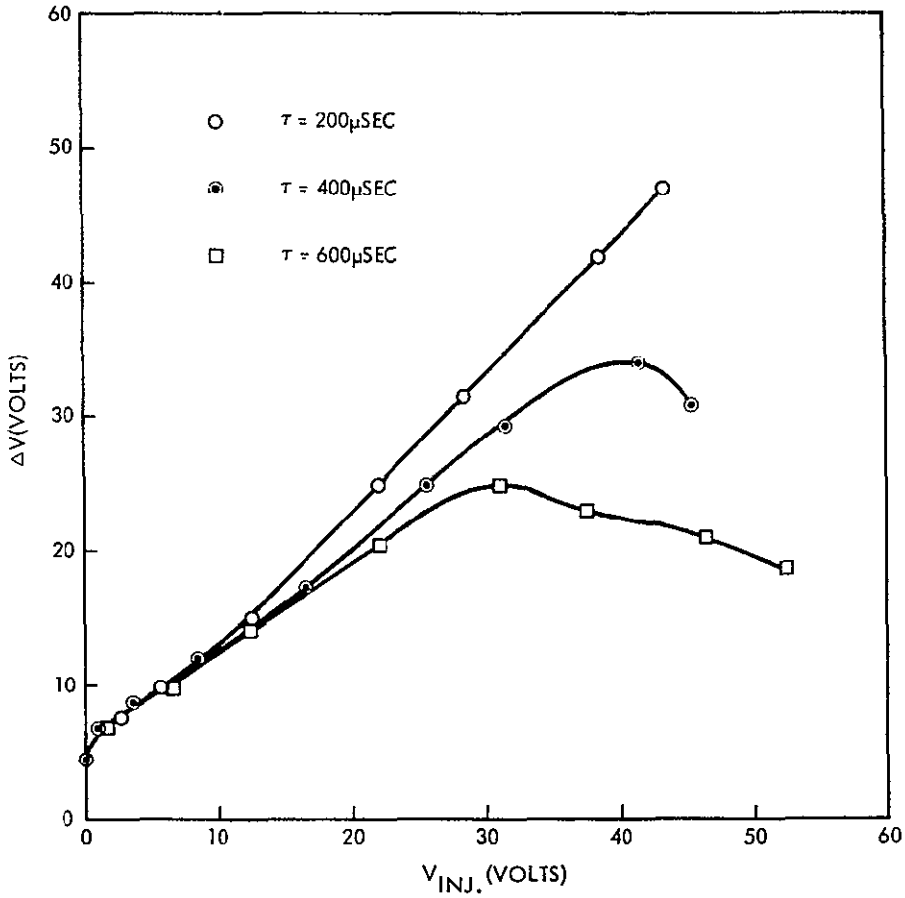

Figure 29. Potential difference between floating potential of wire near source and collector$_1$ as function of V_{inj}. For V_{inj} <10V, the behavior of plasma is nearly identical for all time periods. For V_{inj} >10V, the later two time periods indicate growth of stagnant colony, failure to recover injection potential, and establishment of streaming conditions.

at best are relevant to the vehicular condition. Thus, the period of time required to generate the stagnant colony in a laboratory environment may not be relevant in space. An important feature, however, is the retention of the colony, and, whatever processes may be present which may cause the ejection of a stagnant electron, the rates of these processes are not sufficient to counter the growth rates. In space, the growth rates of a cold colony are related to the allowable back diffusion of these electrons which depends on ambient plasma density and upon "coupling" between the two plasmas. These factors will be discussed in the following section. What the present data suggests is that, unless conditions are present which tend to inhibit the growth of a cold colony, such a colony will be retained.

VIII. THE GROWTH AND RETENTION OF A BACK DIFFUSED COLONY OF ELECTRONS: BI-PLASMA EQUILIBRATION

In the experimental studies, three observed interaction phenomena are of importance. In the first of these, (IV), energetic electrons have been injected and have streamed through a semi-stagnant cold colony of electrons without any significant variation in the properties of that colony. In the second interaction, (V), a condition of moderate injection potential produced neutralizing electrons at elevated temperatures with potential gradients appropriate to the density gradients and to the barometric condition. The contact of this "hot" beam and a cold "space" plasma was allowed to take place with, however, some axial separation between the thrust beam injection region and the initial point of contact of the bi-plasma system. In this axial interval, some fractional recovery of injection potential was realized. In the resulting equilibration, under conditions of balanced electron interchange, the properties of the thrust beam were not markedly different than that experienced in the single beam condition. The third interaction of interest (VII) was the growth and retention, on a quiescent steady state basis, of a cold stagnant colony with freshly injected electrons streaming to the collector. Growth rates for this laboratory environment may depend upon factors that will not be encountered in space.

For the space condition, both ambient plasma density and the geometry of the contact area between the two plasmas may be expected to be key factors in the quantity of back diffusing electrons. If the spacecraft creates a definable wake in the space plasma and if the thrust beam is initially contained in the wake region, then limited coupling between the two plasmas would be expected. This would diminish the back diffusion rates, and, postulating ejection processes which operate at some non-zero level, a condition of minimized influenced of space plasma electrons on thrust beam behavior might be obtained. A dense space plasma whose geometrical contact with the thrust beam is immediate produces strong coupling and possible maximized influence of back diffusing electrons on the thrust beam. Figure 30 illustrates several cases of coupling.

For spacecraft in the interplanetary plasma, long axial lengths of the beam must be considered in order to have any meaningful level of interchange. One may consider the thrust beam as capable of recovering its injection potential and containing within the near regions the injected electrons for dwell times that are appropriate for beams in which the injected electrons both current and charge neutralize the ions. For spacecraft in the ionospheric plasma and with immediate contact between the thrust beam and the space, the back diffusion should be rapid enough to affect the thrust beam materially, to establish the cold colony and to set up a streaming situation for the freshly injected electrons. If this condition were to be possible, some relief might be obtained by "delaying" the coupling between the two plasmas. Figure 31 presents an example of a material structure which "delays" the coupling and allows the thrust beam an opportunity to recover its injection potential before engaging in any substantive interaction with the space plasma.

Two final points must be considered. The first is that throughout the discussion of this paper it has been assumed that the space plasma electrons are "cold" while the thrust beam electrons are "hot." Since the neutralization of an actual thrust beam must utilize a neutralizer with some physical separation from the beam, the injection conditions are likely to lead to "hot" beam neutralizing electrons. Electrons in space, on the other hand, are not energetic, in general, for the main body of these

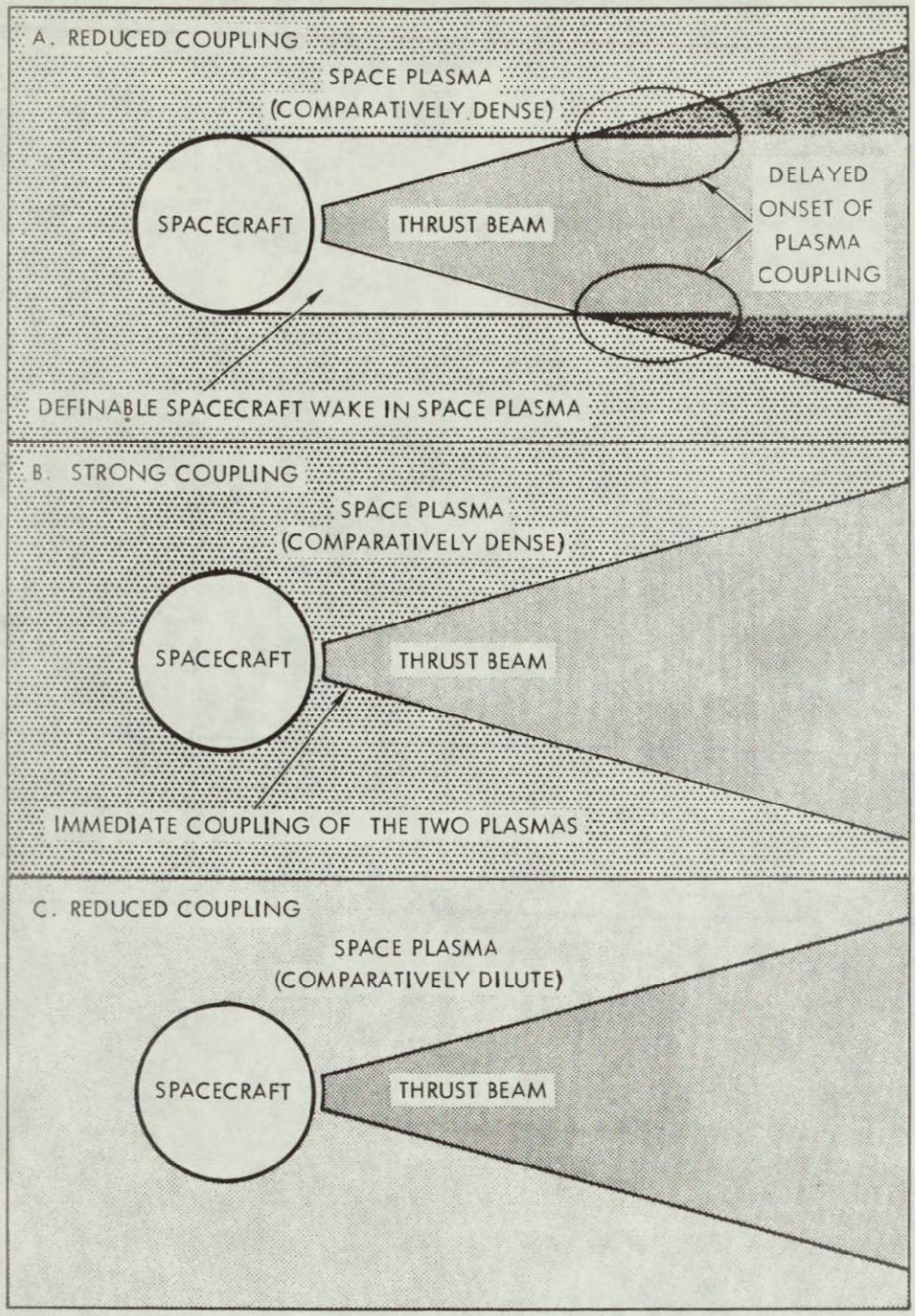

Figure 30. Thrust beam-space plasma coupling
A) Delayed onset of plasma coupling
B) Strong coupling (immediate coupling "dense" plasma)
C) Reduced coupling (immediate coupling "dilute" plasma)

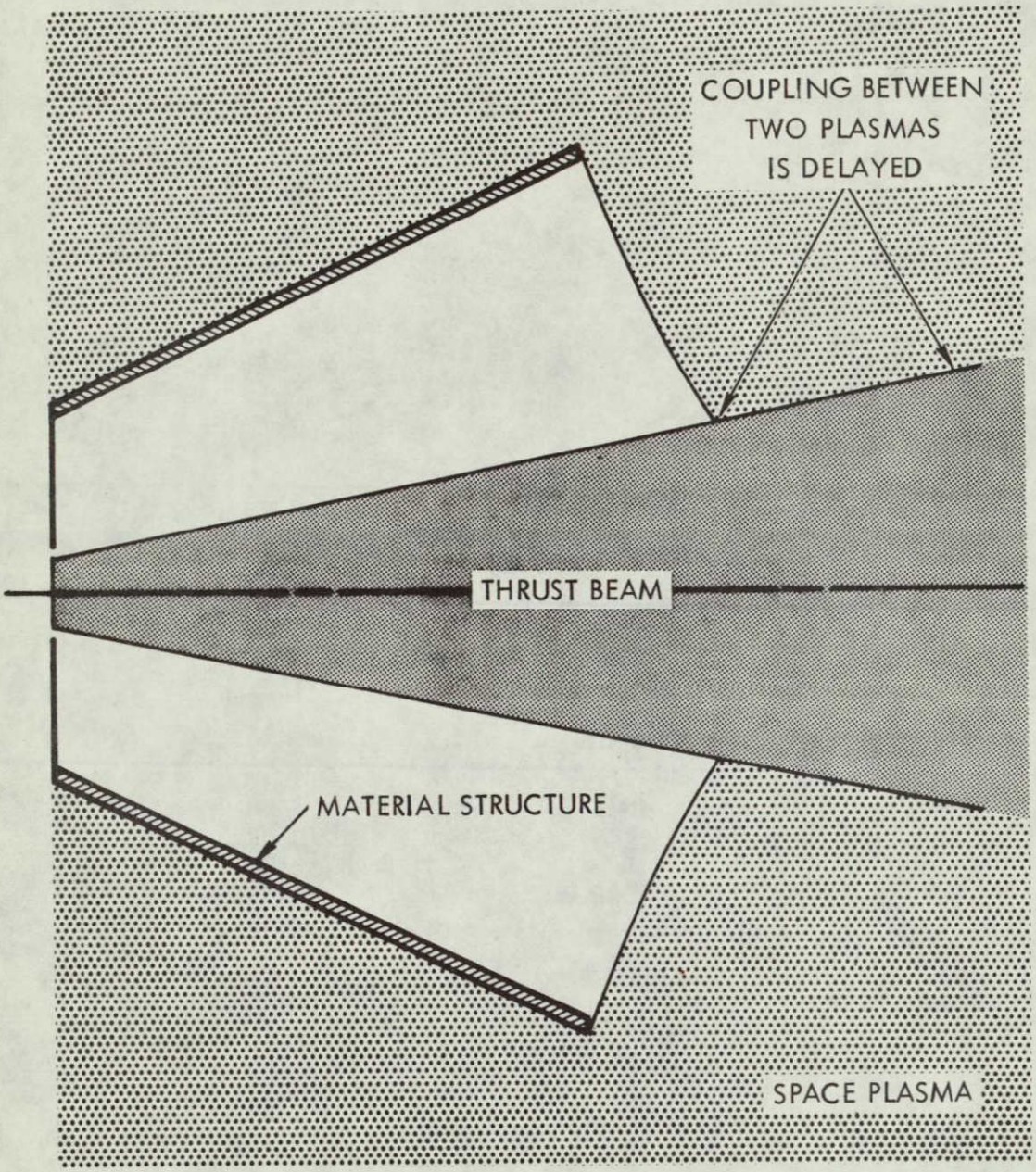

Figure 31. Example of material structure which "delays" coupling between thrust beam and space plasma.

particles. Thus, a "hot" beam and a "cold" space plasma is a likely circumstance. If, however, one considers the general case, the possibility of energetic electrons in the space must also be admitted. For such a condition, then, "hot" electrons from the space could back diffuse into the beam causing increases in beam electron temperature, increased electron pressure effects, and increased particle density gradients. However, the retention of energetic electrons from space in a cold thrust beam is not effective since the energetic electrons are capable of direct escape from the thrust beam potential structure. There is not, thus, the same possible impact upon thrust beam behavior as for the case of a hot thrust beam in a cold space plasma.

The remaining point of discussion is an indicated limitation on injection potential. Previous discussions (Reference 5) have put forward a tentative desirable upper limit on injection potential of 10 volts. The experiments discussed in this paper and the inferences on thrust beam behavior which they provide would only tend to re-emphasize this earlier design point. For injections at this level, the recovery of the injection potential has some possibility of occurrence, unless, of course, there is immediate coupling to a cold dense space plasma. Even if this latter situation should occur, then some possible remedies are available through appropriate bias potentials between the spacecraft and the neutralizer in order to re-establish electrostatic cleanliness on the spacecraft. If, however, injection potentials have progressed beyond the indicated point, recovery of the injection potential may be expected to be even more difficult, and streaming conditions (with attendant electrostatic, magnetic, and space plasma contamination) are a likely steady state occurrence.

IX. FLUCTUATING EQUILIBRATION

The discussion of the previous sections has assumed that the equilibration is a steady state interaction. It is possible, however, to formulate a simple model of the spacecraft-thrust beam-space plasma system in which an oscillatory equilibration could occur. This section will discuss this simple model, noting that any real test of the model must occur in space. To test for the presence of fluctuating equilibria there would require special diagnostic equipment, particularly in band-width capability.

Figure 32 illustrates a spacecraft-thrust beam-space plasma system in which a loop current is present. This loop current could, for example, be the result of a particle drainage to exposed points at elevated potentials on the solar array. This collected current is returned to space through the neutralizer to the thrust beam and thence to the ambient plasma. Because of the driving force of the solar array voltage, a steady state current here does not require any energy flow from the ions to the electrons.

The drainage current loop in Figure 32 may exist on a steady state basis. However, if there is a fluctuation in this drainage, oscillatory phenomena may occur. The elements of the loop are now the L-R-C combination where C is primarily the capacitance between the spacecraft and the space plasma, R is the dynamic resistance for fluctuating currents around the loop which includes the neutralizer injection dynamic resistance, and the dynamic resistance from the thrust beam to the space plasma, and L will require definition.

Figure 33 illustrates a somewhat arbitrarily assumed current flow configuration for the circulating AC current. For this current flow, magnetic fields are generated, and a total magnetic field energy inventory exists. If it is assumed that the geometric dependence of the current flow is of a fixed form for variations in the total magnitude of the flow, then an inductance, L, may be defined where

$$\frac{1}{2} L I^2 = \int_{\text{all space}} W d\tau$$

where I is the total current in the loop and W is the magnetic energy density. For a current as illustrated in Figure 33 and with the geometric dependence in the indicated area, the inductance is

$$L = \frac{\mu_o k \hat{r}}{6\pi} \quad \text{henries.}$$

where $\hat{r}$ is the radius and $k\hat{r}$ is the total length of the cylindrical current flow. For $k \approx 4$ and $\hat{r} = 4$ meters, $L \approx 1$ μhenry.

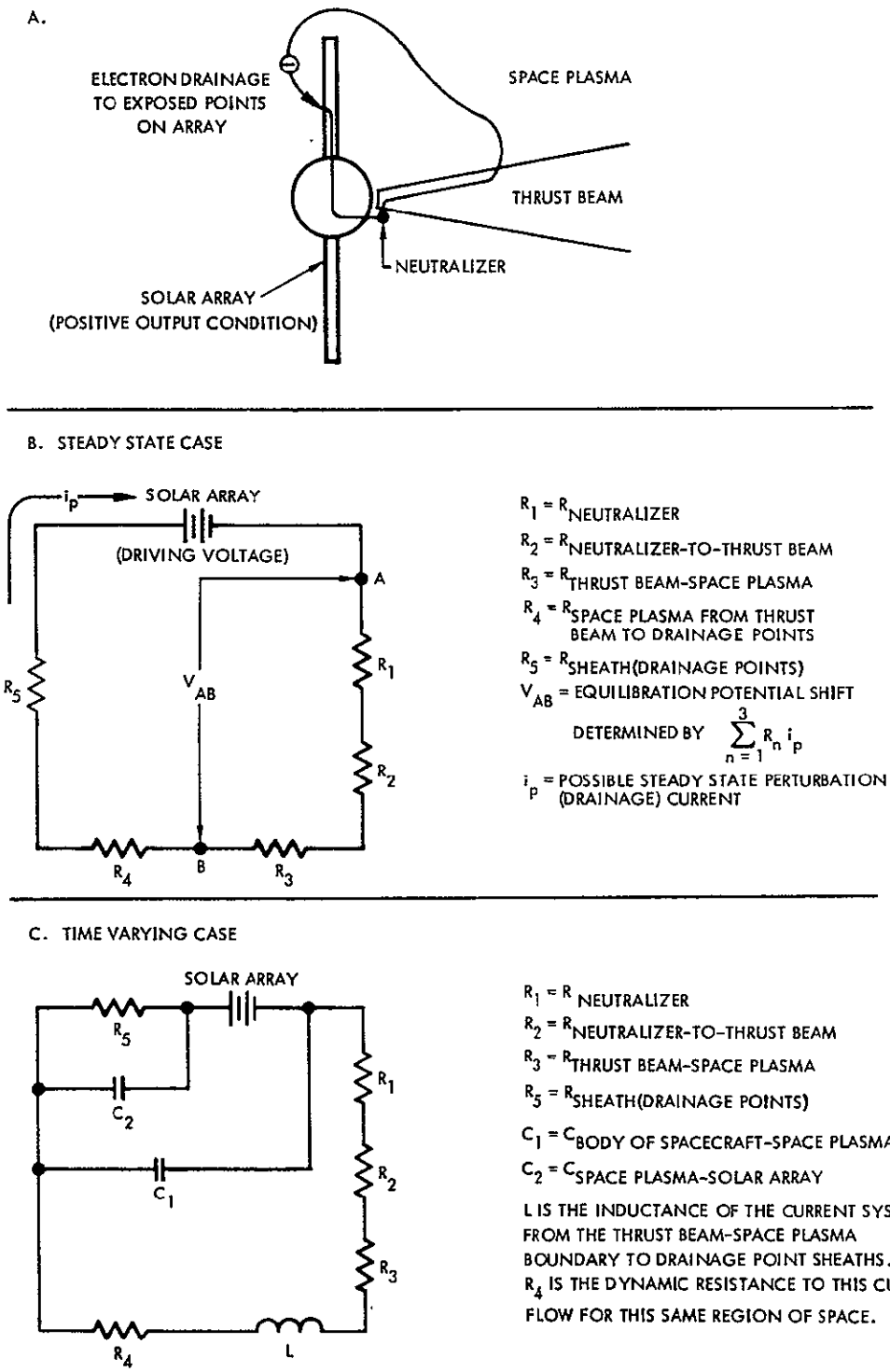

Figure 32. Loop current for spacecraft-thrust beam-space plasma system.
A) Possible current path for system.
B) Equivalent circuit for steady state perturbation (drainage) current loop.
C) Equivalent circuit for time varying perturbation current loop.

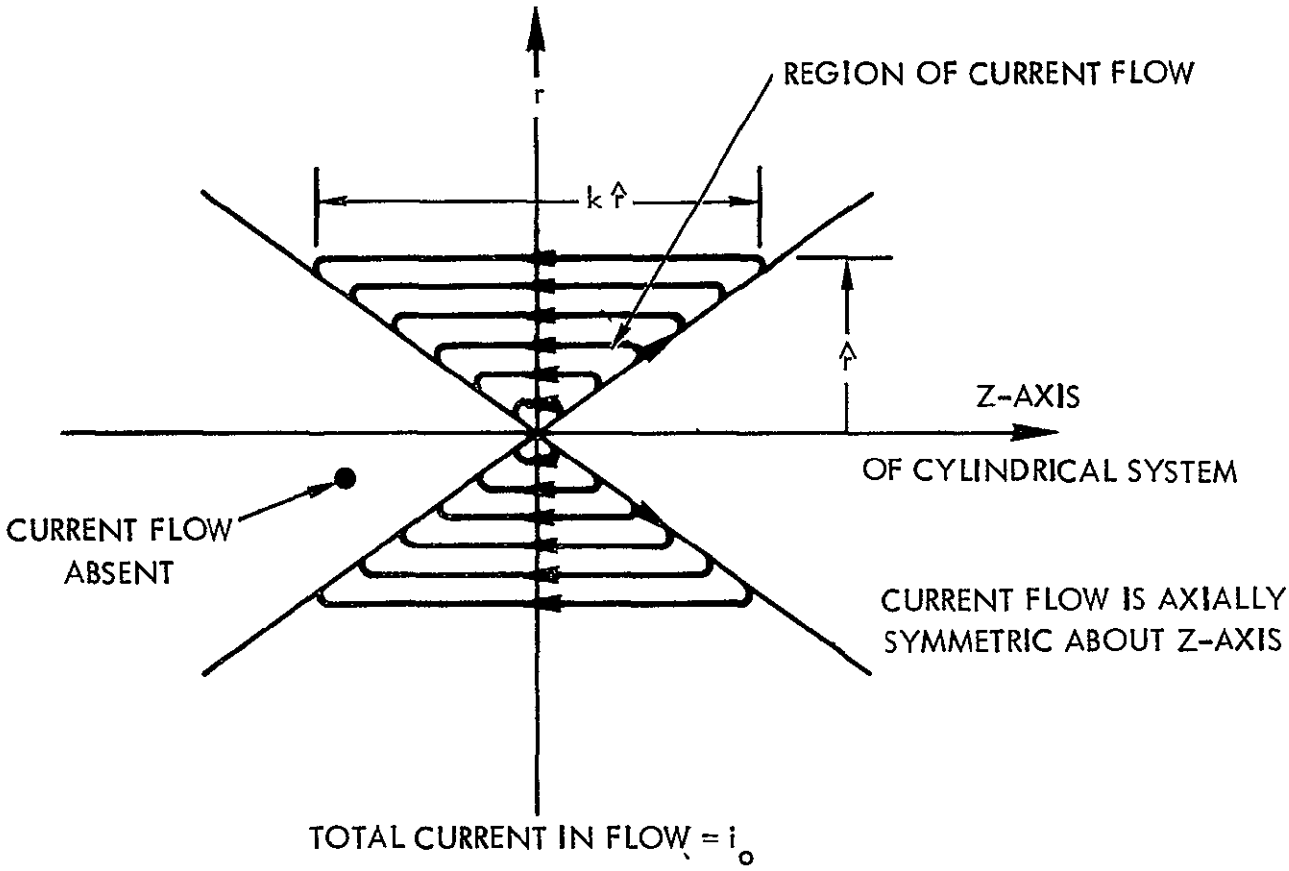

Figure 33. Simple model for computing self-inductance of a circulating current flow. If the current were to be circulating from a thrust beam through a space plasma to a spacecraft, the thrust beam would occupy the cone to the right whose axis is the Z-axis. For Z = 0 plane, total current through circle at r = r is $i_o(1 - r/\hat{r})$. Current flow, thus, is totally contained within $\hat{r}$.

For the spacecraft-space plasma capacitance of C = 10^{-9} farads, the oscillatory frequency of the L-R-C would be of the order of 5 MHz. It is important to note that if such oscillations were to occur, that damping would result because of the positive value of R. A sudden shift in drainage current then could result in a fluctuating equilibration with, however, damping into, again, steady state equilibration. Conditions of over, under, or critical damping will depend upon actual L, R, and C values in the space environment.

The discussion here must be considered conjectural, and laboratory experiments in simulation have not been attempted because of number of unknown factors that might be present in the true vehicular case. The principal point would appear to be that the detection of fluctuating equilibria, if this should occur, will require appropriate diagnostic capability on the spacecraft. Wide band width emissive E-field meters are possible candidates for such diagnosis.

X. SUMMARY

The possible conditions of the electrical equilibration between a thrust beam and an ambient plasma in the completely unbounded geometry of space are not properties that are directly determinable, either through analysis or through laboratory experiments. Analysis and experiments may, however, provide guidance in assessing the various interaction phenomena and allow, at least, qualitative estimates of the conditions that will be obtained in space.

The laboratory tests of single beams at moderate injection potentials have revealed conversion of the injected electrons into Maxwellian distributions. The temperatures of the electrons are in agreement with the values that are obtained from a simple and conservative conversion of injection kinetic energy into both thermal energy and electrostatic potential energy. The relationship between plasma density, electron temperature, and plasma potential is essentially barometric. There would appear to be limitations, however, to the negative going extent of the potential structure in the plasma column. No clear evidence has been obtained for any substantive energy transfer from the ions to the electrons, so it would appear that the plasma

potential will be limited to potentials which do not proceed to any significant amount negative with respect to the neutralizer. If the possible back diffusion of electrons from a space plasma to a beam is assumed as ineffective, then neutralizer equilibration potential would be at or near the space plasma potential. The existence of positive spacecraft equilibration potentials, as discussed for the case of the SERT I spacecraft, do not appear likely, and the evidence supplied by the electric field strength meter performance for that vehicle may be questioned.

For increased injection potentials, the electrons in the plasma are no longer represented by a Maxwellian distribution. The more energetic components of the distribution are in diminished quantity, indicating a preferential escape for those particles. There is also evidence of the accumulation and retention of lower energy electrons, and conditions of streaming of freshly injected electrons are observed. These experiments indicate that the close coupling of "dense" space plasmas to thrust beams with high injection potentials is likely to back-diffuse a cold colony of stagnant electrons, while electrons from the neutralizer stream directly to space. This situation should be avoided if possible since it produces electrostatic contamination, magnetic contamination, and space plasma contamination. A possible technique for reducing the coupling between the thrust beam and the space plasma, to allow the recovery of the injection potential in the beam prior to engaging in the electrical equilibration with the space plasma, has been described. In the very dilute interplanetary plasmas such initial isolation of the two plasmas may not be required.

The dynamic resistances of the injection region and the thrust beam have been examined. For measured bi-plasma equilibration, the thrust beam has exhibited negative dynamic resistance. However, the net dynamic resistance from the neutralizer to the space plasma has been demonstrated to be positive. Thus, equilibration is stable, and possible fluctuations in the equilibration should undergo damping rather than growth.

A limitation on injection potential has been discussed. If this injection may be maintained at the level of 10 volts or less, and unless strong coupling to a "dense" space plasma exists, then conditions for the

recovery of the injection potential in the thrust beam are likely. In a dense space plasma (such as the lower ionosphere), it may be necessary to delay the coupling, even for the reduced level of injection potential given here. For that fraction of the injection potential not recovered, relief would be obtainable through appropriate bias potentials between the spacecraft and the neutralizer. Within this limitation on injection potential and through remedies of applied bias potentials, one may conclude that electrostatic cleanliness may be achieved for the spacecraft. The limitation on electron streaming removes possible conditions of magnetic contamination. Finally, electrical efficiency is maintained through the recovery of the electron injection energy, this quantity having already been reduced in its initial magnitude. For these several conditions, the operation of electric thrusting units on spacecraft should be compatible with the simultaneous operation of the scientific payload on the craft.

REFERENCES

1. "Spacecraft-Space Plasma Equilibria for Passive and Active Spacecraft," J. M. Sellen, Jr., AIAA Electric Propulsion and Plasmadynamics Conference, Colorado Springs, Colorado, Sept. 11-13, 1967. AIAA Preprint 67-702.

2. "Thrust Beam Equilibration Models," J. M. Sellen, Jr., Section IV.D., Study of Electric Spacecraft Plasmas and Field Interactions, TRW 07677-6013-R000, May 1968.

3. "Measurements of Equilibration Potential Between a Plasma 'Thrust' Beam and a Dilute 'Space' Plasma," H. S. Ogawa, R. K. Cole, and J. M. Sellen, Jr., AIAA 7th Electric Propulsion Conference, Williamsburg, Virginia, March 3-5, 1969. AIAA Preprint 69-263.

4. "Study of Electric Spacecraft Plasmas and Field Interactions," J. M. Sellen, Jr., AIAA 7th Electric Propulsion Conference, Williamsburg, Virginia, March 3-5, 1969. AIAA Preprint 69-276.

5. "Interaction of Spacecraft Science and Engineering Subsystems with Electric Propulsion Systems," J. M. Sellen, Jr., AIAA 6th Annual Meeting, Anaheim, California, October 20-24, 1969, AIAA Preprint 69-1106.

6. "The Generation and Diagnosis of Synthesized Plasma Streams," J. M. Sellen, Jr., W. Bernstein, and R. F. Kemp, Rev. Sci. Instr. 36, 316 (1965).

7. "Observations of Neutralized Ion Thrust Beams in the 25-Meter NASA Testing Chamber," J. M. Sellen, Jr., R. F. Kemp, and R. H. Hieber, TRW 8603-6039-KU-000, July 1964.

8. "Beam Neutralization Tests of a Flight Model Electron Bombardment Engine," R. F. Kemp, J. M. Sellen, Jr., and E. V. Parwlik, AIAA Preprint 62-2663 (November 1962). Also, NASA TN-D1733, July 1963.

9. "Environmental Effects on Laboratory and In-Flight Performance of Neutralization Systems," J. M. Sellen, Jr., and R. J. Cybulski, AIAA Preprint 65-70 (1965). Also, NASA TM X-52093.

10. "Oscillations in Synthetic Plasma Streams," W. Bernstein and J. M. Sellen, Jr., Phys. Fluids, 6, 1032, 1963.